The break-out behaviour of a suction anchor embedded in a granular soil.

SAHOTA, B.S.

1979

THE BREAK-OUT BEHAVIOUR OF A SUCTION ANCHOR EMBEDDED IN A GRANULAR SOIL

by

Baldev Singh Sahota

A thesis submitted to

The Council for National Academic Awards

for the Degree of Master of Philosophy

School of Mechanical and Offshore Engineering

Robert Gordon's Institute of Technology Aberdeen

July, 1979

ABSTRACT

The thesis describes an experimental investigation into the uplift behaviour of hemispherical suction anchors embedded in saturated sand. Anchor types are briefly discussed. Some existing theories related to plate-type anchors, for uplift foundations, and inverted cup-type surface suction anchors are reviewed. The experimental data and their interpretation are also discussed.

The experimental work comprised flow measurement tests on model suction anchors, pull-out tests on the model anchors with or without applied suction pressure, pull-out tests on the anchor shaft with or without suction pressure and pull-out tests on the prototype suction anchor. The primary investigation is directed towards the 70 mm and 102 mm suction anchors. Anchor loads, anchor displacements, cavity suction pressures, pore pressures above and below the anchor, and anchor embedment depths were recorded.

Suction anchors develop high pull-out loads primarily due to the applied suction pressure with embedment depth. The behaviour of an embedded-type suction anchor in saturated sand is governed by a large number of factors. These factors include depth of anchor embedment, anchor diameter, shaft diameter, filter area, sand density, and applied suction pressure. The author's results are plotted on Vesic's (1971) and, Das and Seeley's (1975) graphs for the correlation of the experimental test data. The plotted test data appeared to be in limited agreement, which is not unexpected because of the new parameter introduced by the applied suction pressure.

The research investigation is concluded and suggestions are made for further experimental and analytical work.

ACKNOWLEDGMENTS

The work described in this thesis was carried out in the School of Mechanical and Offshore Engineering, Robert Gordon's Institute of Technology, Aberdeen, and supported by a Science Research Council grant awarded to Mr. Q. Wilson.

The author is deeply indebted to his Director of Studies Mr. Q. Wilson of the School of Mechanical and Offshore Engineering, Robert Gordon's Institute of Technology, Aberdeen and External Supervisor Mr. T. W. Finlay of the Department of Civil Engineering, The University, Glasgow, for their valuable support. The author also extends his thanks to Mr. J.G. Black for his help.

Thanks are also due to the workshop staff for their help but particularly to the Project Technician, Mr. A. Whyte who took a keen interest in making and assembling the various parts of the test apparatus, which required considerable physical effort.

The author also expresses his thanks to Mr. F. Billington, Operations Manager for arranging time off from work in order to complete this thesis, and thanks are also due to Miss A. Gregory and Mrs. G. Macdonald for typing the thesis often under the difficult situations of Seaway Diving (UK) Ltd., Aberdeen.

Finally the author wishes to express his deepest love and appreciation to his wife, Harmit, who made this research study possible.

DECLARATION

This is to certify that the work described in this thesis is the result of the investigation conducted by the candidate during the research study except where specific reference is made to other investigators.

Candidate:

Director of Studies:

C O N T E N T S

Page

SYMBOLS

The following is a list of the more important symbols used in this thesis. Symbols generally are defined in the text.

a	dimensional factor, Matsuo's (1967) Theory
A	area
b	dimensional factor, Matsuo's (1967) Theory
B	width, diameter of anchor
B_o	diameter of anchor shaft
B_2	dimension in Matsuo's (1967) Theory
c	soil cohesive strength
C_{1-4}	expressions in Vesic's (1963 and 1965) Shallow Anchor Theory.
d_a	vertical displacement of anchor
d_s	anchor shaft burial depth
D	embedment depth of anchor
D_1	dimension in Matsuo's (1967) Theory
D_2	dimension in Matsuo's (1967) Theory
e	void ratio
e_{max}	maximum void ratio
e_{min}	minimum void ratio
f	friction resistance of soil on the anchor stem
F	force, vertical component of limiting frictional force
$\overline{F}_c$, $\overline{F}_q$	cavity breakthrough factor, Vesic's (1963 and 1965) Theory
F_{1-7}	factors in Matsuo's (1967) Theory
H	limited extent of displacement zone above deep anchor footing.
K	coefficient of earth pressure
K_o	coefficient of earth pressure at rest
K_p	coefficient of passive earth pressure
K_{pv}	coefficient in Meyerhof and Adams' (1968) Theory
K_u	uplift coefficient in Meyerhof and Adams' (1968) Theory
K_1, K_2	factors in Matsuo's (1967) Theory
L	skirt length of suction anchor

l working length of anchor stem in Mariupol'skii's (1965) Theory

$\bar{N}_q$ break-out factor in sand, Vesic's (1971) Theory

p_{uc} ultimate cavity pressure

p_1 anchor cavity suction pressure

p_2 pressure below anchor

p_3 pressure above anchor

p_4 pressure above top of anchor

q overburden pressure

Q total cohesive force over failure surface, Mariupol'skii's (1965) Theory

Q_u ultimate uplift resistance

S amount of anchor displacement, Mariupol'skii's (1965) Theory

s' shape factor, Meyerhof and Adams' (1968) Theory

t thickness of anchor

T time, tensile region near soil surface in shallow anchor case

T_v vertical component of shearing, Balla's (1961) Theory

T_v' vertical component of resultant shearing, Matsuo's (1967) Theory

V_o volume of anchor

V_{1-5} various volumes of soil

W weight of anchor

W_a buoyant weight of anchor

W_{1-5} various weights of soil volume

α Earth Cone angle, angle in Vesic's (1963 and 1965) Theory

γ density of soil

δ Earth pressure friction angle

ϑ angle, Matsuo's (1967) Theory

λ coefficient of anchor dimensions, Balla's (1961) Theory

μ micron

ρ ratio of logarithmic spiral, Matsuo's (1967) Theory

ρ_o original radius of logarithmic spiral Matsuo's (1967) Theory

σ_r radial pressure

φ angle of shearing resistance

CHAPTER 1

INTRODUCTION

1.1 GENERAL

An anchor is a sub-structural member which transmits a tensile force from a main structure to a surrounding soil or rock and is attached to the structure with a suitable anchor tendon or shaft or mooring line. The uplift resistance of the anchor during pull-out is the sum of the resistance mobilised by the anchor and any other forces mobilised due to adhesion and friction along the embedded length of the anchor tendon.

Engineers have always been interested in the use of anchors for stabilising structures subjected to uplift forces. Typical examples of these structures are suspension bridges, arch bridges, transmission towers, pipe lines, structures on which hydrostatic forces are exerted by submerged or semi-submerged equipments and other low density structures. Recently, there has been an increasing demand for buried anchors to stabilise structures on land and at sea. The forces imposed upon structures are firstly, due to a strong wind on land and secondly due to a combination of currents, waves, wind and tides at sea. These forces are not static in nature but are dynamic in their application. Wind or wave force or combinations of both forces have no set intensity or frequency of occurrence but are random in functions.

Considerable progress has been made in developing the experimental investigation and theoretical analysis of the behaviour of buried anchors subjected to static and dynamic uplift forces. For example, special testing procedures have been employed to find the failure surface which develops during pull-out of embedded anchors. Still, at present the less commonly attempted research investigations on the uplift resistance capacity of anchors in soils require a great deal of attention to overcome the unresolved problems.

1.2 TYPES OF ANCHORS

Anchors may be classified into the following categories and their characteristics are identified as follows:-

1. Ground Anchors

2. Rock Anchors

3. Marine Anchors

1.2.1 Ground Anchors

Ground anchors are generally used in soils ranging from soft silts to gravels and their types are bored or underreamed, plate or slab, grouted type, etc. Some examples and uses of ground anchors are shown in Fig. 1.1.

1.2.2 Rock Anchors

Rock anchors are usually tendons or cables held in position by grouting or some other suitable means and placed in a known size of hole in rock. Rock anchors are employed to stabilise fractured, fissured or jointed rock and their types are rawlplug, grouted type, slot and wedge type, etc. Fig. 1.2 shows some examples and uses of rock anchors.

1.2.3 Marine Anchors

Marine anchors are of various types and are capable of providing uplift resistance in shallow or deep water. Marine anchors are employed by boats, buoys, ships, semi-submersible

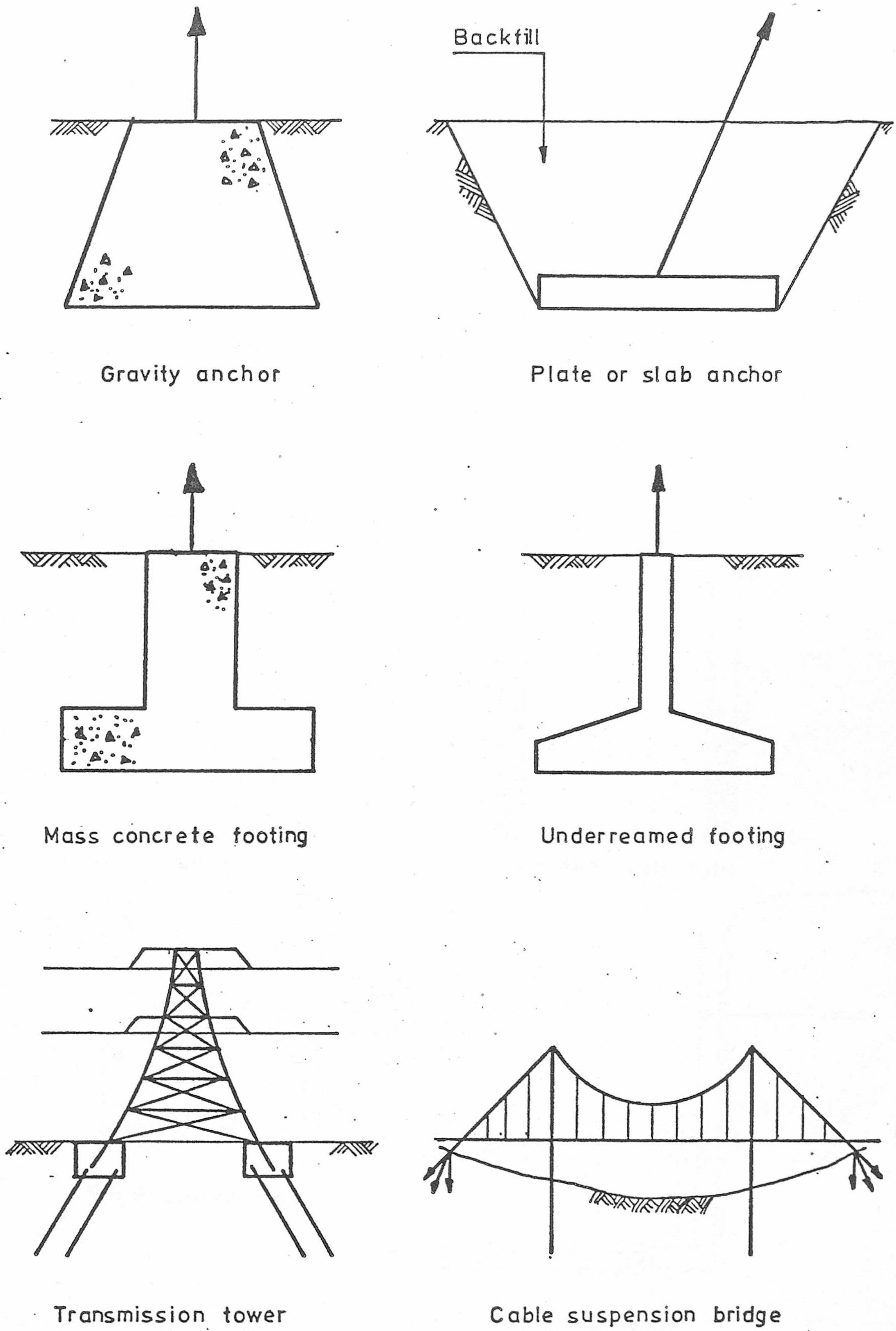

Fig. 1.1 Some examples and uses of ground anchors.

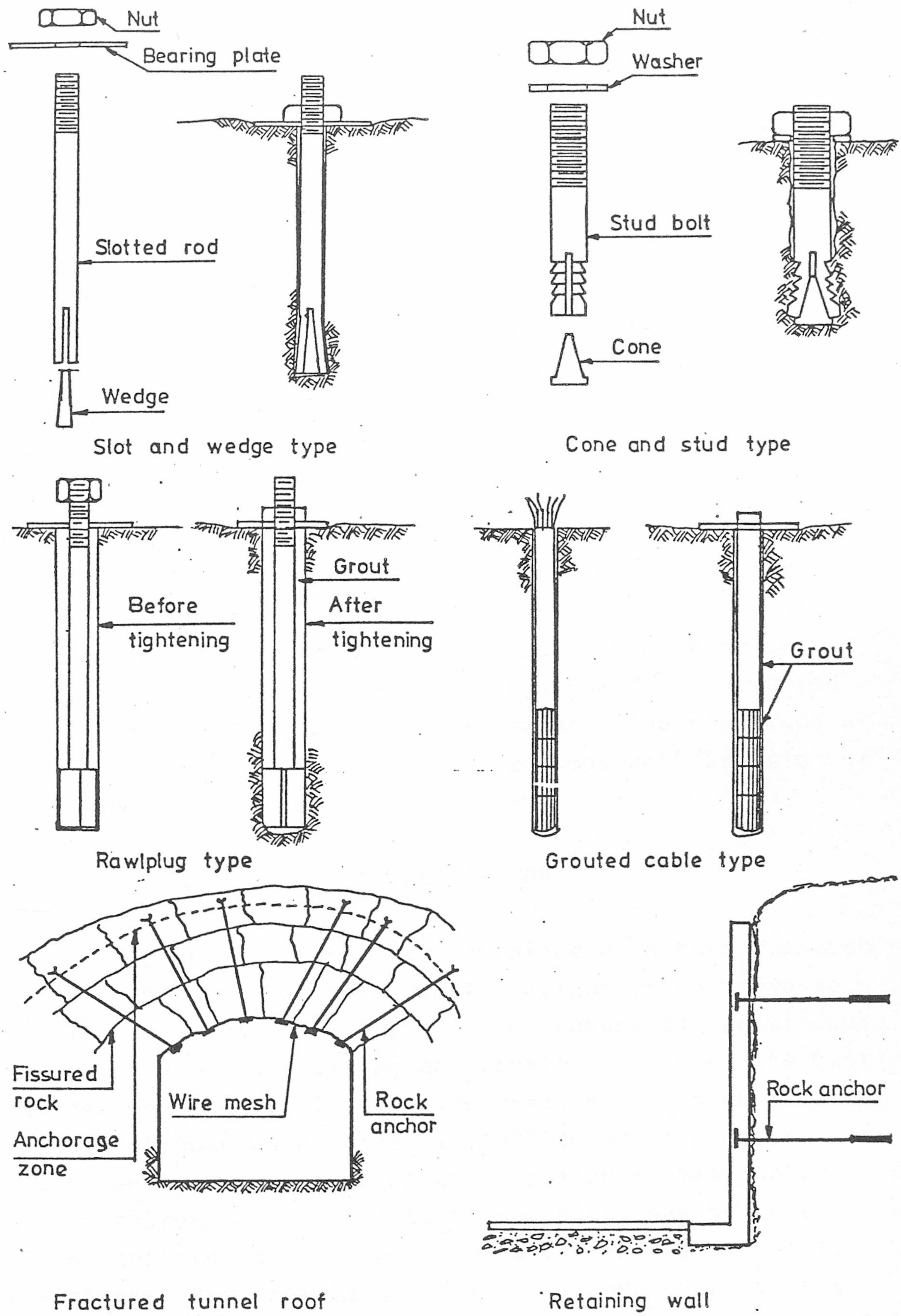

Fig. 1.2 Some examples and uses of rock anchors.

structures, bottom resting equipments, etc. The types of these anchors are dead weight, conventional anchors, free-fall, drilled, driven, propellant-actuated direct embedment, Vibrated direct-embedment anchors, etc. In 1977, a new form of marine anchor, the embedded suction anchor was proposed by research workers at Robert Gordon's Institute of Technology, Aberdeen. Some examples of marine anchors, with applications, are illustrated in Fig. 1.3 to Fig. 1.6.

1.3 APPLICATIONS OF ANCHORS IN PRACTICE

A primary application of anchors is to stabilise structures which are subjected to uplift forces. The anchors can be used directly to transmit forces from weak strata to sound strata, join fractured rocks, tie back retaining walls, transmission pylons, buoyant foundations, submerged or semi-submerged equipments, to anchor pipe lines on the sea bed etc., and the anchors may be single or in groups. Selection of the anchor type can be considered after investigating the soil parameters, the magnitude of force to be stabilised and the magnitude and direction of displacement which can be tolerated.

1.4 NEED FOR RESEARCH INVESTIGATION

Only marine anchors are considered in this research study. The need for research investigation on improved mooring continues on a world scale because the continuous growth of ocean operations and construction over the last two decades has resulted in increased application of low density structures anchored in shallow or deep water; and a substantial mooring is often required in deep water, due to the extreme storm conditions, where the use of conventional ships' anchors is ruled out due to the excessive uplift resistance, far from land. This puts into question the economics of transporting heavy masses of concrete, steel, etc., to act as anchors for such systems. The quest is for

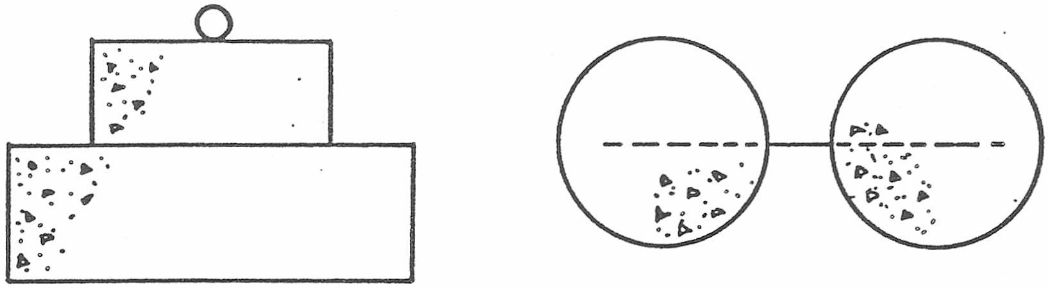

Mass anchors

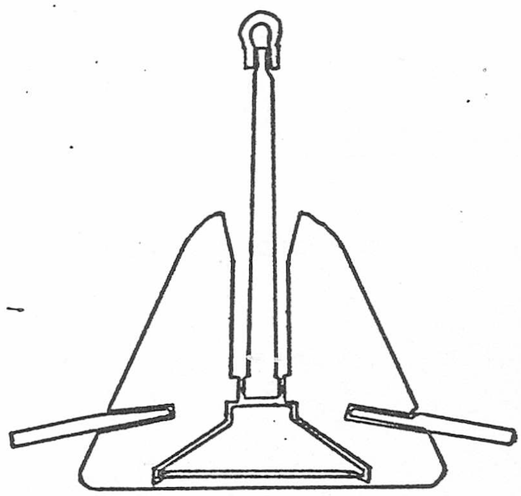

Drag anchors

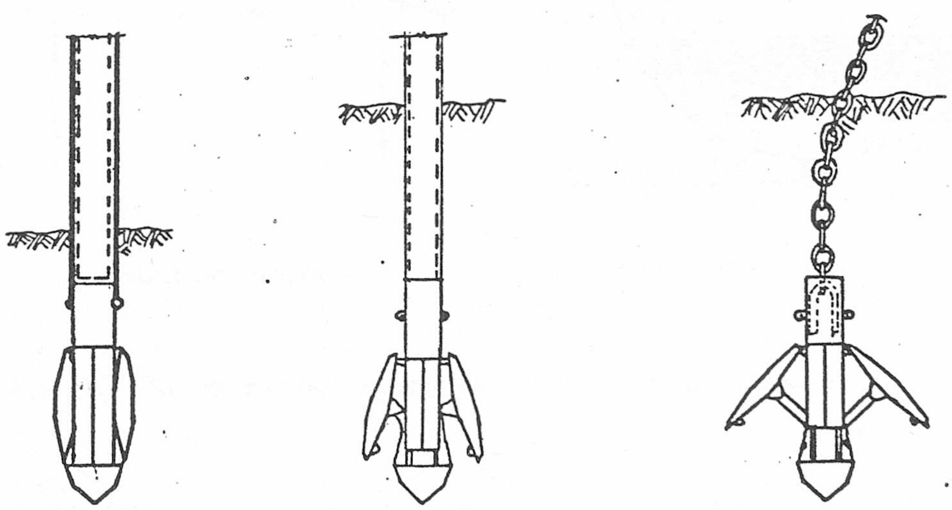

Initial driving position   opening position   in-service position

Umbrella pile anchor

Fig. 1.3 Some examples of marine anchors.

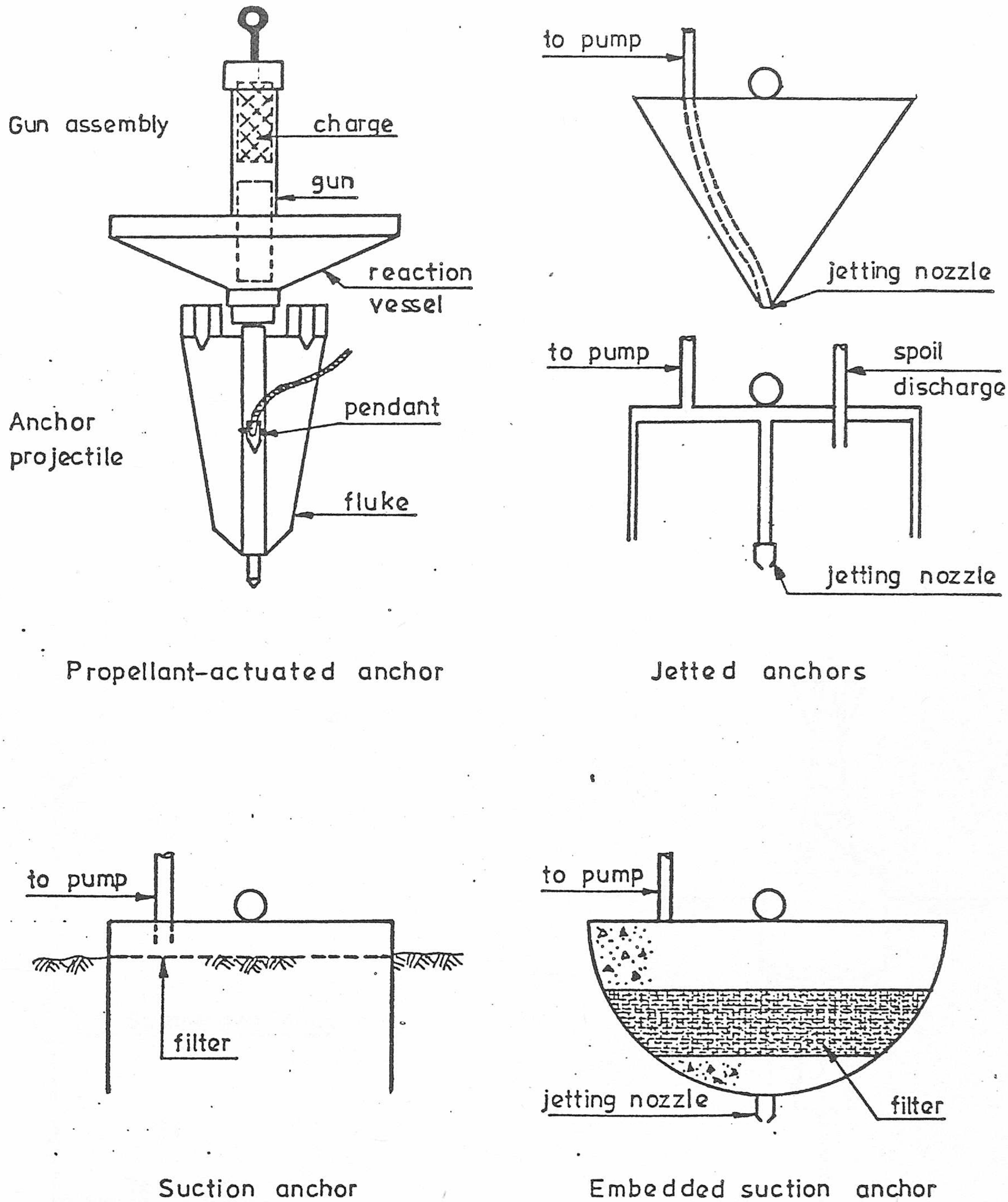

Fig. 1.4 Some further examples of marine anchors.

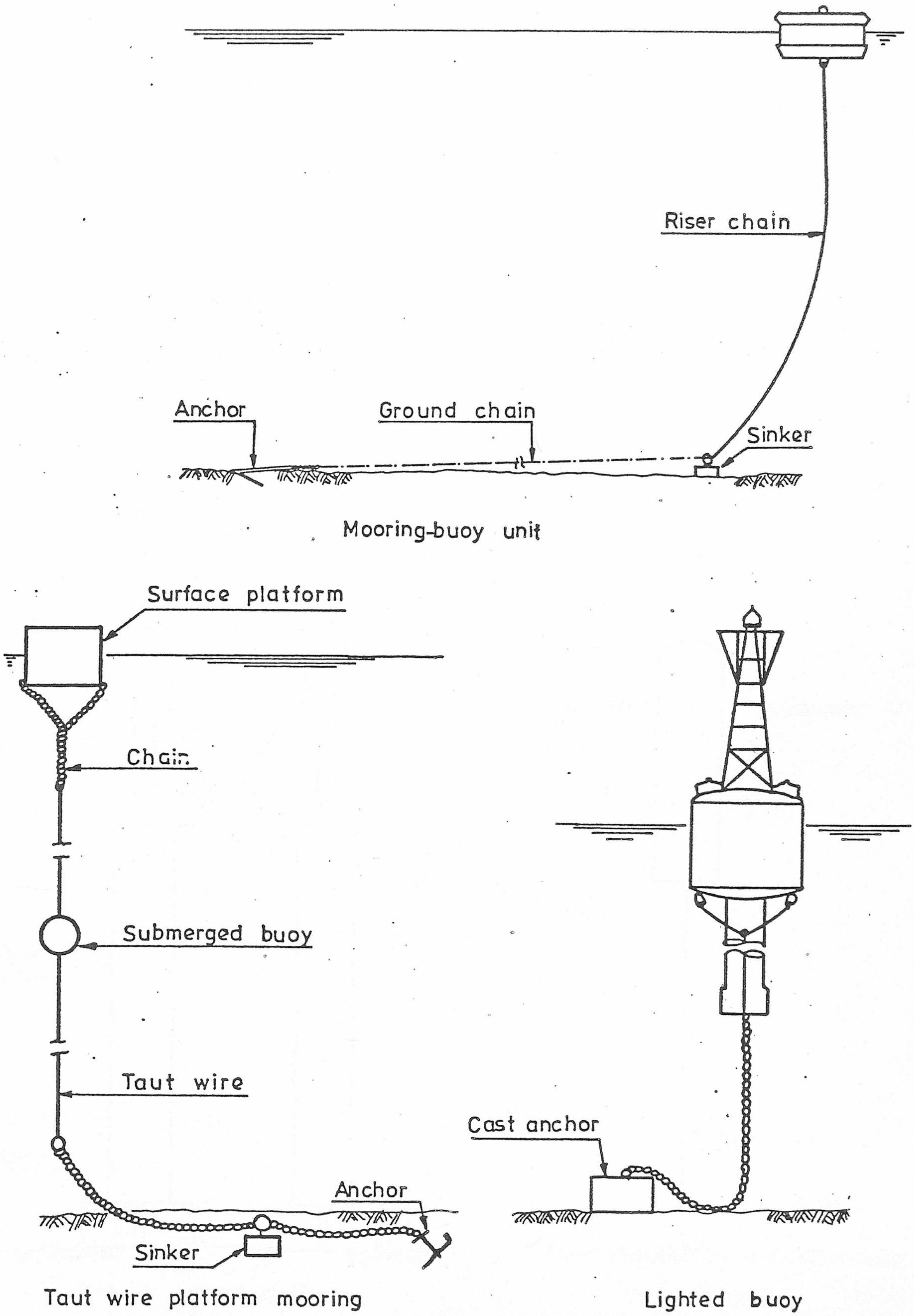

Fig. 1.5. Some applications of marine anchors.

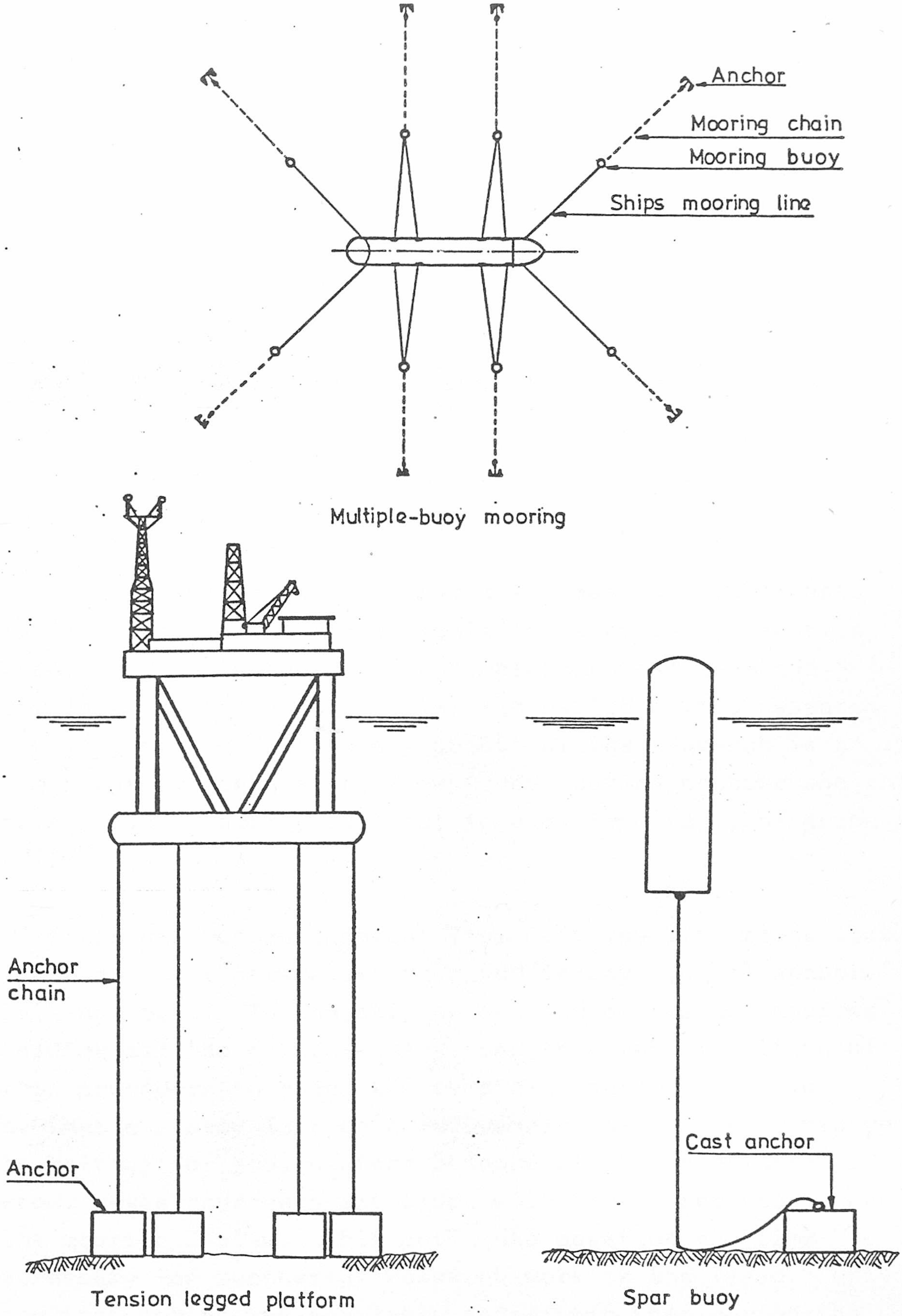

Fig. 1.6. Some applications of marine anchors.

anchors which can resist uplift forces, which are highly efficient, reliable, light weight, small in size and simple to handle and maintain. The embedded type anchors are likely to meet most of the above requirements.

1.5 PURPOSE AND SCOPE OF THE PRESENT INVESTIGATION

It is hopefully believed that a better understanding of the embedded suction anchor problem, which is the subject of this research investigation, will assist engineers in future design, and that the information collected will be of use to researchers for developing a theoretical analysis of the anchor, soil behaviour and in planning for future research work.

The experimental programme is based on model tests in the laboratory and full-scale tests at sea on suction anchors of hemispherical shape which were designed and developed by the author during the period of the research investigation. The primary object of the research is to study the break-out behaviour of embedded suction anchors and the pore pressure during pull-out in a minimum range of granular soils.

It has become apparent from past investigations that there are many parameters involved in any typical anchor pull-out test. To investigate any one parameter requires holding all the others steady, and then the repetition of this procedure to cover the remaining parameters. To achieve a steady load on a full-scale test at sea comes down to waiting for good weather because of the interaction of wind, waves, currents and tides with the moored vessel and the mooring system. This puts into question the time necessary for successful research work in the field. Only one test period was available and within that period the number of tests that could be completed was severely limited. Because of this, the investigation was based principally on model tests.

Many series of tests were performed in the laboratory on hemispherical anchors which were developed with different suction filter area, filter position and diameter. The experimental test results have been compared among the model anchors and a full-scale anchor, and also results have been correlated with the theoretical analysis of the observed behaviour of model plate anchors. The research work is concluded and recommended for further work.

CHAPTER 2

LITERATURE REVIEW ON UPLIFT CAPACITY OF FOUNDATIONS

2.1 INTRODUCTION

Dead weight anchors represent an early solution to the problem of resisting uplift forces. They are simple and their holding capacity is easily calculated since this relies on self weight. Dead weight anchors become large as holding capacity is increased and become impractical because they are cumbersome and inefficient. However, at some stage, it was realised by investigators that there was a great demand for anchors to stabilise structures subjected to uplift forces, and a more fundamental approach to predict the uplift resistance of the more sophisticated anchor types was required.

In recent years, investigators have proposed theoretical solutions to the anchoring problem. Most of the theories are based on model-scale study and have been derived for cohesionless soils, cohesive soils and also soils possessing friction and cohesion. A few of these studies apply to shallow anchors only, some to deep anchors and others to anchors at all depths. Various sizes and shapes of anchors, single or in groups, were employed in model studies under a variety of soil types and conditions. Empirical and semi-empirical analyses were used to develop a relationship between anchor geometry, anchor burial depth and soil parameters. Field studies were also performed to evaluate the accuracy of the empirical equation for predicting the anchor's pull-out resistance.

A shallow burial depth of the anchor may be defined as when the slip failure surface in the soil mass reaches to the ground surface at an ultimate load, and up to this burial depth the anchor is called a shallow anchor. A deep burial depth of the anchor may be defined as one whose ultimate load does not affect the ground surface and beyond this burial depth, the anchor is known as a deep anchor.

Uplift resisting theories for buried plate anchors are discussed briefly in the following sections to illustrate the development of the solutions to the anchor problem. Research investigations on surface-attaching suction anchors are then reviewed in order to develop a framework of ideas of relevance to the present study.

2.2 THEORETICAL DEVELOPMENTS

Traditional methods were used for many years to calculate the uplift resistance of shallow anchor footings. During the last two decades, many methods have been proposed to compute the uplift behaviour of shallow and deep anchor footings of different shapes. The more recent methods reflect the growing understanding of soil mechanics principles in obtaining a solution to the uplift resisting problem.

2.2.1 Earth Cone Method

The ultimate uplift resistance is assumed to be equal to the sum of the dead weight of footing and the weight of soil contained in the cone truncated by the bottom of the footing slab as shown in Fig. 2.1. The ultimate uplift resistance Q_u is given by:

$$Q_u = W + \gamma(V_1 - V_o) \qquad \text{.........................(2.1)}$$

The volume of earth in the truncated cone for a round slab

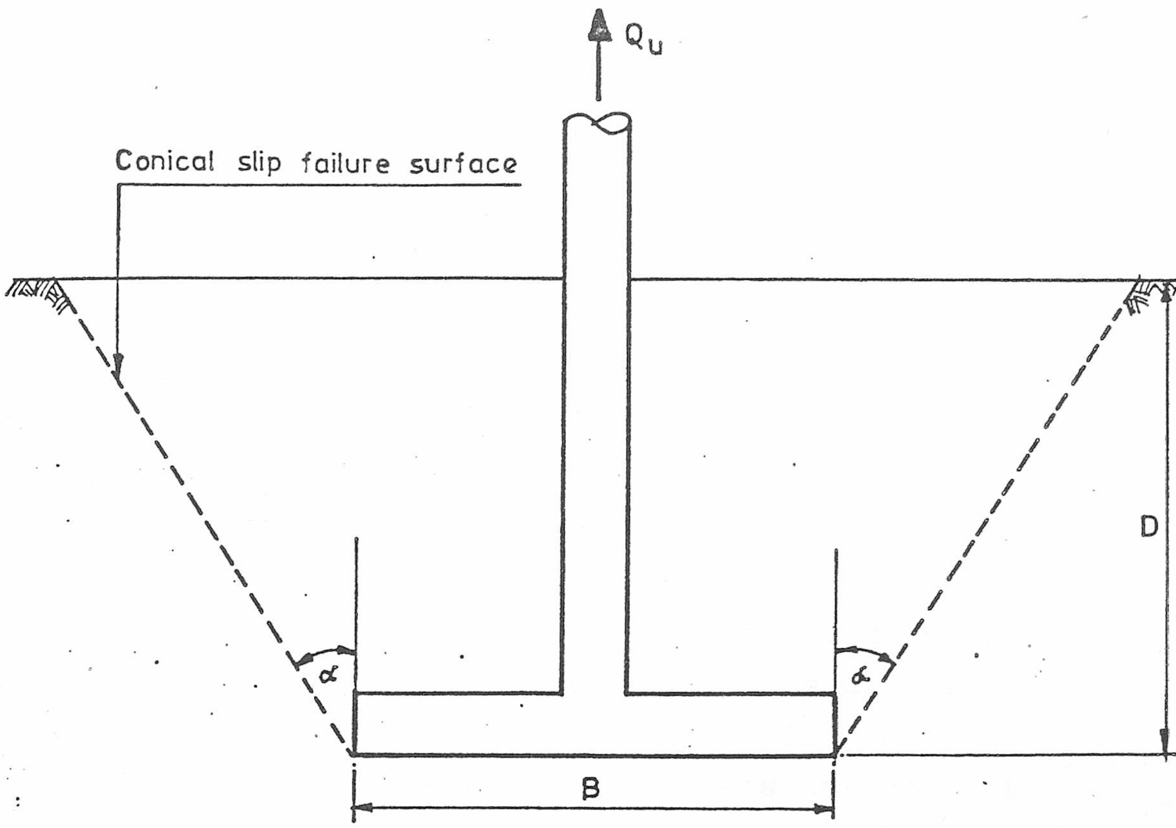

Fig. 2.1. Earth cone theory

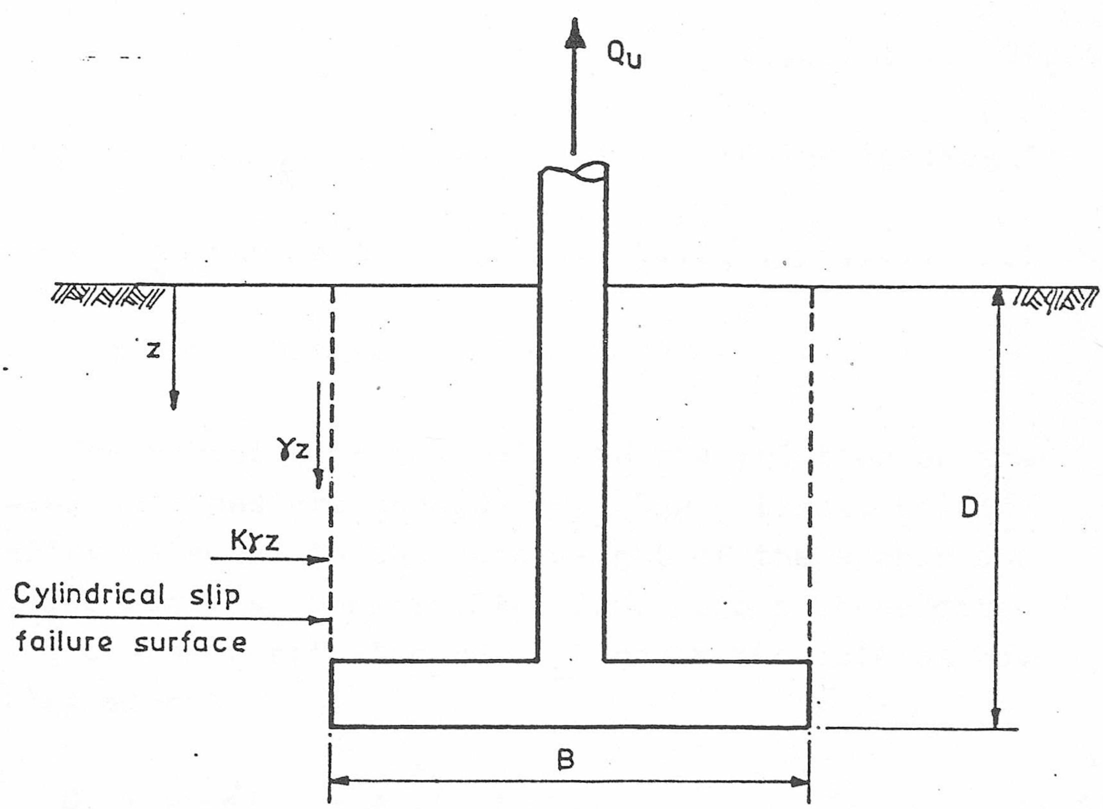

Fig. 2.2. Earth pressure and shearing theories

is given by:

$$V_1 = \frac{\pi D}{4}(B^2 + 2BD\tan\alpha + \frac{4}{3}D^2\tan^2\alpha) \quad \ldots\ldots\ldots\ldots (2.2)$$

The magnitude of angle α changes according to the type of soil but α is the angle which is formed by the conical surface against vertical. Soil mechanics principles are not taken into consideration, therefore the shear failure in the earth body is neglected.

2.2.2 Earth Pressure (Friction Cylinder) Method

The ultimate uplift capacity is assumed to be equal to the dead weight of the anchor, plus the weight of soil lying vertically on the anchor footing slab and the frictional force on the vertical surface through the outside edge of the slab at the condition of earth pressure at rest as shown in Fig. 2.2. Then:

$$Q_u = W + \gamma(V_2 - V_o) + F \quad \ldots\ldots\ldots\ldots (2.3)$$

where, the frictional force F for a circular footing is:

$$F = \frac{\pi}{2}K_o\gamma BD^2\tan\delta \quad \ldots\ldots\ldots\ldots (2.4)$$

2.2.3 Shearing Method

The cohesion of the soil and the friction on the sliding surfaces are considered. The ultimate uplift capacity is equal to the dead weight of the anchor and enclosed soil as shown in Fig. 2.2, plus a shear force T acting on the vertical surface through the outside edge of footing slab.

$$Q_u = W + \gamma(V_2 - V_o) + T \quad \ldots\ldots\ldots\ldots (2.5)$$

where the shear force T on the cylindrical slip failure surface is:

$$T = \pi cBD + \frac{\pi}{2}K\gamma BD^2\tan\varphi \quad \ldots\ldots\ldots\ldots\ldots\ldots\ldots (2.6)$$

2.2.4 Balla's (1961) Theory: (Fig. 2.3)

Balla performed his research studies to evaluate the resistance of breaking out of mushroom type foundations for pylons and disagreed with the traditional methods because these methods underestimate the pull-out capacity at shallow depths and overestimate at deep depths. He approximated the observed slip failure surface to an arc of a circle starting with a vertical tangent to the edge of the anchor slab and intersecting the ground level at an angle of $(\pi/4 - \varphi/2)$. The centre of this arc lies on a horizontal line through the top of the anchor slab and its radius is given by:

$$r = \frac{D - t}{\sin(\pi/4 - \varphi/2)} \quad \ldots\ldots\ldots\ldots\ldots\ldots\ldots (2.7)$$

Balla derived the overall resistance against breaking out as:

$$Q_u = W_1 + T_v + W_2 \quad \ldots\ldots\ldots\ldots\ldots\ldots\ldots (2.8)$$

where W_1 = weight of the breaking-out soil solid of revolution

$$= (D - t)^3\gamma F_1(\varphi,\lambda) \quad \ldots\ldots\ldots\ldots\ldots\ldots\ldots (2.9)$$

where $F_1(\varphi,\lambda)$ is a factor depending on the friction angle of the soil and on a coefficient characteristic for the shape of the foundation body.

W_2 = difference in weight between the anchor material and the soil for the volume of the anchor shaft.

T_v = shearing resistance over the sliding surface

$$= (d-t)^3 \gamma \left[\frac{c}{\gamma} \frac{1}{d-t} F_2(\varphi,\lambda + F_3(\varphi,\lambda) \right] \quad \ldots\ldots(2.10)$$

where F_2 and F_3 are factors depending on φ and λ.

2.2.5 Vesić's (1963, 1965 and 1971) Theory: (Fig. 2.4)

Vesić proposed a different analytical approach to the uplift resistance problem in which he considered an explosive charge placed in an earth medium at moderate depth from the surface and put forward the problem of expansion of cavities close to the surface of a semi-infinite rigid-plastic solid. He assumed that the cylindrical or spherical cavity expands at a limiting pressure and due to this a slip failure surface occurs above the cavity. The solution to the three-dimensional axially-symmetric problem was obtained by introducing the assumption that the normal and shear stress distributions including the angle along the slip surfaces are equivalent to those found in the corresponding two-dimensional case. He also assumed that the slip failure surface with a circular arc tangential to the expanded cavity meets the soil surface at an angle of $\pi/4 - \varphi/2$. Using an equation derived by Brinch Hansen (1953) for the two-dimensional case the ultimate pull-out resistance is given by:

$$Q_u = W_3 + W_4 + T\cos\alpha - N\sin\alpha \quad \ldots\ldots\ldots\ldots\ldots(2.11)$$

where T and N were taken by Vesić from Brinch Hansen and are functions of φ and α.

The ultimate cavity pressure p_{uc} was determined from an equation of vertical equilibrium of the entire ruptured mass above the cavity. Then:

$$p_{uc} = c\bar{F}_c + \gamma D\bar{F}_q \quad \ldots\ldots\ldots\ldots\ldots\ldots\ldots\ldots(2.12)$$

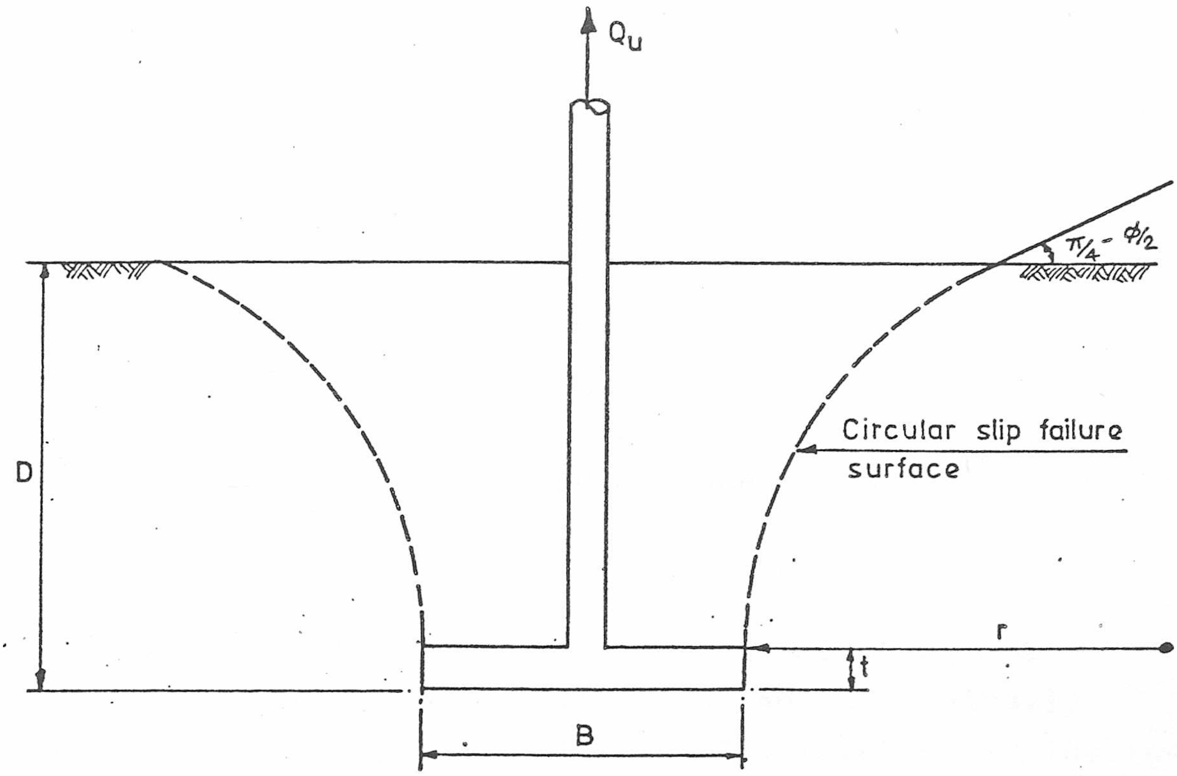

Fig. 2.3. Balla's Theory: Circular slip failure surface.

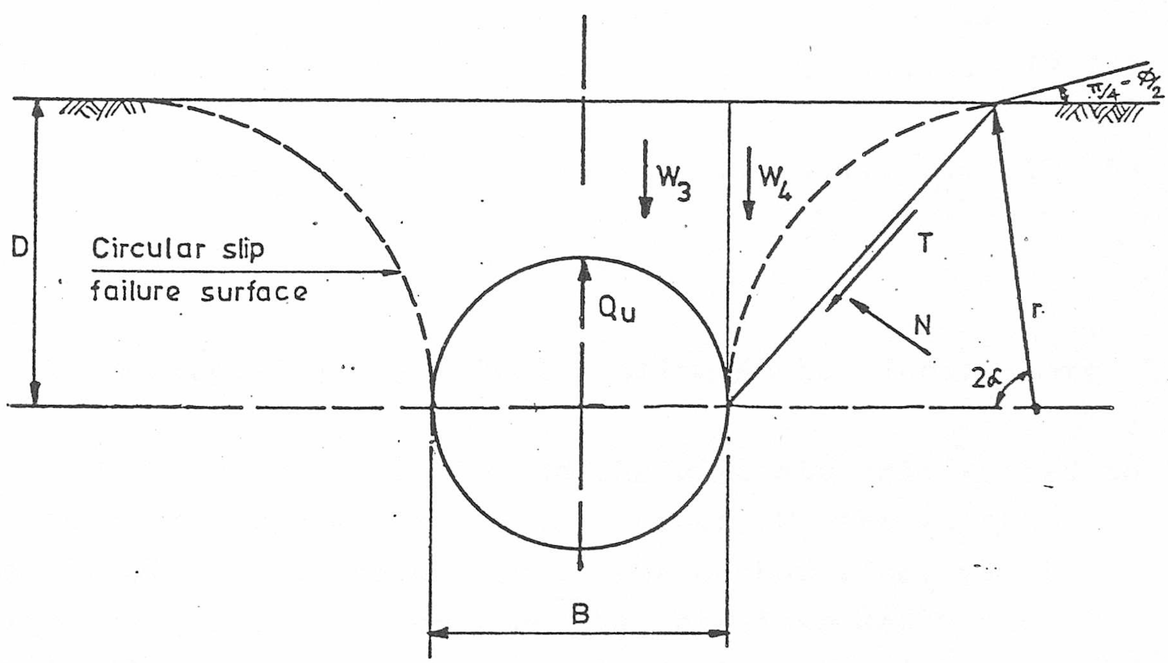

Fig. 2.4. Vesic's Theory: Expansion of a spherical cavity close to the ground surface.

in which $\overline{F}_c$ and $\overline{F}_q$ = the cavity breakthrough factors, which depend on the shape and relative depth of the cavity, as well as on the angle of shearing resistance of the soil. Where:

$$\overline{F}_q = 1.0 + \frac{B}{3D} + 2C_1\frac{D}{B} + 4C_2\left\{\frac{D}{B}\right\}^2 \quad \text{..............(2.13)}$$

and, $$\overline{F}_c = 2C_3\frac{D}{B} + 4C_4\left\{\frac{D}{B}\right\}^2 \quad \text{.........................(2.14)}$$

C_{1-4} are expressions in φ and α. When $\varphi = 0$ then $\overline{F}_c$ and $\overline{F}_q$ reduce to relatively simple terms.

Esquivel-Diaz (1967) adjusted the volume of the hemispherical cavity to be filled with soil, originally neglected, whose weight was $(16 \div 3)\pi B^3\gamma$ which would increase the unit pressure acting on the anchor plate by $\gamma B/3$. In addition to this quantity the equation 2.12 for cohesionless ($c = 0$), would give the ultimate pull-out pressure of the anchor plate:

$$p_{uc} = \gamma D F_q + \frac{\gamma B}{3} \quad \text{.............................(2.15)}$$

$$= \gamma D\overline{N}_q \quad \text{.............................(2.16)}$$

2.2.6 Mariupol'skii's (1965) Shallow Anchor Theory: (Fig. 2.5)

Mariupol'skii considered the ultimate uplift load to be equal to W the weight of the anchor, W_1 the weight of the circular earth column above the anchor slab, γV_2 the weight of the conical part of the entrained earth plus Q the total cohesive force to failure along the lateral surface of the 'separation cone'. Then, the ultimate load on the anchor:

$$Q_u = W + W_1 + \gamma V_2 + Q \quad \text{.......................(2.17)}$$

$$\text{where } Q = \pi B\left[cD + \tan\varphi\left(K\gamma \frac{D^2}{2} + \int_0^D \sigma_r dz\right)\right] - \gamma V_2 \quad \text{........(2.18)}$$

where σ_r designates the additonal radial stresses created by pressing the anchor slab on to the overlying earth column in a cylindrical section with radius B/2. The function σ_r is determined from the equations of equilibrium. Then the total ultimate load on the anchor is:

$$Q_u = W + \frac{\pi}{4}(B^2 - B_o^2)\frac{\gamma D\left\{1 - \left(B_o/B\right)^2 + 2K_o\left(D/B\right)\tan\varphi\right\} + 4c\,D/B}{1 - \left(B_o/B\right)^2 - 2nD/B}$$

$$\text{................(2.19)}$$

where n is a certain dimensionless function of the angle of internal friction of the soil φ and is determined from experimental data.

2.2.7 Mariupol'skii's (1965) Deep Anchor Theory: (Fig. 2.6)

Mariupol'skii proposed that when a deep anchor reaches the limiting condition, a conical wedge is formed immediately above the anchor slab, forcing the soil lying above it apart and to the sides then allowing the anchor to move upwards at a practically constant load. The soil wedge had the shape of a truncated cone with slightly convex generatrix and the angle made at the apex was close to 90^o. He assumed that upon reaching the limiting condition the work of withdrawing the anchor plate to height S is equivalent to the work done when expanding a certain cylindrical cavity in the soil of height S from its diameter B_o to B. He considered the 'useless' work expended

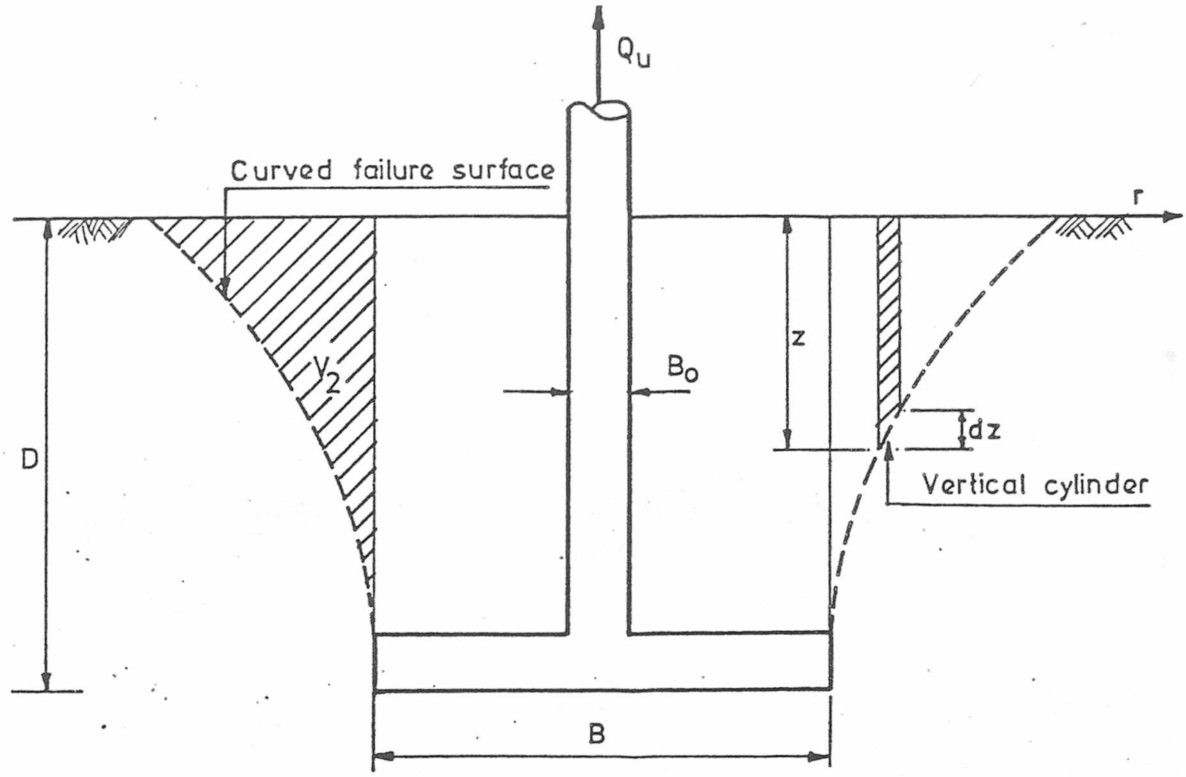

Fig. 2.5. Mariupol'skii's Theory : Failure surface for a shallow anchor.

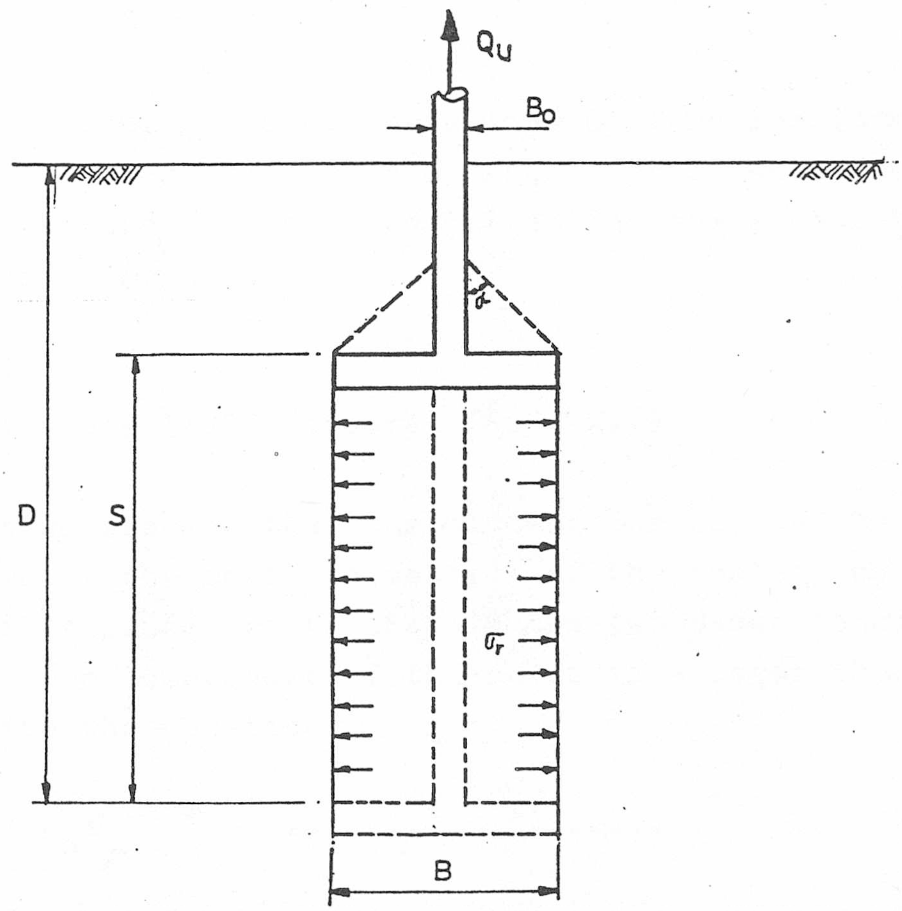

Fig. 2.6. Mariupol'skii's Theory ; Failure surface for a deep anchor.

to overcome friction between the surface of the soil wedge and the surrounding soil. Then:

$$P_p = \frac{\sigma_r \pi(B^2 - B_o^2)}{4(1 - 0.5\tan\varphi)} \qquad \text{.........................(2.20)}$$

where, P_p = ultimate load transmitted to the soil by the anchor slab

and, σ_r = radial pressure

Finally, Mariupol'skii derived an expression for the total ultimate load on a deep anchor as:

$$Q_u = W + P_p + f\pi B_o l \qquad \text{.........................(2.21)}$$

where, f = friction resistance of soil on the anchor stem and l = working length of anchor stem and assumed to be equal to $S - (B - B_o)$.

When finding the ultimate load Q_u from the formulae 2.19 and 2.21 the smaller value should be selected because the soil failure may occur on extracting the anchor by two different schemes.

2.2.8 Matsuo's (1967) Theory: (Fig. 2.7)

Matsuo assumed that the sliding surface can be determined at the meridian section of the footing by means of a similar procedure to that in the two dimensional problem. The lower part of the curve is a logarithmic spiral with the equation:

$$\rho = \rho_o e^{\vartheta \tan\varphi} \qquad \text{.................................(2.22)}$$

The upper part of the sliding surface is a straight line from A and meets the ground surface at an angle of $(\pi/4 - \varphi/2)$.

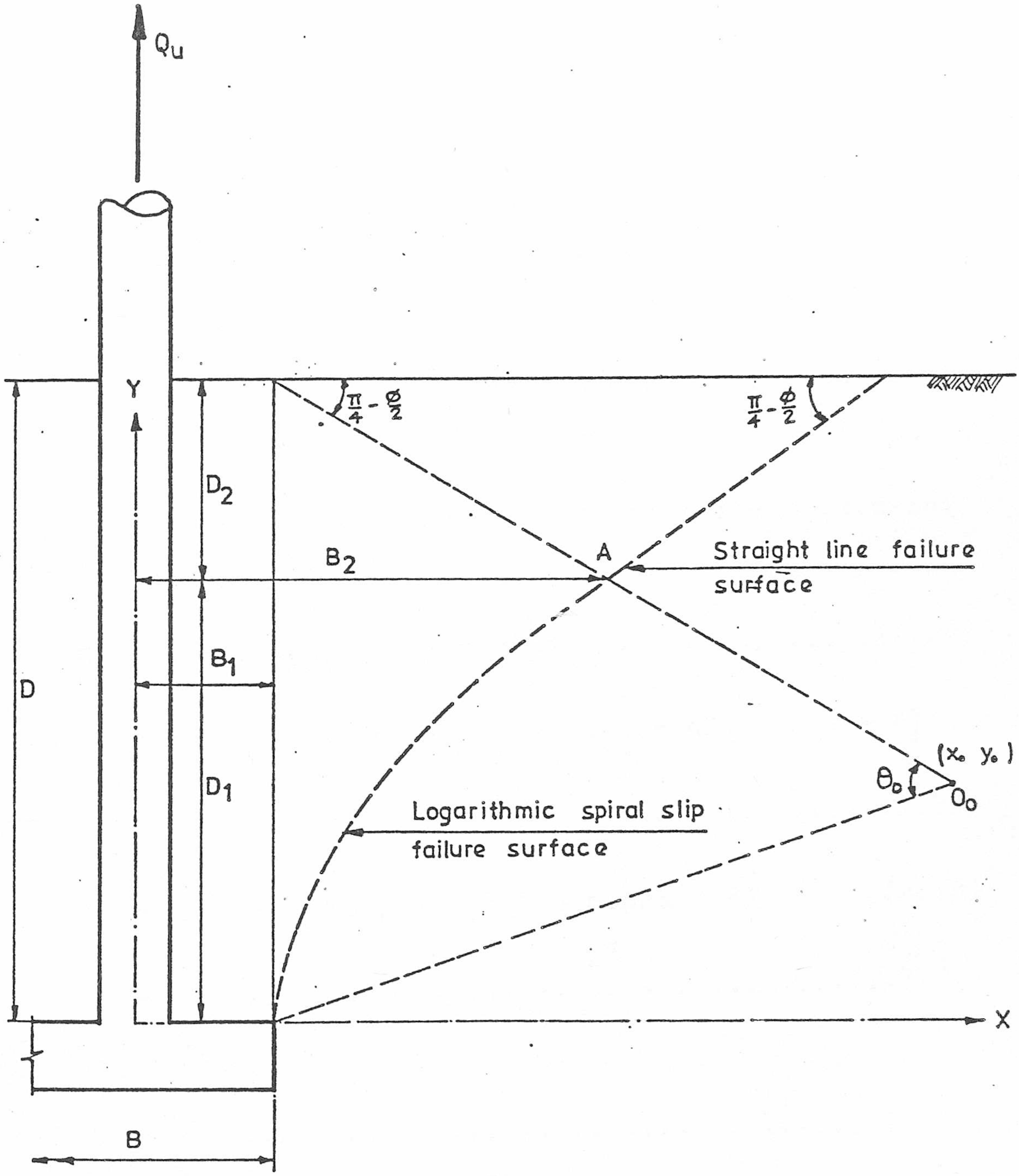

Fig. 2.7. Matsuo's Theory : Logarithmic spiral and straight line slip failure surfaces.

The slip occurs along the sliding surface when there is a minimum pressure on the anchor and this pressure may be found by taking moments about O_o. On determining the sliding surface, the ultimate uplift resistance Q_u can be expressed as:

$$Q_u = W + \gamma V_4 + T'_v \quad \text{.............................(2.23)}$$

where V_4 = volume of soil mass included in the sliding surface,

and T'_v = vertical component of the resultant shearing resistance acting on the slip failure surface.

Matsuo derived complex expressions for the vertical component for cohesion and cohesionless soils.

The ultimate uplift resistance for soils possessing cohesion and friction is:

$$Q_u = W + \gamma(B_2^3K_1 - V_5) + cB_2^2K_2 \quad \text{...............(2.24)}$$

where $K_1 = \pi\left[(a - 1)(a^2F_1 + aF_2 + abF_3 + bF_4 + F_5) + b\right]$

$$\text{..............(2.25)}$$

$$K_2 = \pi\left[(a - 1)(aF_6 + F_7) + b(b\tan\alpha + 2)\right] \quad \text{.....(2.26)}$$

$$a = \frac{x_o}{B_2} \quad \text{.....................................(2.27)}$$

$$b = \frac{D_2}{B_2} \quad \text{......................................(2.28)}$$

and F_{1-7} are factors depending on ϑ_o, x_o, φ, B_2 and D_2.

2.2.9 Meyerhof and Adams' (1968) Theory: (Fig. 2.8)

Meyerhof and Adams proposed an approximate general theory of uplift resistance in soil based on theoretical considerations and test observations. The theory is derived for a strip of continuous footing and is then modified for use in sands and clays for a required footing type and for group action. For example, the analysis for strip footings can be extended to circular footings by finding the shearing resistance from cohesion and passive earth pressure inclined at δ on a vertical cylindrical surface through the footing. Then, ultimate uplift resistance Q_u for shallow depths ($D < H$) is given by:

$$Q_u = \pi cBD + s'\left(\frac{\pi}{2}\right)\gamma BD^2K_u\tan\varphi + W + W_5 \quad \ldots\ldots.(2.29)$$

where, s' = shape factor governing the passive earth pressure on a convex cylindrical wall.

W_5 = weight of the lifted soil in the breaking-out cylinder.

Similarly the uplift resistance for great depths ($D > H$) is given by:

$$Q_u = \pi cBH + s'\left(\frac{\pi}{2}\right)\gamma B(2D - H)HK_u\tan\varphi + W + W_5 \quad \ldots(2.30)$$

where, $K_u = K_{pv}\tan\varphi$ ....(2.31)

K_{pv} = vertical component of the coefficient of passive earth pressure.

$= K_p\tan\delta$ ....(2.32)

where, K_p = coefficient of passive earth pressure.

and, $\delta = \frac{2\varphi}{3}$ ....(2.33)

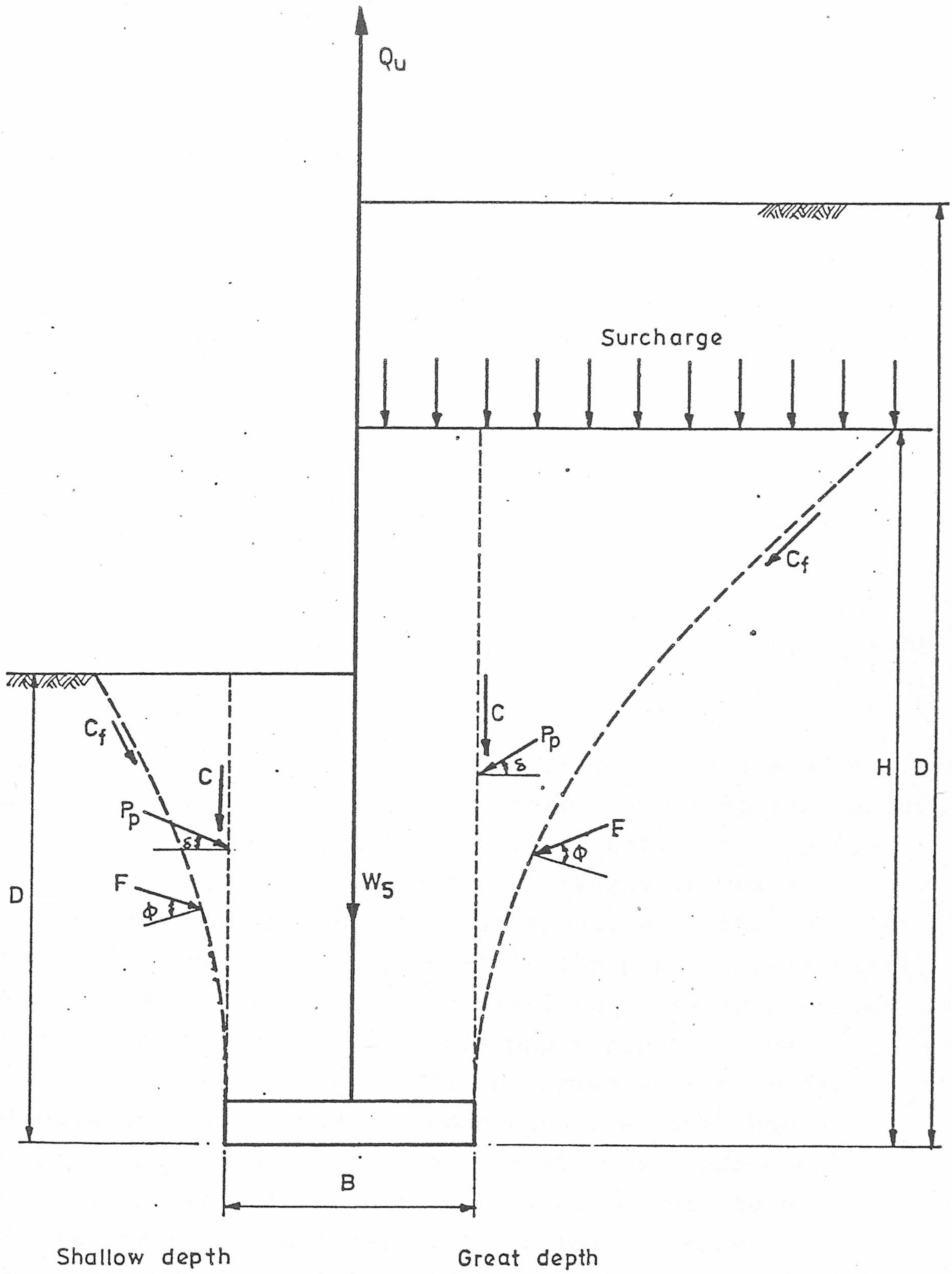

Fig. 2.8. Meyerhof and Adams' Theory : Failure surfaces of soil for shallow and great depths.

2.3 DISCUSSION OF EXISTING SHALLOW ANCHOR THEORIES

The Earth Cone Method (Fig. 2.1) does not take into consideration the knowledge of soil mechanics and therefore the actual important phenomenon of shear failure in the earth body is neglected.

The Earth Pressure Method (Fig. 2.2) does not take into consideration the shear failure in the soil mass, like the Earth Cone Method, and also discards the effect of cohesion of the soil.

The Shearing Method (Fig. 2.2) is better than the Earth Cone and the Earth Pressure Methods because it considers the shear in the soils. The deficiency in this method is the simplifying assumption of a vertical slip failure surface for those soils which possess internal friction.

Balla (Fig. 2.3) was the first to propose a simplified analysis for a circular plate, under the assumptions about the failure slip surface. He applied Kotter's equation to determine the distribution of stresses in the slip surface and assumed that the distribution in the axially symmetrical case is the same as in the plane strain case. However, according to Vesić (1971), the numerical values of the factors F_2 and F_3 in his paper appear to be incorrect. Sutherland (1965) performed work on model studies and site tests and concluded that the theory proposed by Balla would underestimate the loads mobilised in dense cohesionless soils. This would lead to an unsafe error on shaft raising problems and an error on the safe side for pylon foundations. The theoretical loads would be overestimated for loose cohesionless soils which would give safe errors for shaft raising and unsafe errors for pylon foundations.

Vesić's theory for the problem of expansion of cavities close to the surface of a semi-infinite rigid-plasic solid (Fig. 2.4) takes into account both normal and shear components of stress on the slip failure surface. Esquivel-Diaz (1967) modified the approach to include the weight of soil required to fill half the cavity, as it was originally neglected, and he added that, in computing the uplift capacity, the compressibility and frictional properties of the soil should also be taken into account.

Mariupol'skii (Fig. 2.5) assumed the maximum shear stress is mobilized in every vertical cylindrical surface around the anchor axis and the failure occurs in tension at different points along the slip failure surface. Vesić (1971) determined by experiments the values of the n parameter in Mariupol'skii's equation and reported that the agreement between theory and experiments is of very limited meaning. The assumptions made in analysing the state of stress in the soil wedge above the anchor are entirely arbitrary and in contradiction with the elementary theory of earth pressure.

Matsuo (Fig. 2.7) assumed that the sliding surface was composed of a logarithmic spiral and a tangential straight line. He concluded that the sliding surface from the edge of the footing slab does not reach the ground surface at the maximum value of uplift resistance. He also added that the ultimate resistance by the calculation method modified on the basis of the mentioned fact in the text is in good agreement with that by test.

Meyerhof and Adams (Fig. 2.8) simplified the approximate general theory for uplift capacity by considering the forces acting on a cylindrical surface above the foundation. Shape factors were applied to the general equation expression to account for the three-dimensional effect of individual square or circular footings.

Their expression for uplift resistance is partly theoretical and partly empirical.

2.4 DISCUSSION OF EXISTING DEEP ANCHOR THEORIES

Deep anchors tunnel towards the surface under uplift load and their peak uplift capacity would be reached at relatively deep displacements. The deep anchor theory should follow this failure mechanism and take into consideration that the cohesionless soil is compressed and that shearing takes place around the anchor footing.

Mariupol'skii (1965) assumed that the work done by the anchor during vertical displacement should be equal to the work needed to expand a vertical cylindrical cavity. He determined the ultimate pressure by trial and error from a lengthy equation. However, this could be done more conveniently by using a rigorous solution as proposed by Vesić.

Baker and Kondner(1966) established an empirical relationship for their deep anchors and pointed out that care should be taken in using the relationship, as the ratio between the sand particle size and anchor size were different in the model scale and the prototype.

Meyerhof and Adams (1968) restricted the application of their assumed sliding surface to a height H above the footing.

Vesic (1971) presented analyses involving break-out of objects embedded in the ocean bottom. He concluded that no equation, no matter how elaborate, could be fully satisfactory for all varieties of soil conditions as well as for methods of placement and types of objects to be pulled-out.

Ashbee's (1969) finite element analysis should be suitable for both shallow and deep anchors. The analysis shows, for a soil with friction and cohesion, that the peak stresses at various points in the soil mass are not reached simultaneously. This is a valid observation which was not considered by any of the previous theories.

2.5 PREVIOUS LABORATORY SCALE TEST WORK

None of the researchers has presented an exhaustive study in one paper because of the number of variables involved. Main points are noted from specific papers as follows:-

Balla (1961) performed a limited number of model tests on the pull-out loads developed in an air dried sand with $\varphi = 36^{o}$ to 38^{o} and moisture content = 10 to 12 percent. The diameters of the mushroom foundation models were 60, 90 and 120 mm.

Sutherland (1965) carried out model studies on shaft raising through cohesionless soils with $\varphi = 31^{o}$ for the loose state. Twenty-three pull-out tests were made on the dense sand and twenty-two on the loose sand using the first container. The diameter of the discs ranged from 38 mm to 152 mm and $D/_{B}$ values were 1 to 5.

Baker and Kondner (1966) carried out their experimental tests on 25, 38, 51 and 76 mm diameter anchor plates in an air-dry uniform silica sand with $\varphi = 42^{o}$.

Matsuo (1967) performed a large number of tests on different anchor geometries and varied the soil conditions in different soils. He concluded from the uplift tests on footings buried in sand that the observed sliding surface and the ultimate uplift resistance of the footings are in good agreement with those obtained by the theory. The effect of buoyancy on the uplift resistance is remarkable. Approximately there was no difference between the uplift load/displacement curve for load control and displacement control.

Howat (1969), Carr (1970) and Yilmaz (1971) reported that the uplift capacity increases with an increasing effective depth.

Shallow failure occurs when the soil above the anchor footing moves along a well defined surface which is accompanied by radial and circumferential surface cracks. Deep failure occurs when the anchor tunnels under pull-out which forces the soil to compress and shear around the anchor footing. The relative depth ratio varies from $D/_B$ = 3 to $D/_B$ = 12 at which shallow anchor failure ceases and deep failure begins. Howat (1969) performed some deep tests in moist sand and observed his critical $D/_B$ = 10 and claimed that at greater depths the footing 'tunnelled' through the sand until the $D/_B$ ratio was reached then a failure surface would reach to the soil surface. Carr (1970) found the tunnelling effect in deep failure and that the peak shear stresses occurred near the anchor footing. Hence slip failure occurred around the anchor footing and the surface of the inactive sand wedge which was located on top of the anchor footing and moving with the anchor. Kalajian (1971) confirmed the existence of this inactive soil wedge which was located on top of his anchor footing. Healey (1971) found the value of $D/_B$ at commencement of deep failure to increase with the increasing density of sand.

2.6 PREVIOUS FIELD SCALE TEST WORK

Tests on anchors are carried out commonly on sites to prove anchor uplift design capacity. It is rare for the pull-out test data to include load displacement, soil displacement and stresses near the anchor footing. Most of the published data on anchor pull-out tests are for shallow anchors.

Balla (1961) reported a limited number of field tests which were performed by Fielitz and by the firm Brown-Boweri in Altheim.

Sutherland (1965) reported nine tests for shaft raising operations in sand where the diameter of the shaft was 2.387 m.

Baker and Kondner (1966) reported two tests performed on Webb-Lipow type anchors buried in a relatively uniform fine sand with $\varphi = 37^{o}$ in which ground water was encountered at a depth of about 1.8 m below the surface.

The uplift capacity increases with the $D/_B$ ratio and also if the anchors have enlarged bases. A higher factor of safety is required for working loads where creep is critical. Anchor shape and perimeter effect the load to be mobilised by the anchor.

2.7 A BRIEF REVIEW ON SUCTION ANCHORS

Mackereth (1958) was the first to use a suction anchor for fastening a piston corer during a sampling operation in soft soils. Goodman et al (1961) carried out a model test study to determine the pull-out resistance of an inverted cup-type anchor subjected to different vacuum pressure in moist soils (sand, silt and clay), demonstrated that vacuum anchorage in moist soil is feasible and considered the application for military field equipment. Rosfelder (1966) considered the use of hydrostatic pressure to perform work for anchoring purposes in the marine application. Etter and Turpin (1967) studied underwater suction anchors for manoeuvring a small rescue vehicle to achieve a hatch-to-hatch union with an abandoned submarine and considered that a suction anchor is not only a feasible solution to this particular anchoring problem, but perhaps the only possible solution. Tudor (1967) and Chmelik (1968) showed increasing interest towards the development of a new anchoring system which would possess a high degree of mobility relative to break-out resistance. Al-Awadi (1971) performed his studies on 'sheet-and-slab' and 'cut-off-wall-and-slab' type model suction anchors of different base area under laboratory conditions. Brown and Nacci (1971) investigated a cup-type model anchor for the development of a short term high efficiency underwater suction anchor, tested it in a granular soil and reported the basic components and construction of the anchor. Lewis (1971) reported that a suction anchor had been used successfully for obtaining a vertical reaction for bottom coring platforms which were operated on marine cohesive soils. Baird and Nacci (1972) used triaxial tests to simulate actual failure conditions on laboratory sedimented kaolinite clay and silt for the investigation of shear strength parameters applicable to predict ultimate pull-out forces on a hydrostatic anchor. During 1972, Shell attempted to use a 2.7 metre diameter suction anchor to develop a reaction force for pushing instruments into sandy seabeds and their equipment was designed to accommodate a cone penetrometer which could be jacked into the soil through the centre of the anchor. Valent et al (1973) performed tests for preconsolidation on cohesive soils for seafloor foundations while using a suction anchor. Schofield (1974) proposed a different type of surface attachment anchor which included an anchor structure built of interconnecting beams and covered by an extended impermeable sheet. The sheet is probably a very useful part for increasing the anchor pull-out resistance. Wang et al (1975) performed a detailed study on model suction anchors varying in diameter from 114 to

337 mm. Helfrich et al (1976) observed directly the failure mode of the suction anchor and provided additional test data on a 400 mm suction anchor which was tested in submerged sand. Wang et al (1977, 1978) extended their study and developed a general break-out capacity equation which provided a method of assessing the value of an anchor by predicting the anchor capacity from anchor geometry, suction pressure intensity and soil properties. Wilson and Sahota (1977, 1978) performed studies on inverted cup-type and hemispherical-type suction anchors with jets added for embedment and conducted their experimental investigation in the laboratory and at sea in cohesionless soils. The excessive water present in the close vicinity of the anchor, due to jetting, was extracted through the filter of the anchor by using a pump and this extraction of water restored the strength of the disturbed soil.

Two theories will be considered for determining break-out force of an inverted cup-type suction anchor. The theories were proposed by Brown and Nacci (1971) and Wang et al (1977 and 1978). As far as the author knows there is no theory in existence which takes into consideration the behaviour of an embedded suction anchor.

2.7.1 Brown and Nacci (1971) Theory: (Fig. 2.9)

Brown and Nacci (1971) considered a hydrostatic anchor placed on the seabed. They suggested that in addition to the pressure forces, several body and friction forces would act on the anchor. A force balance on the anchor yields the following equation:-

$$F_b = W_a + W_p + F_{so} + F_p \quad \ldots\ldots\ldots\ldots\ldots\ldots (2.34)$$

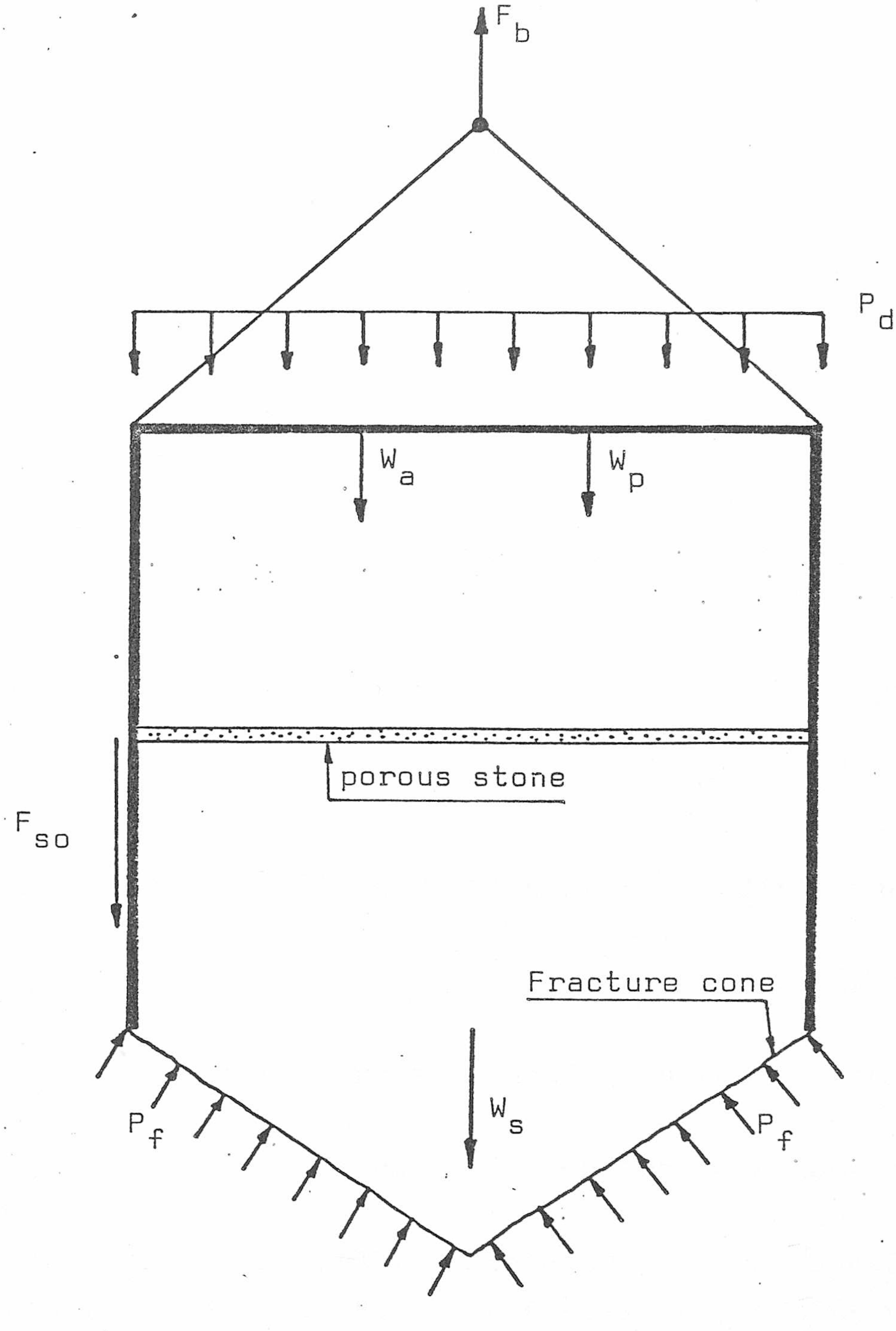

Fig. 2.9 Brown and Nacci Theory: Forces on hydrostatic anchor and fractured sediment cone.

where F_b = break-out force

W_a = buoyant weight of anchor

W_p = buoyant weight of pump

F_{so} = shear forces between the soil and the anchor skirt surface

F_p = force resulting from the pressure difference

Later, they added the forces which act on the fracture cone during anchor break-out. The force equilibrium now becomes:

$$F_b = W_a + W_p + W_s + F_{so} + F_s \quad \text{..............(2.35)}$$

where W_s = buoyant weight of soil

F_s = force resulting from the pressure difference

and $$F_s = \frac{\pi B^2}{4}(p_d - p_f) \quad \text{........................(2.36)}$$

where p_d = hydrostatic pressure acting on top of the anchor.

p_f = average pressure acting on fracture cone surface.

Brown and Nacci (1971) concluded that the anchor developed resistance to pull-out forces by the differential pressures developed by pumping. Further, they added, "the anchor provides an effective means for short-term anchorage on sands and provides a high holding power to anchor weight ratio".

2.7.2 Wang, Demars and Nacci's (1977 and 1978) Theory: (Fig. 2.10)

Wang et al (1977) considered the break-out resistance of an anchor by estimating all vertical forces which act to maintain static equilibrium. Forces which act on the anchor are shown in Fig. 2.10 and include the break-out force Q_u, the buoyant weight of the anchor W_a, the buoyant weight of the attached soil wedge W_s, the friction and adhesion F along exterior wall surface, and the resultant of vertical intergranular pressure $\sigma_{3f'}$ over the area A of the time of failure. Force equilibrium yields:

$$Q_u = W_a + W_s + F + A\sigma_{3f'} \quad \ldots\ldots\ldots\ldots\ldots\ldots (2.37)$$

where $\sigma_{3f'} = \sigma_{1f'}\tan^2\alpha' - 2c'\tan\alpha' \quad \ldots\ldots\ldots\ldots (2.38)$

$$\sigma_{1f'} = K_o\sigma_o' \quad \ldots\ldots\ldots\ldots\ldots\ldots\ldots\ldots\ldots\ldots (2.39)$$

and $\alpha' = (45^o - \varphi/2) \quad \ldots\ldots\ldots\ldots\ldots\ldots\ldots\ldots (2.40)$

Further, they proposed a general equation for the anchor capacity per unit area:

$$q = q_o + \lambda\Delta p \quad \ldots\ldots\ldots\ldots\ldots\ldots\ldots\ldots\ldots\ldots\ldots (2.41)$$

where q_o = anchor capacity at no-pump condition

λ = slope per linear relationship between anchor capacity and suction.

and $\Delta p = p_a - p_s$ = suction pressure

Wang et al (1978) contributed a basis for anchor design for practical applications and put forward a

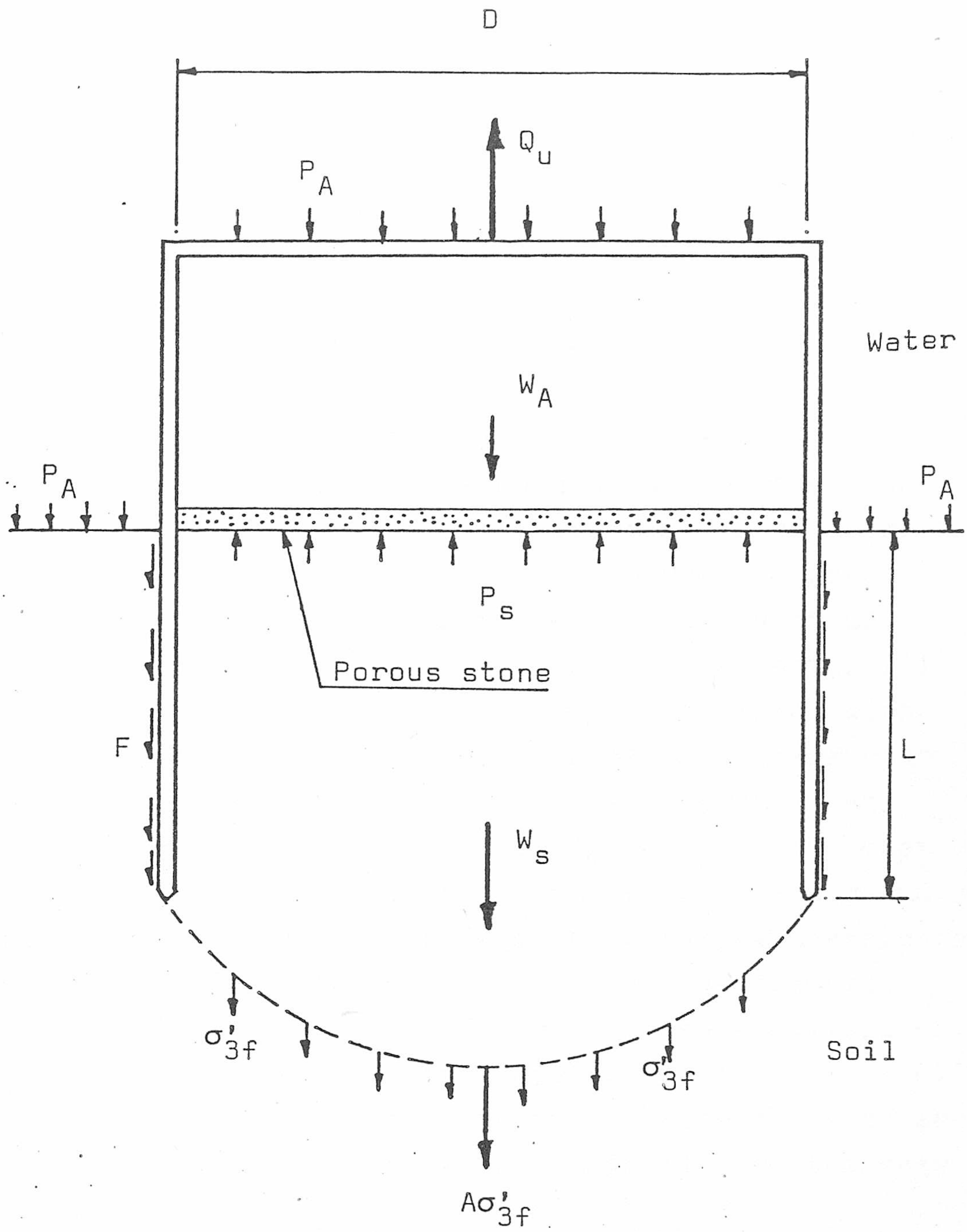

Fig. 2.10 Wang et al Theory: Force components on a test anchor

general equation for net break-out capacity:

$$q_{net} = q_o + \lambda\Delta p \quad \text{.........................} (2.42)$$

2.7.3 Discussion on the Experimental Investigations

Brown and Nacci (1971) conducted 14 tests in loose sand and 15 tests in dense sand on a 254 mm diameter inverted cup-type suction anchor. Laboratory tests exhibited that the suction cavity pressure was within 5 percent of the pressure on the base of the porous stone. The fracture cone had an angle of about 20 to 30 degrees to the horizontal, but in some cases only a partial cone was observed. Tests which were performed at low suction pressure did not exhibit the conical failure pattern, in fact, the skirt cavity was only partially filled with soil after break-out. If the ratio of anchor diameter to skirt embedment is constant (B/L = Constant), an increase in the anchor diameter would increase the mass of the failure cone as a function of the cube of the diameter, whereas, the force resulting from the pressure difference increases as a function of the square of the diameter. Therefore, for a given B/L and given pressure difference, the break-out of small diameter anchors would be controlled by the pressure difference force and the break-out of large diameter anchors would ideally be controlled by the mass of the failure cone.

Helfrich et al (1976) performed tests on a 400mm suction anchor buried in medium to fine sand and found pull-out force to be linearly related to the suction pressure. The maximum pull-out force and the weight of sand pulled-out were directly related to the flowrate, which was an easier parameter to measure than the suction pressure. Despite the difference in L/B ratio, the rate of pumping possibly may contribute to the development of either a local-shear or a conical-shear failure surface.

Wang et al (1975, 1977 and 1978) concluded that the break-out force reached a peak at almost the same vertical displacement for all anchors tested in sand, silt and clay, however, a greater displacement was required to reach the peak break-out force for the long-skirt anchors than the short-skirt anchors. The peak force diminished faster for the short-skirt anchors than for the long-skirt in all test soils. The soil wedge remained in the shape of an inverted cone having its base at the tip of the anchor wall with a cone angle of approximately 30^o in sand, and for silt and clay the soil wedge did not have a shape as regular as that of sand. When tested on medium fine sand, silt and clay, the anchor capacity appeared to vary uniquely and linearly with suction pressure for constant anchor diameter to skirt ratio and increasing angle of friction of the test soil. They also concluded on the basis of the study that short-skirt anchors are more effective in cohesionless soils, whereas in clay long-skirt anchors are preferable. Further, they concluded that there are several factors governing the performance of suction anchors: anchor geometry (diameter and skirt length), soil properties (internal friction angle, and cohesion) and suction.

Wilson and Sahota (1977) concluded during their investigation into deep burial that the inverted cup-type model anchor was affected by buoyancy during jetting and was floating in the fluidized sand. They confirmed this by fluid pressure and vertical force measurements on models which revealed that the uplift was due to the difference in pressure gradient between the clear water inside the anchor and the fluidized sand passing from the jets up the outside of the anchor. On their 600 mm cup anchor, a large plug of soil was extracted from the seabed when break-out occurred, and this was held by the anchor as long as suction was maintained.

Wilson and Sahota (1978) studied buried suction anchors and stated that deeply-embedded suction anchors have certain features in common with buried plate anchors. Considered in this context the new parameter introduced was the reduction in pore pressure in the surrounding soil and the influence of this pressure on the force required for pull-out. All pull-out tests were performed after anchor embedment had created a pit of disturbed soil within a region of naturally consolidated material. Further, they concluded that the extent on the application of anchor suction and the relative contributions made by applied suction and overburden require further exploration by extension of the range of suction pressures and burial depths.

Most of the suction anchors considered by the investigators are surface attachment anchors and, to-date, very few anchors exist as embedment suction anchors.

2.8 COMMENTS ON THE FOREGOING THEORIES AND EXPERIMENTAL WORK

Fig. 2.11 and Fig. 2.12 are taken from Meyerhof and Adams' (1968) paper and show a comparison of theory with model tests and full-scale tests for footings in sand. The test results show a wide scatter of points which the authors say is to be expected due to the different types and densities of sand used.

Fig. 2.13 shows the plot of break-out factor $\overline{N}_q$/relative depth $D/_B$ which belongs to Vesić's (1971) paper and indicates the expected trend of increase of break-out factors with depth only at shallow depths. There is a characteristic relative depth, $D/_B$ for each soil, beyond which the anchor footing starts behaving as a deep anchor and beyond this the final values of break-out factors

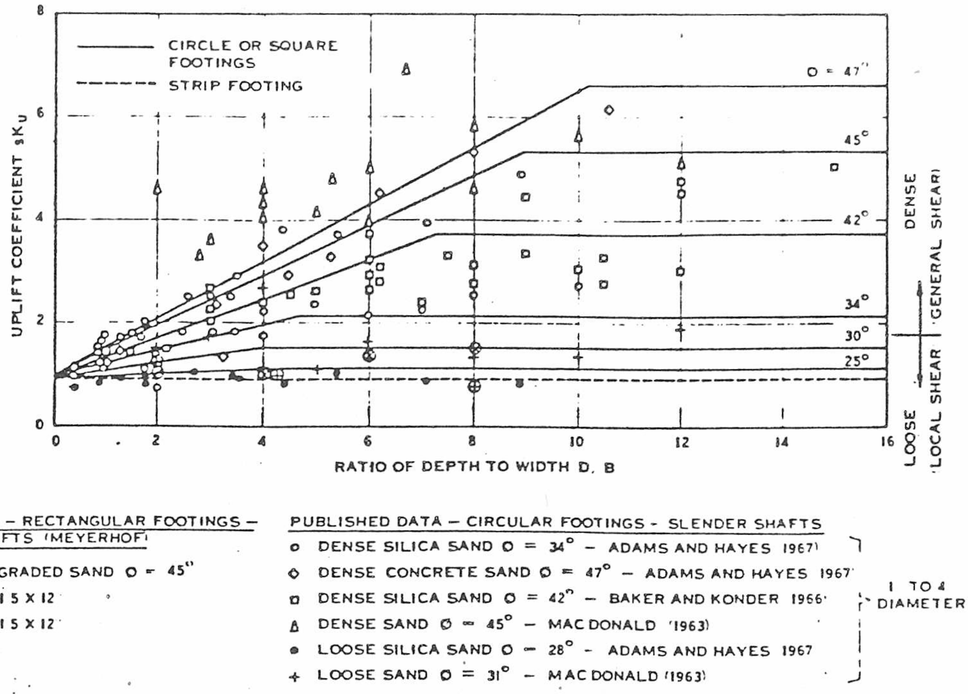

Fig. 2.11 Comparison of theory and model tests for footings in sand - Meyerhof and Adams (1968)

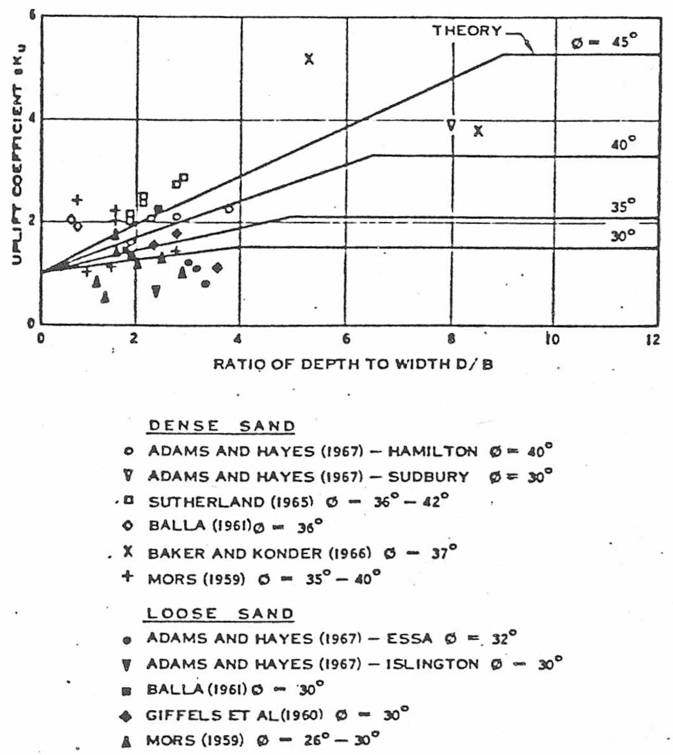

Fig. 2.12 Comparison of theory and full-scale tests in sand - Meyerhof and Adams (1968)

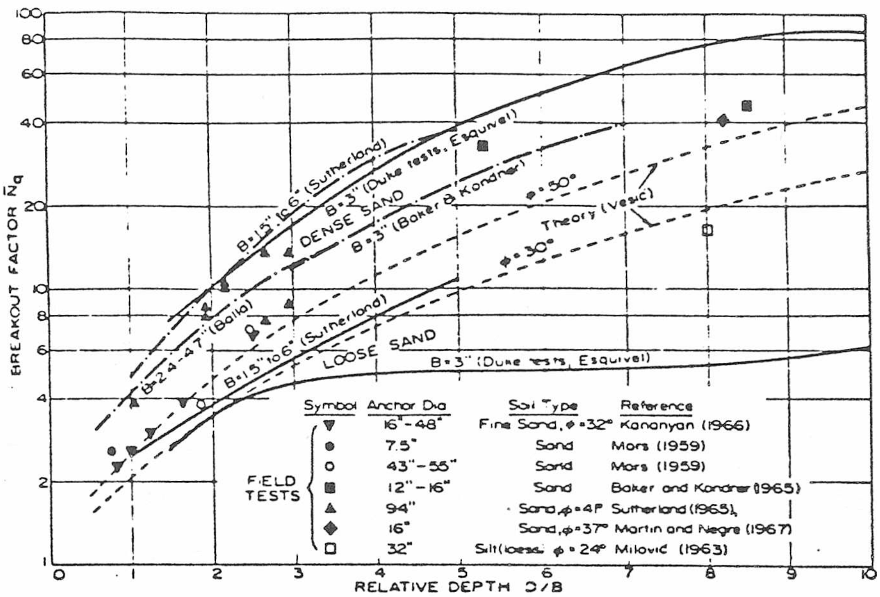

Fig. 2.13 Break-out factor $\overline{N}_q$ in sands - Vesić (1971)

become constant. This value of relative depth for sands increases with relative density from about 3 for loose sands to over 10 for dense sands. Observations show that the absolute magnitude of observed break-out factors does not agree with theory. The difference is most pronounced in dense sand where the observed factors are over 100% higher than the theoretical ones.

Examination of the published work indicates that a direct comparison can be made between the test results using the parameters proposed by the various investigators for a specific problem of the ultimate uplift force. Fundamental properties affecting the soil behaviour are still ignored, such as the change in density and stresses due to installation.

The development of finite element technique appears to be very useful in the soil mechanics field and it may provide the right solution.

CHAPTER 3

TEST ANCHORS AND EXPERIMENTAL INVESTIGATION

3.1 INTRODUCTION

It has become apparent that there are many parameters involved in any anchor pull-out test. The tests may be conducted in at least two ways, firstly by performing a small number of tests and recording every possible parameter for each of test and secondly, by performing a large number of tests and recording the information as the tests progress gradually.

Pull-out investigation of the test anchors was conducted initially in a relatively simple manner, before moving on to the instrumented anchor tests. The initial tests were performed on a 145 mm self-burying suction anchor embedded at various depths in the submerged sand in the testing tank. It became clear from the investigation that a number of suction anchors and solid anchors were needed to draw a satisfactory conclusion about the break-out performance of a suction anchor. In all six model anchors and one prototype suction anchor were fabricated.

The principles and physical details of the hemispherical anchors are outlined below. The test apparatus and the properties of the soil are briefly discussed. 476 tests were performed on the various types of model anchors in the laboratory and 11 tests were also conducted on a 600 mm suction anchor at sea. 296 tests on model anchors are tabulated in Appendix 1. All the tests were performed under a vertical load and control of anchor displacement.

Anchor pull-out force or resistance is the maximum force produced by the anchor during the pull-out and it does not include the submerged weight of the anchor but includes the skin friction force mobilised by the anchor shaft.

3.2 PRINCIPLE OF THE HEMISPHERICAL SUCTION ANCHOR

Water under pressure is supplied to a system of water jets through a jet supply line and is shown in Fig. 3.a. The anchor can be bu-ried in a cohesionless soil bed by using the pressurized water jets which fluidize the soil bed sediments underneath and around the anchor. The desired burial depth of the anchor is achieved by forcing the underlying soil particles to move upward as shown in Fig. 3.b. Once the required embedment depth is achieved the water supply to the jets is cut-off and suction is applied from the suction line. Water is extracted from the annular suction cavity, which reduces the pressure in the anchor cavity, then the porewater pressure in the surrounding soil, and the continuation of dewatering reduces the volume of water present in the fluidized soil. The strength of the cohesionless soil can be restored within a short period by means of de watering and allows the anchor to be brought into almost immediate use. A further strength from the anchor can be achieved by means of supplying and continuing a further suction pressure which densifies the local soil close to the anchor as shown in Fig. 3.c. The anchor retains a soil plug around the suction cavity as long as the suction is kept on and the soil plug is shown in Fig. 3.d. after the anchor being pulled out from the soil bed.

3.3 DETAILS OF TEST ANCHORS

Model anchors above 100 mm were designed to resist a pull of 2.0 kN and below 100 mm the anchors were designed to take an uplift resisting force of 1.0 kN. A full-scale anchor was designed for an uplift force of 100 kN.

The physical parameters of the seven hemispherical anchors are shown in Table 3.1.

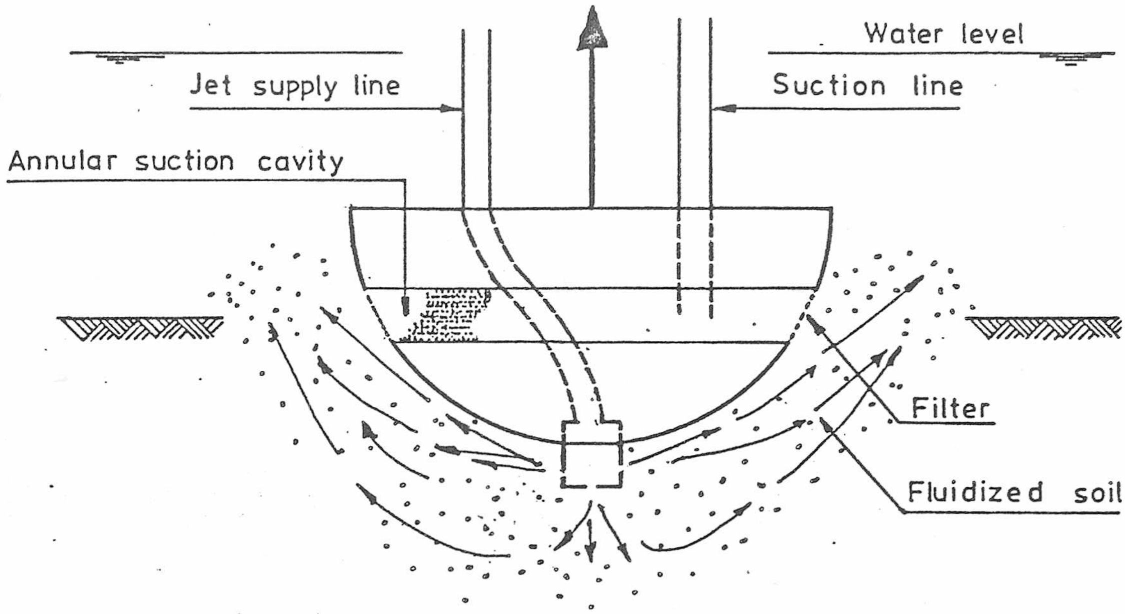

Fig 3.a Water jet supply only

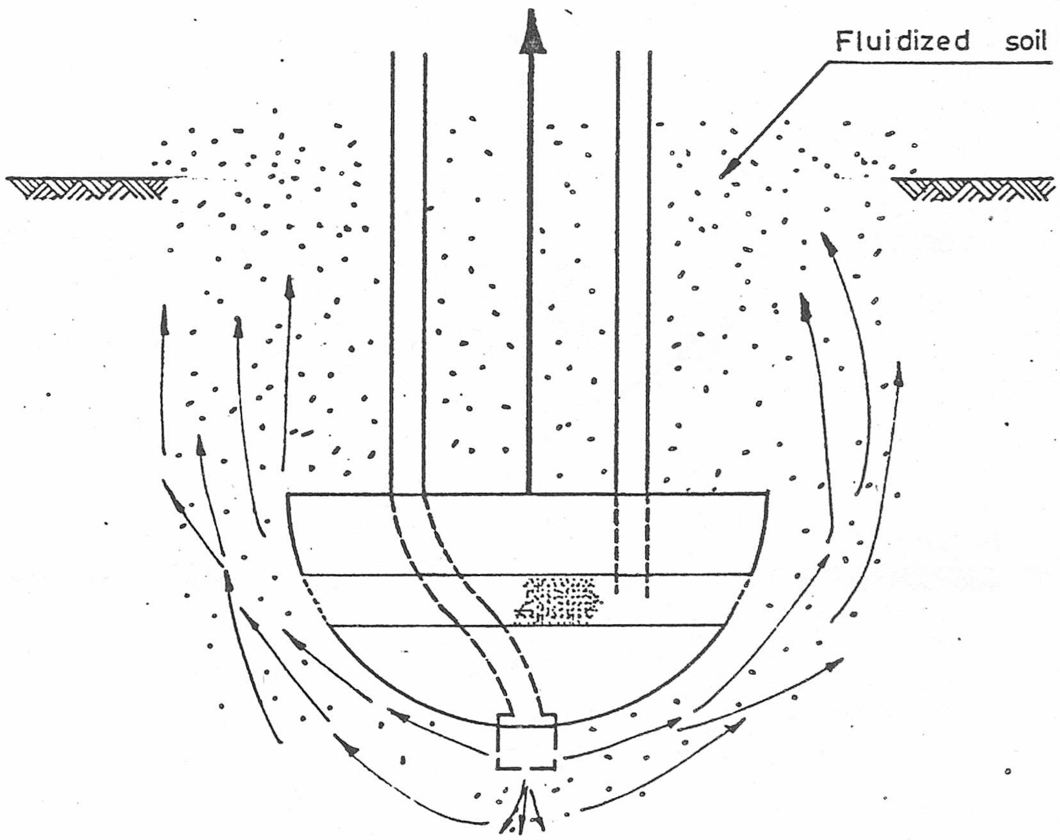

Fig. 3.b Further burial with jets only.

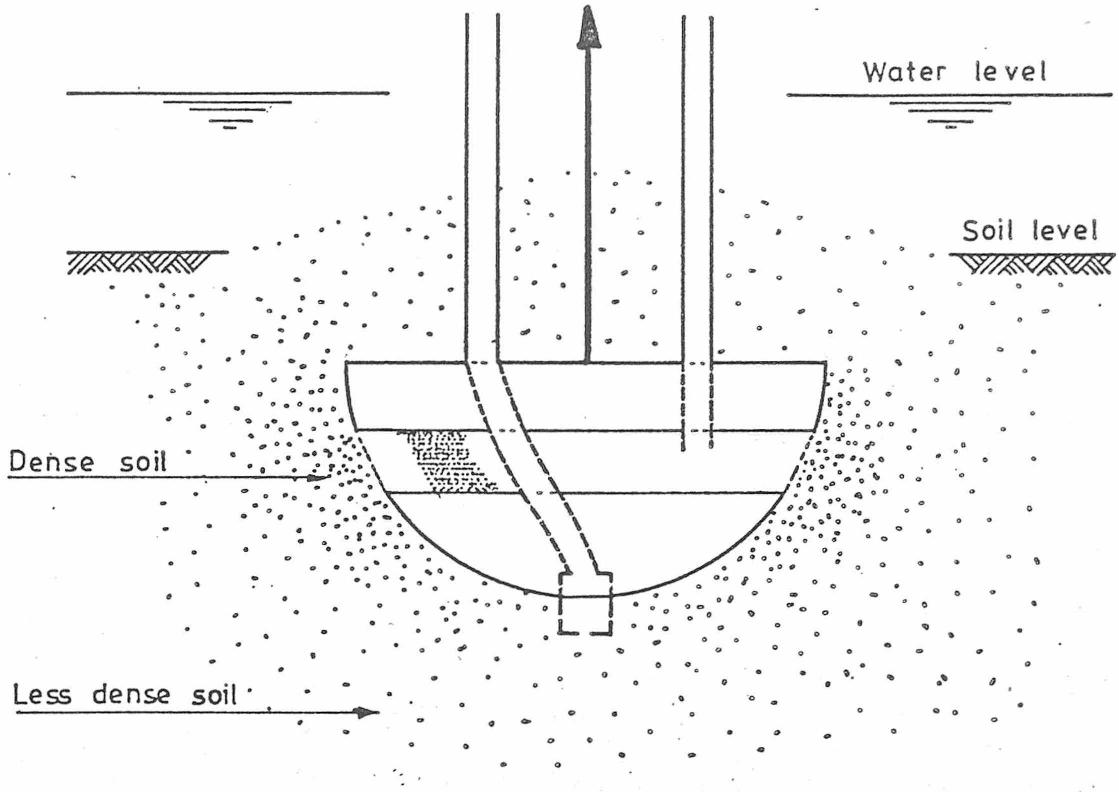

Fig. 3.c Pulling out with suction on.

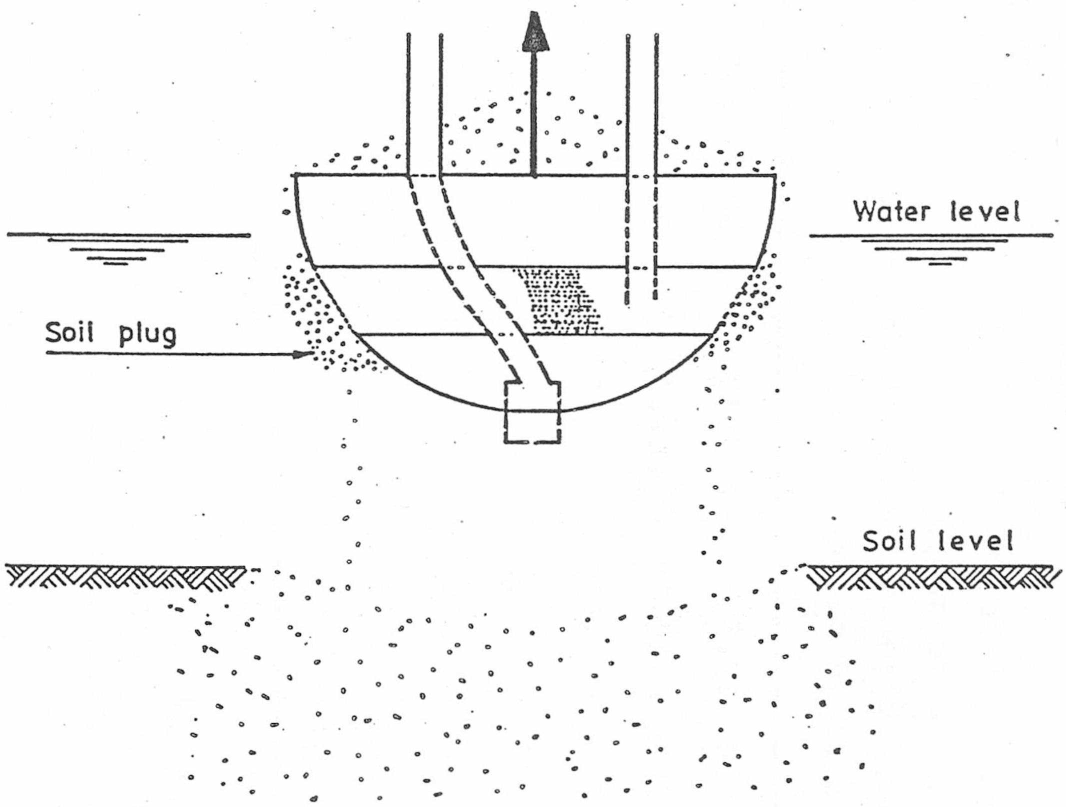

Fig. 3.d Soil plug retained after break-out.

Table 3.1 Physical parameters of the hemispherical anchors

S. No.	Anchor diameter (mm)	Weight in air (N)	Anchor plan area A (mm^2)	Suction filter perimeter (mm)		Suction channel width (mm)	Suction filter area, a (mm^2)	Filter size (μm)	Area ratio a/A	Filter area ratio	Fig. No.
				top	bottom						
1	70[a]	2.22	3849	0	0	0	0	-	0	0.0	3.1
2	70[b]	2.39	3849	216	181	14.04	2787	100	0.724	0.574	3.1a
3	70	2.88	3849	209	182	7.87	1539	100	0.40	0.317	3.2
4	102	7.43	8171	310	263	16.95	4856	100	0.594	1.0	3.3
5	108[c]	7.36	9161	0	0	0	0	-	0	0.0	3.4
6	145[d]	15.30	16513	358	196	35.0	9695	100	0.587	1.996	3.5-3.6
7	600	1512	282743	1430	910	123	143910	100	0.509	29.64	3.7-3.10

a: 70 mm solid anchor

b: 70 mm suction anchor with no pipes

c: 108 mm solid anchor

d: Wilson's anchor

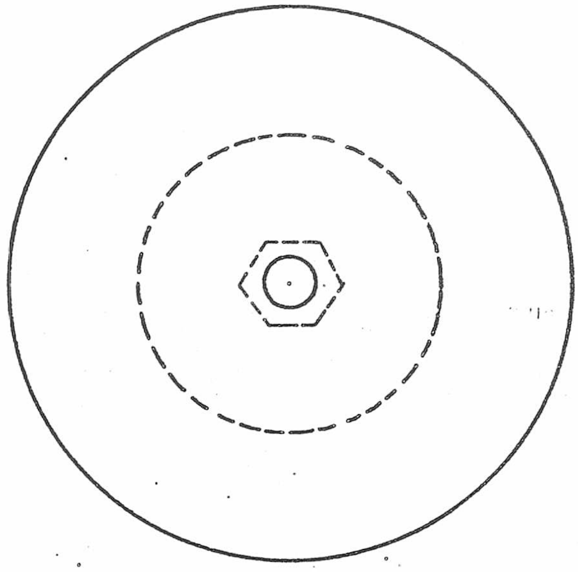

Scale 1:1

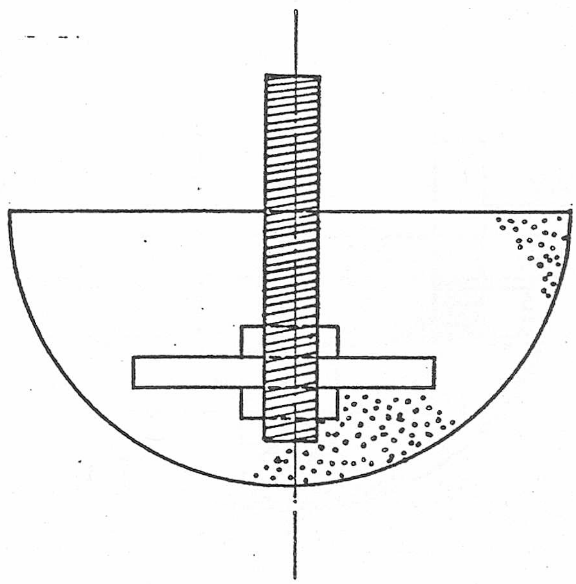

Fig. 3.1 Plan and section through the 70 mm solid anchor.

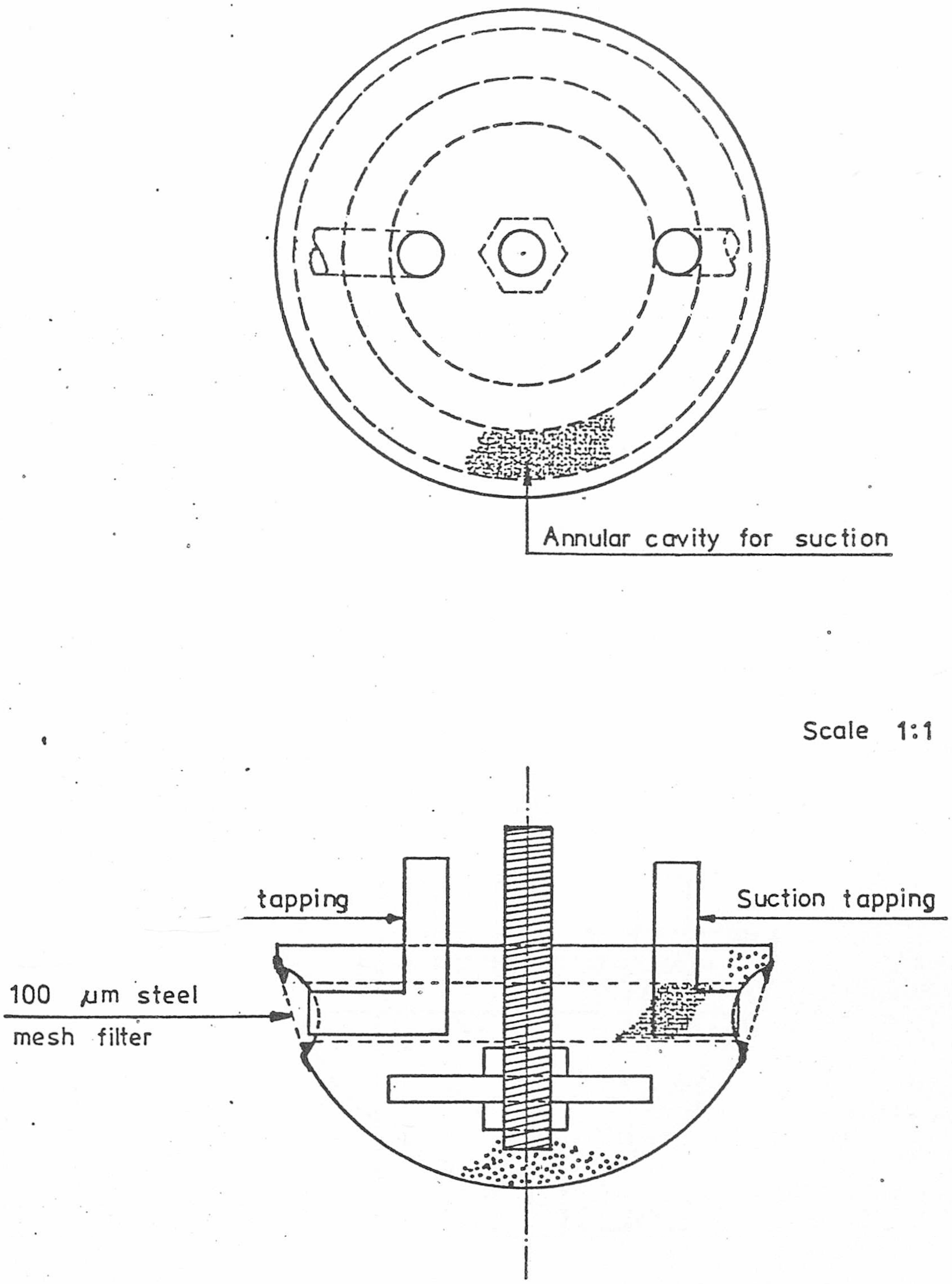

Fig. 3.1a Plan and section through the 70 mm suction anchor with a single suction tapping.

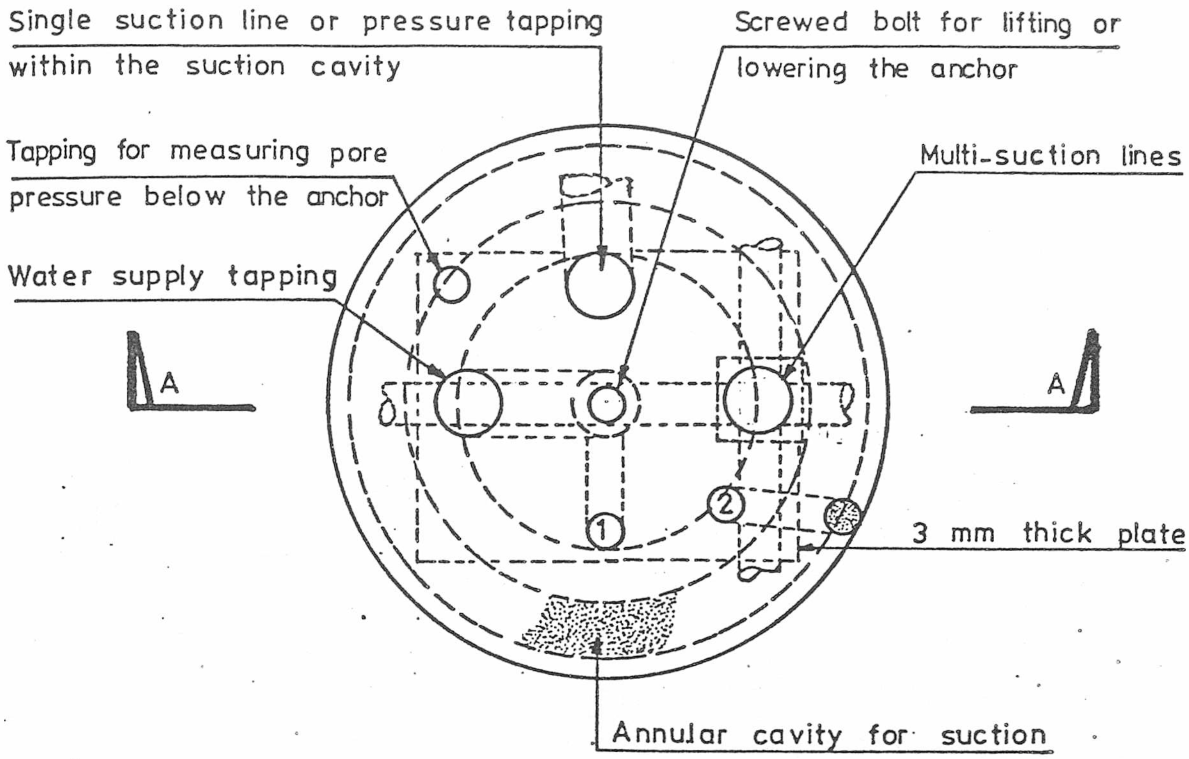

1. Tapping for measuring fluid pressure at the nozzle entry.
2. Tapping for measuring pore fluid pressure on top of the anchor.

Scale 1:1

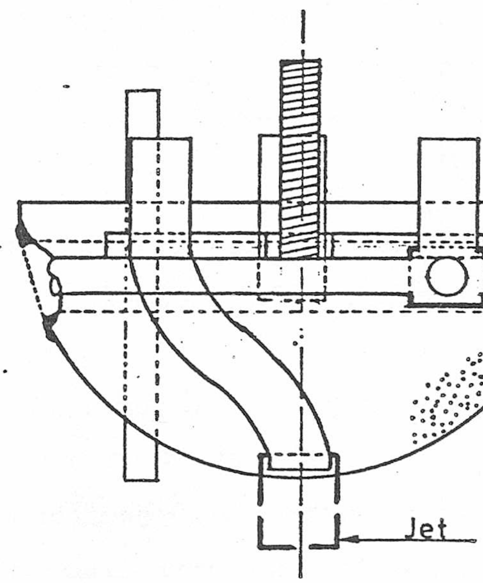

Fig. 3.2 Plan and section A – A through the 70 mm suction anchor with a multi suction lines.

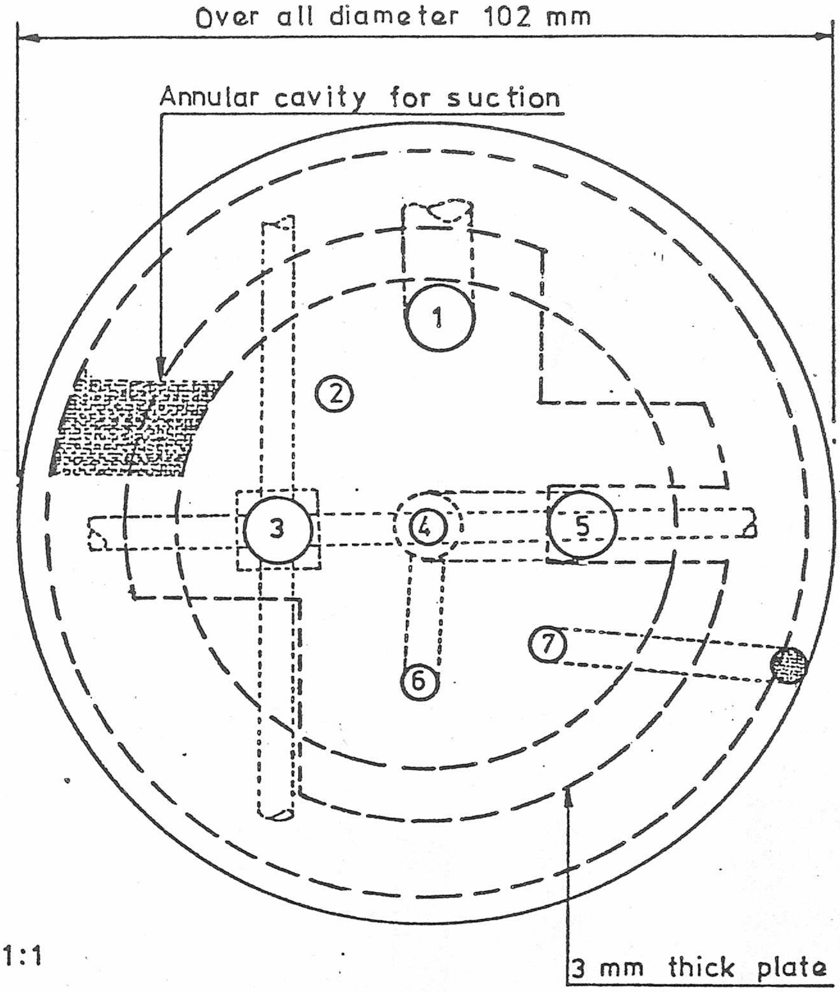

Scale : 1:1

1. Single suction line or pressure tapping within the suction cavity
2. Tapping for measuring pore fluid pressure beneath the anchor
3 Multi-suction lines
4 Screwed bolt for lifting or lowering the anchor
5 Tapping for water supply to jets
6 Tapping for measuring fluid pressure at the nozzle entry
7 Tapping for measuring pore fluid pressure on top of the anchor

Fig. 3.3 Plan on 102 mm suction anchor.

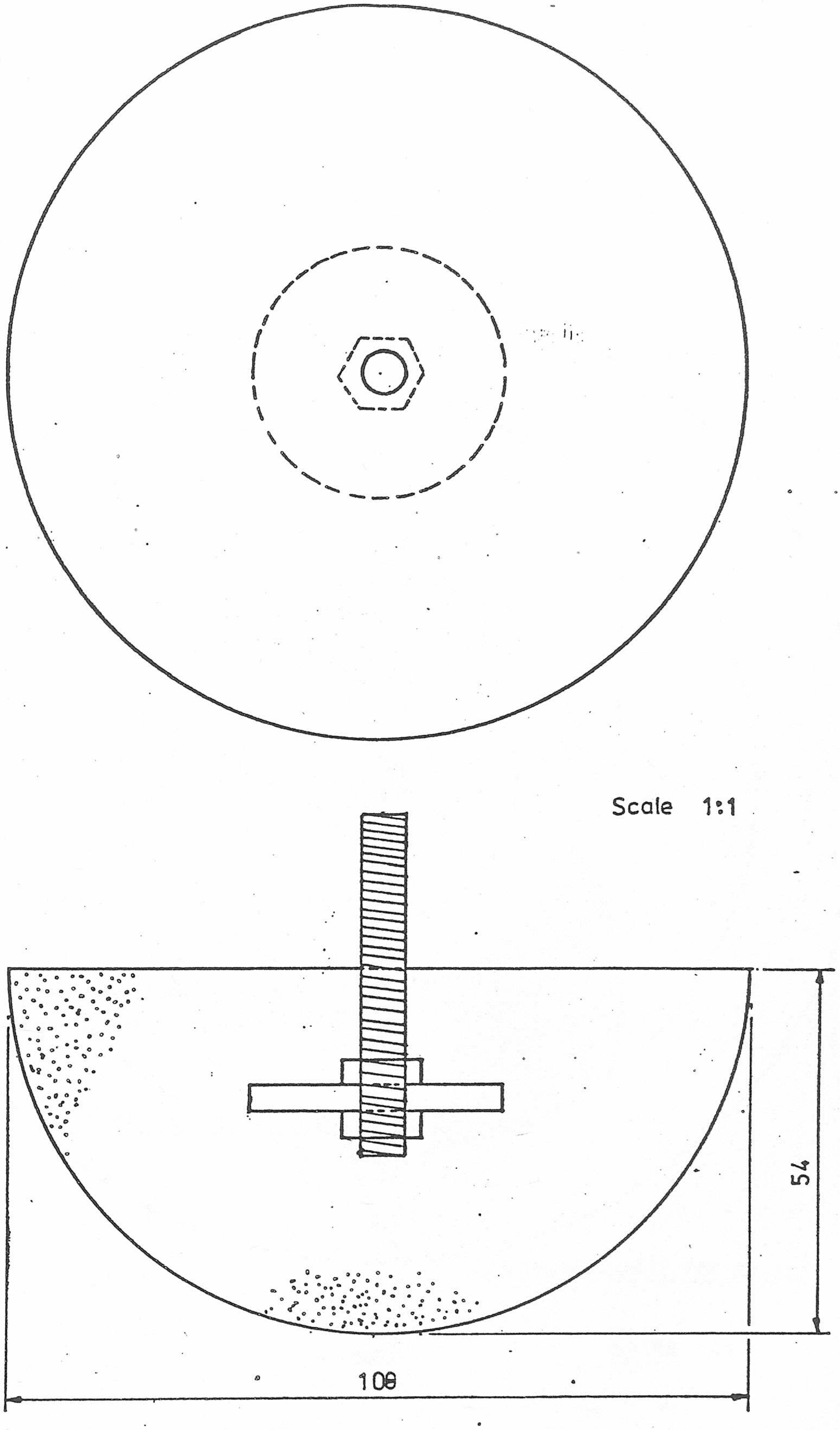

Fig. 3·4 Plan and section through the 108 mm solid anchor.

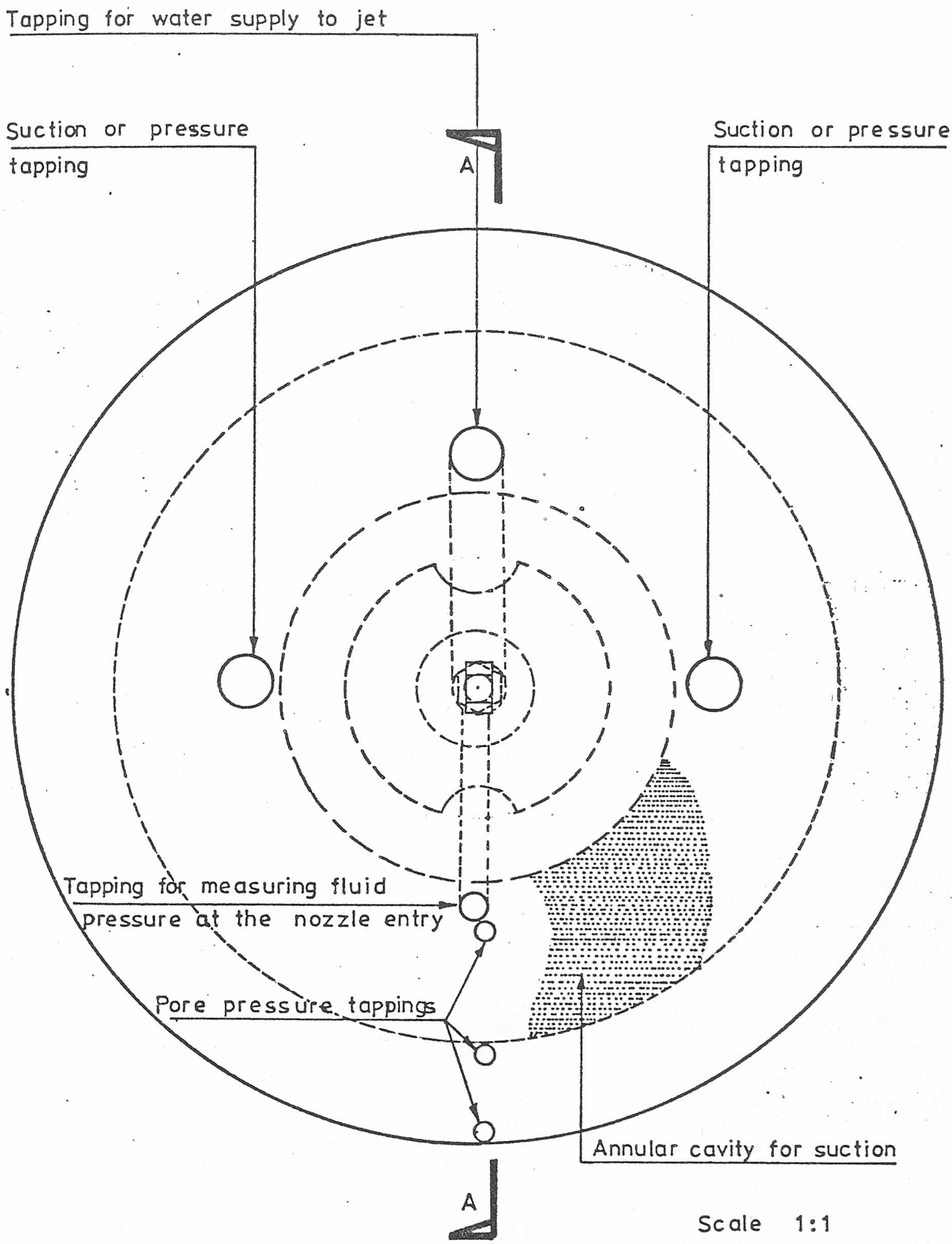

Fig. 3.5 Plan on 145 mm suction anchor.

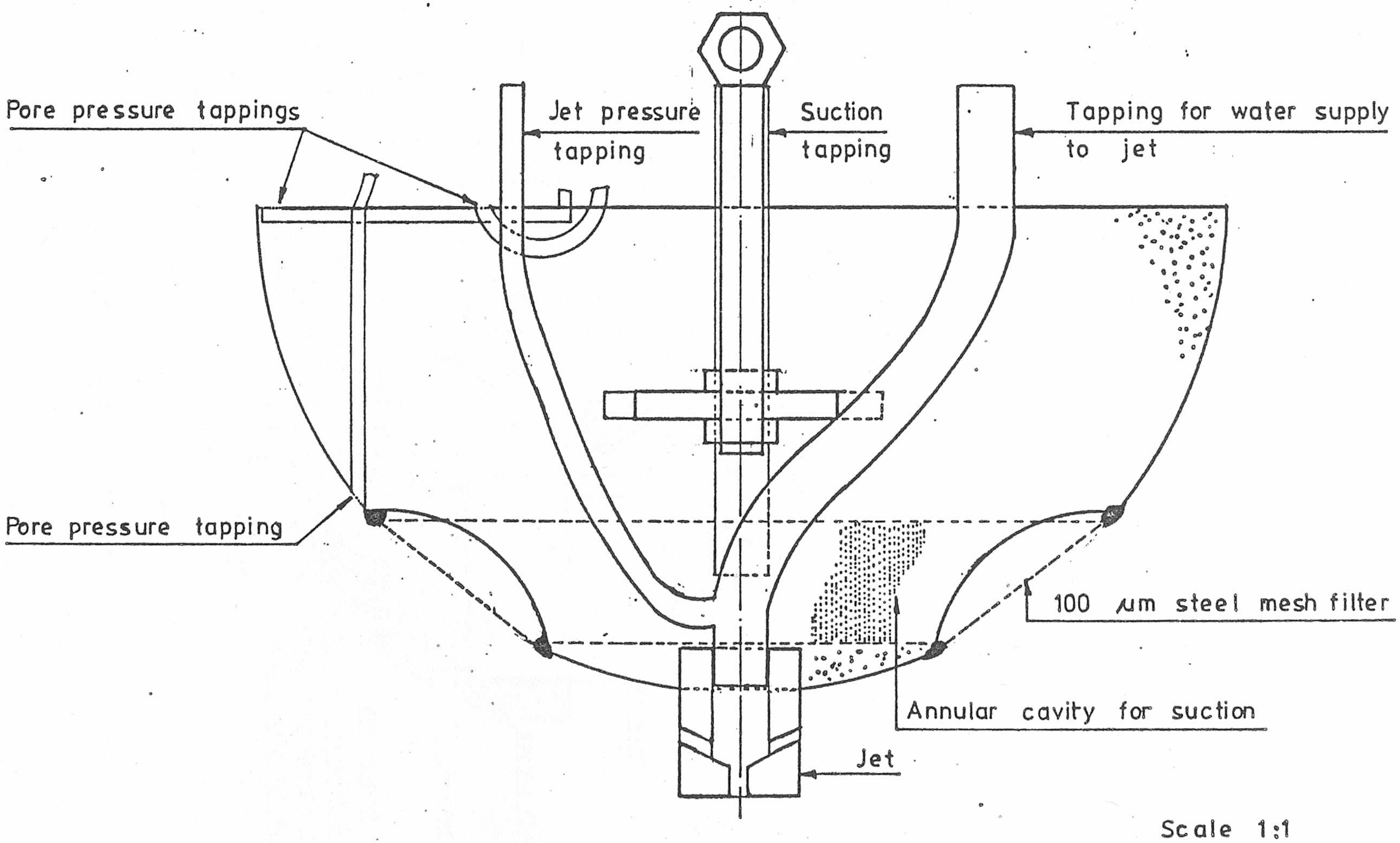

Fig. 3·6 Section A – A through the 145 mm suction anchor.

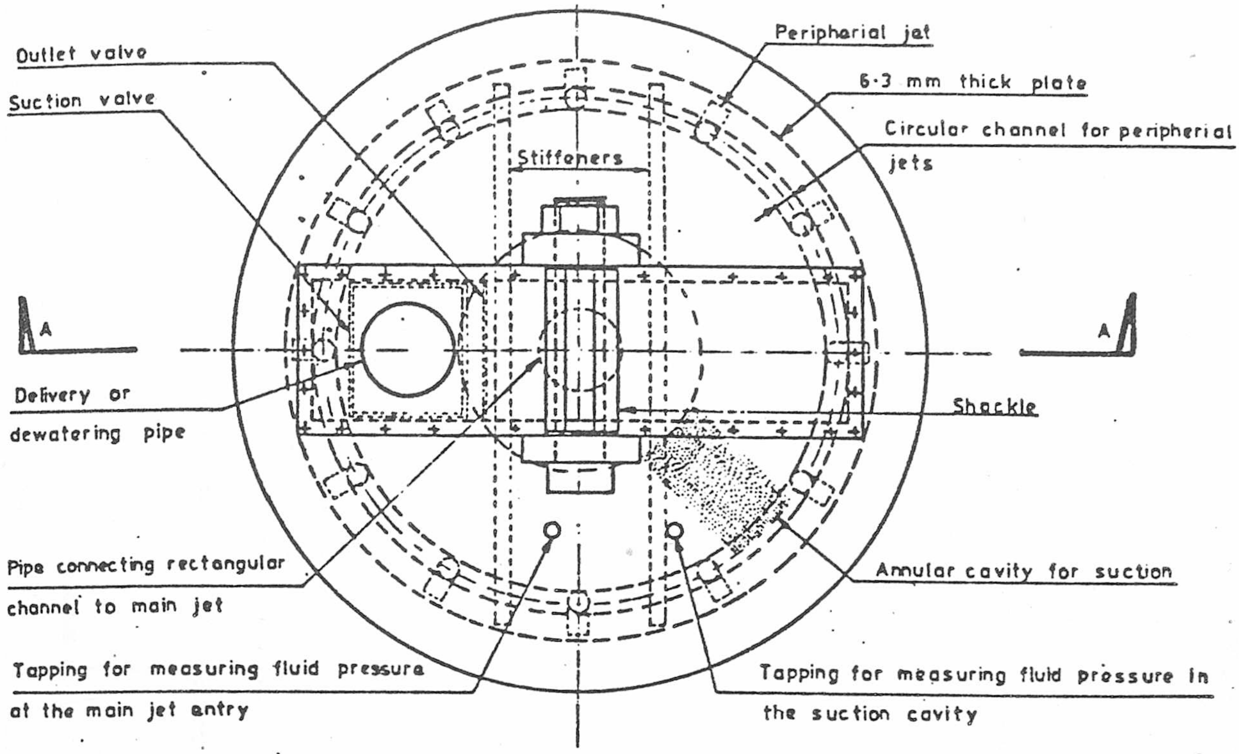

Fig. 3·7 Plan on 600 mm suction anchor

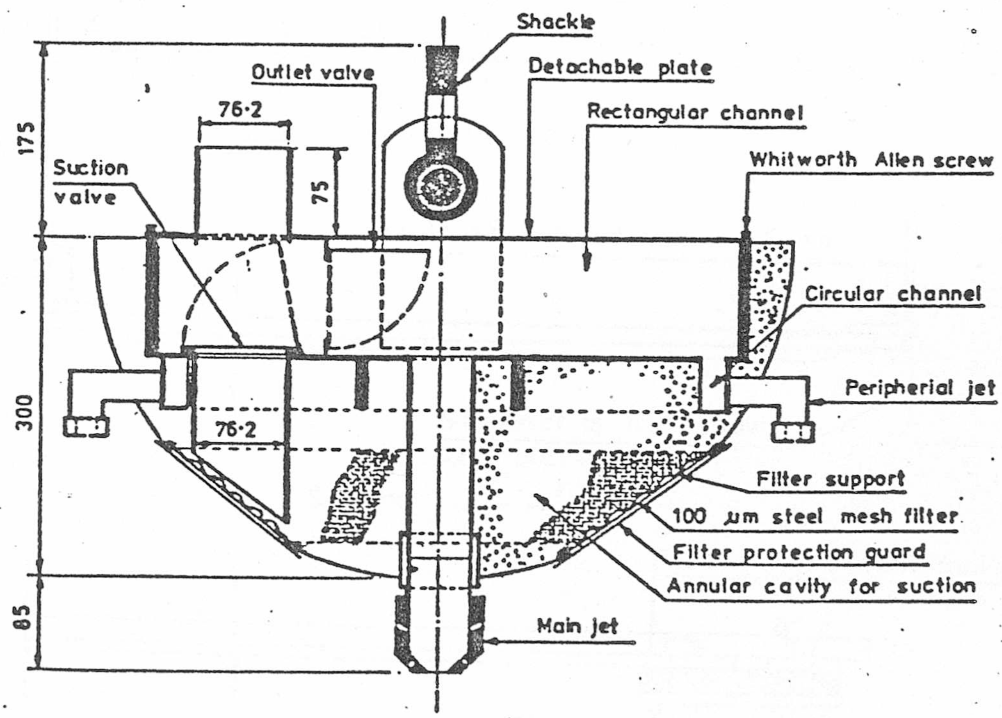

Fig. 3·8 Section A–A through the 600 mm suction anchor.

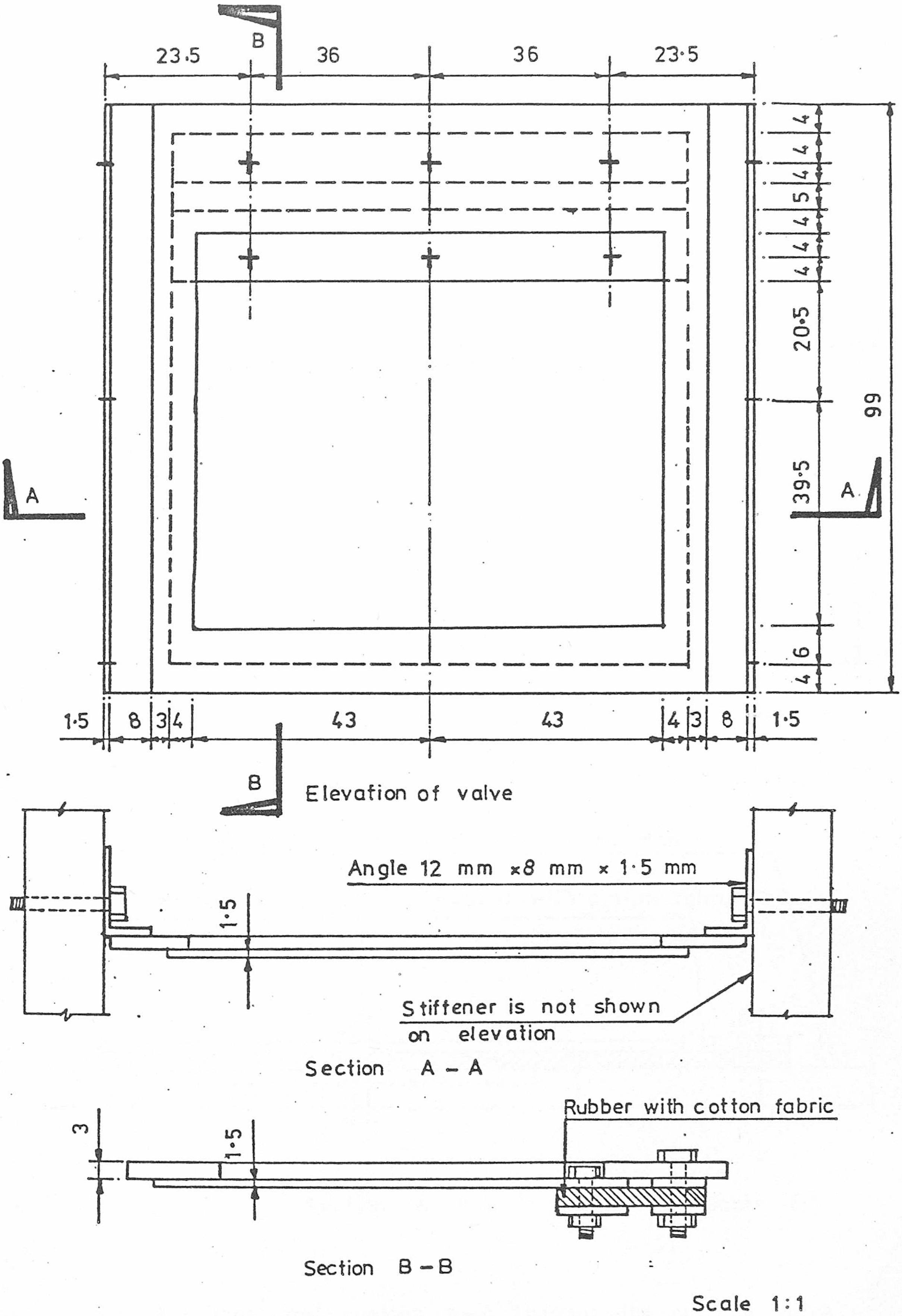

Fig. 3·9 Elevation and sections of the outlet valve.

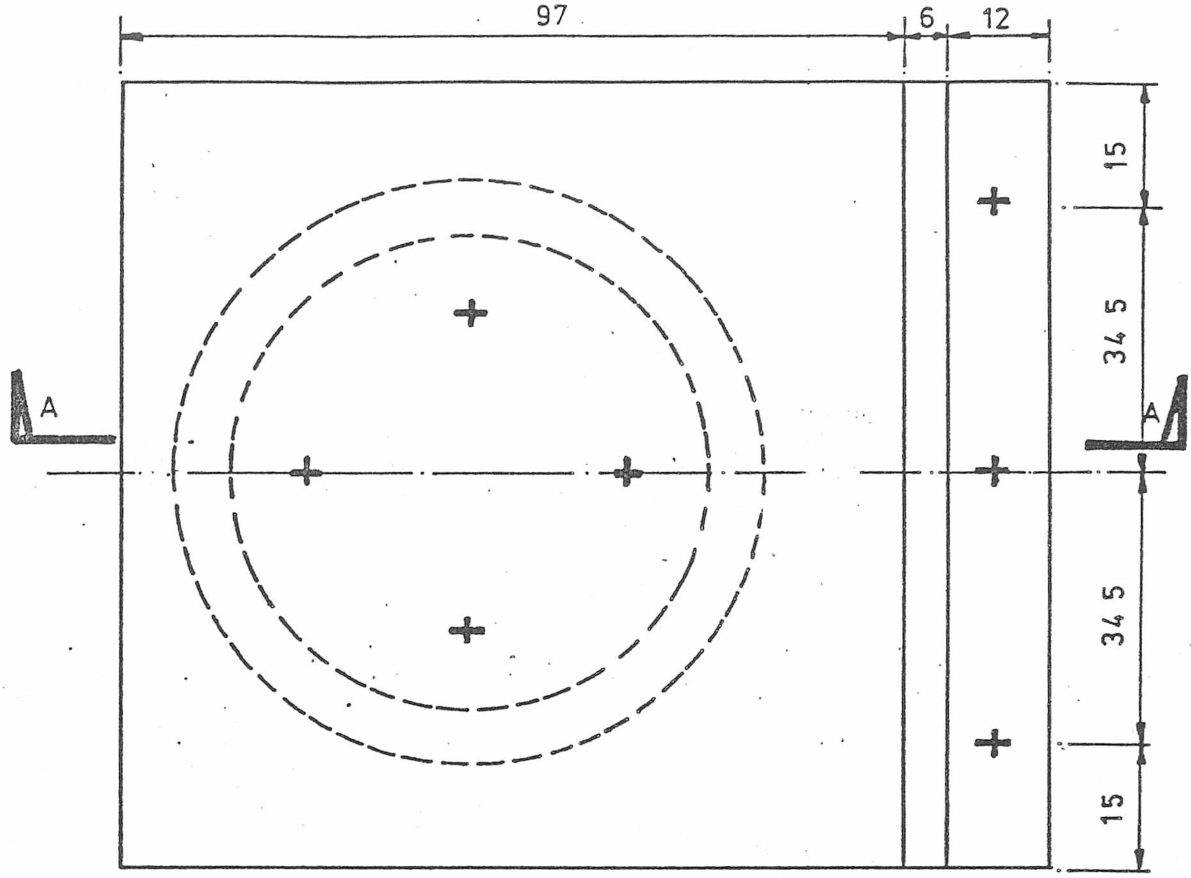

Plan on suction valve

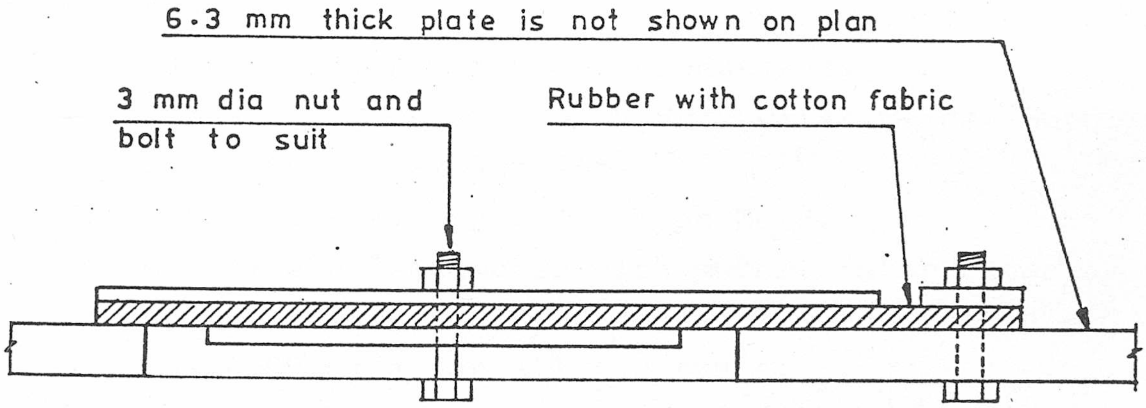

Section A A

Scale 1:1

Fig. 3·10 Plan and section A–A through the suction valve.

The materials used for model anchors were mainly brass and concrete. Mild steel and concrete were used to fabricate the full-scale anchor. The concrete mix was one part of cement and two parts of building sand. 100 µm steel mesh was used as a filter for all suction anchors.

3.4 DETAILS OF TEST APPARATUS

The experimental investigation of the break-out behaviour of suction anchors is sub-divided into two parts, firstly the model-scale and secondly the full-scale anchors. The apparatus used for model anchors and full-scale anchors is dealt with separately.

3.4.1 Test Apparatus for Model Anchors

The following test apparatus was used for the model anchors:-

1. Testing tank: An extended oil drum 850 mm deep by 750 mm wide with 40 mm of concrete screed layed inside on the bottom of the tank. Depth of sand beds before start and at the end of test programme were 645 mm and 630 mm respectively.
2. Pressurized water supply from water mains: Supplied water to the anchor jets.
3. Mono self-priming pump: Type ML/2.
4. Hounsfield Tensometer with motor: Motor capacity was 0.186 kW. Pull-out speed was controlled and was 0.60 mm/s for all the tests.
5. Rig with platform: It supported the Hounsfield Tensometer, motor and further loads in addition to its own weight.
6. Chain and 13.43 mm diameter stainless steel hollow pipe: Burial depth of the anchor was increased or decreased by adding or reducing the chain repectively. The stainless steel pipe was used as an anchor shaft and was sealed to air at the top end.

7. Force transducer: Generally the force transducer was calibrated to 600 N, checked for calibrations at the start and end of the test and finally calibrated to 1400 N at the end of the test series.
8. Dead weights: The weights were used to calibrate the load transducer.
9. Pressure transducers: Three pressure transducers were used for the 102 mm suction anchor programme. Each of the pressure transducer had a pressure range of 0 to 138 kN/m^2 and was calibrated with a water manometer.
10. Two chart recorders: Three pressures and one uplift load were automatically recorded. Each chart recorder had three channels.
11. Peekel type 581 DNH Universal Carrier Measuring Amplifier.
12. Stop clock: For some pull-out test series the time period was kept constant.
13. Heathkit regulated power supply and digital volt meter: The volt supply to pressure transducers was monitored by the power supply meter.
14. Vacuum gauge: The pressure range of the vacuum gauge was 0 to 100 kN/m^2.
15. Water measuring containers: The containers had a capacity of 20000 ml, 5000 ml and 2000 ml. They were used when determining the water flow through the suction filter of 145 mm, 102 mm and 70 mm suction anchors at a specific burial depth and suction pressure.
16. Locating plate with pressure probes: The anchor shaft and the pressure probes were guided by the locating plate.

Fig. 3.11 shows the photograph of all the model anchors, Fig. 3.12 and Fig. 3.13 represent the photograph of test setup. Fig. 3.14 shows the locating plate with anchor shaft and pressure probes.

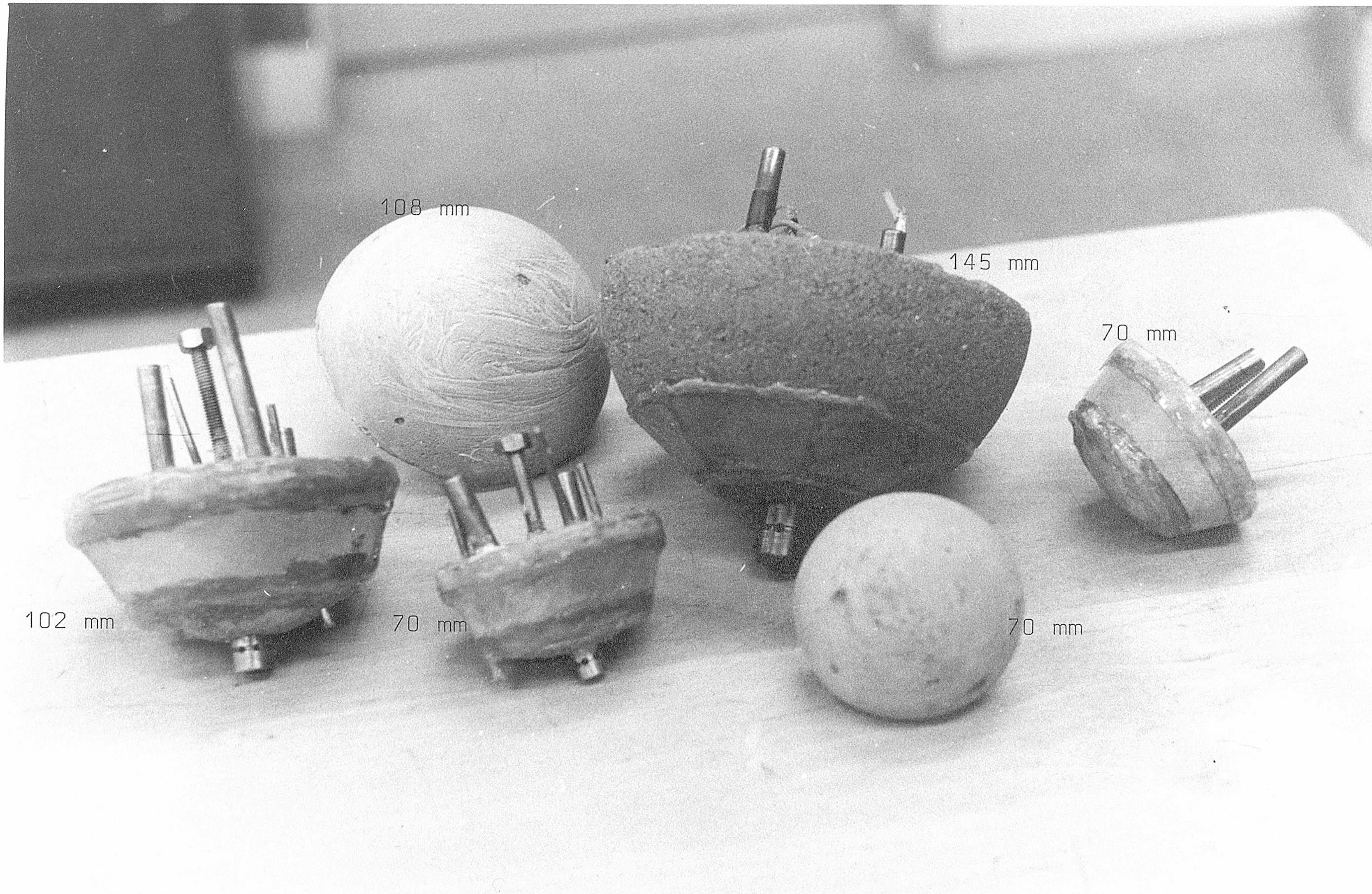

Fig. 3.11 Photograph of hemispherical solid and suction anchors.

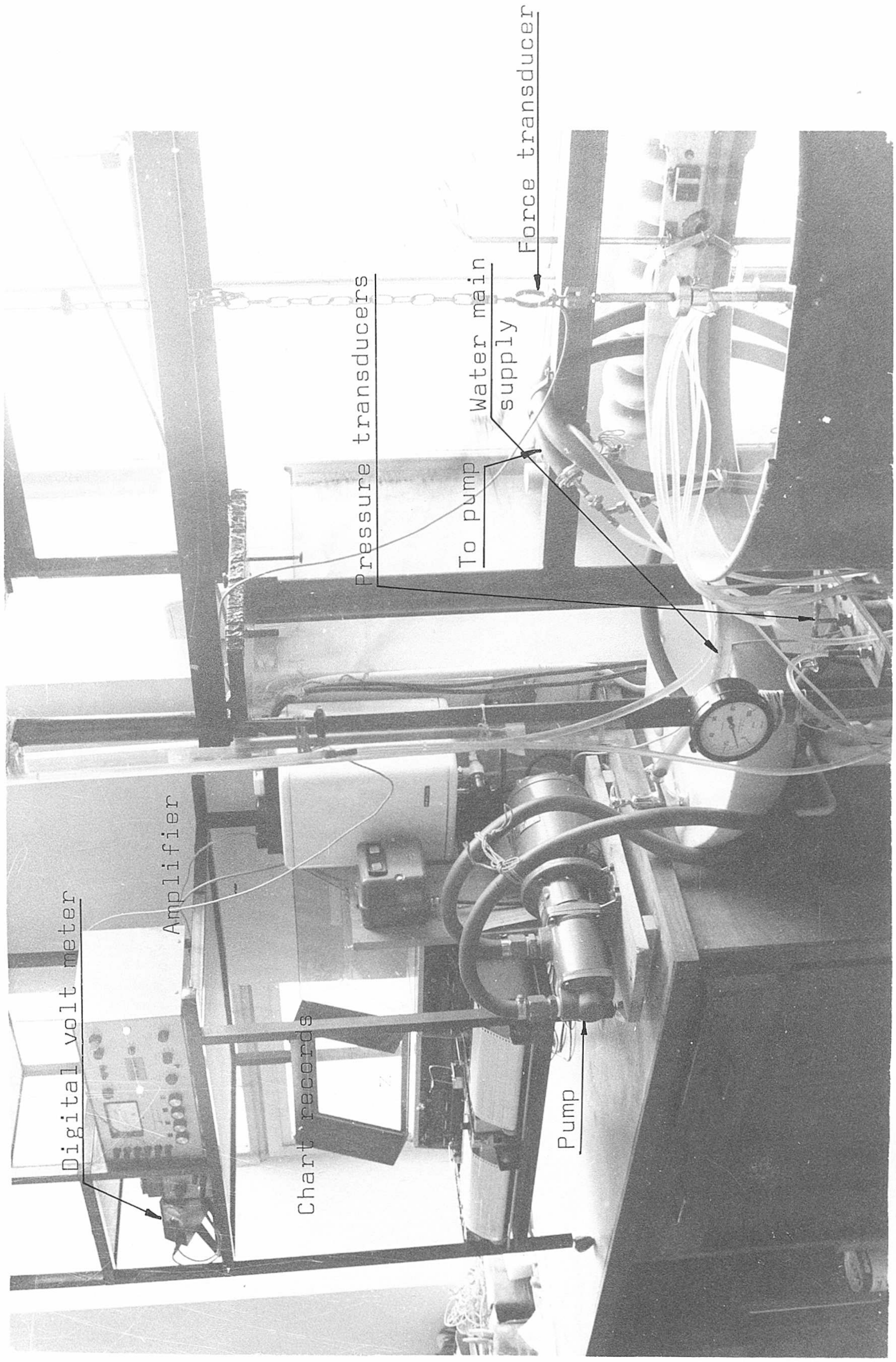

Fig. 3.12 Photograph showing details of test set-up excluding the Hounsfield Tensometer and the motor.

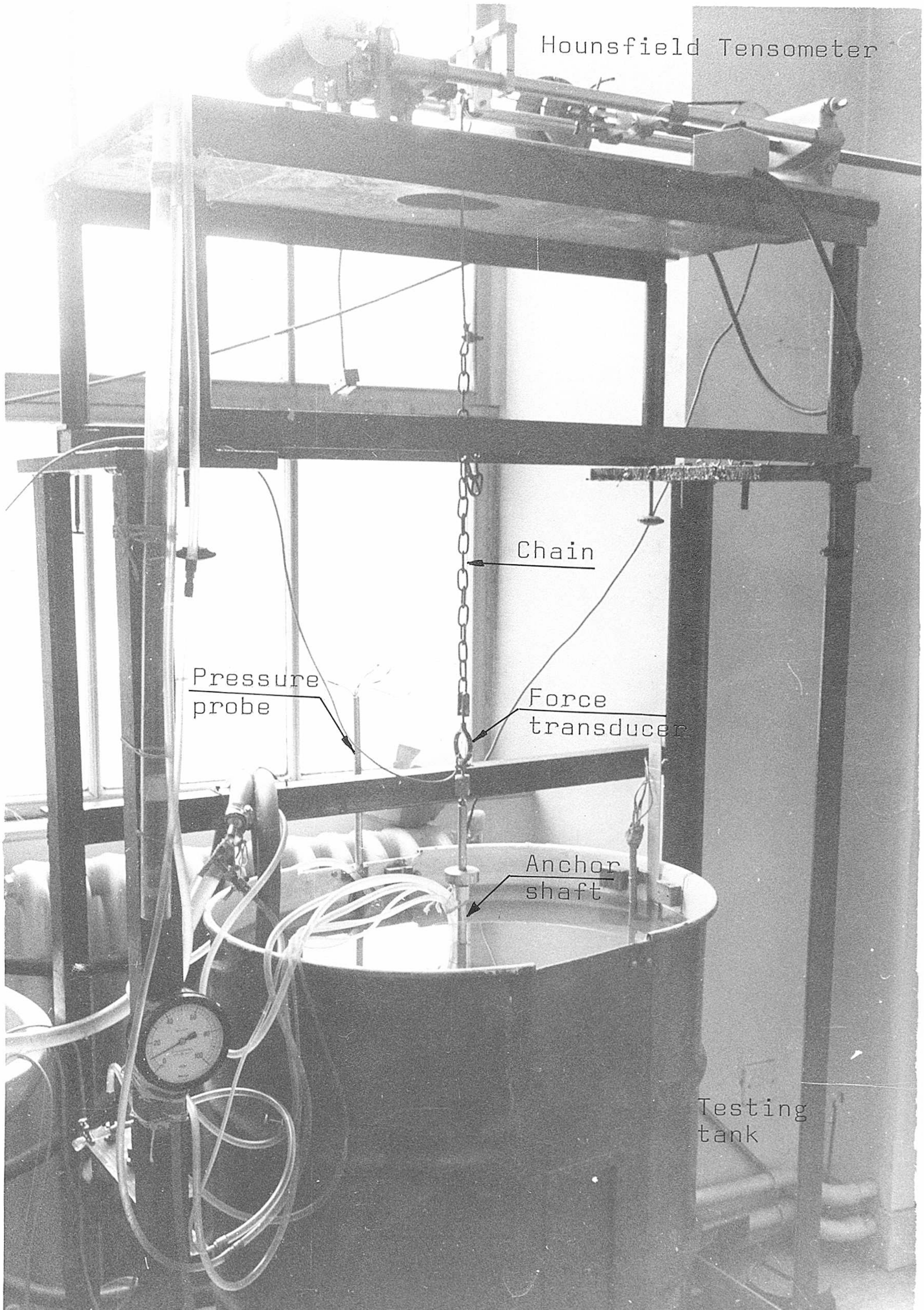

Fig. 3.13 Photograph showing the part of the apparatus set-up with the Hounsfield Tensometer.

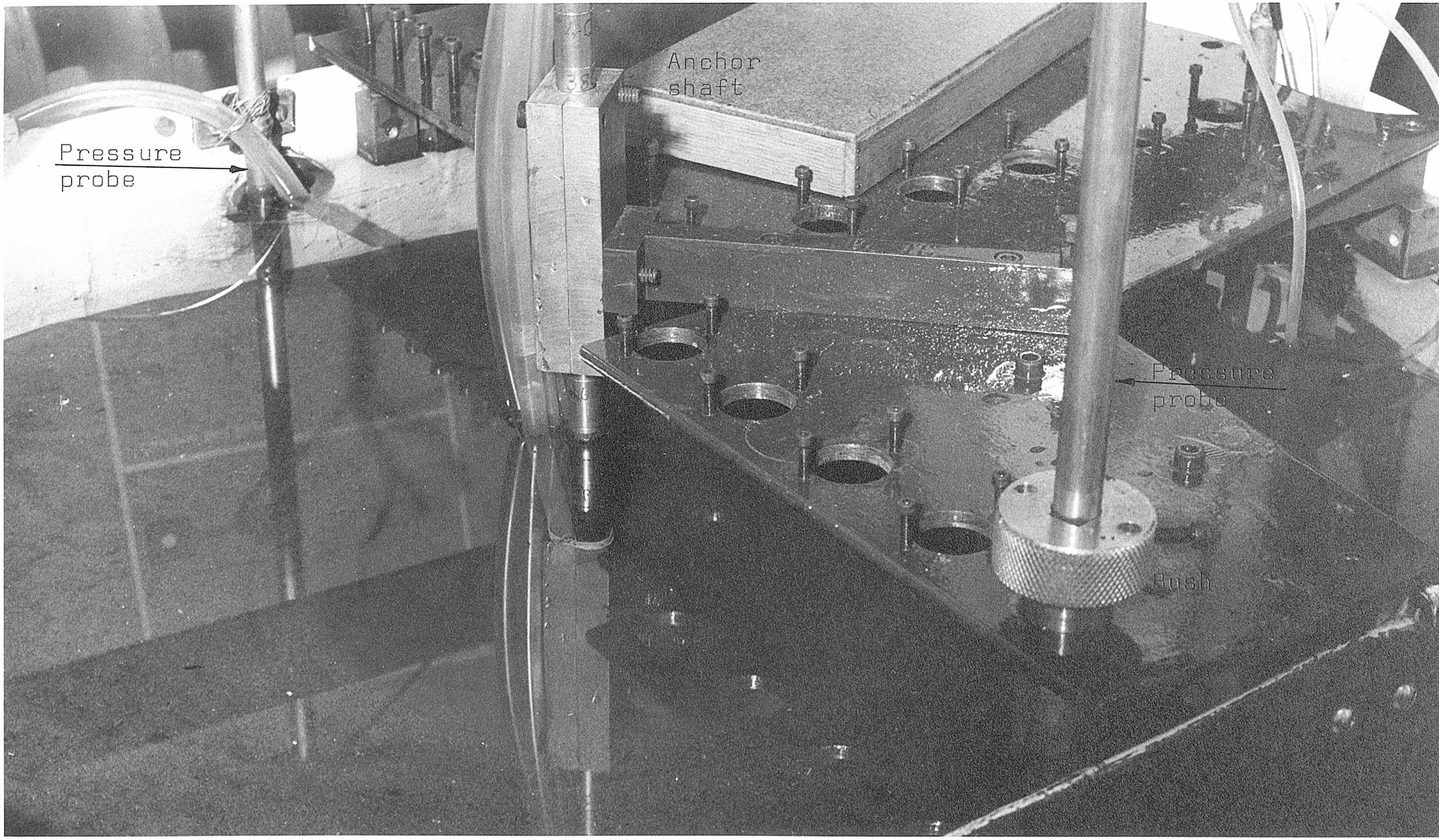

Fig. 3.14 Photograph of the locating plate with the anchor shaft and pressure probes.

3.4.2 Test Apparatus for the Full-scale Anchor

The following was the apparatus which was utilized during the field programme:-

1. 60 ton schooner Robert Gordon: Chain, winch and other facilities. Fig. 3.15 shows the Robert Gordon while a test was in progress.
2. A pump (22kW diesel engine) with a pipe system as shown in Fig. 3.16. Delivery inlet and outlet pipe was 76 mm diameter armoured hose. Orifice plate was located at a distance of 1150 mm from the 90° bend which was on the upstream end and 380 mm from the downstream end. The pipe used in this section was 76 mm in diameter and was a straight copper pipe.
3. Force transducer originally calibrated to 110 kN and then recalibrated to 60 kN.
4. Pressure transducer was used during only part of the testing programme because it was damaged. The pressure range of the transducer was 0 to 517 kN/m^2.
5. One three pen chart recorder was used for the recording of anchor load and suction pressure inside the anchor box.
6. Two vacuum gauges, two pressure gauges and one pump gauge were used to measure the pressures at the suction cavity and just before the main jet, either side of the orifice plate and at the pump respectively.
7. Peekel type 581 DN^{H} Universal Carrier Measuring Amplifiers.
8. Cassette recorder for voice recording the required information from tests.

3.5 PROPERTIES OF SOILS USED IN THE UPLIFT RESISTANCE TESTS

Marine soils were used in this investigation. Soil No. 1

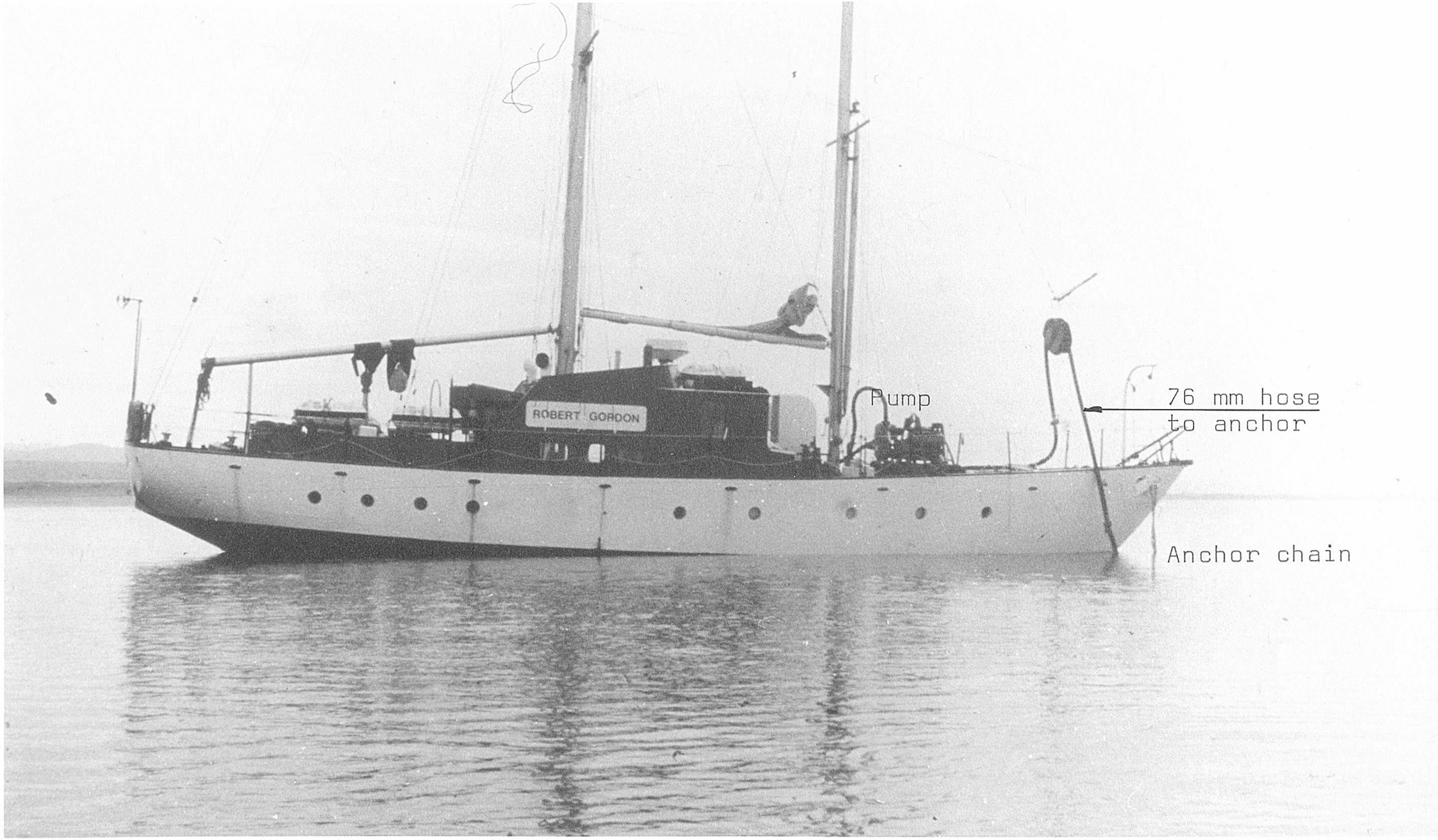

Fig. 3.15 Photograph of the 60-ton schooner Robert Gordon during a sea test when the test was in progress and uplift force = 37 kN.

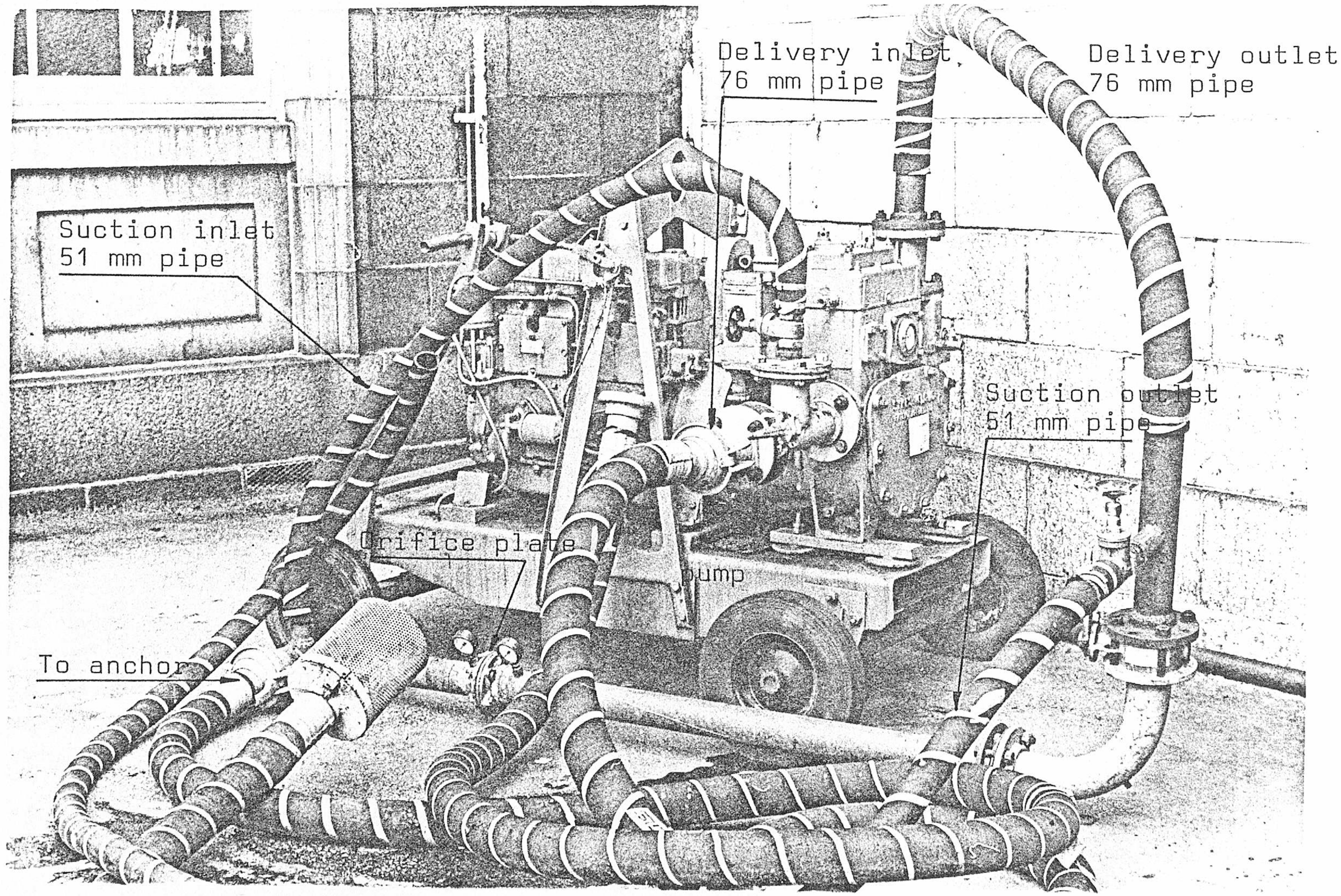

Fig. 3.16 Photograph of pump and pipe system

in the testing tank was from Aberdeen beach and it was washed to remove salt. Soils No. 2 to 5 were collected at the end of the prototype suction anchor tests at sea in the Moray Firth area and the soil samples were put in plastic bags and brought to the laboratory for the determination of soil properties.

The test anchors were forced to bury in the sand bed of the testing tank and similarly in the sea bed by providing pressurized water to the jets or in front of the test solid anchors. By performing this, the soil layers were all disturbed. Soil particles were allowed to fall naturally and settle for natural consolidation or consolidation by means of de watering. Suction pressure in the anchor suction cavity was controlled for all of the suction anchor tests. Due to the applied suction pressure the soil was densified close to the anchor suction cavity. This effect put into question what porosity should be taken into account and ruled out the possibility of using porosity control after deposition or porosity control during deposition.

Particle size distribution curves were drawn for Soils No. 1 to 5 and shown in Fig. 3.17. Soil No. 1 is fine sand and Soils No. 2 to 5 are medium-fine sand. Soils No. 2 to 5 were collected from the top of the anchor when the anchor was brought to the surface at the end of the pull-out test and these results represent only the true grading of the sample collected.

Two acrylic cylinders with the top end open and a 100 µm steel mesh attached to the bottom were used to determine the saturated bulk density and their volumes were $148.9 \times 10^{-6} m^3$ and $140.9 \times 10^{-6} m^3$. The cylinders were buried for 24 hours in the submerged sand in the testing tank. The top was levelled with a knife and the cylinders were dried from outside. The weights were noted and then the densities were

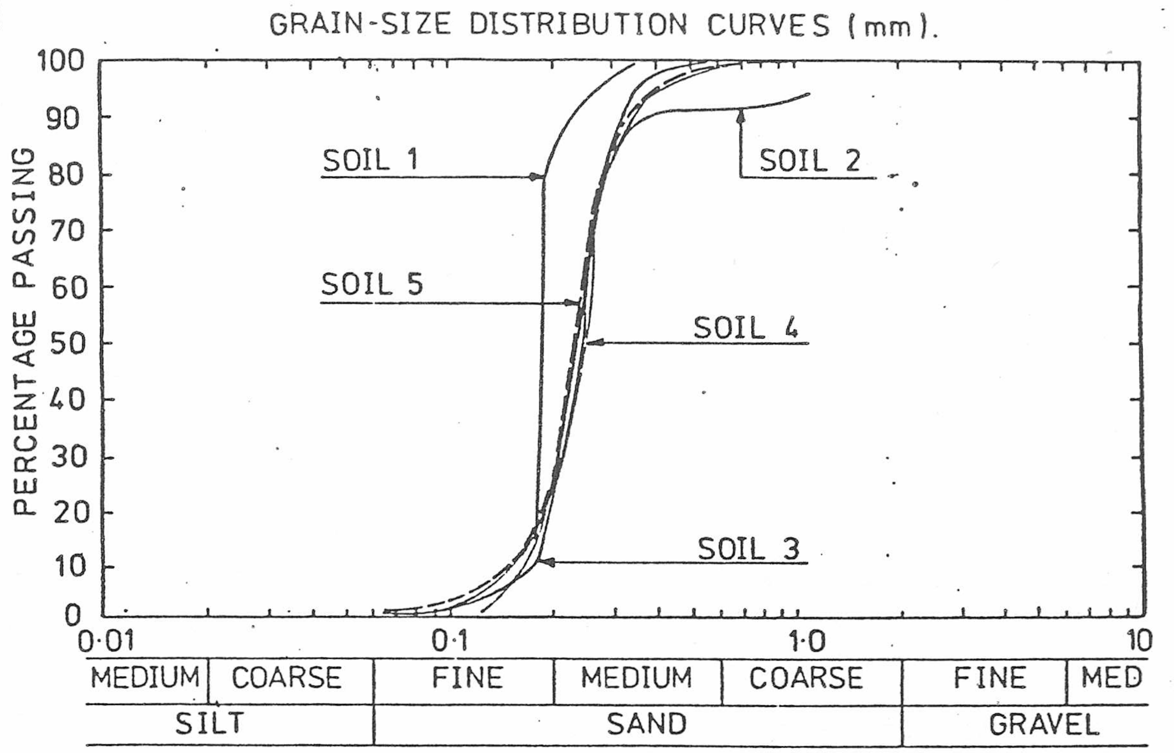

Fig. 3.17 Particle size distribution curves.

found. To confirm the accuracy of this method a 500 ml jar was used. The difference was not more than 1.5%.

The maximum and minimum density tests were conducted by using the methods originally suggested by Kolbuszewski (1948 (a)).

Conventional shear box tests were performed on dry and wet sands. The moisture contents of the wet sand were also determined.

A constant head permeability test was also conducted for the soil No. 1.

The soil properties are briefly summarized in Table 3.2.

3.6 TESTING PROGRAMME

During the experimental programme, it was considered that the current research work based on the break-out behaviour of a suction anchor embedded in a granular soil needed to be experimentally widened, which would help to plan future work. Therefore the testing programme is subdivided as follows:-

1. Flow measurement test on model suction anchors.
2. Pull-out tests on the model anchors with no suction.
3. Pull-out tests on the model suction anchors.
4. Pull-out tests on the anchor shaft with or without suction pressure.
5. Pull-out tests on the prototype suction anchor.

3.6.1 Flow Measurement Tests on Model Suction Anchors

The flow measurement tests were conducted on 70 mm, 102 mm and 145 mm suction anchors. The anchor was lowered to the required burial depth by using the anchor jets and

Table 3.2 Properties of the soils

Details		Types of soil			
	Soil 1	Soil 2	Soil 3	Soil 4	Soil 5
Specific gravity	2.667	2.627	2.640	2.644	2.659
Bulk density (sat.) kN/m^3	19.13	-	-	-	-
Moisture content in %	28.3	-	-	-	-
Maximum dry density kN/m^3	16.01	-	15.88	-	15.97
Minimum dry density kN/m^3	13.74	-	13.47	-	13.53
Void ratio, e	0.754	-	-	-	-
Maximum void ratio, e_{max}	0.905	-	0.905	-	0.927
Minimum void ratio, e_{min}	0.634	-	0.631	-	0.633
Relative density	0.557	-	-	-	-
Loose φ (dry)	29^o	30^o	33^o	32.5^o	32^o
Dense φ (dry)	37^o	38^o	36^o	37^o	38^o
Loose φ (wet)	-	29.5^o	29^o	31^o	29^o
Dense φ (wet)	-	36^o	40.5^o	40^o	39.5^o
Moisture content at dense φ in %	-	27.2	25.0	24.3	24.0
Uniformity coefficient C_u	1.13	1.82	1.46	1.63	1.58
Coefficient of curvature	1.00	1.24	1.00	1.16	1.11
Permeability coeff. at 18^oC by expt. mm/s	0.46	-	-	-	-
Permeability coeff. by Hazen's formula mm/s	0.26	0.20	0.31	0.26	0.24

Hounsfield Tensometer. The jet supply was cut off and the pump was put on to provide a suction pressure to the anchor suction cavity. The required suction pressure was achieved either by increasing or lowering the pressure in the suction cavity and this pressure was read on a water manometer in terms of a difference in water levels. The sand was levelled. Water flow was measured in a 20 000 ml container. The time range for flow measurement was 1.5 minutes to 12 minutes for high cavity suction to low cavity suction pressure respectively. Water level in the tank was kept to an approximately constant level because the water was sucked from the measuring container to tank at the end of the flow measurement test and by doing this, there was minimum disturbance to the soil. Similarly, the procedure was repeated for further water flow measurement tests.

43, 44 and 50 water flow measurement tests were conducted on 70 mm, 102 mm and 145 mm suction anchors respectively. The water temperature was also recorded. Fig. 3.18, 3.19 and 3.20 show the plot of suction pressure against flow at different depths for 70 mm, 102 mm and 145 mm suction anchors respectively. Further, these graphs are cross plotted to give anchor cavity suction pressure against anchor embedment depth and are shown in Fig. 3.21, 3.22 and 3.23 for 70 mm, 102 mm and 145 mm suction anchors respectively.

3.6.2 Pull-out Tests on the Model Anchors with no Suction

The anchors were buried to the required depth by using a jet supply in front of them and lowering the anchor by using the Hounsfield Tensometer. The jet supply was with-drawn on achieving the desired burial depth. The soil was levelled. The anchor was left at least 10 hours in the sand bed before the pull-out test began. The time range for the test was 0.5 hour to 72.5 hours. 96, 21, 16 and 20 tests were conducted on the 70 mm, 102 mm, 108 mm and 145 mm anchors

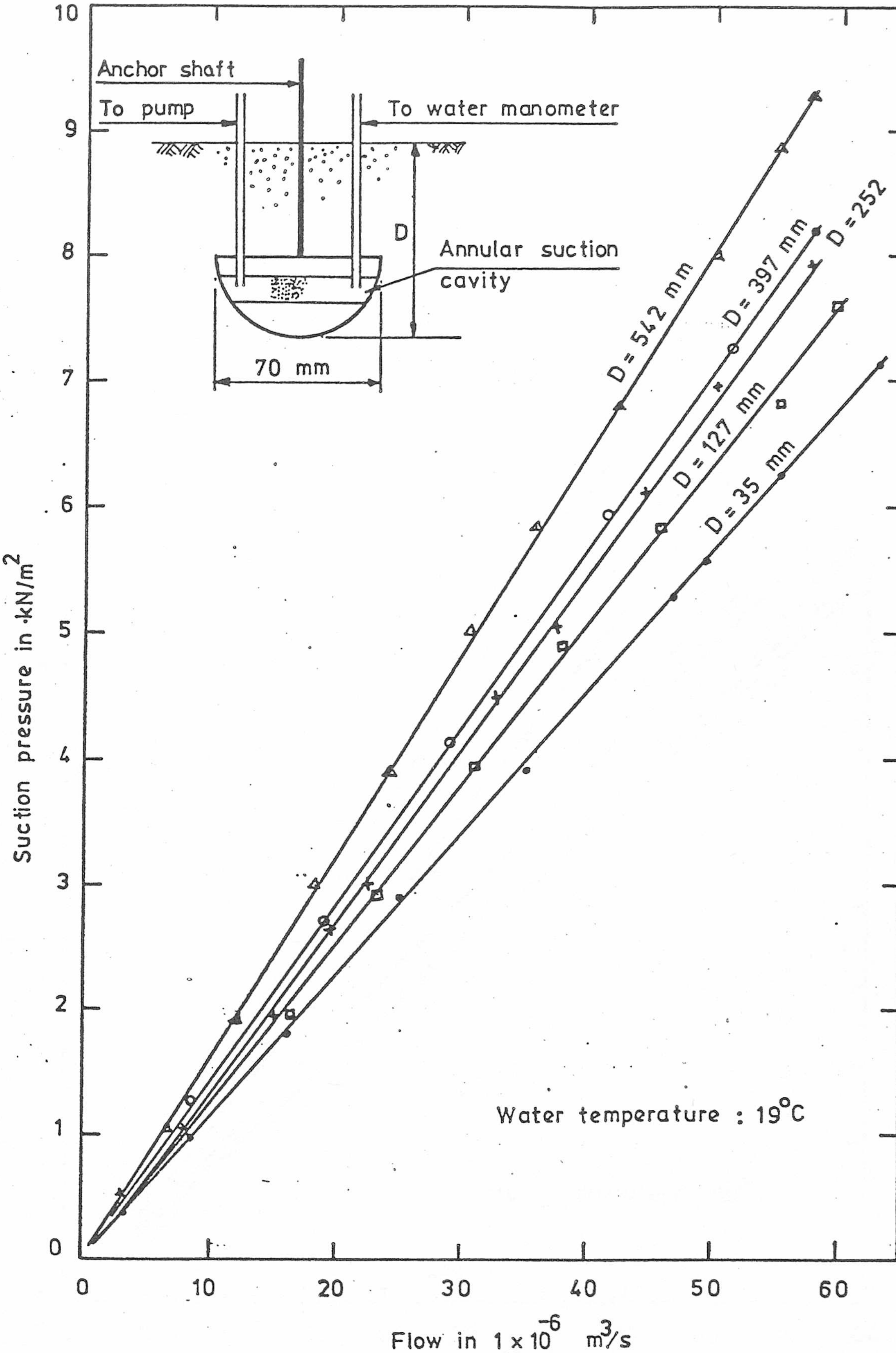

Fig. 3·18 Suction pressure/flow at different depths for 70 mm suction anchor.

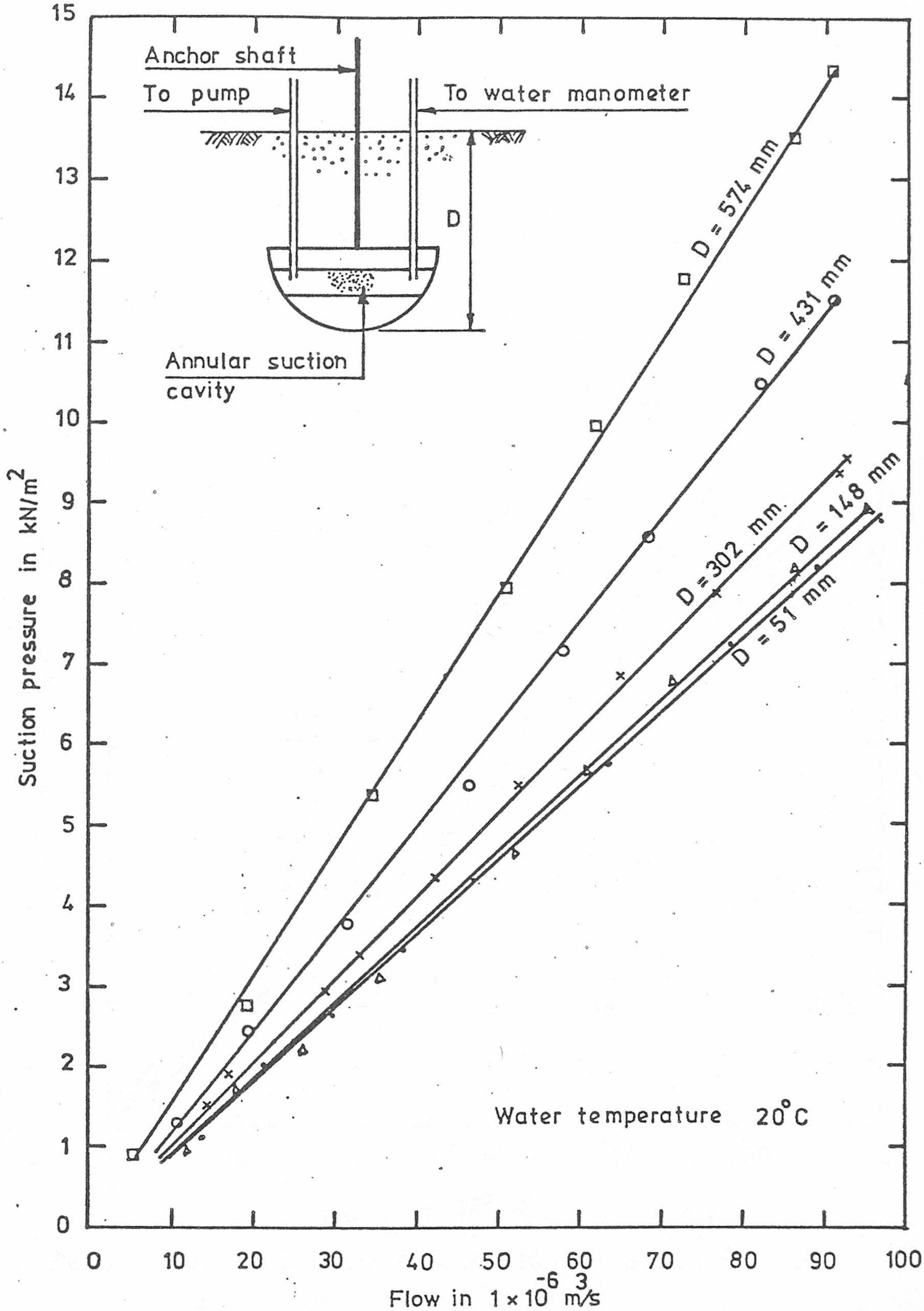

Fig. 3.19 Pressure/flow at different depths for 102 mm suction anchor.

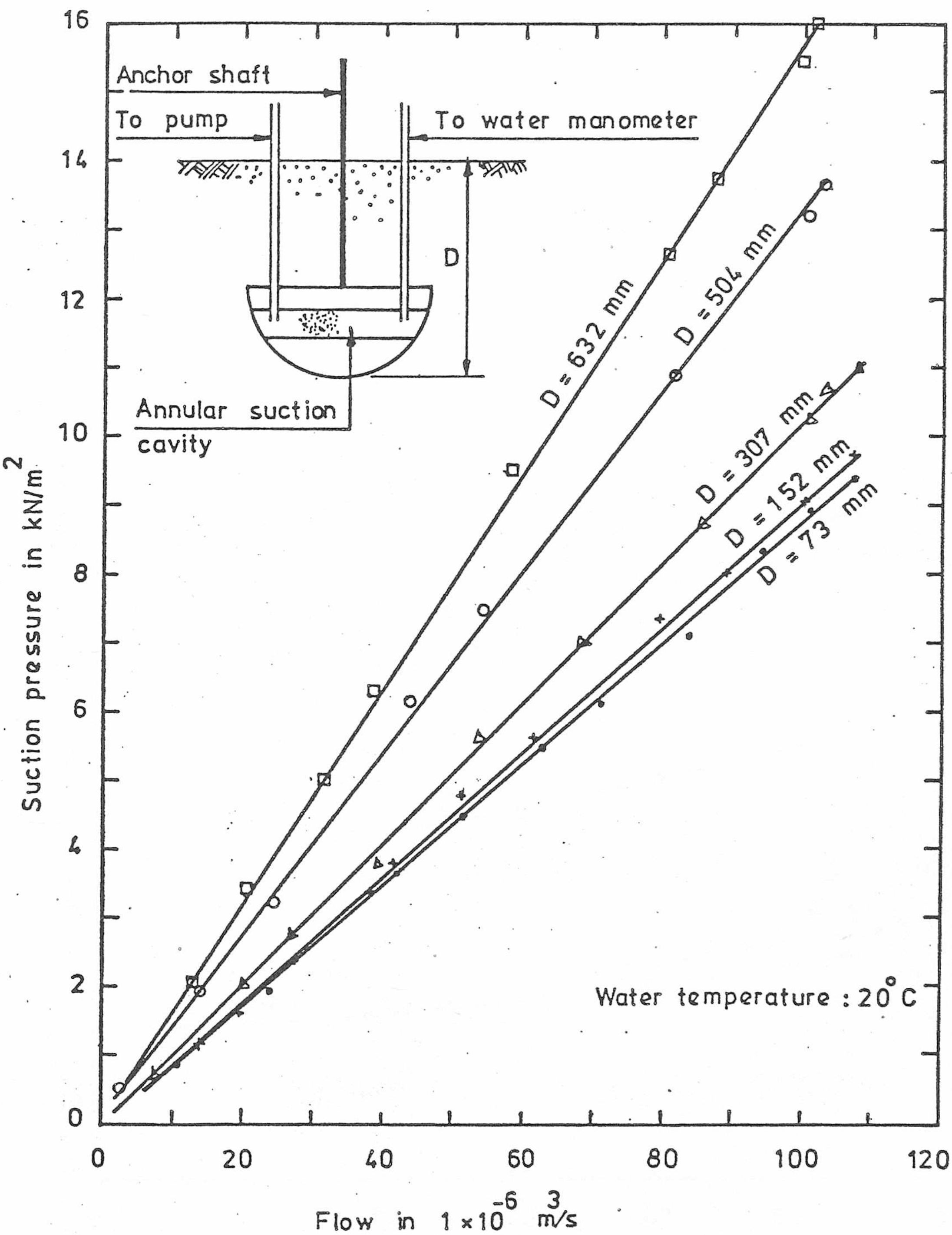

Fig. 3.20 Suction pressure/flow at different depths for 145 mm suction anchor.

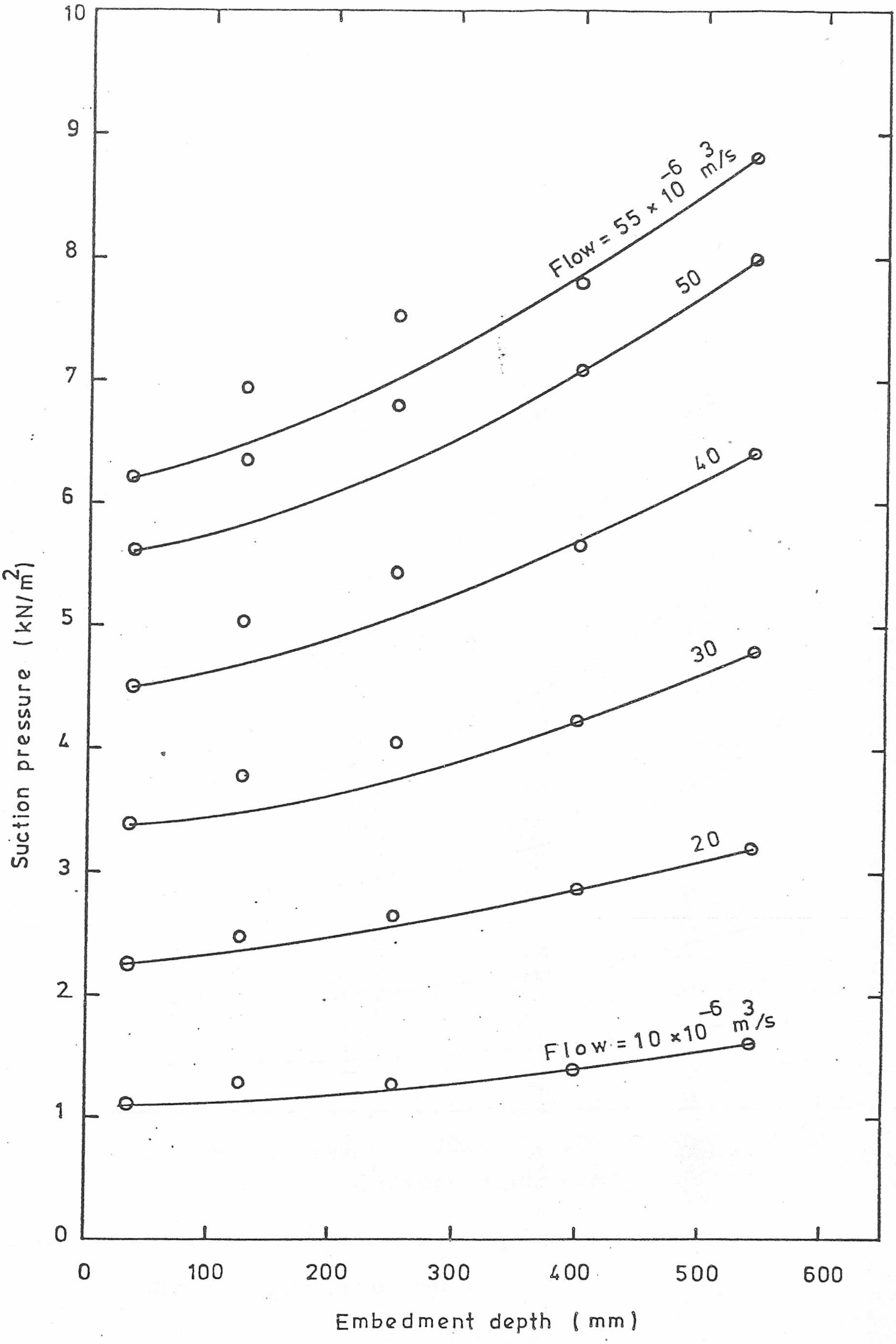

Fig. 3.21 Plot of suction pressure against embedment depth for 70 mm suction anchor.

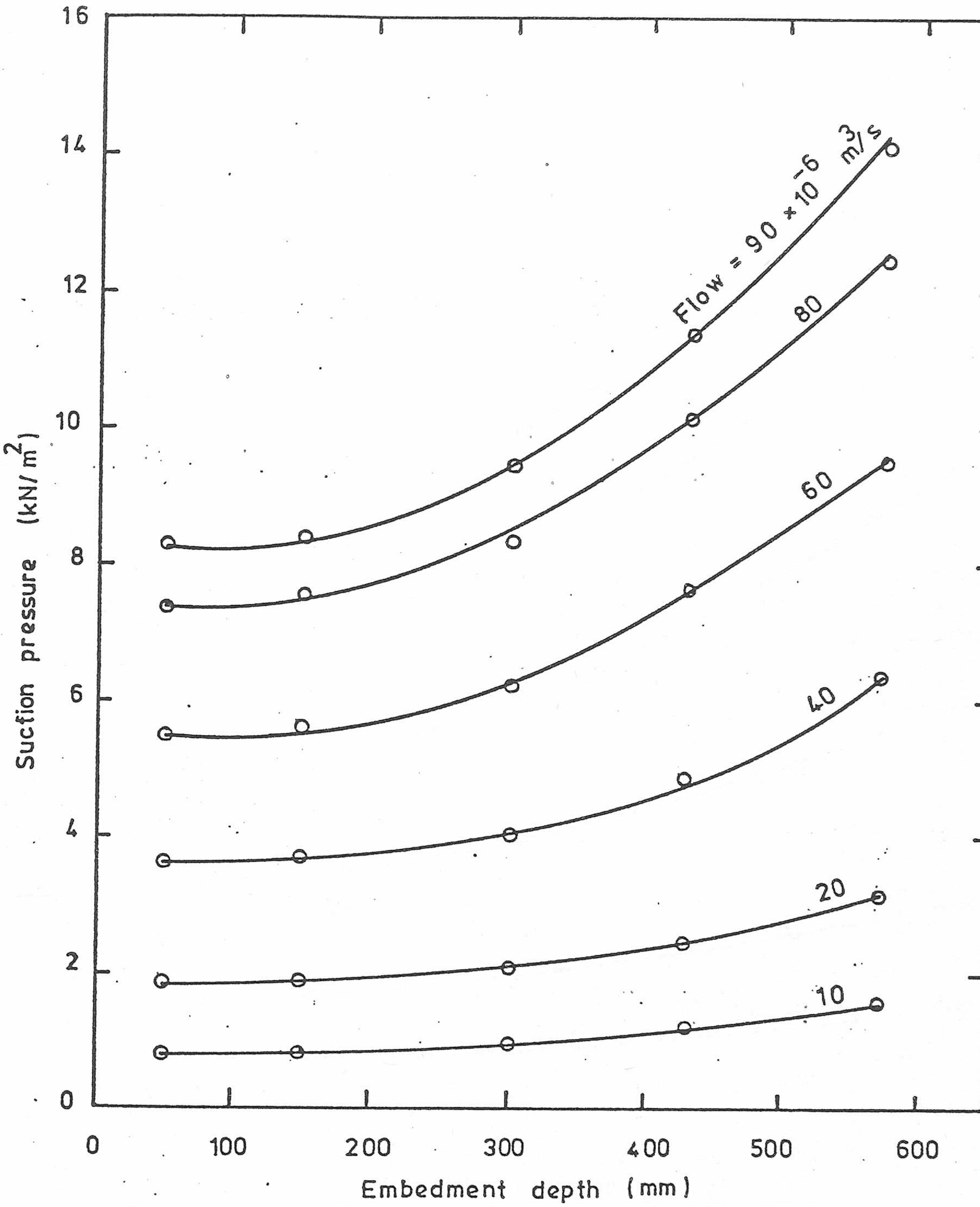

Fig. 3.22 Plot of suction pressure against embedment depth for 102 mm suction anchor.

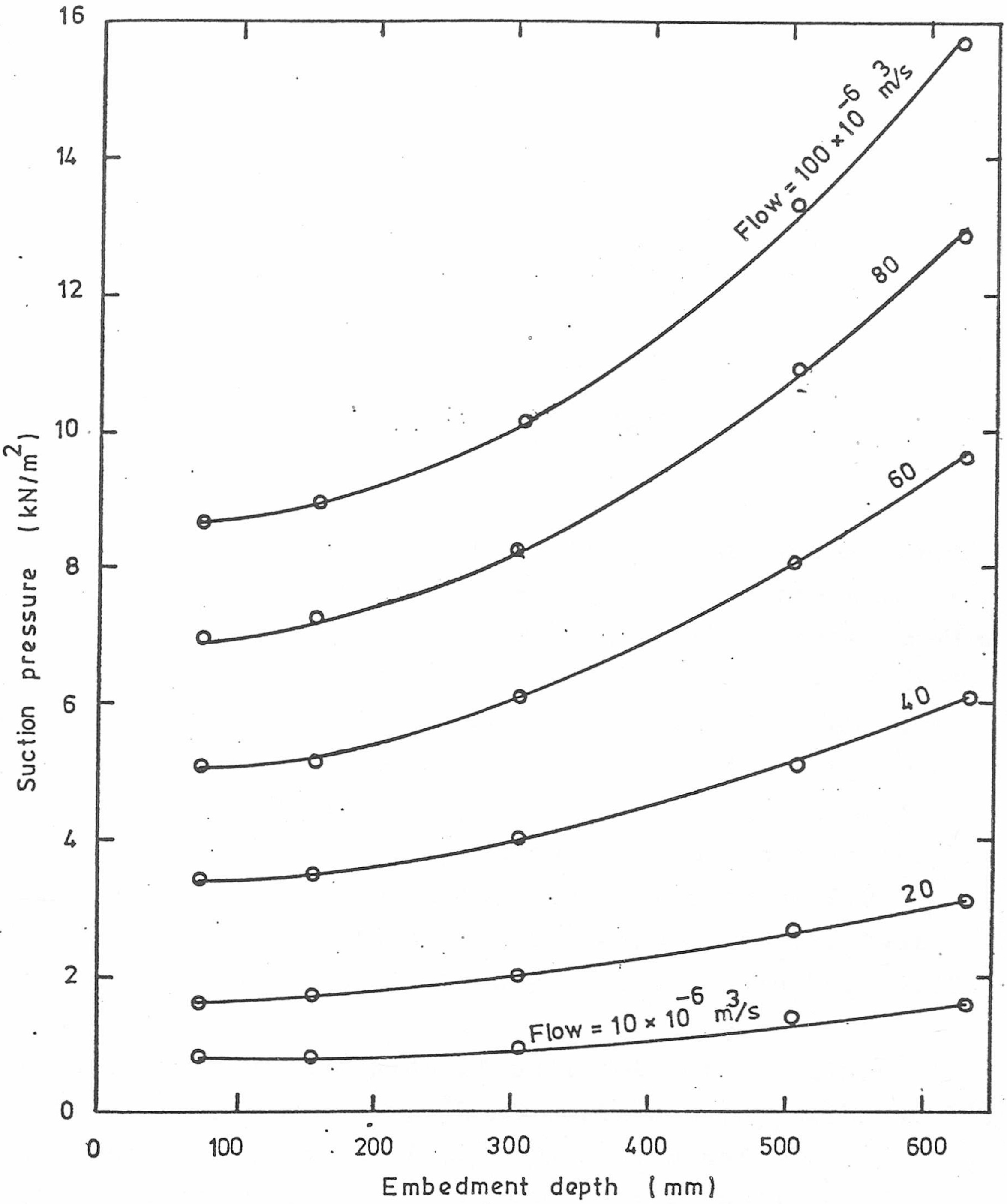

Fig. 3·23 Plot of suction pressure against embedment depth for 145 mm suction anchor.

respectively. Fig. 3.24 and 3.25 show the plot of pull-out resistance against burial depth for the anchors.

3.6.3 Pull-out Tests on the Model Suction Anchors

The model suction anchors were buried in the test sand by fluidizing the sand by jetting and lowering the anchor simultaneously by using the Hounsfield Tensometer. The jet supply was cut off and the required suction was put on. The sand at the surface was levelled. The anchor was pulled-out until it reached a maximum force and in some cases the anchor was brought to the surface. For additional tests, the sand in the tank was resurfaced after burying the anchor to a desired depth. The anchors were tested at various depths.

Fig. 3.26 shows the pull-out force against burial depth for the 70 mm and 102 mm suction anchors with a maximum suction pressure obtained from the pump in the anchor suction cavity. Fig. 3.27 shows the plot of pull-out force against anchor burial depth with a constant anchor suction cavity pressure of 6.0 kN/m^2. For this graph, the time range was selected at 2, 5, 10, 12 and 15 minutes to verify the time factor for suction before commencement of pull-out in the submerged sand. 20 and 33 tests were performed at 5.0 and 7.5 kN/m^2 anchor suction cavity pressure and the test results for the 70 mm suction anchor are shown in Fig. 3.28.

Fig. 3.29 shows the plot of pull-out force against anchor burial depth for the 102 mm suction anchor with suction pressures of 0, 2.5, 5, 6, 7.5, 10 and 12.5 kN/m^2. Further, this graph is cross plotted to give pull-out force against cavity suction pressure and is shown in Fig. 3.30.

187 and 136 tests were carried out on the 70 mm and 102 mm suction anchors respectively.

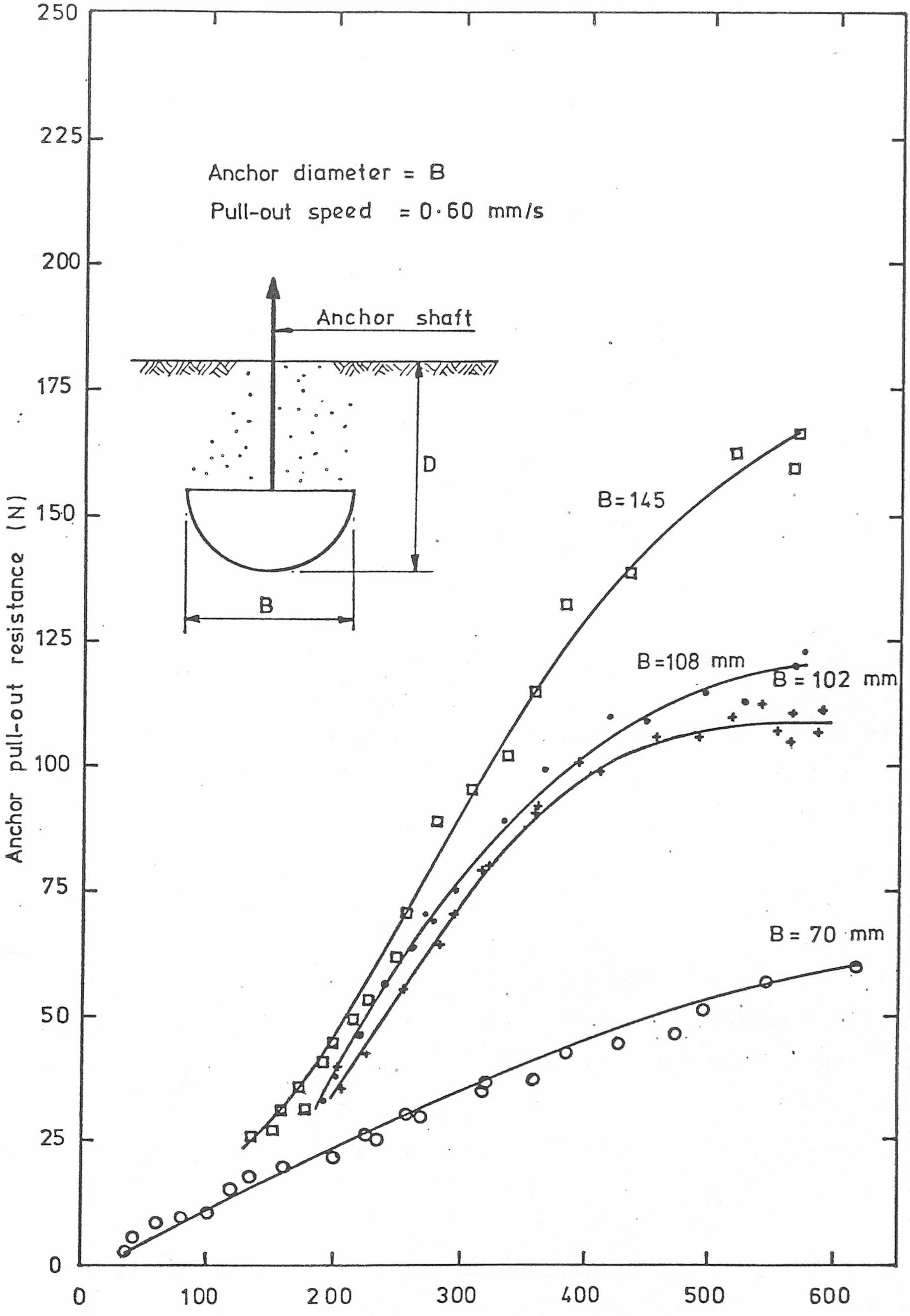

Fig. 3·24 Pull-out resistance/burial depth for 70, 102, 108 and 145 mm anchors with suction pressure = 0 kN/m^2.

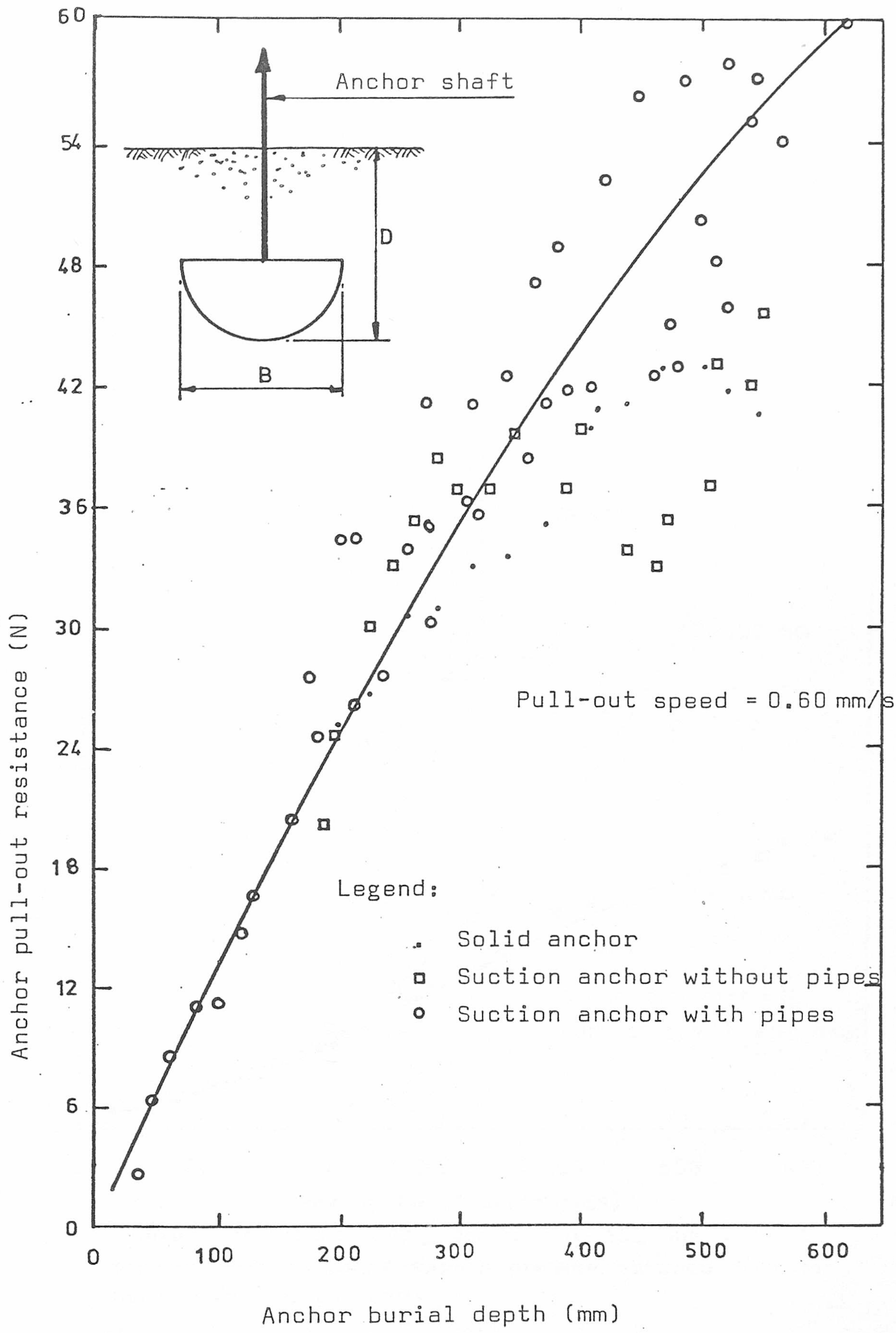

Fig. 3.25 Pull-out resistance/burial depth for 70mm solid anchor and suction anchor with or without pipes

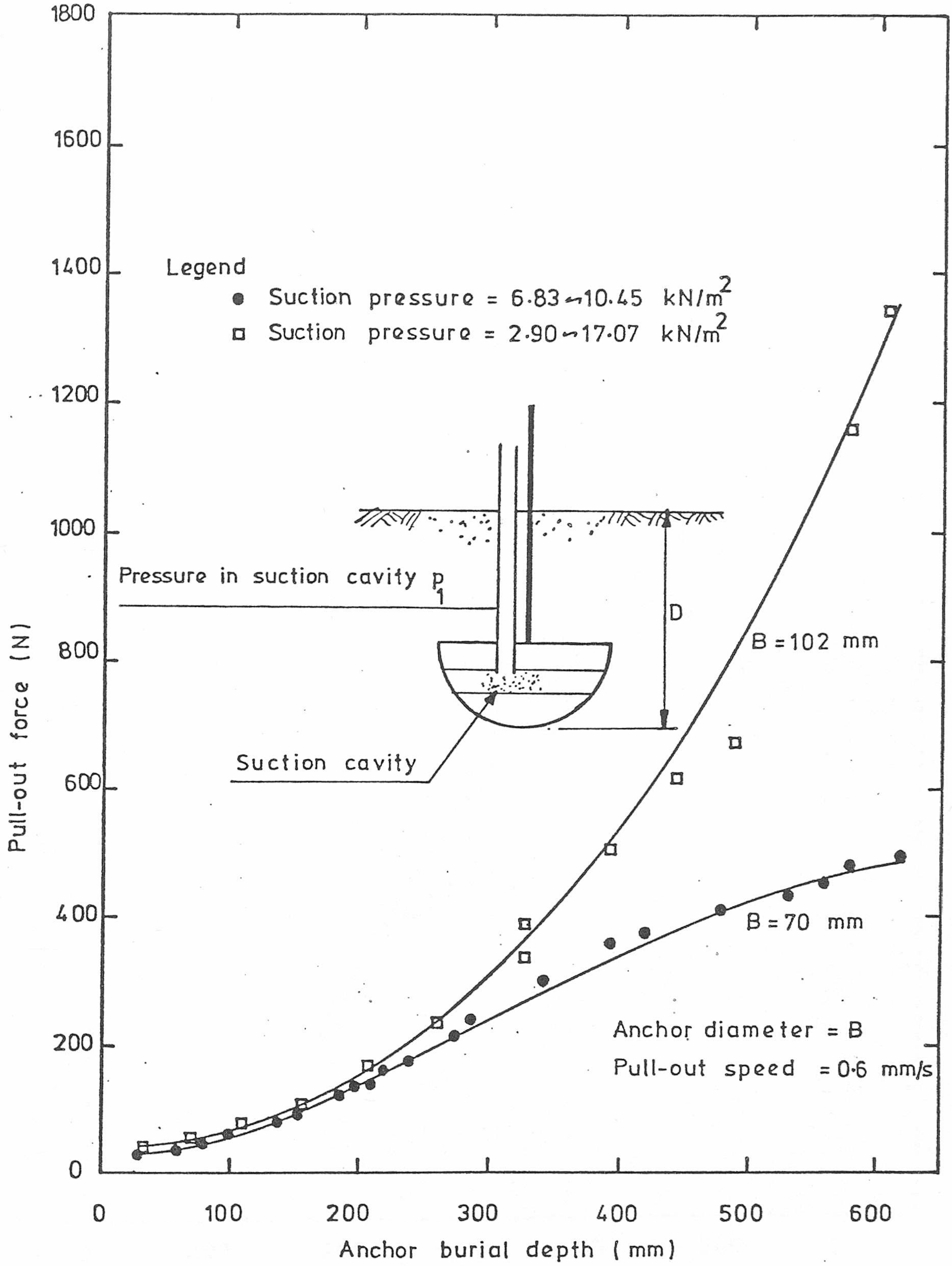

Fig. 3·26 Pull-out force/burial depth for 70 and 102 mm suction anchors with maximum suction pressure obtained from the pump in the suction cavity.

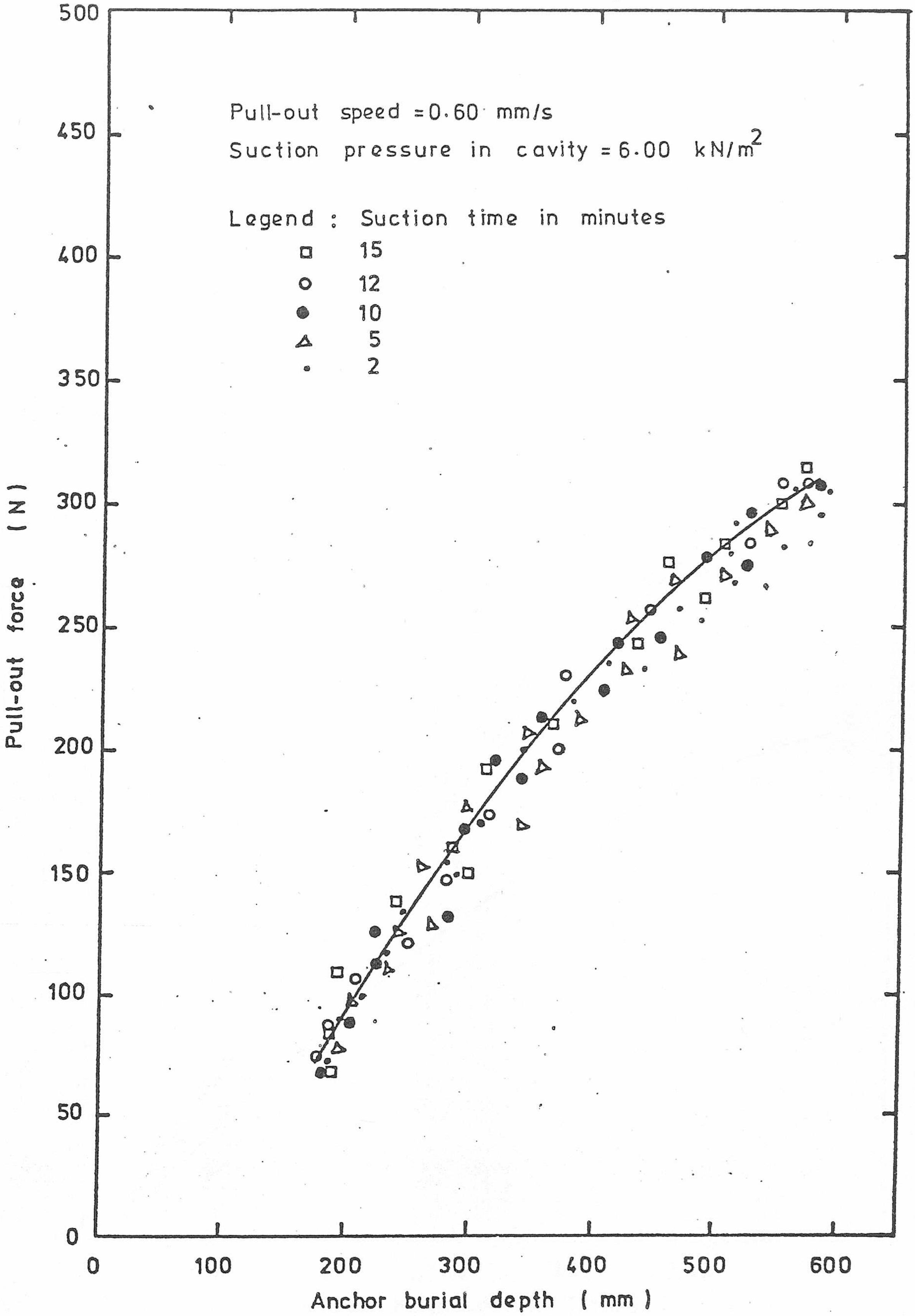

Fig. 3·27 Pull-out force / anchor burial depth for 70 mm suction anchor.

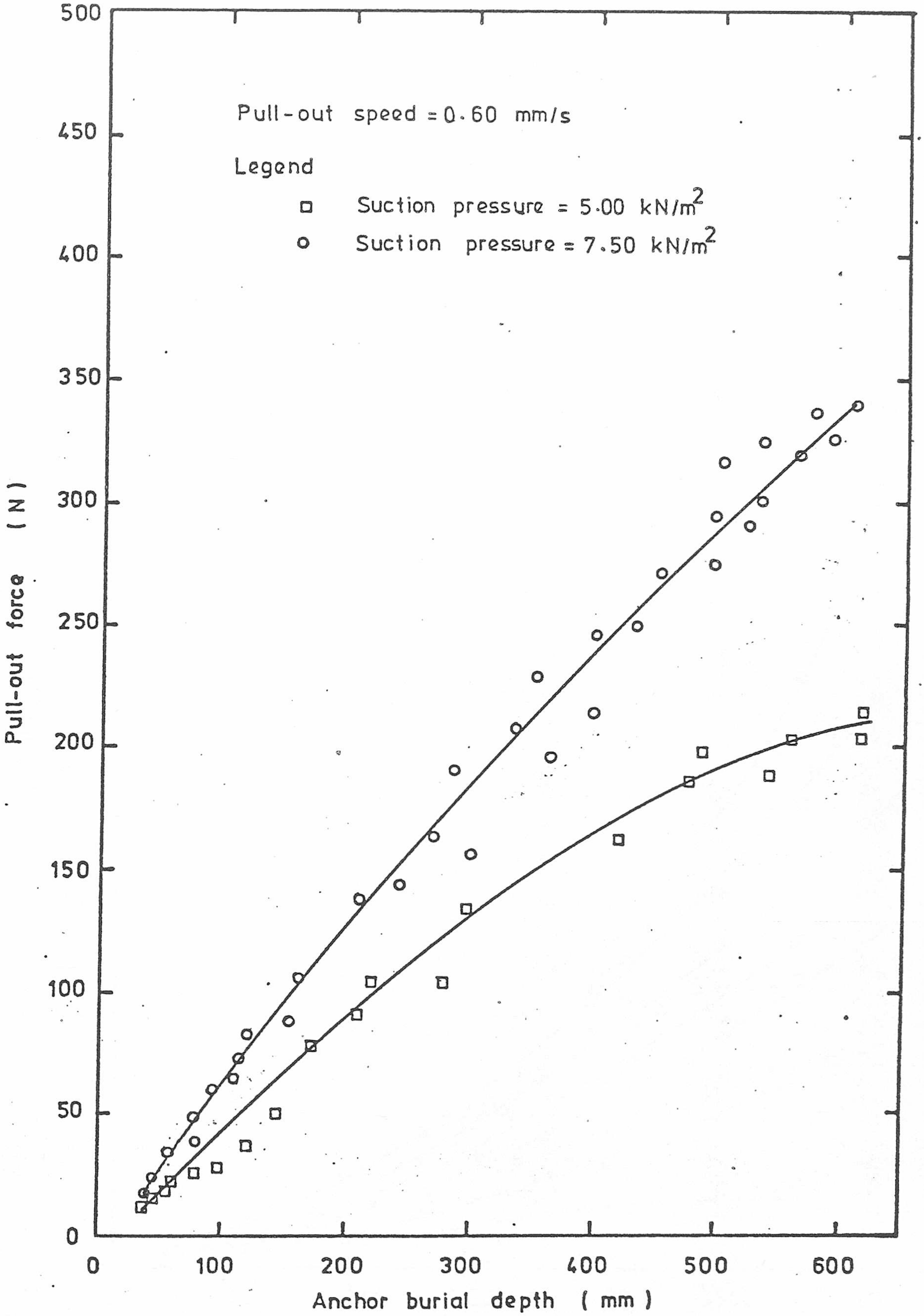

Fig. 3·28 Pull-out force / anchor burial depth for 70 mm suction anchor.

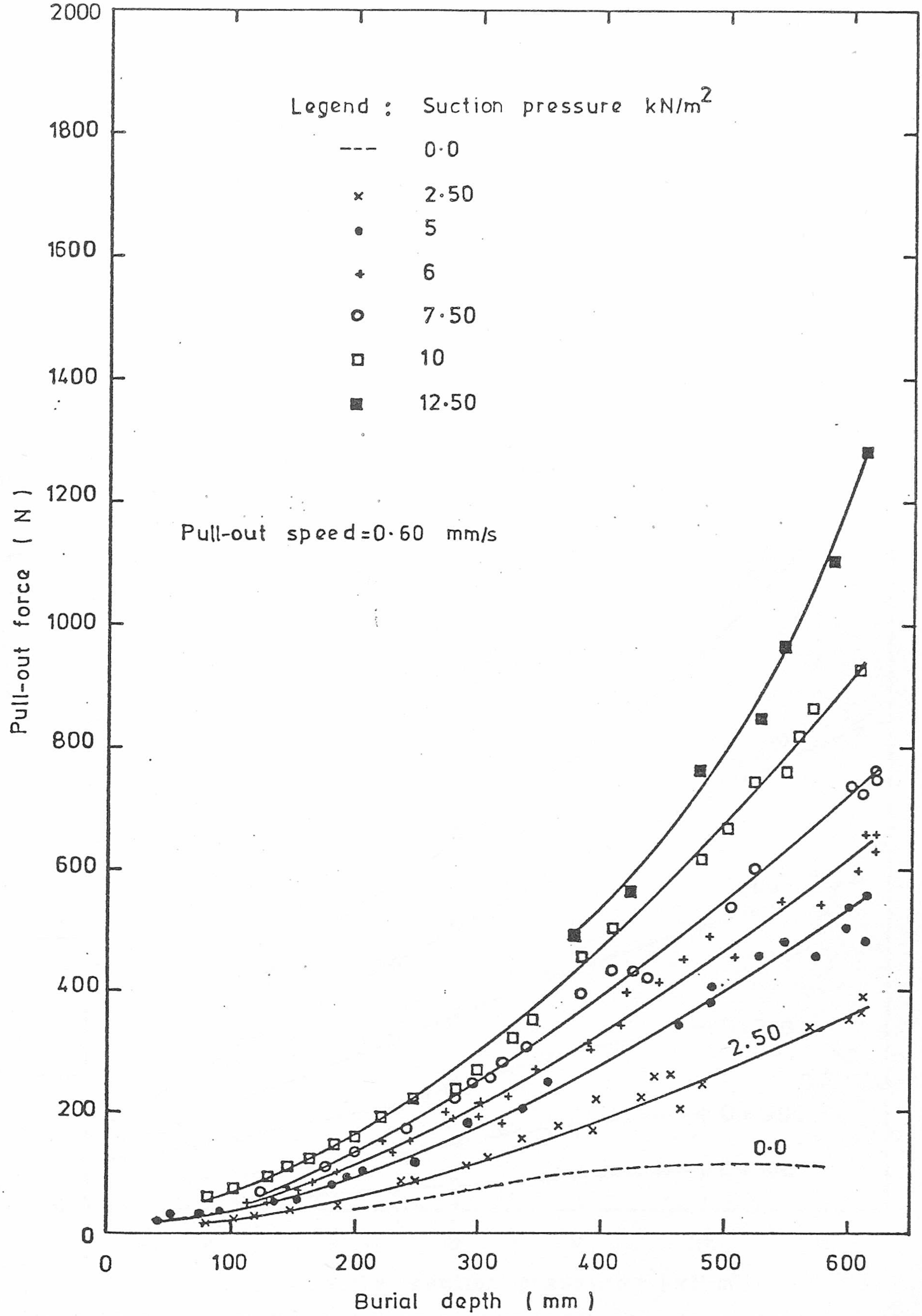

Fig. 3·29 Pull-out force / anchor burial depth for 102 mm suction anchor.

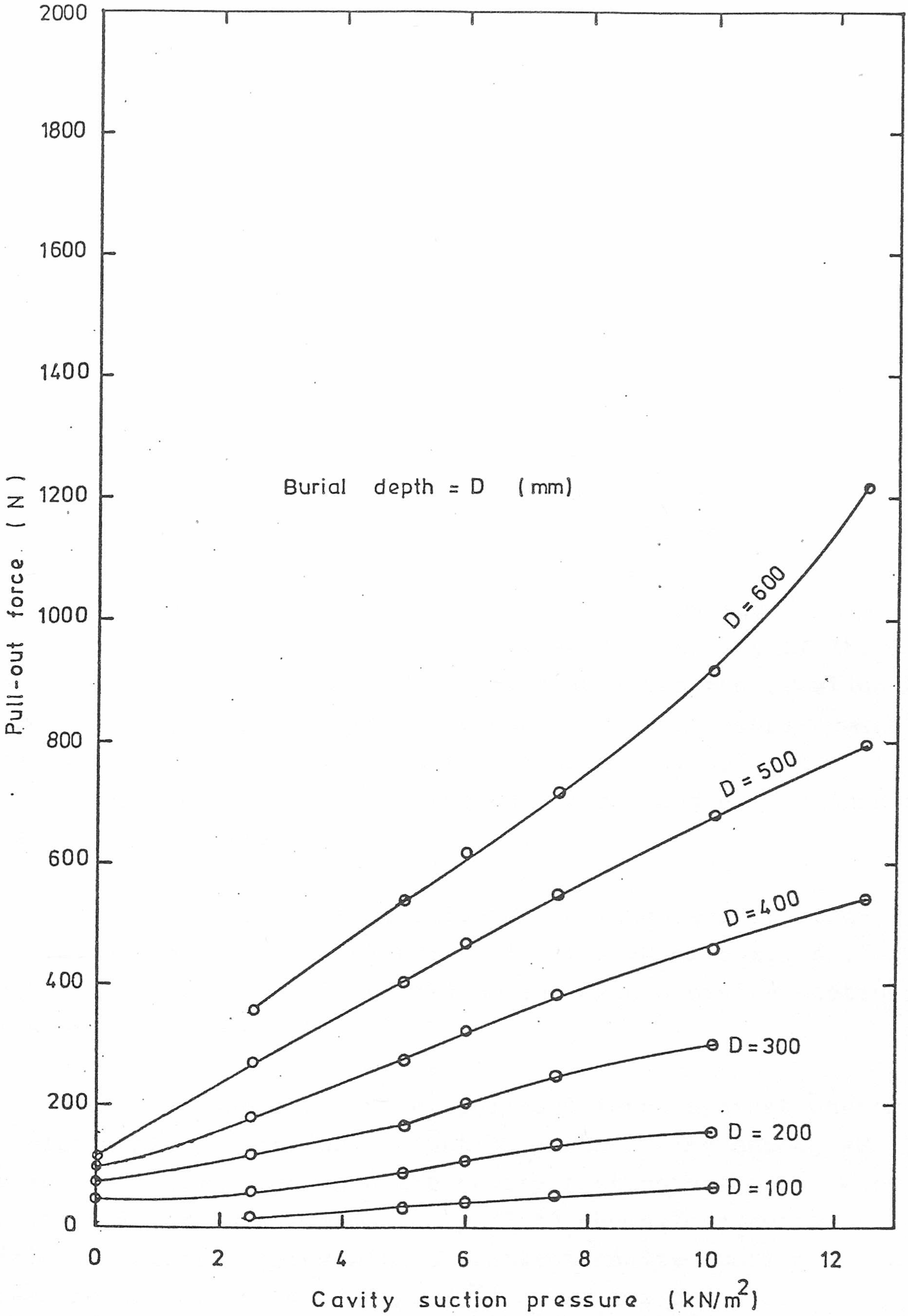

Fig. 3·30 Plot of pull-out force against cavity suction pressure at different depths for 102 mm suction anchor.

Three water manometers were used to measure the pressure within the anchor suction cavity, and above and below the 70 mm suction anchor.

Three pressure transducers were used to determine the pore water pressures above, below and above the top of the 102 mm suction anchor. The anchor cavity pressure was measured by the water manometer. The values of these pressures are plotted against force during pull-out and are shown in Fig. 3.31 to 3.38. The anchor suction cavity pressures ranged from 5.0 to 16.42 kN/m^2. Fig. 3.39 shows the relationship between the pore pressures below and above the anchor before pull-out at 5, 10 and 12.5 kN/m^2 suction cavity pressure. The pore pressure above the anchor became zero when the anchor was at or above the surface level but the pore pressure below the anchor remained with some pressure as long as the annular suction cavity of the anchor was covered with sand. Fig. 3.40 shows the relationship between the three pressures and the anchor displacement. Pressure p_1 in the suction cavity, pressure p_2 below the anchor and pressure p_3 above the anchor reduced as the anchor displacement increased.

Fig. 3.41 shows the relationship between anchor pull-out force and anchor displacement for the 70 mm suction anchor at a burial depth of 594 mm and with a cavity suction pressure of 8.50 kN/m^2.

Fig. 3.42 shows a plot of pull-out force against anchor displacement for the 102 mm suction anchor. The anchor was buried to 614 mm depth and the cavity suction pressures were 5.0, 15.94 and 16.42 kN/m^2. Fig. 3.43 shows four tests at different burial depths with a constant cavity suction pressure of 10.0 kN/m^2. Fig. 3.44 shows two tests at a cavity suction pressure of 12.0 kN/m^2 for 589 mm and 609 mm burial depth.

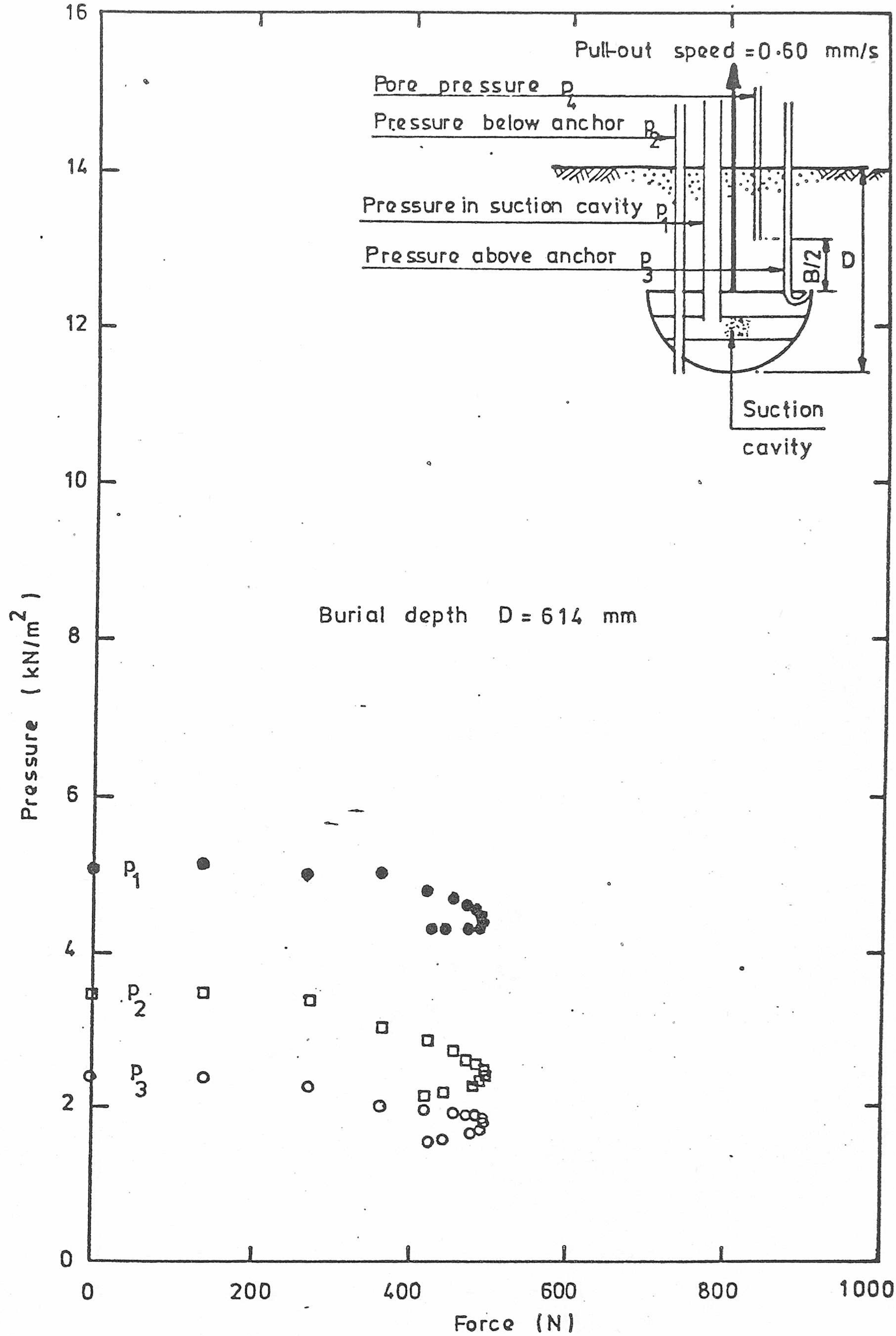

Fig. 3.31 Pressure against anchor pull-out force for 102 mm suction anchor.

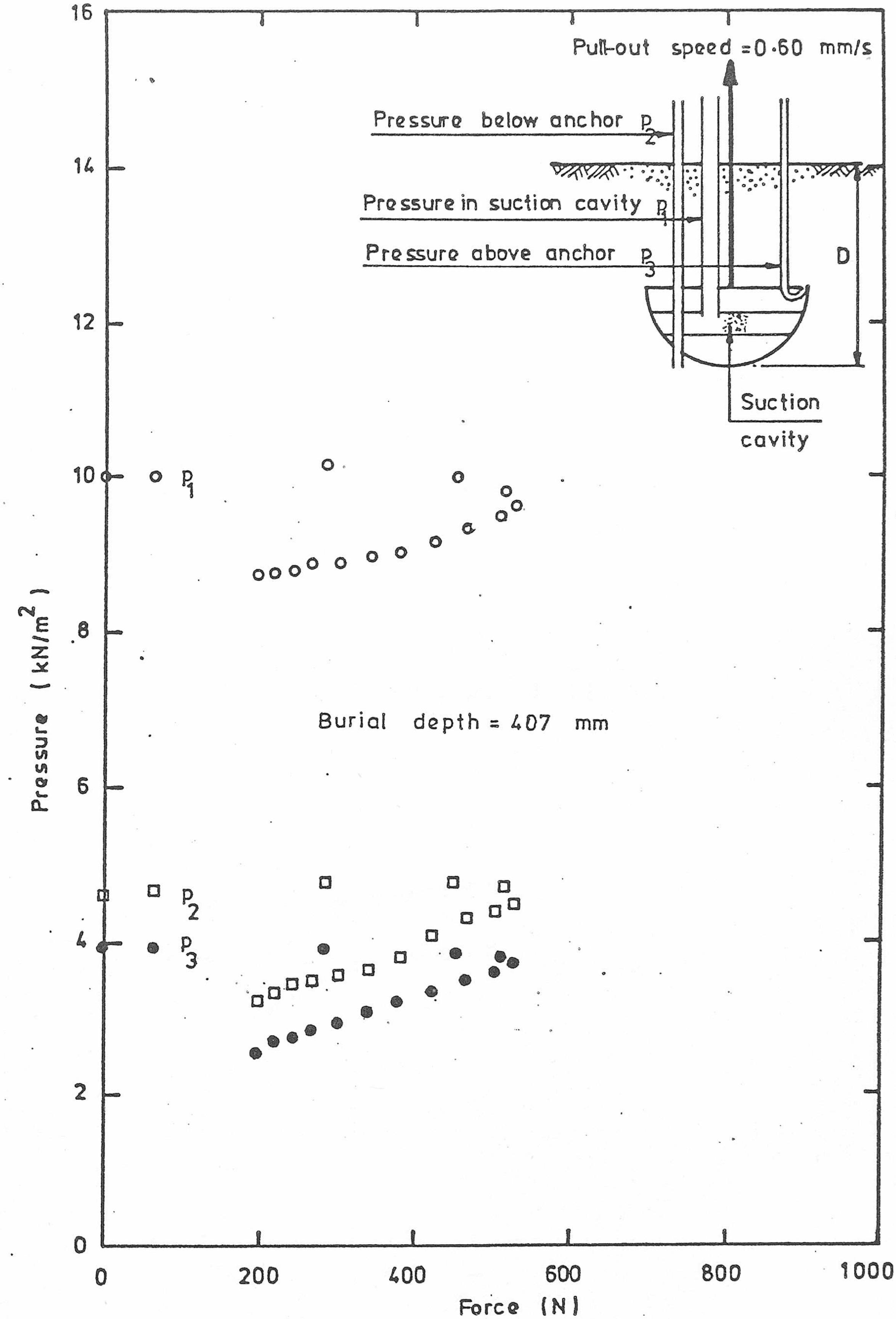

Fig. 3·32 Pressure against anchor pull-out force for 102 mm suction anchor.

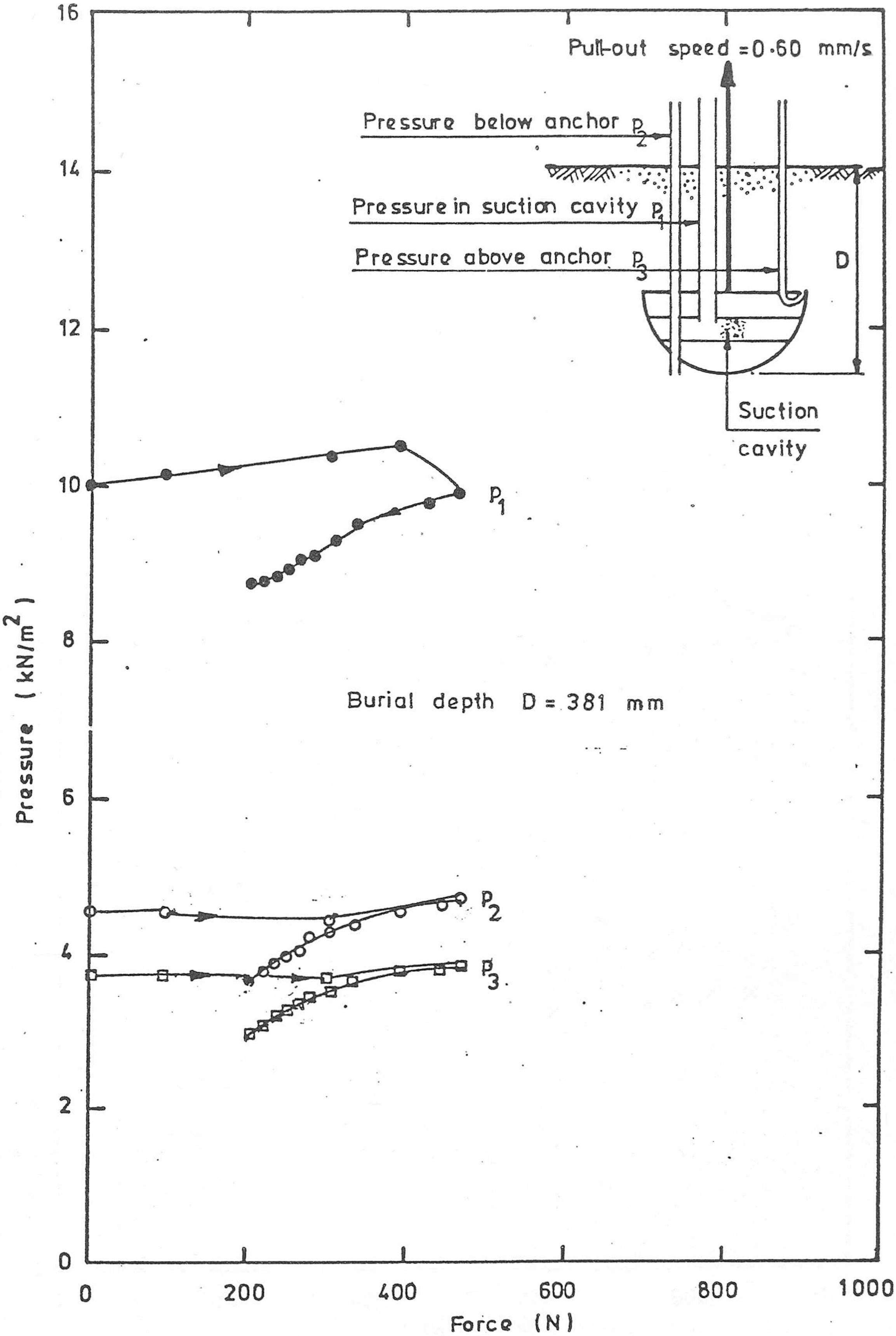

Fig. 3·33 Pressure against anchor pull-out force for 102 mm suction anchor.

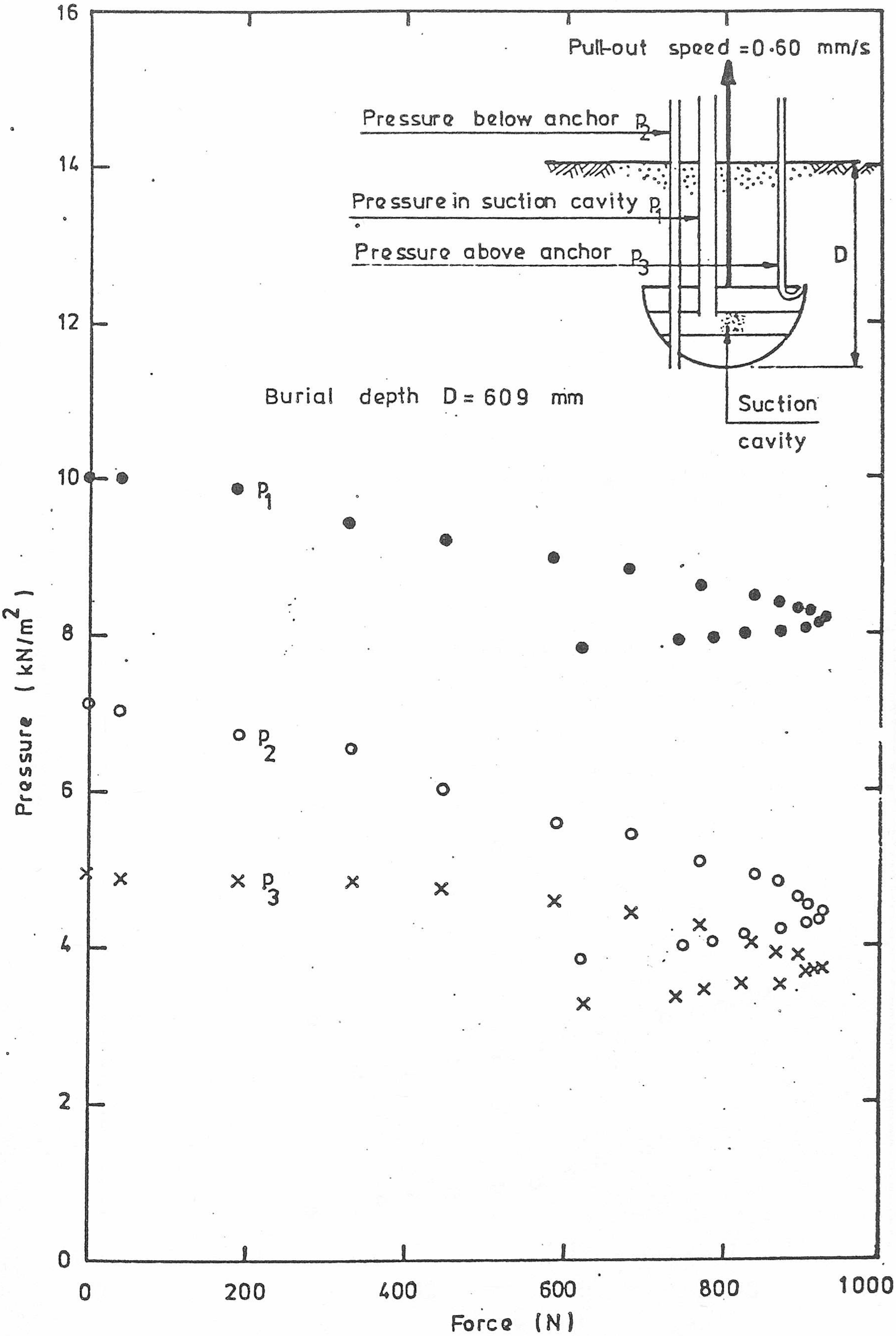

Fig. 3.34 Pressure against anchor pull-out force for 102 mm suction anchor.

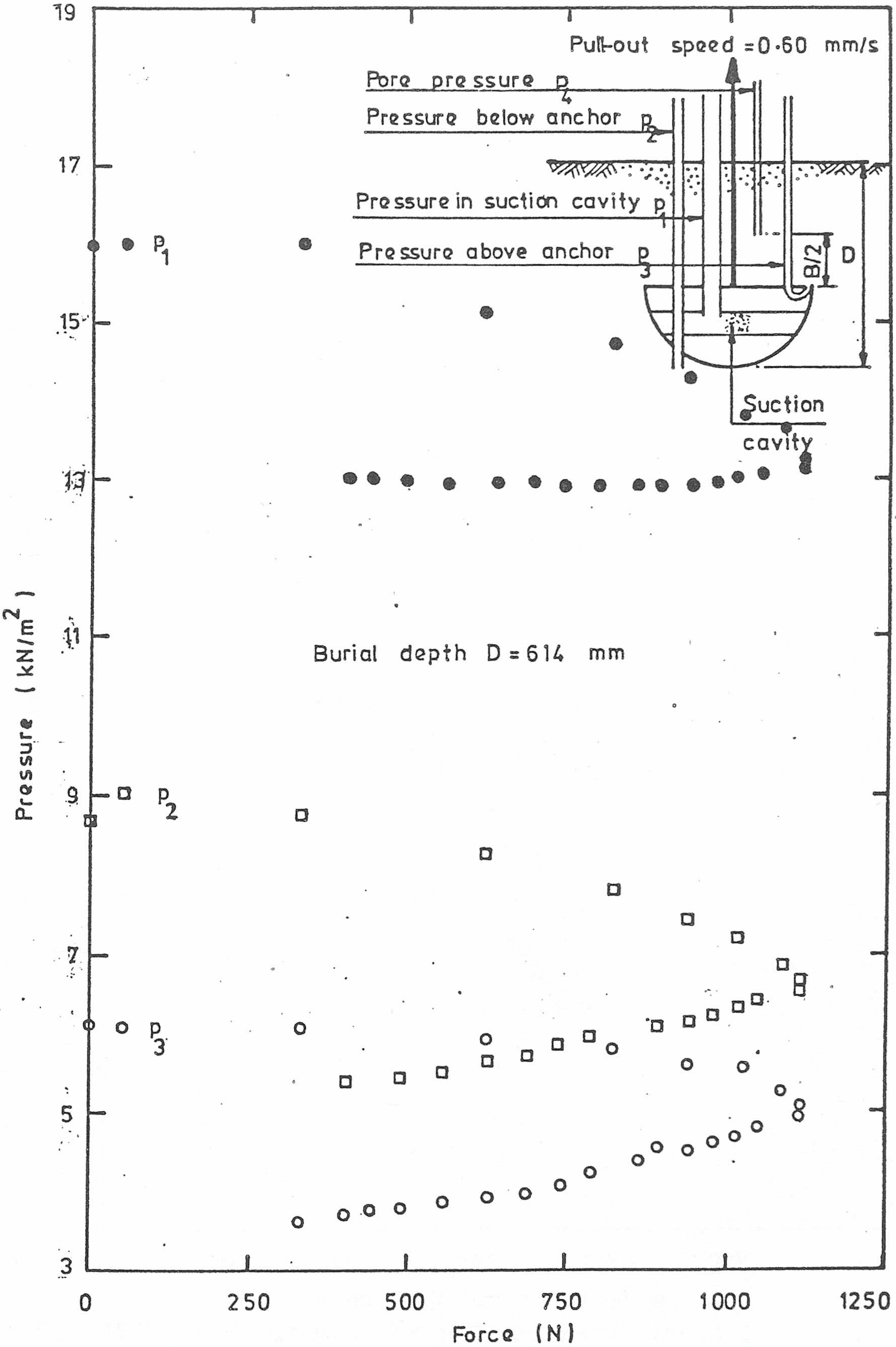

Fig. 3·35 Pressure against anchor pull-out force for 102 mm suction anchor.

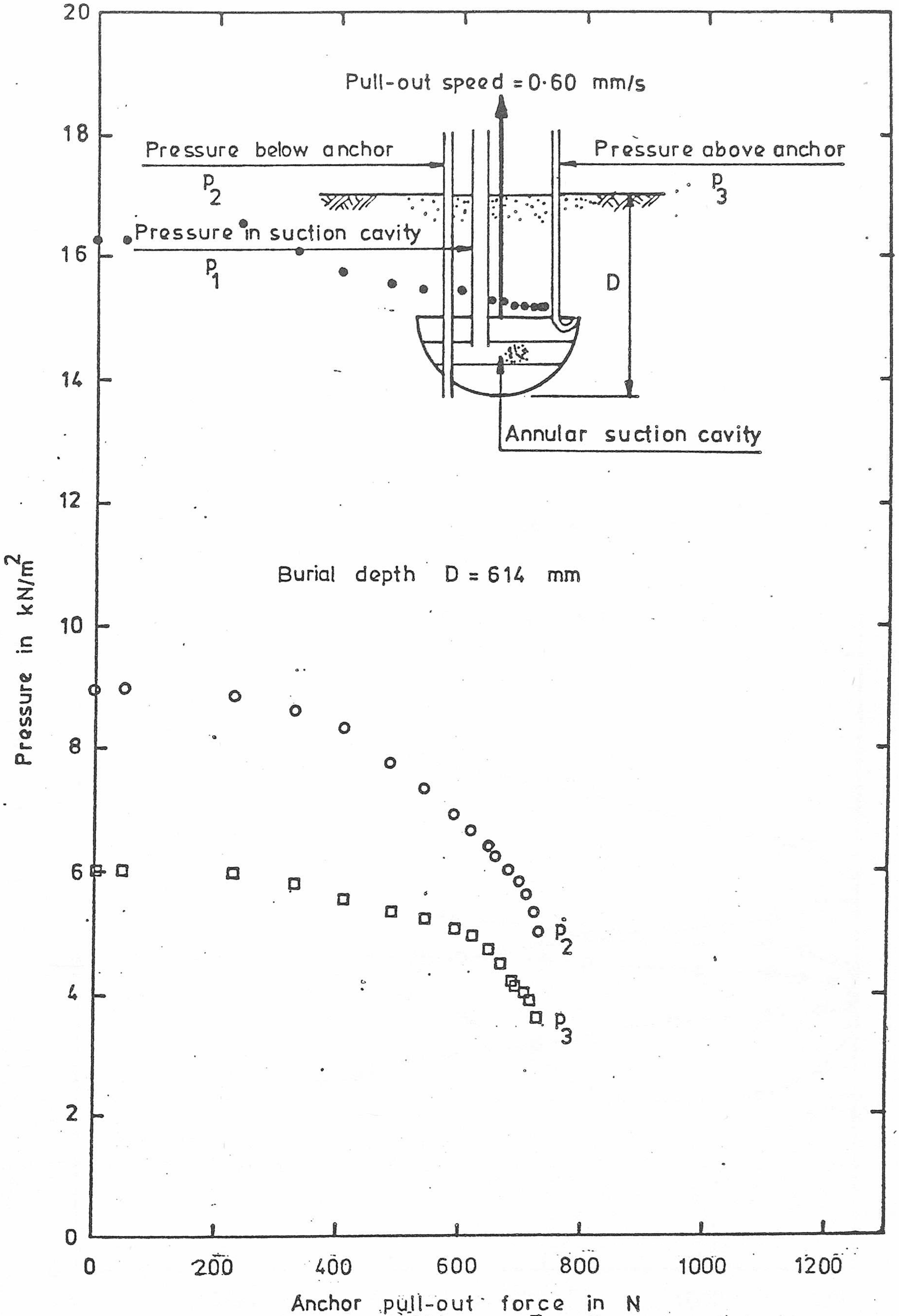

Fig. 3·36 Pressure against anchor pull-out force for 102 mm suction anchor.

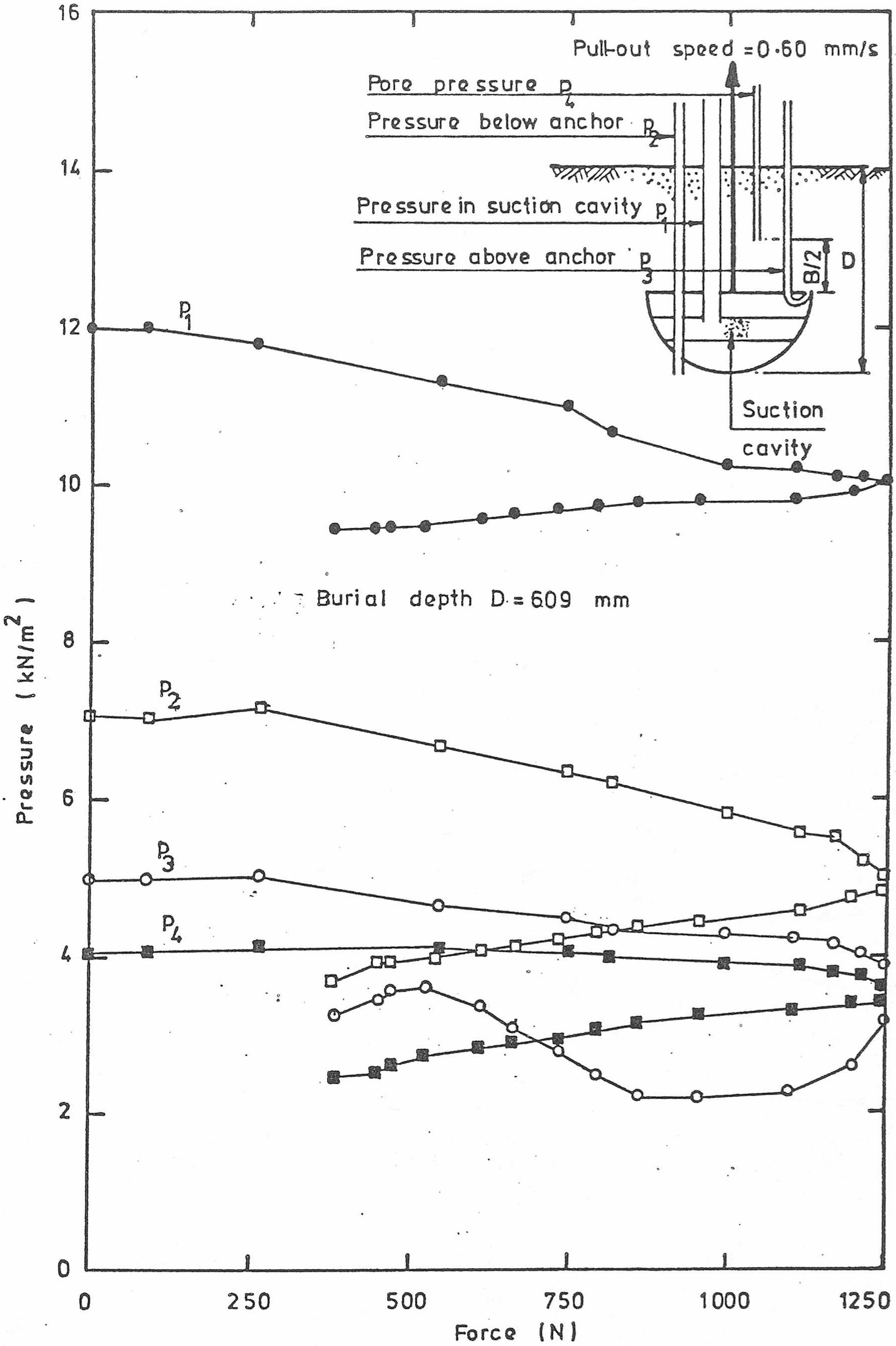

Fig. 3·37 Pressure against anchor pull-out force for 102 mm suction anchor.

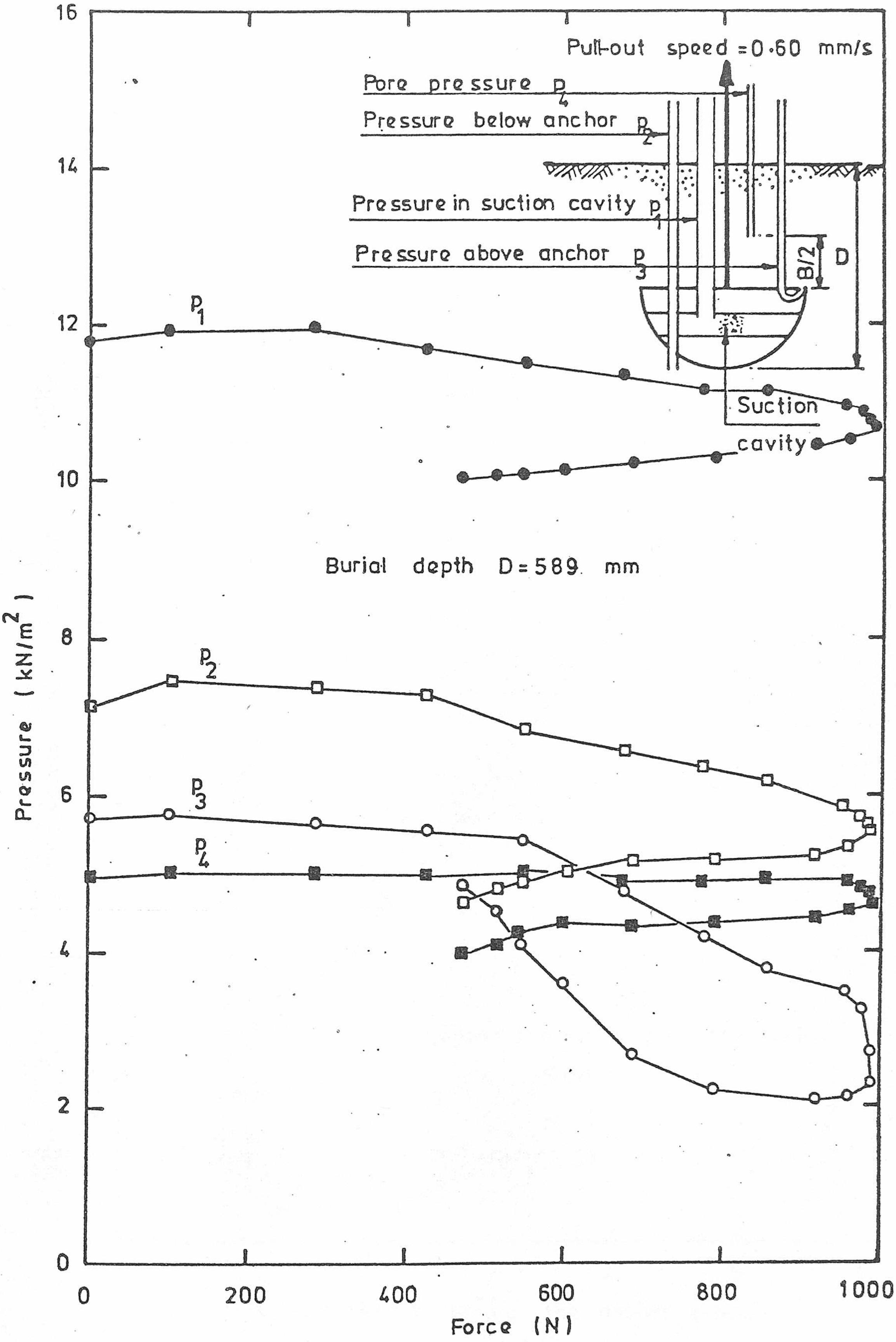

Fig. 3·38 Pressure against anchor pull-out force for 102 mm suction anchor.

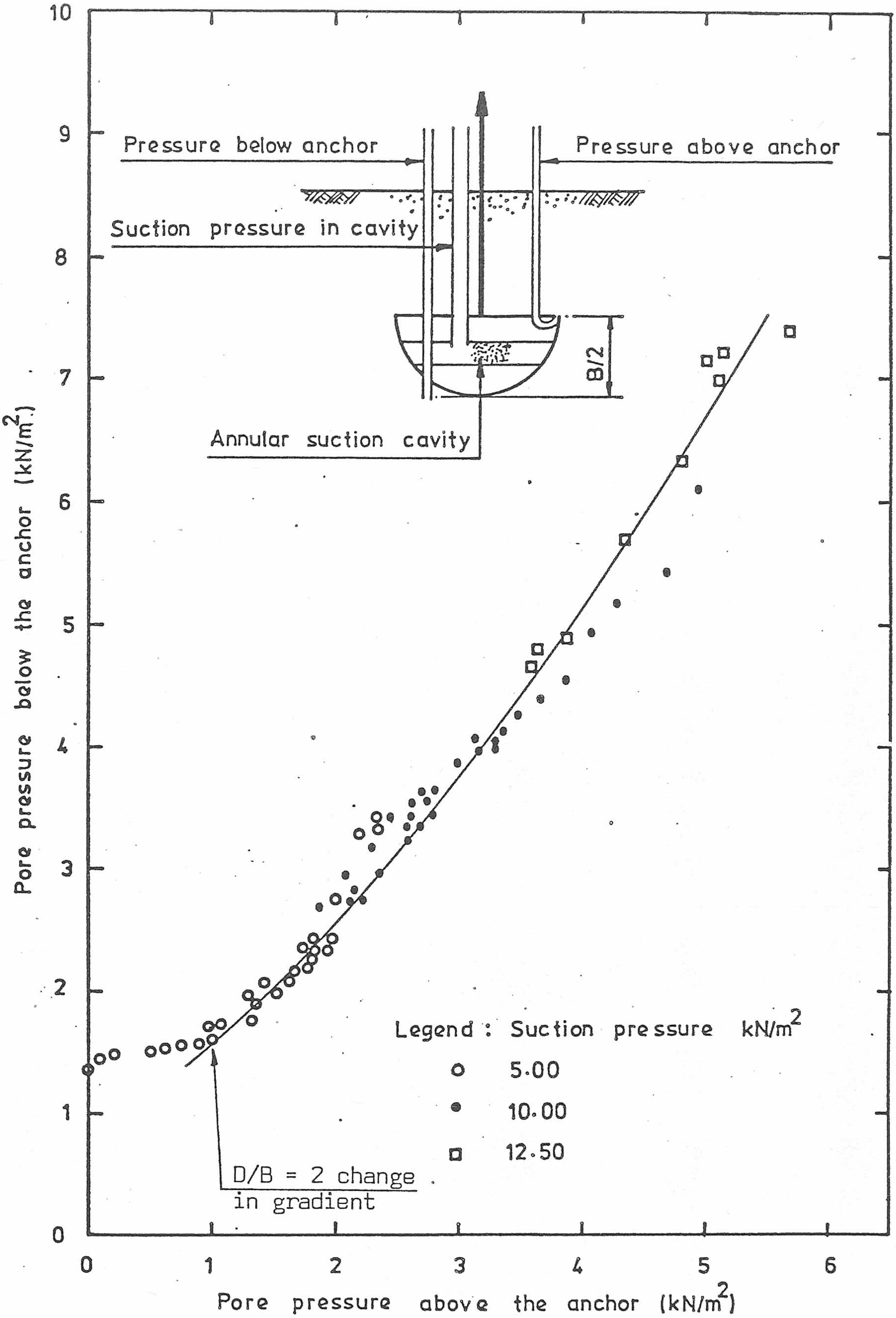

Fig. 3.39 Relationship between pore pressures below and above the 102 mm suction anchor.

PAGE NO 98 BLANK.

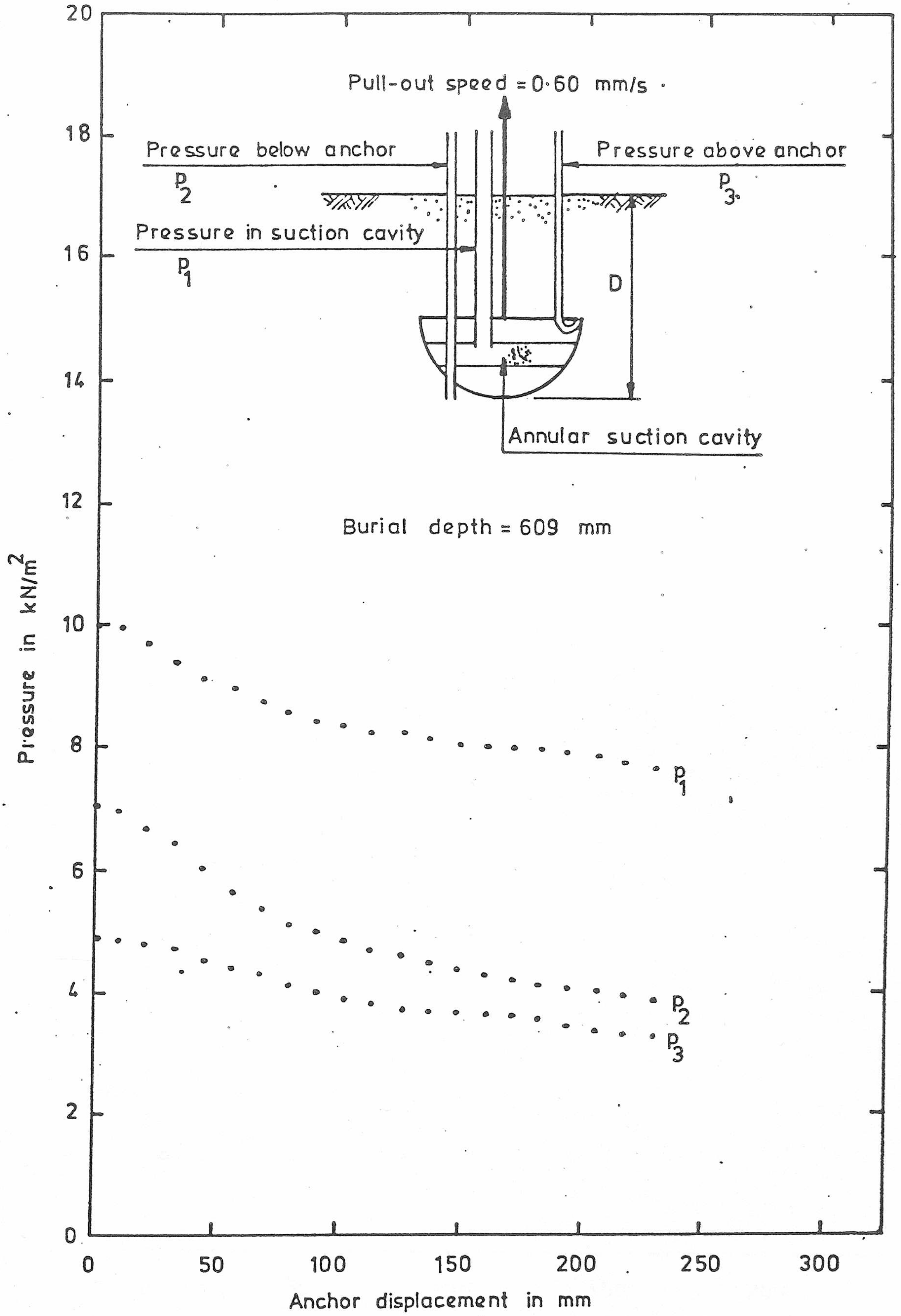

Fig. 3·40 Pressure against anchor displacement for 102 mm suction anchor.

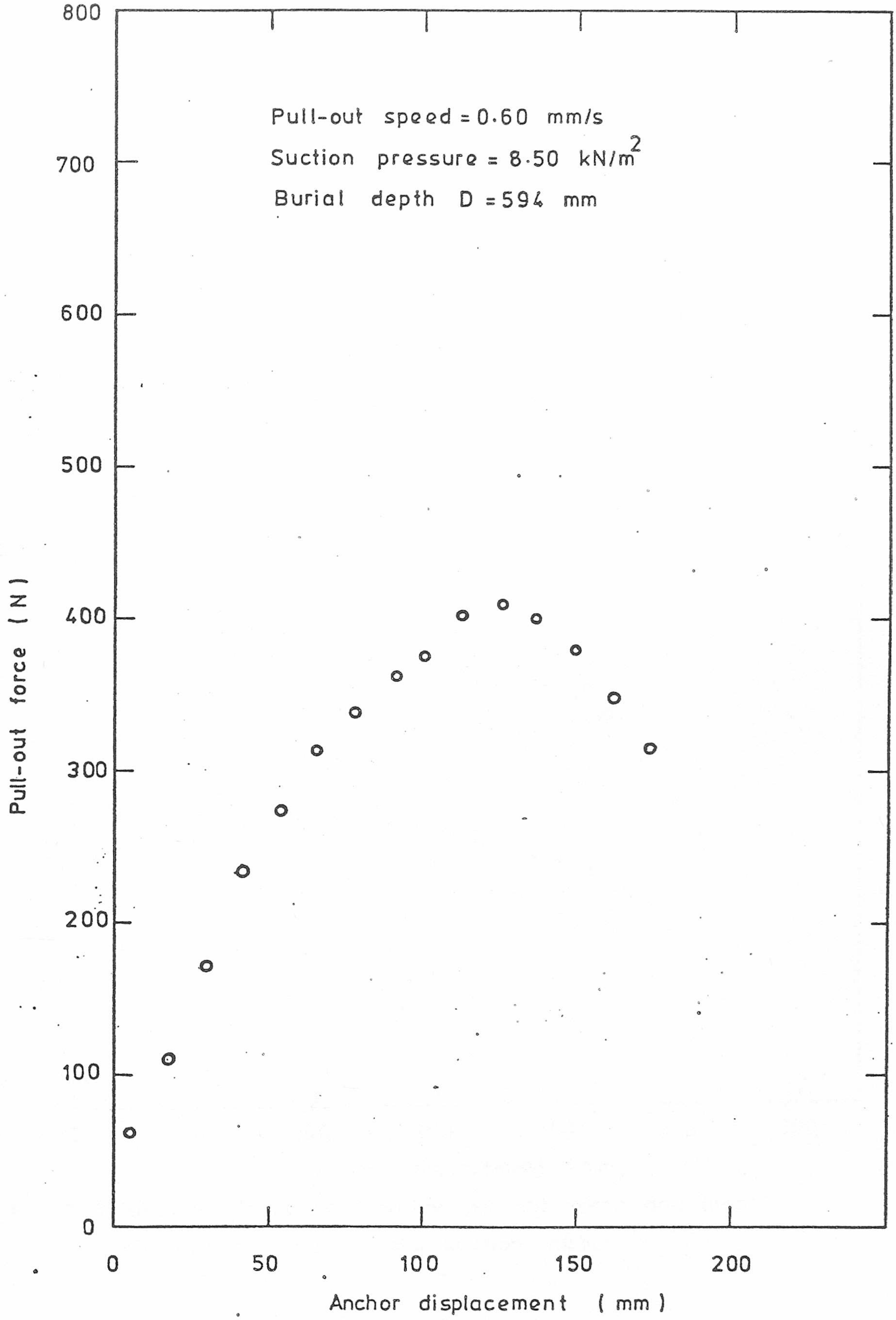

Fig. 3.41 Relationship between anchor pull-out force and anchor displacement for 70 mm suction anchor.

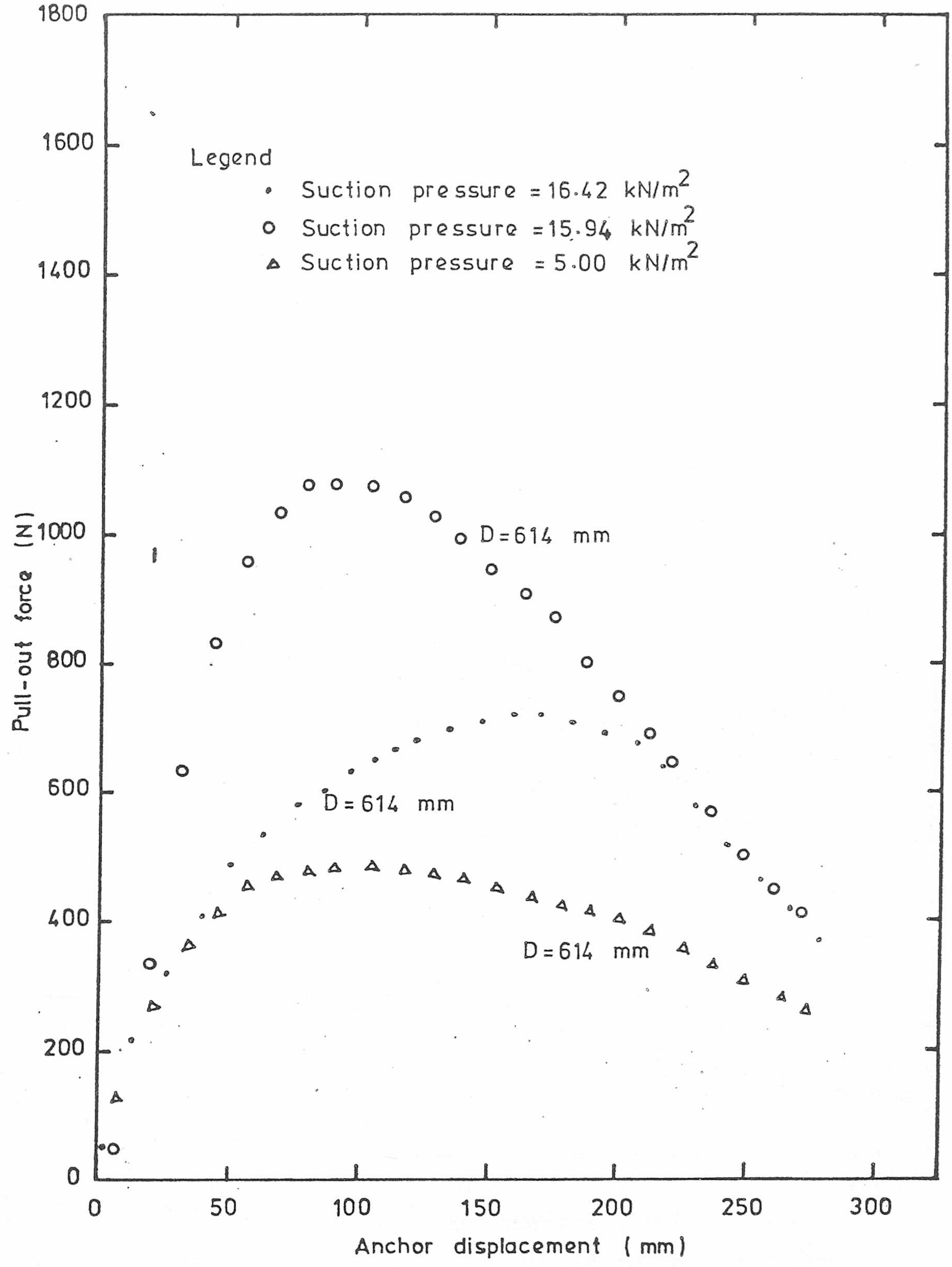

Fig 3.42 Relationship between anchor pull-out force and anchor displacement for 102 mm suction anchor

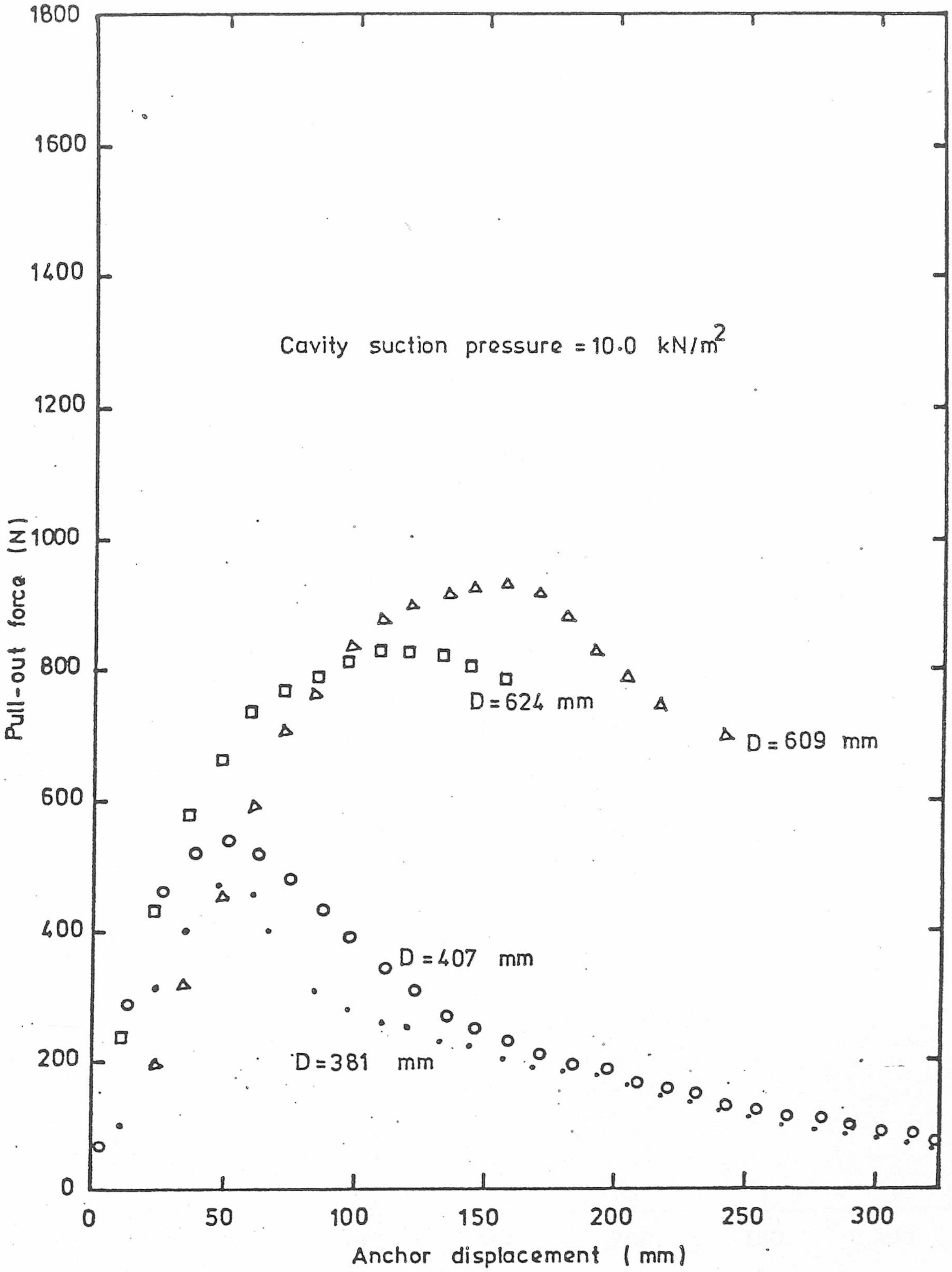

Fig 3.43 Relationship between anchor pull-out force and anchor displacement for 102 mm suction anchor

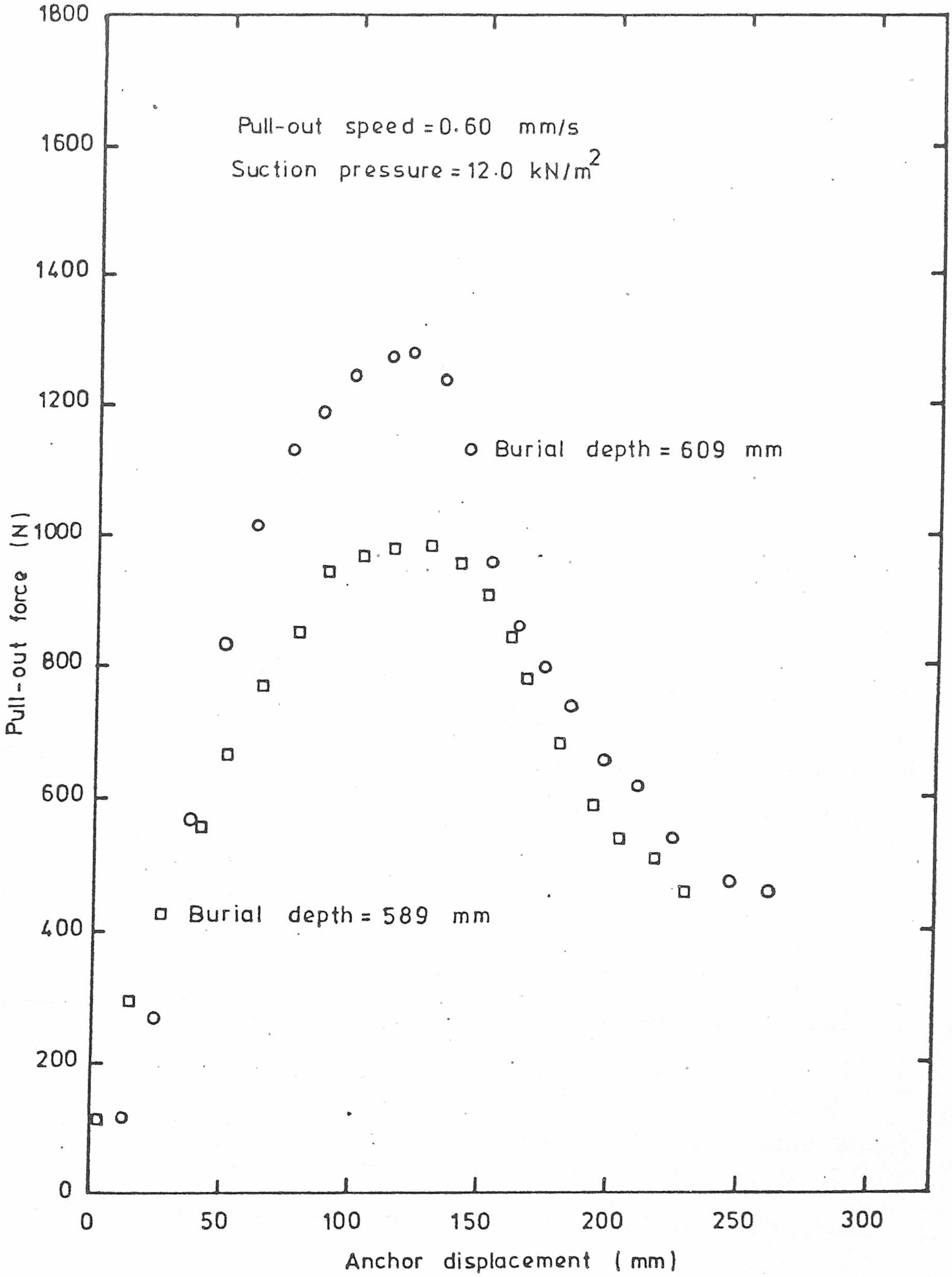

Fig 3.44 Relationship between anchor pull-out force and anchor displacement for 102 mm suction anchor

3.6.4 Pull-out Tests on the Anchor Shaft with or without Suction Pressure

The first test series on the anchor shaft was without suction pressure. The anchor shaft was pushed into the sand bed vertically to the required burial depth by using the dead weights on top of the anchor shaft and was located by the locating plate as shown in Fig. 3.14. The sand was levelled at the surface. The shaft was left buried at least 12 hours in the sand before the pull-out test took place. The shaft was pulled-out beyond the limit of maximum frictional force. More tests on the anchor shaft were conducted at different depths.

The second series of pull-out tests on the anchor shaft was with suction pressure. The anchor shaft was pushed vertically into the sand bed by using the locating plate as mentioned above. The 102 mm suction anchor was located by hand about 40 to 50 mm below the bottom of the anchor shaft. There was no connection between the anchor shaft and the suction anchor. The anchor shaft and the anchor were placed at the desired burial depth and the required suction pressure in the anchor cavity was achieved. The sand was levelled. The shaft was pulled out by the Hounsfield Tensometer. Additional tests were performed in a similar manner for various burial depths.

Fig. 3.45 shows the relationship between anchor shaft skin friction force and shaft burial depth with suction pressures of 0.0, 7.5 and ranging from 8.49 to 22.51 kN/m^2.

3.6.5 Pull-out Tests on the Prototype Suction Anchor

A 600 mm hemispherical suction anchor was used for sea tests. A load cell with a tensile capacity of 100 kN, a pressure transducer with a pressure range of 0 to 517 kN/m^2, an orifice plate in the pipe system with pressure gauges either side, a pressure gauge

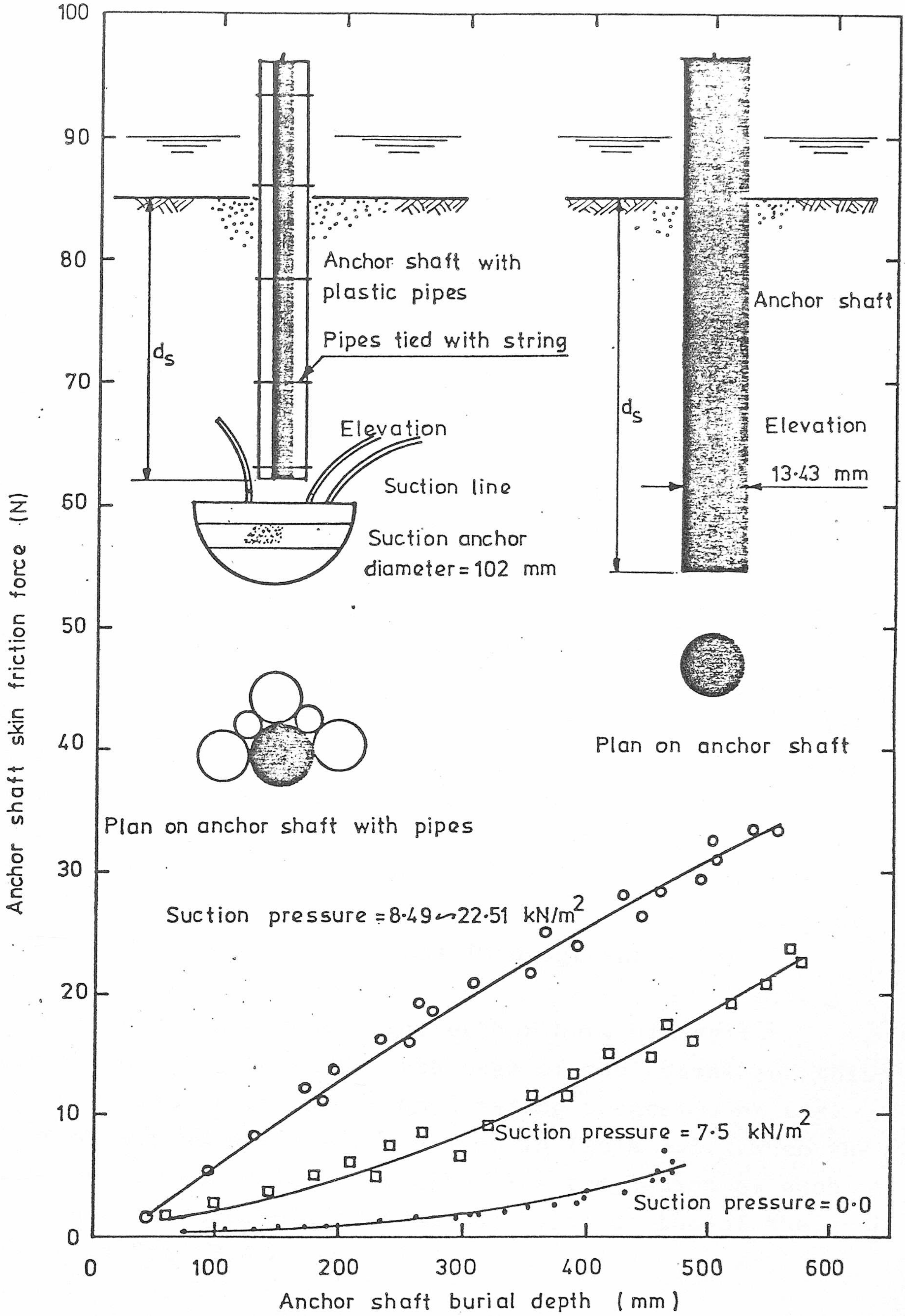

Fig. 3·45 Anchor shaft skin friction force/burial depth with or without suction pressure ahead of the anchor shaft.

attached to the pump (22 kW diesel engine) between the inlet and outlet, one vacuum and pressure gauge close to the main jet and a vacuum gauge were used to determine the pull-out force, anchor depth and water pressure inside the anchor box, water flow measurement, head of water on the pump gauge, water pressure at main jet and negative water pressure in the anchor suction cavity. Readings of the load cell and pressure transducer were automatically recorded on a chart recorder. The readings from the pressure gauges were manually recorded.

The anchor was buried by using the jet supply from the pump situated on the vessel. The anchor was attached to the 76 mm hose at the outlet delivery end with extension pipes. The arrangement of the pump and the pipe systems are shown in Fig. 3.16. The jetting was turned off and the suction was put on. The soil was not levelled in these tests. All tests were performed from the Institute's 60-ton schooner 'Robert Gordon' using the vessel's anchor chain and windlass. The tests were conducted during calm sea conditions in shallow water and in a cohesionless soil bed. All tests were started at the rise of tide to achieve tension in the anchor line and finished before the turn of the tide. A nylon rope was used to minimise the effect of the pulsating force. Fig. 3.15 shows a photograph of the 60-ton schooner 'Robert Gordon' while a test was in progress.

During the sea tests, the author hurt him-self accidently due to the sudden stoppage of the vessel and this led to curtailment of the anchor testing programme at sea. The tests carried out are summarized in Table 3.3. When the suction anchor was pulled-out after the completion of each test, generally a sample of sand was lying on top of the anchor as shown in Fig. 3.46

Table 3.3 Summary of the 600 mm anchor test results

1	2	3		4	5	6	7	8
Test No.	Burial depth D (m)	Pull-out force (kN) Maximum steady	Mimimum impulse	Suction pressure (kN/m^2)	$\frac{D}{B}$	$\frac{Q_u}{\gamma' AD}$	$\frac{p_1}{\gamma' D}$	Remarks
1	2.3	-	-	-	-	-	-	Discontinued due to leaks.
2	2.3	6.0	-	0	3.9	1.00	0	Pull-out doubtful.
3	5.0	-	-	22	-	-	-	Discontinued beyond pull-out capacity & damaged the load cell.
4	-	-	-	-	-	-	-	Discontinued due to damage to the pressure transducer.
5	5.0	15.5	27.0	0	8.4	0.71, steady, 1.24, impulse	0	Suction initially but reducing to zero due to leaks. Anchor retrieved by jetting

Table 3.3 (cont'd)

1	2	3		4	5	6	7	8
Test No.	Burial depth	Pull-out force (kN) Maximum steady	Minimum impulse	Suction pressure (kN/m^2)	$\frac{D}{B}$	$\frac{Q_u}{\gamma' AD}$	$\frac{p_1}{\gamma' D}$	Remarks
6	3.6	29.0 no pull-out	38	0 finally	6.0	2.97 steady, 3.94 impulse	0 finally	Some suction initially, reducing to a small value due to leaks.
7	2.20	13.6 pull-out	Calm	9 to 14 estimated	3.67	2.34	1.66 to 2.54 estimated	High suction at beginning, estimated from pump gauge.
8	2.92	17.5 pull-out	calm	2.5	4.87	2.31	0.49	Good suction at beginning but low suction at pull-out.
9	3.40	32.5	46.5	22	5.67	3.69	4.00	No pull-out.
10	2.18	37	calm	19	3.63	6.56	3.52	No pull-out.
11	2.18	37 pull-out	calm	15	3.63	6.56	2.73	Since no failure obtained pump turned off & suction pressure allowed to reduce naturally.

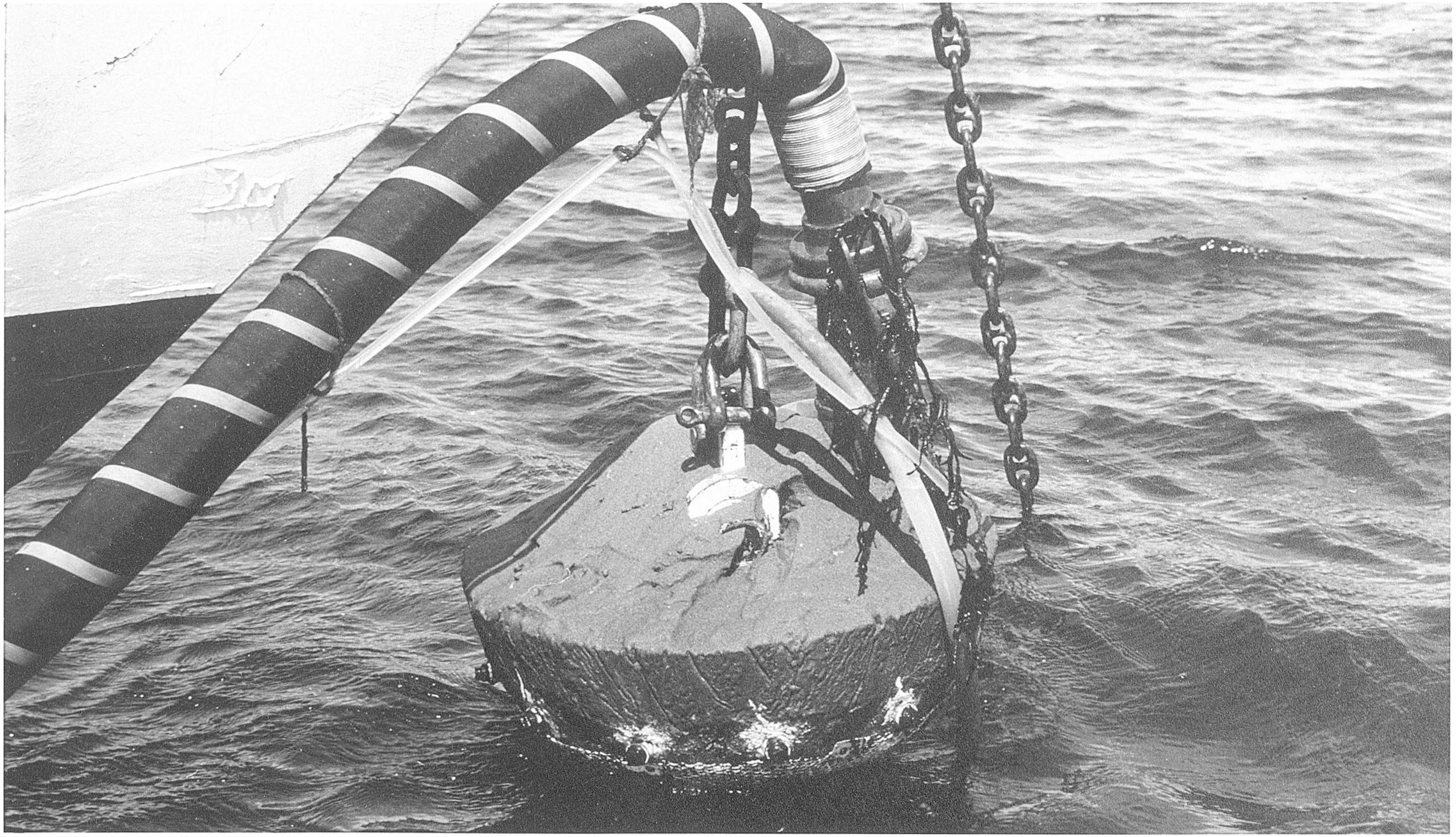

Fig. 3.46 Photograph of the 600 mm suction anchor pulled-out to surface after a test.

3.7 PHOTOGRAPHIC ILLUSTRATION OF THE SUCTION ANCHOR

The 102 mm suction snchor was chosen for the photographic illustration. Fig. 3.47 shows a photograph of the crater formed due to the applied suction pressure of 10.54 kN/m^2 at the anchor suction cavity after the jets were turned off and also due to the effect of jetting because the sand particles were carried away.

The anchor was buried to a depth of 551 mm. A suction pressure of 12.45 kN/m^2 was achieved and the sand surface was levelled. The anchor was pulled-out at a speed of 0.60 mm/s and stopped about 15 to 20 seconds for taking photographs. Fig. 3.48 shows a photograph of the sand displacement close to the anchor shaft when the anchor was raised 150 mm from its initial position. Fig. 3.49 shows a further displacement of the sand at an anchor total movement of 406 mm. Fig. 3.50 shows the displaced sand when the anchor was raised by a total distance of 539 mm. Fig. 3.51 shows a photograph of the anchor and sand when further displaced. Fig. 3.52 shows that some sand remains attached to the anchor suction filter. The suction filter remained covered with sand as long as suction was continued.

The final sand movement at surface level was 89 mm. The approximate diameter of the displaced sand was 275 mm with the suction pressure and 320 mm without the suction pressure.

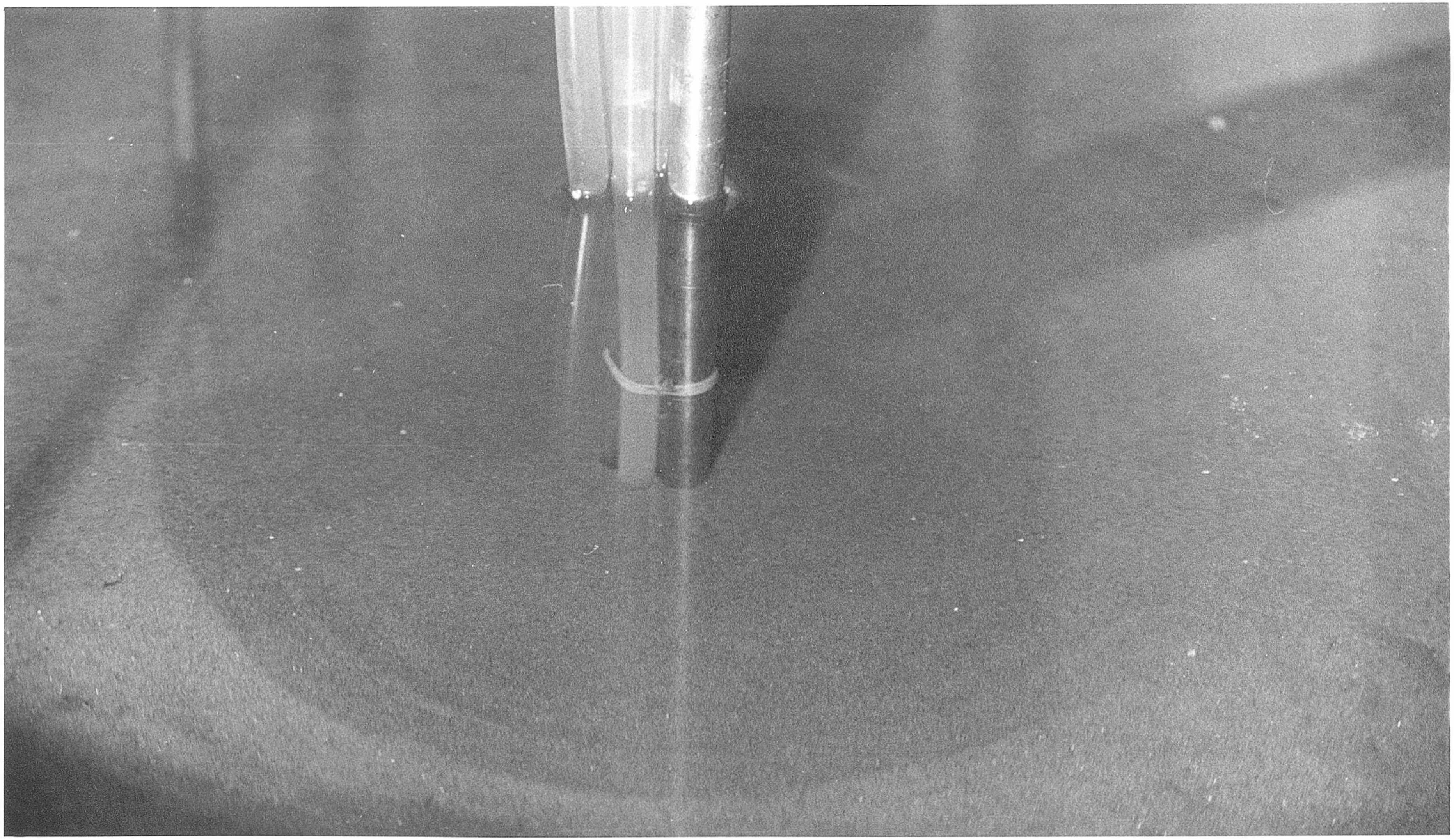

Fig. 3.47 Photograph of the crater formed by the jetting and the suction pressure of $10.54\ kN/m^2$ at the anchor suction cavity.

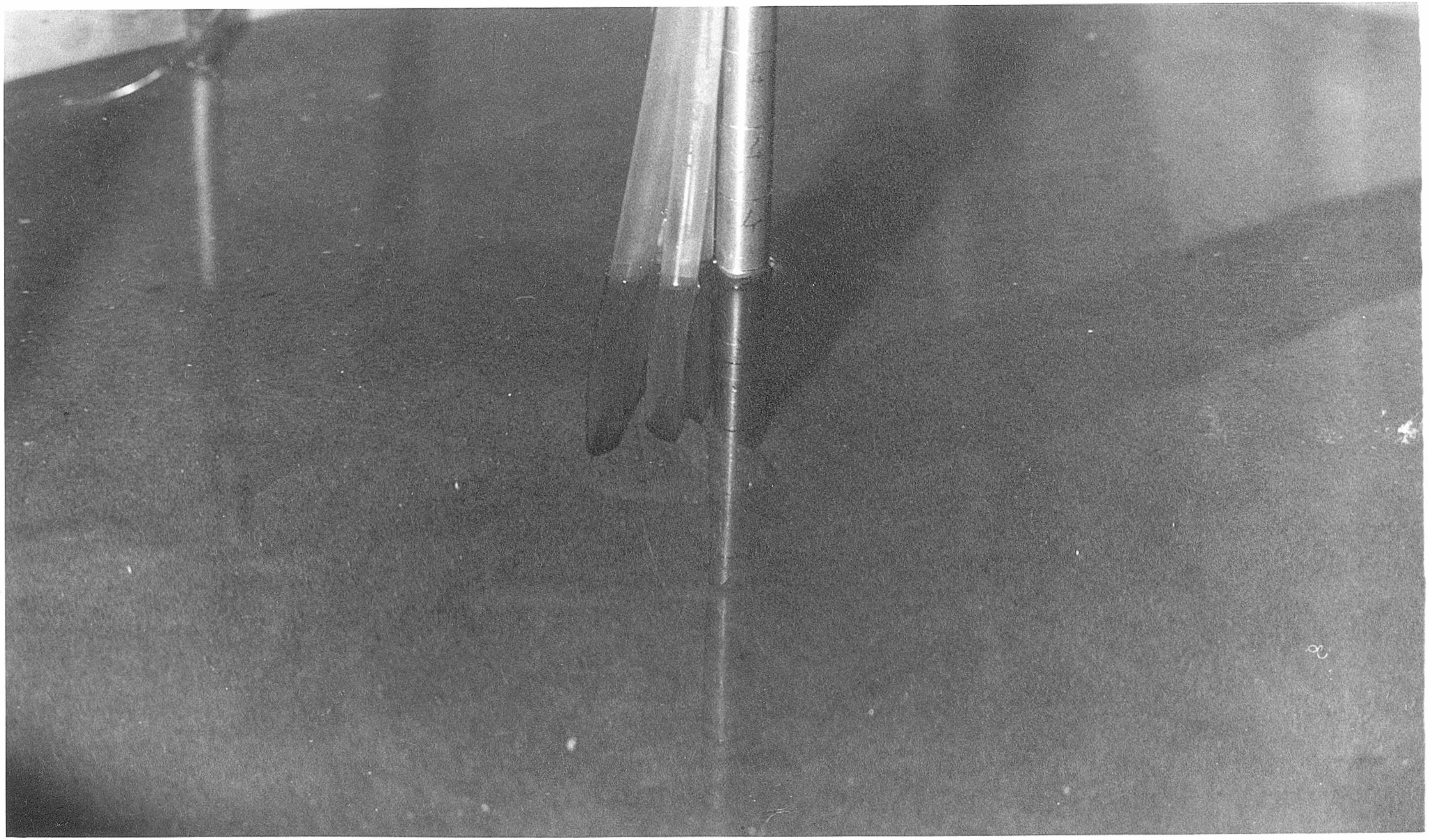

Fig. 3.48 Photograph of the sand displacement when the anchor was moved by a distance of 150 mm.

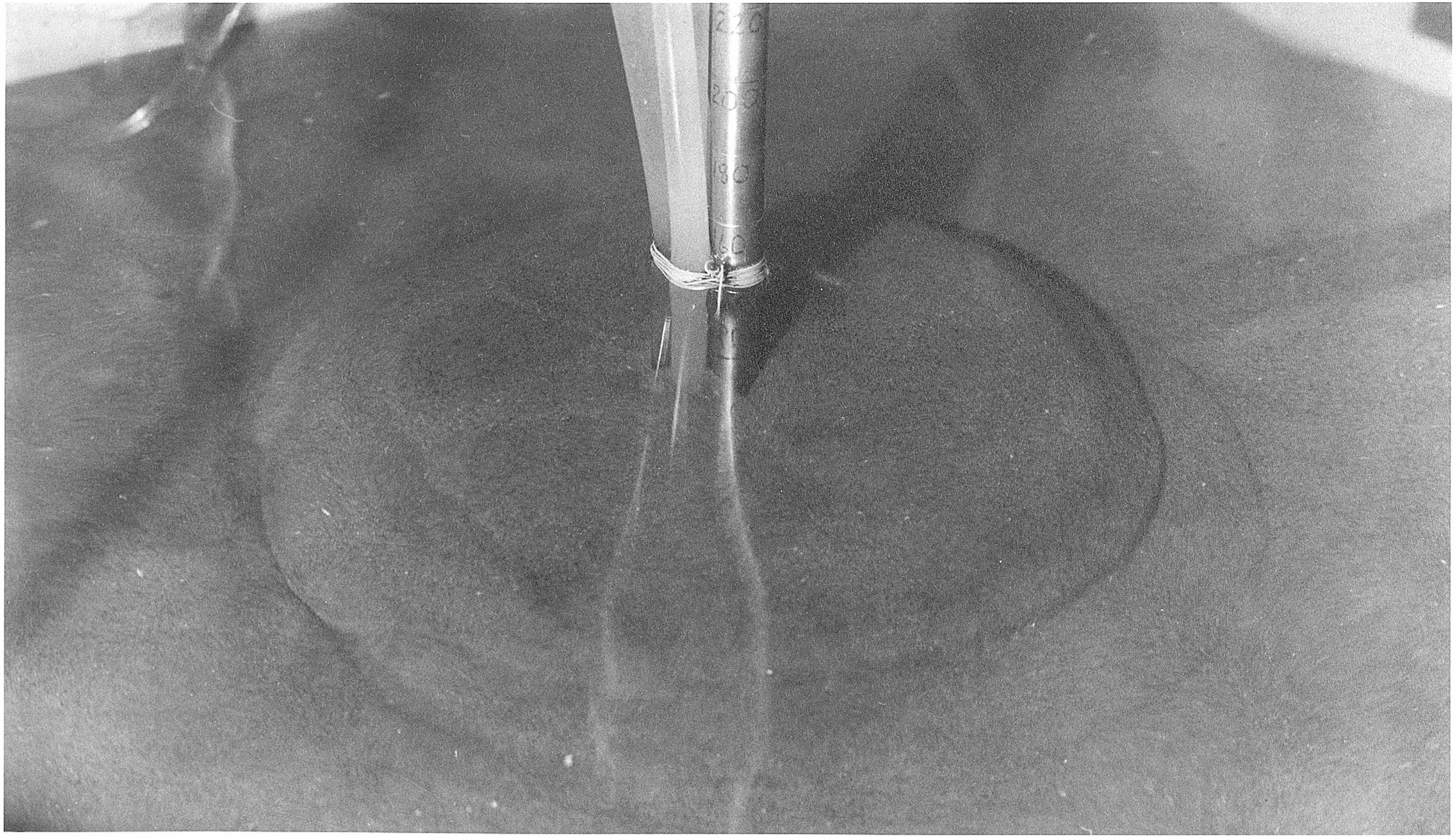

Fig. 3.49 Photograph of the sand displacement when the anchor was moved by a distance of 406 mm.

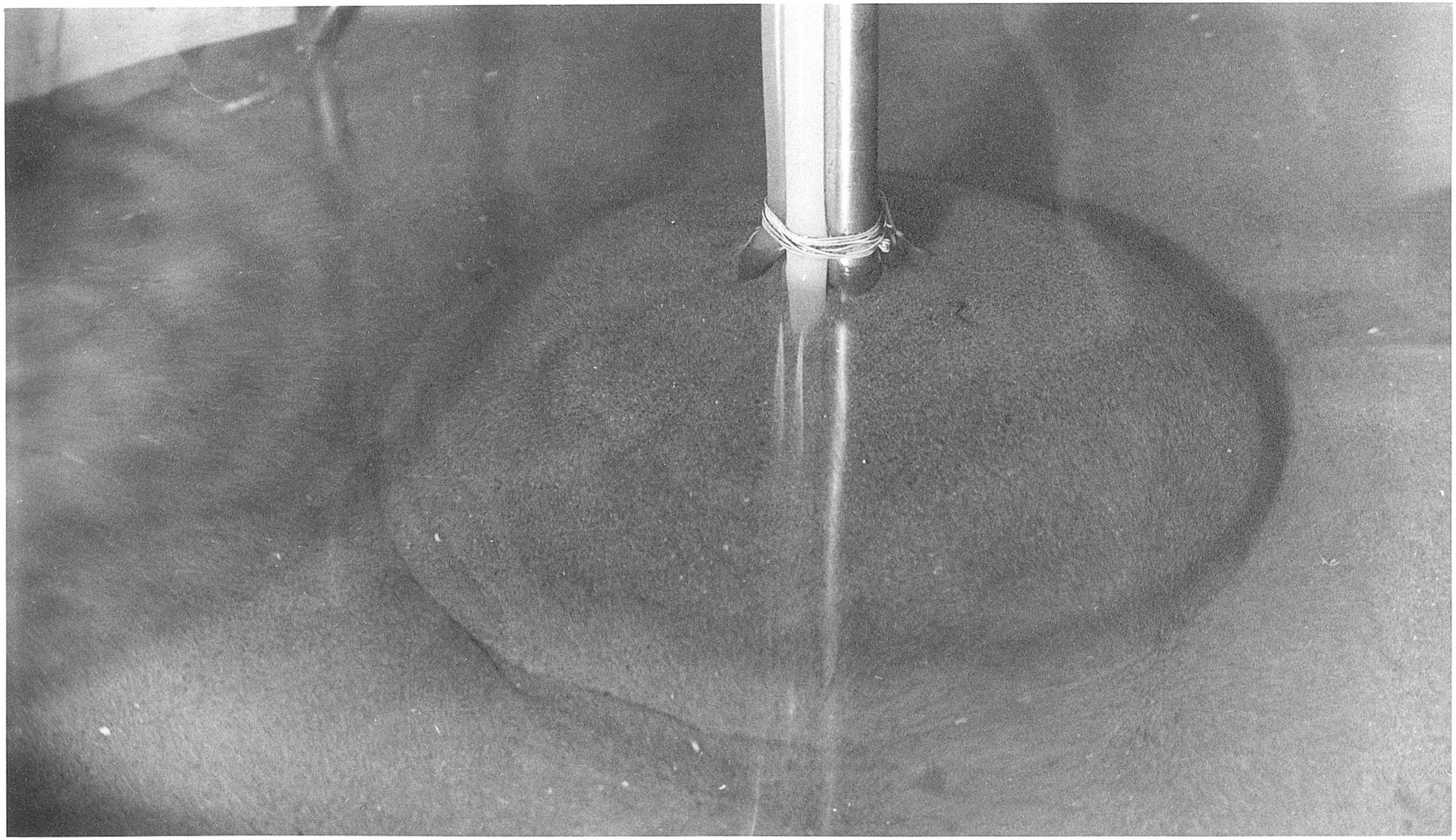

Fig. 3.50 Photograph of the displaced sand when the anchor was moved by a total distance of 539 mm.

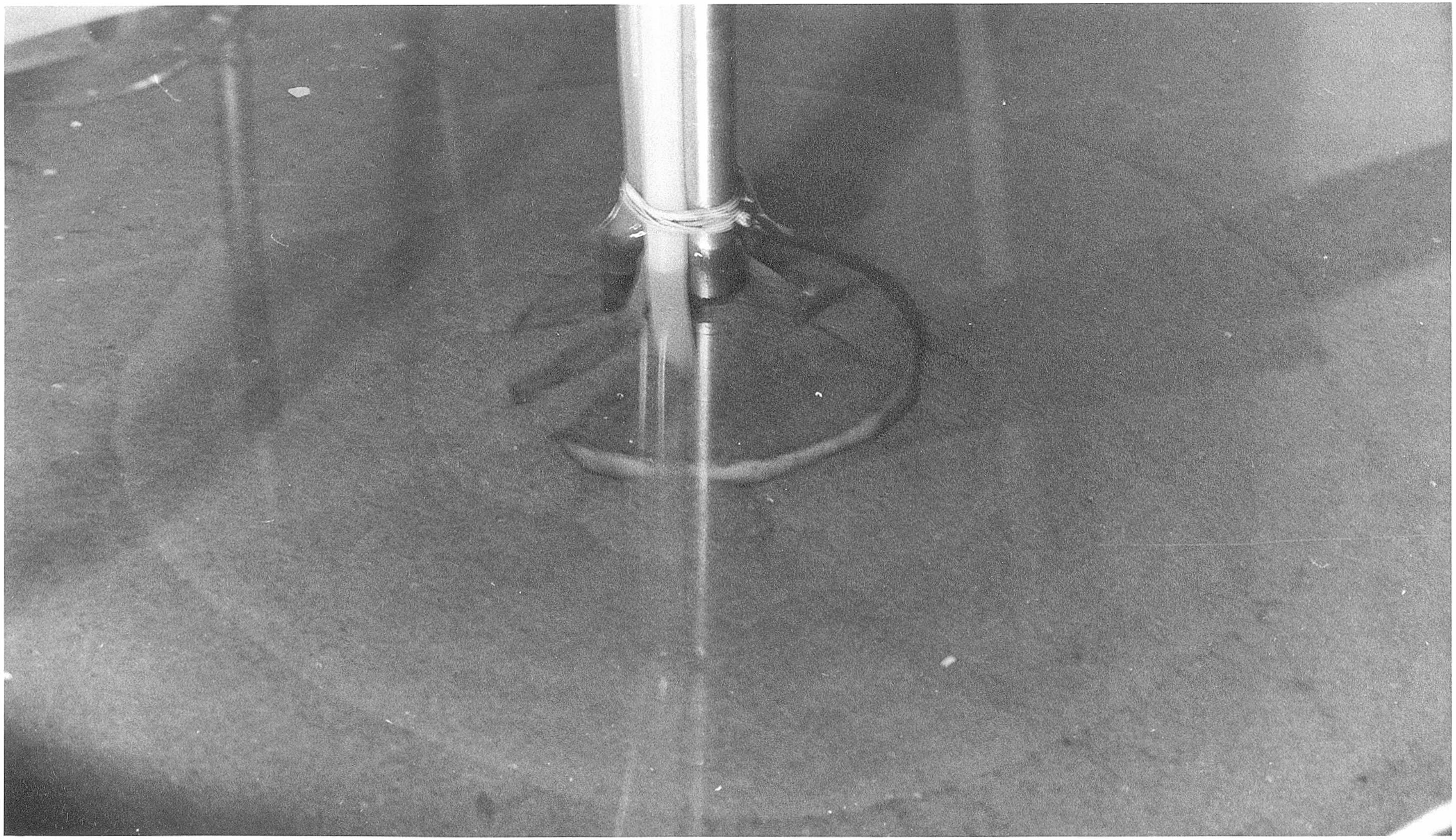

Fig. 3.51 Photograph of the anchor and sand displacements.

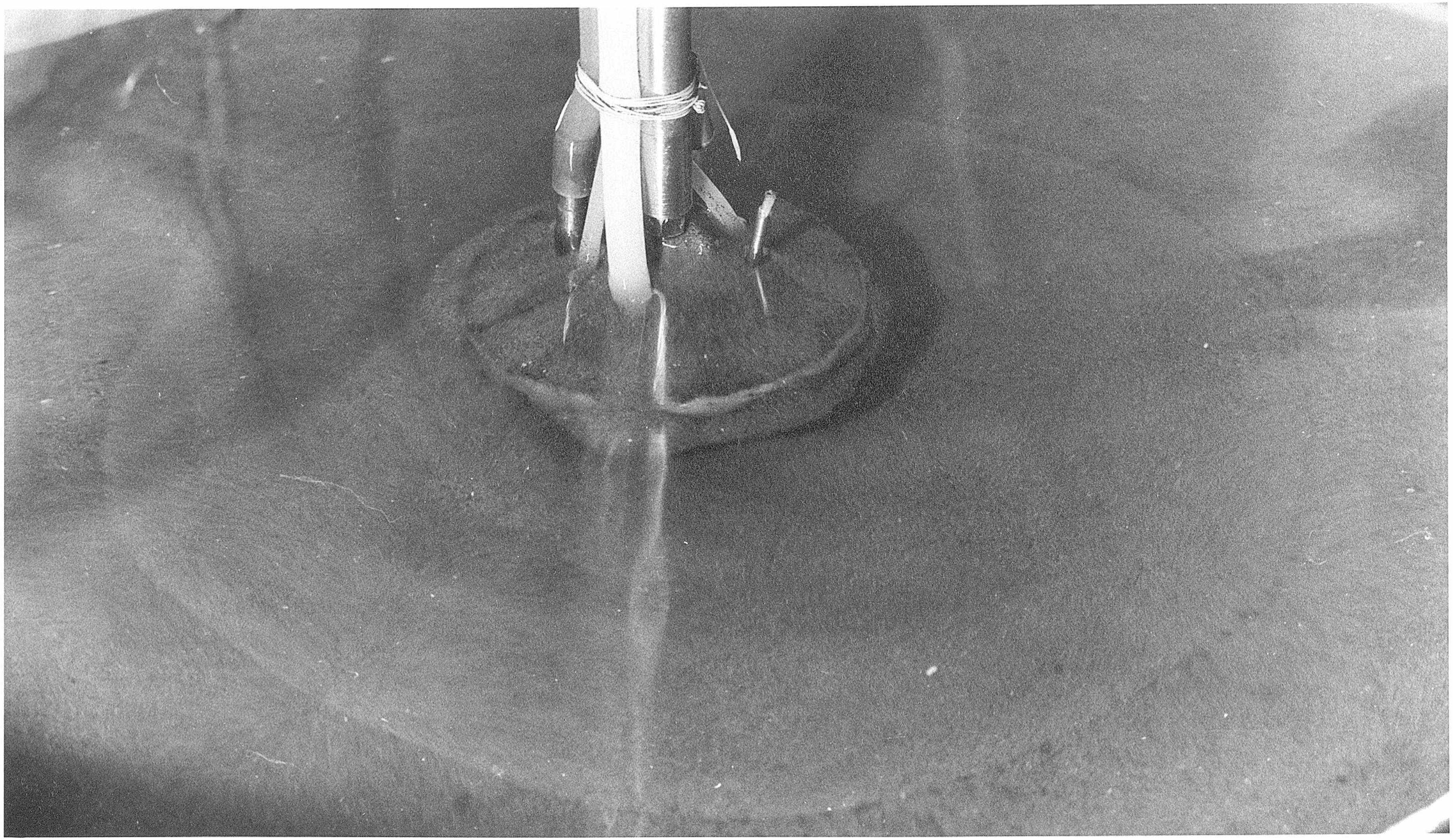

Fig. 3.52 Photograph of a further displacement of the anchor and the sand.

CHAPTER 4

GENERAL DISCUSSION

4.1 INTRODUCTION

As far as the author knows, this is the first study in which embedded suction anchors of the type described earlier have been subjected to uplift pull. It was realised at the commencement that this is a large research project requiring consideration of many parameters before the behaviour of such anchors is fully understood.

In general, brief information will be given on the experimental investigation and where necessary detailed information on the uplift test data will be reported. Comments will be made firstly on the present experimental investigation, secondly on the test data analysis for uplift resistance and comparing uplift tests with some of the theories discussed in Chapter 2.

4.2 EXPERIMENTAL INVESTIGATION

Six model-scale anchors and one prototype anchor were tested to evaluate their uplift resistance capacity in the laboratory and at sea respectively. Their physical details are listed in Table 3.1. Different ratios of filter area to anchor plan area were employed, but with the same type of filter, to investigate the effect on the pull-out resistance of the anchors. A number of tests were performed with various cavity suction pressures, different suction times and various embedment depths for water flow measurement through the anchor filter and for pull-out resistance of the anchors. All the tests conducted are plotted in Chapter 3.

4.2.1 Properties of the Test Soils

The particle size distribution curves are plotted in Fig. 3.17. The soils possess similar gradings. Soils No. 2 to 5 were collected from the anchor top after completing the test and these results represent the true particle grading only of the collected soil samples; but they confirm that the seabed is a cohesionless soil. The angle of internal friction φ, in loose and dense state, was investigated by using a conventional shear box apparatus. A number of shear box tests were also carried out on Soils No. 2 to 5 in the wet state and their moisture contents were also found. The relative density of Soil No. 1 is 0.557 and this indicates that the sand is in a medium state. All the soil particles round in shape and the sands are uniformly graded. The permeability coefficient of Soil No. 1 was found by using a constant head permeability apparatus. The permeability coefficients were also evaluated by using Hazen's formula for all the soils. The coefficient of permeability of 0.26 mm/s was determined by using Hazen's formula for Soil No. 1, but by the experimental test, this coefficient was 0.46 mm/s. This indicates that Hazen's formula underestimates the coefficient of permeability by 43.5% for Soil No. 1.

4.2.2 Flow Measurement Tests on Model Suction Anchors

The flow measurement tests were performed on 70 mm, 102 mm and 145 mm suction anchors to determine the relationship between the applied suction pressure in the anchor suction cavity and the water flow through the suction cavity of the anchor. The water level in the testing tank was kept approximately constant. The sand was levelled for all tests to avoid an uneven surface. The results are plotted for 70 mm, 102 mm and 145 mm suction anchors in Fig. 3.18 to 3.20 respectively. The plots of the test results show a linear relationship between cavity suction and flow rate at a given burial depth. The cross-plot presentations in Fig. 3.21

to Fig. 3.23 indicate that if a specific water flow through the anchor cavity is required to be maintained then a higher suction pressure is needed at a deep burial in comparison with a shallow burial. For example, to achieve a water flow of $100 \times 10^{-6} m^3/s$ through the anchor suction cavity for the 145 mm suction anchor buried at 100 mm and 600 mm deep in the sand bed, from Fig. 3.23, the required suction pressure will be 8.88 kN/m^2 and 15.5 kN/m^2 respectively.

4.2.3 Pull-out Tests on the Model Anchors with no Suction

Fig. 3.24 shows a plot between pull-out resistance and anchor burial depth for 70 mm, 102 mm, 108 mm and 145 mm anchors. The pull-out force of the 70 mm anchor is increasing at a slower rate even beyond a burial depth of 600 mm. Curves for the 102 mm and 108 mm anchors appear to be following a similar pattern. The pull-out force of the 102 mm anchor has reached a maximum value at about 550 mm. The 145 mm anchor curve is still rising at a steeper slope even beyond 550 mm. Fig. 3.25 shows some more test results for the 70 mm anchors. Three series of tests were performed; for example, one on the solid anchor, one on the suction anchor without pipes and one on the suction anchor with pipes. The test results indicate a rather wide scatter of points, which is to be expected due to the anchor being with or without pipes. One test series indicates a good agreement of test results within the series and overall this series is in reasonable agreement with the other test series.

4.2.4 Pull-out Tests on the Model Suction Anchors

Fig. 3.26 shows the relationship between pull-out force and burial depth for the 70 mm and 102 mm suction anchors with the maximum suction pressure obtained from the pump in the suction cavity. The pull-out force for both curves is increasing in a similar pattern up to a burial depth of 250 mm and then the 102 mm anchor curve is rising at a steeper slope in comparison with the 70 mm anchor curve. Fig. 3.26 also defines the limit of maximum suction pressure which can be achieved for these anchors by the pump.-

84 tests were conducted on the 70 mm suction anchor at a constant anchor suction pressure of 6.0 kN/m^2 but varying the suction time from 2 to 15 minutes. The test results are plotted in Fig. 3.27 and show a random scatter though in general they are in good agreement. From this, it appears that for the test sand, the suction time beyond 2 to 15 minutes range does not affect the pull-out capacity of the anchor.

Fig. 3.28 shows the relationship between pull-out force and anchor burial depth for the 70 mm suction anchor with suction pressures of 5.0 kN/m^2 and 7.5 kN/m^2. The test results indicate a rather wide scatter of points. This is due to the unknown period required for suction time because the tests reported in Fig. 3.27 were not fully investigated prior to the pull-out test data plot Fig. 3.28.

Fig. 3.29 shows the relationship between pull-out force and anchor burial depth for the 102 mm suction anchor with a suction pressure range of 0.0 kN/m^2 to 12.5 kN/m^2. All the curves with suction pressure applied show a good relationship among themselves and follow a similar pattern. Pull-out force increases with increasing burial depth and cavity suction pressure. These curves are cross-plotted in Fig. 3.30 to give the relationship between the anchor pull-out force and anchor cavity suction pressure at given depths. It appears from this plot that the pull-out force increases approximately linearly with an increase in suction pressure. It also shows that the rate of change of pull-out force with cavity suction pressure increases with increasing burial depth. The same data are plotted in non-dimensional terms in Fig. 4.1 and 4.2.

4.2.5 Pore Pressure Distribution

Three pressure transducers were used to determine the pore water pressures below (p_2), above (p_3) and above top (p_4) the 102 mm suction anchor. A water manometer was used to measure the pressure p_1 in the anchor cavity. Fig. 3.31 to 3.38 show the relationship between pressures p_1, p_2, p_3 (and where applicable the pressure p_4) and the pull-out force. During the start of the anchor pull-out test, the pressures p_1 and p_2 generally increased by 4.5% and 2% respectively, but for one test in Fig. 3.34, where all the pressures decreased. Pressure p_3 generally reduced. Table 4.1 shows the change of pressures as percentages at the ultimate pull-out force. There is only one test at the ultimate pull-out force during which pressures were increased, e.g. $p_1 = 0\%$, $p_2 = 4.5\%$ and $p_3 = 3.3\%$. This is shown in Fig. 3.33.

Fig. 3.39 shows the relationship between pore pressures below and above the 102 mm suction anchor before the pull-out test was started. Suction pressures of 10.0 kN/m^2 and 12.5 kN/m^2 were obtained at relative depths deeper than D/B = 0.78 and D/B = 3.5 respectively. For the 5.0 kN/m^2 pressure, the anchor top was brought to the sand surface and on doing this, the pressure on top of the anchor was completely eliminated. At D/B = 2, a change in gradient occurs as shown in Fig. 3.39. The pore water suction pressure below the anchor increases rapidly after reaching the relative depth D/B = 2 from the sand surface.

4.2.6 Vertical Displacement of the 70 mm and 102 mm Suction Anchors

Vertical displacements of the anchor are not corrected to take into consideration the elongation of the anchor shaft, chain and wire rope. Also the initial tensioning effect of the chain and the wire rope was ignored. The effect due to the elongation of chain and shaft is negligible in comparison with the anchor displacements. But, the initial tensioning effect of the wire rope may be significant for small anchor displacements though it does not make a significant change in the anchor displacement at pull-out.

Pressures p_1, p_2 and p_3 versus anchor displacement are shown in Fig. 3.40. During this test, the pressures were reducing as the anchor was advancing towards a greater displacement. Fig. 3.41 to 3.44 show relationships between pull-out force and anchor displacement. The cavity suction pressure and anchor burial depth are also stated in these figures. In Fig. 3.41, the 70 mm suction anchor with suction pressure of 8.50 kN/m^2 gives an ultimate pull-out force of 416 N. The graph is a straight line in the early stage and later becoming a curve. Fig. 3.42 shows plots of pull-out force against anchor displacement for the 102 mm suction anchor. Three curves are plotted in this figure at a constant burial depth of 614 mm with suction pressures of 5.0, 15.94 and 16.42 kN/m^2. At these pressures the ultimate pull-out forces are 486, 1073 and 724 N and the anchor displacements are 94, 92 and 170 mm respectively. It appears from this graph that the maximum ultimate load is at the minimum anchor displacement with suction pressure of 15.94 kN/m^2 and the maximum anchor displacement is for the maximum suction pressure of 16.42 kN/m^2 which is giving a relatively low pull-out force. Fig. 3.43 shows the relationship between pull-out force and anchor displacement for different depths at a constant cavity suction pressure of

10.0 kN/m^2. Anchor displacements for burial depths of 381 and 407 mm are of similar pattern. At shallow burials, the pull-out force reaches its maximum value at a relatively small displacements. Fig. 3.44 shows the relationship between pull-out force and anchor displacement for the 102 mm suction anchor at burial depths of 589 and 609 mm with a constant suction pressure of 12.0 kN/m^2. The pull-out force increases linearly within the elastic limit of the soil. The force rapidly decreases on reaching the peak value as the anchor displacement advances. Two tests of the 102 mm suction anchor reached a peak pull-out force at displacements of 50 mm and are shown in Fig. 3.43. For the other tests, the ultimate pull-out force is not reached until the anchor is at least displaced by 100 mm.

4.2.7 Pull-out Tests on the Anchor Shaft with or without Suction Pressure

Fig. 3.45 shows the plot of anchor shaft skin friction force against burial depth with or without suction pressure ahead of the anchor shaft. Consider the test results of Fig. 3.24, 3.29 and 3.45. The anchor shaft skin frictional force increases the ultimate pull-out resistance of the 70, 102, 108 and 145 mm anchors up to 10%, 5.5%, 5% and 3.75% respectively, which is without a suction pressure. The 102 mm suction anchor at a cavity suction pressure of 7.5 kN/m^2 would have its ultimate pull-out force increased by up to 2.75% due to the frictional resistance of the anchor shaft.

In this study, the influence of the anchor shaft on the anchor pull-out forces is ignored because the effect of 2.75% on the pull-out resistance of the 102 mm suction anchor is not considered to be high enough for an allowance to be necessary.

Table 4.1 Changes of pressure in percentages at the ultimate pull-out force.

Fig. No.	$\frac{D}{B}$	$\frac{d_a}{B}$	Changes of pressure in %				Remarks for pressures
			P_1	P_2	P_3	P_4	
3.31	6.02	0.92	10.0	27.1	20.3	---	reduced
3,32	3,99	C.50	3.6	3.3	5.4	---	reduced
3.33	3.74	0.47	0.0	4.5	3.3	---	increased
3.34	5.97	1.41	18.1	36.4	23.9	---	reduced
3.35	6.02	0.90	16.8	22.7	15.3	---	reduced
3.36	6.02	1.67	6.2	46.8	41.6	---	reduced
3.37	5.97	1.06	15.8	23.5	21.1	15.2	reduced
3.38	5.77	1.21	10.3	24.2	61.1	6.7	reduced

d_a/B = displacement factor

4.2.8 Pull-out Tests on the Prototype Suction Anchor

Pull-out tests on the 600 mm suction anchor are listed in Table 3.3 with the concluding remarks. Burial of the anchor was achieved as soon as possible after the anchor was lowered on to the sea bed because the rise of tide could lead to a false burial depth. Tension on the anchor cable was primarily achieved by the rise of tide because the anchor winch capacity of the 'Robert Gordon' was limited to 10 kN. Initial loads on the anchor were applied up to 5 kN. Further loads on the anchor were gradually increased because of the rise of tide.

Test No. 11 is plotted in Fig. 4.1 and is in good agreement with the plots of the 102 mm suction anchor.

4.2.9 Photographic Illustration of the 102 mm Suction Anchor

Fig. 3.47 to 3.52 show the photographs of the testing tank, anchor buried in the sand and the anchor above the sand surface level. Initially the anchor was embedded to a relative depth of D/B equal to 5.40 and sand displacement was not observed at the initial pull-out stage. Once the soil was displaced around the anchor shaft it formed a shape like a dome. As the anchor displacement advanced further and further, the dome became bigger and bigger as shown in Fig. 3.48 to 3.50. The vertical sand movement was 89 mm at the dome apex and its diameter was 275 mm. The dome collapsed when the suction was put off.

4.2.10 Testing Tank

The testing tank appeared to be limited in boundaries for the suction anchors tested. Two analogue tests were conducted to analyse the affect of fluid flow through the anchor filter.

4.3 COMMENTS ON THE PRESENT EXPERIMENTAL INVESTIGATION

The comments will be made on the followings:-

1. Anchor burial depth
2. Anchor displacement
3. Density of the sand in the testing tank
4. Suction pressure

4.3.1 Anchor Burial Depth

In this study, the anchor burial depth, D is considered to be that depth from soil surface to the bottom of the embedded anchor. When comparing the test results with other investigators' results, the anchor burial depth, D is considered, as the distance between soil surface level and the top of the embedded anchor.

4.3.2 Anchor Displacement

Anchor displacement was measured by the uniform speed of the moveable part of the Hounsfield Tensometer unit as all the anchor tests were pulled-out by the Hounsfield Tensometer. The pull-out force was continuously recorded on the chart recorder and hence the anchor displacement was calculated from the constant speed of the chart recorder. The anchor displacement was only considered from when the anchor started to pick-up loads during pull-out. The anchor displacement factors, d_a/B varied up to a value of 1.87

4.3.3 Density of the Sand in the Testing Tank

Other investigators, for example, El-Rayes (1965), Howat (1969), Carr (1970), Yilmaz (1971), Harvey and Burley (1973), McMullan (1974), etc., maintained their desired densities when they conducted their pull-out or push-out tests on anchors. If the density was controlled for this study, it could be easily disturbed by the applied suction pressure therefore, no steps were taken into consideration to control the density of the sand in the testing tank. It was observed during the determination of sand density that the applied suction pressure increased the density to some degree, and the effect due to the suction pressure was further not investigated because the sand was denser close to the anchor suction cavity and becoming less dense as the distance was becoming larger from the suction cavity. This puts into question, what density should be taken into consideration under various suction cavity pressures! To overcome the density problem, a submerged density of 9.32 kN/m^3 was considered to be adequate and used in all calculations.

4.3.4 Suction Pressure

The pumps used for the model suction anchors and the prototype suction anchor were above water level. Suction pressure produced by the pumps was marginally reduced as the distance became larger from the anchor suction cavity.
In general, the effect due to the applied suction pressure created a local change in pressure close to the anchor and this effect was recorded. These pressures were (in descending order) the anchor cavity pressure p_1, pressure below the anchor p_2, pressure above the anchor p_3 and, in the cases above the top of the anchor p_4. The suction pressure measured, the pressure in the suction cavity of the anchor was considered to be a reference suction pressure.

4.4 DATA ANALYSIS AND COMPARISON WITH EXISTING THEORIES

Test data will be analysed by using non-dimensional parameters for the possible correlation of the results of the 102 mm suction anchor tests with the behaviour of the 600 mm suction anchor. The primary physical quantities for the present work in terms of π-functions are:

$$\pi_1 = \frac{Q_u}{\gamma' AD} = \overline{N}_q \qquad \text{.............................}(4.1)$$

$$\pi_2 = \frac{p_1}{\gamma' D} \qquad \text{.............................}(4.2)$$

$$\pi_3 = \frac{p_1}{\gamma' B} \qquad \text{.............................}(4.3)$$

$$\pi_4 = \frac{D}{B} \qquad \text{.............................}(4.3)$$

$$\pi_5 = \frac{d_a}{B} \qquad \text{.............................}(4.4)$$

where Q_u = ultimate uplift resistance
γ' = submerged density of the soil
A = area of the anchor
$\overline{N}_q$ = break-out factor
D = embedment depth of the anchor
p_1 = anchor cavity suction pressure
B = diameter of the anchor
d_a = vertical displacement of the anchor

Fig. 4.1 shows the non-dimensional relationship between $Q_u/\gamma' AD$ and burial depth ratio D/B at given non-dimensional parameters $p_1/\gamma' B$ for the 102 mm suction anchor and the 600 mm suction anchor. The plot of $p_1/\gamma' B = 0$ forms a concave downwards shape and gives a characteristic relative depth, $D/_B = 3.5$, beyond which the anchor starts behaving as a deep anchor and beyond which the break-out factor might have been expected to become constant. In this case, it does not. The plot of $p_1/\gamma' B = 2.63$ shows that the break-out factor varies approximately linearly with the D/B ratio. The plot of $p_1/\gamma' B = 5.26$, 10.52 and 13.15 show a similar upward trend for break-out factor beyond D/B = 1.5. The curve for $p_1/\gamma' B = 5.26$ shows a

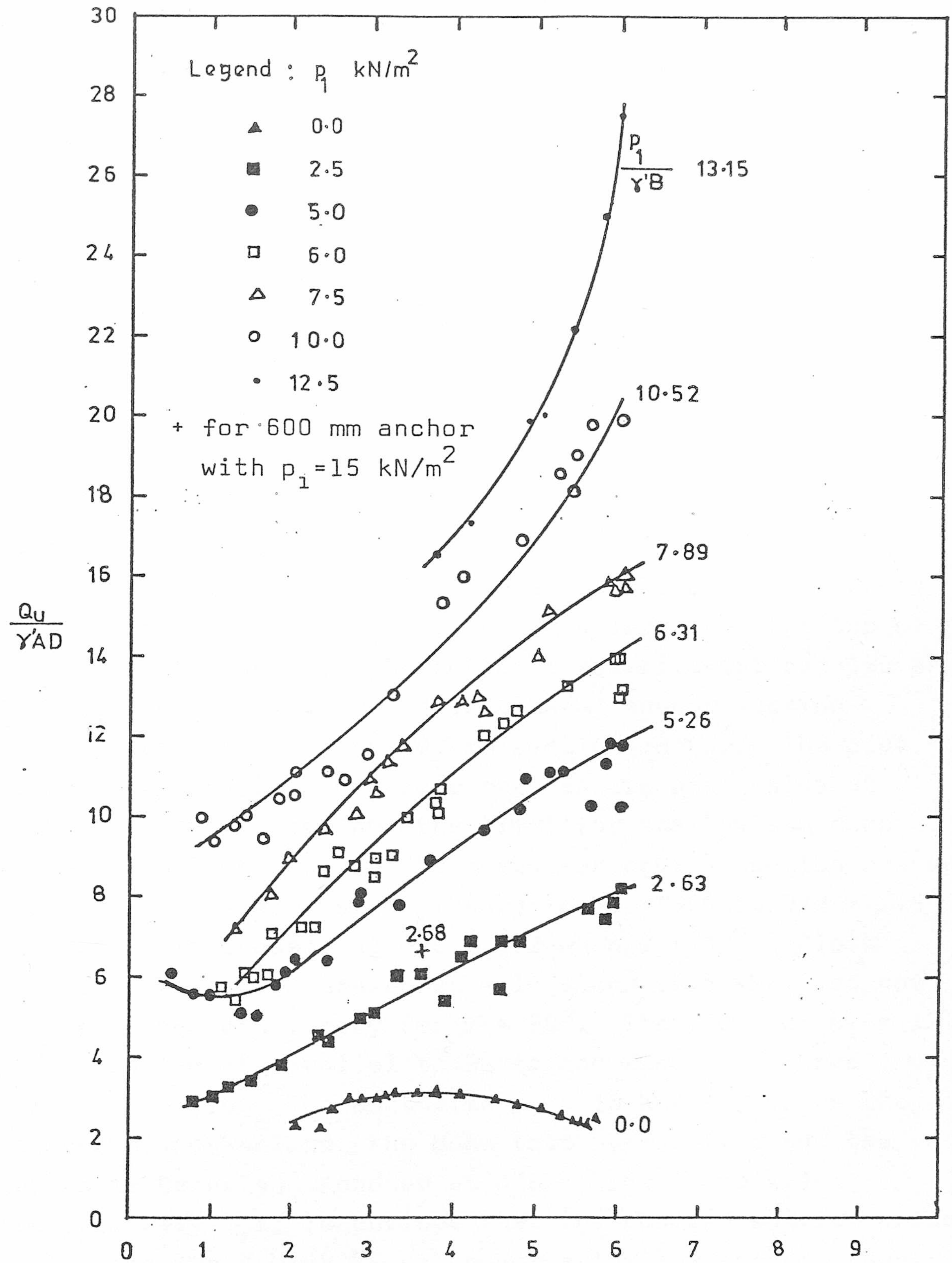

Fig. 4.1 Plot of $\frac{Q_u}{\gamma' AD}$ against D/B for 102mm suction anchor and one test for 600 mm suction anchor.

downward trend for the break-out factor when D/B is less than 1.5. The plot of $p_1/\gamma'B$ = 6.31 and 7.89 shows a concave downwards shape though the break-out factor is in a rising trend as the D/B ratio increases. One test of the 600 mm suction anchor is also plotted and it shows good agreement with the model tests.

Fig. 4.2 is an alternative presentation of the data which gives the relationship between the break-out factor and $p_1/\gamma'D$ at given $p_1/\gamma'B$. It appears from these plots that the break-out factor increases sharply with decreasing $p_1/\gamma'D$.

Fig. 4.3 shows the plot of break-out factor $\overline{N}_q$ against relative depth D/B which belongs to Vesić's (1971) paper. $\overline{N}_q$ and D/B values are recalculated to place on the same basis as Vesić. The anchor burial depth, D is considered as the distance between soil surface level and the top of the embedded anchor. The author's experimental results are plotted for 0, 2.5, 10 and 12.5 kN/m^2 anchor suction cavity pressure for the 102 mm suction anchor. The plot for zero cavity suction pressure reaches its peak value at D/B = 3 and this defines the limit for shallow and deep anchors in loose sand. The curve for cavity suction pressure = 2.5 kN/m^2 crosses Vesic's Theory for φ = 50° at D/B = 2.5 and later it crosses at D/B = 4.2 when φ = 30°. Plots for cavity suction pressures = 10.0 and 12.5 kN/m^2 do not cross to Vesic's Theory for φ = 50°. The plot for p_1 = 12.5 kN/m^2 is almost parallel to Baker and Kondner's curve from D/B = 4 to 5.5. The plot with p_1 = 10 kN/m^2 crosses the curves of Sutherland, the Duke test by Esquivel and the curve of Baker and Kondner at D/B = 2.8, 3 and 4.4 respectively. It is obvious that the applied suction pressure will lead to a high $\overline{N}_q$ value for a shallow anchor. None of the theories appear to give a good correlation with the experimental data, which is not unexpected.

Fig. 4.4 shows a plot of break-out factor of shallow

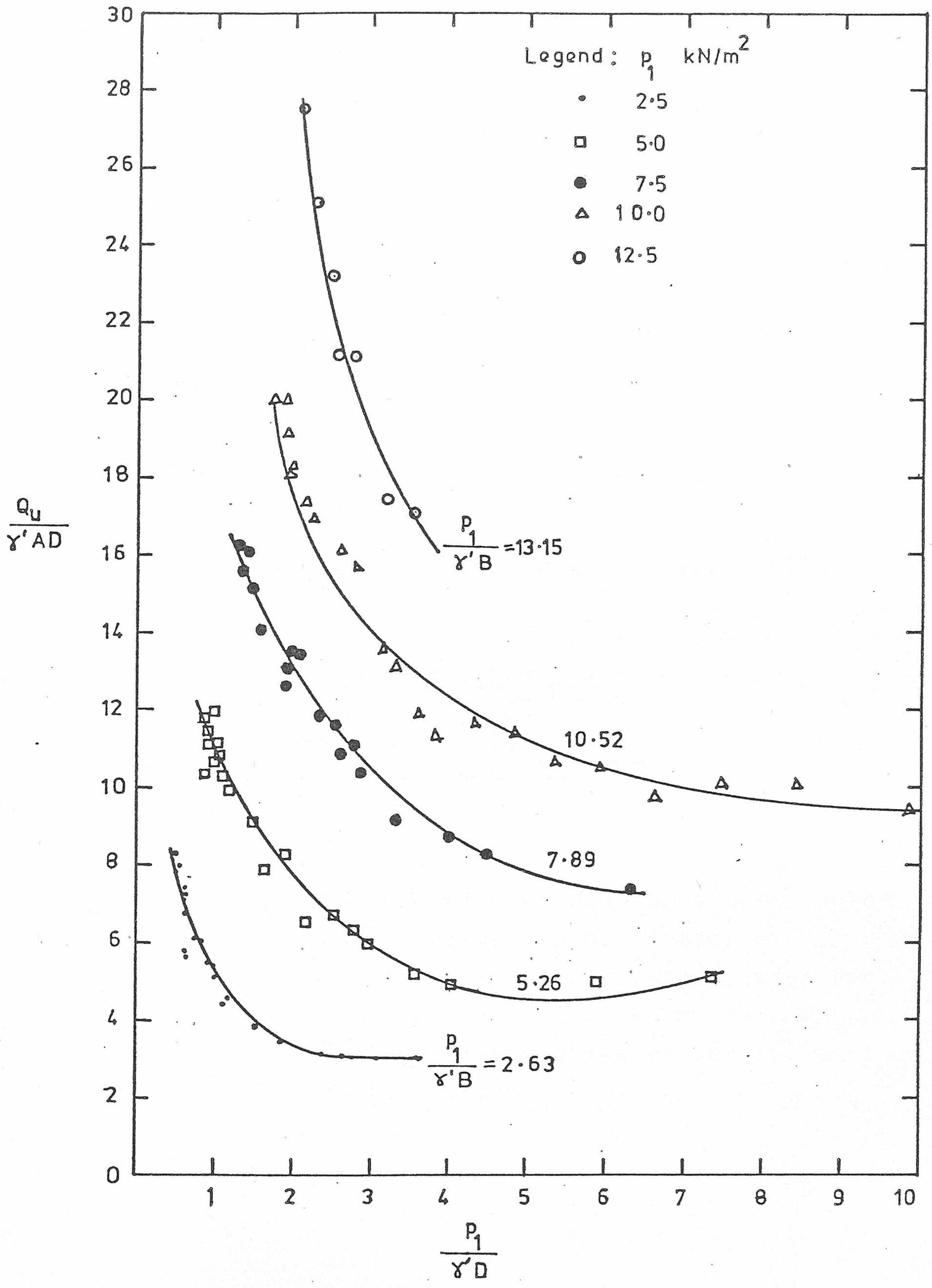

Fig. 4.2 Relationship between $\frac{Q_u}{\gamma' AD}$ and $\frac{P_1}{\gamma' D}$

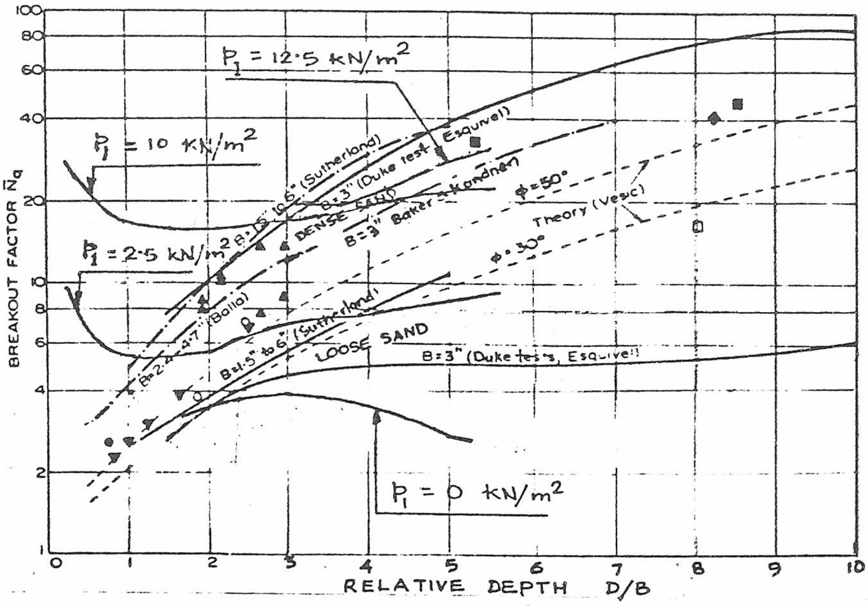

Break-out factor $\bar{N}_q$ in sands - Vesic (1971)

	Symbol	Anchor Dia	Soil Type	Reference
	▼	16"-48"	Fine Sand, $\phi = 32°$	Kananyan 1966
FIELD TESTS	●	75"	Sand	Mors (1959)
	○	43"-55"	Sand	Mors (1959)
	■	12"-16"	Sand	Baker and Kondner (1965)
	▲	94"	Sand, $\phi = 41°$	Sutherland (1965)
	◆	16"	Sand, $\phi = 37°$	Martin and Negre (1967)
	□	32"	Silt (loess) $\phi = 24°$	Milovic (1963)

Fig. 4.3 Relationship between break-out factor and relative depth. Author's experimental results are plotted for 0, 2.5, 10 and 12.5 kN/m^2 anchor suction cavity pressure for 102 mm suction anchor.

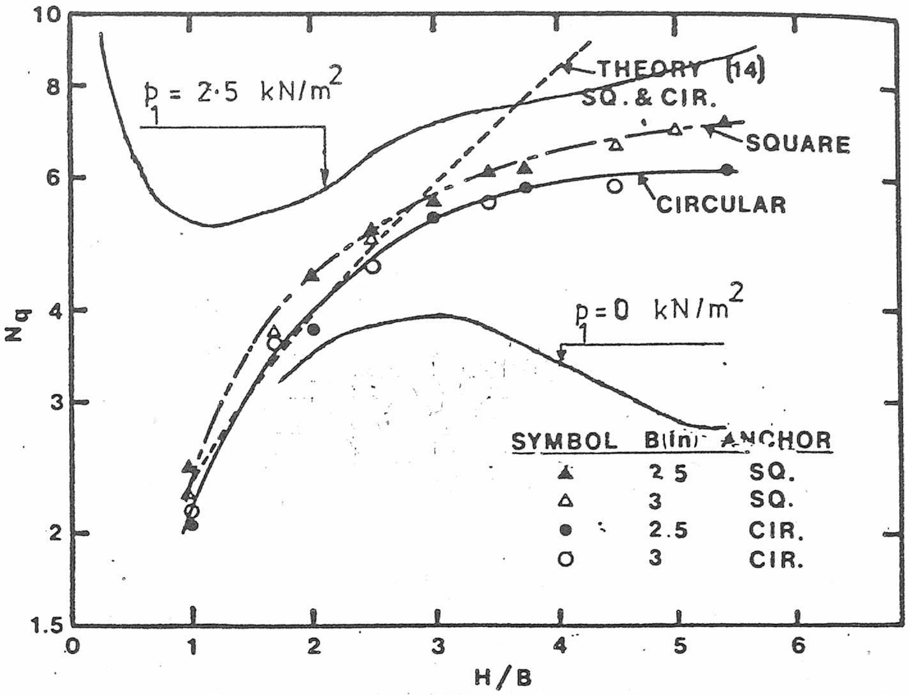

Break-out factors of shallow anchors
After Das and Seeley (1975)

Theory (14): Meyerhof, G.G. and Adams J.I., (1968). "The ultimate uplift capacity of foundations". Canadian Geotechnical Journal, Vol. 5, No. 4, Aug., pp. 225 - 224.

Fig. 4.4 Relationship between break-out factor and relative depth. Author's experimental results are plotted for 0 and 2.5 kN/m^2 anchor suctions cavity pressure for 102 mm suction anchor.

anchors after Das and Seeley (1975). The author's experimental results are plotted for 0 and 2.5 kN/m^2 anchor suction cavity pressure for the 102mm suction anchor. The plot for $p_1 = 0$ kN/m^2 is much below the experimental results of Das and Seeley (1975) and also Meyerhof and Adams' (1968) Theory. The plot for $p_1 = 2.5$ kN/m^2 appeared to show a similar relationship with Das and Seeley's experimental circular curve at D/B = 2 to 5. Meyerhof's and Adams' theoretical curve for square and circular anchor footings crosses the plot for $p_1 = 2.5$ kN/m^2 at D/B = 3.7.

Fig. 4.5 shows the relationship between anchor pull-out pressure and anchor displacement factor for the 70mm and 102 mm suction anchors. The 70 mm suction anchor gives the anchor displacement factor, $d_a/B = 1.87$ at peak pull-out pressure. The d_a/B value appears to be high in comparison with the d_a/B values of the 102 mm suction anchor. At maximum anchor pull-out pressure, the 102 mm suction anchor gives $d_a/B = 0.90$ and 0.92 for applied suction pressures of 15.94 and 5.0 kN/m^2 respectively at a constant burial depth.

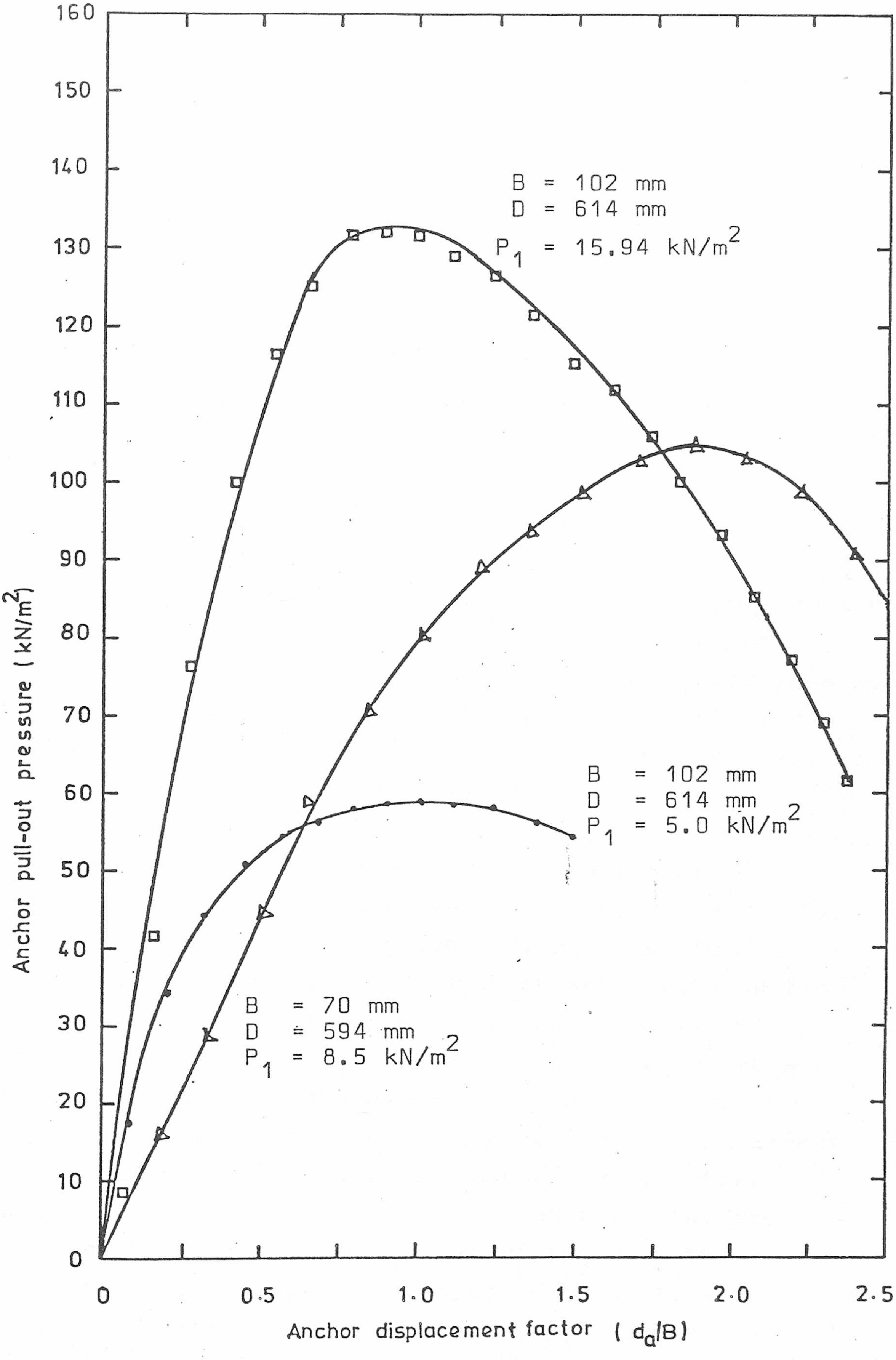

Fig. 4·5 Pull-out pressure against anchor displacement factor.

CHAPTER 5

CONCLUSIONS AND SUGGESTIONS FOR FURTHER WORK

5.1 CONCLUSIONS

The results of the present investigation concerning the suction anchors in the cohesionless soil are concluded as follows:-

The water flow rate through the anchor varied linearly with cavity suction pressure at constant burial depth. A higher applied suction pressure was required at a deep burial in comparison with a shallow burial for a given flow rate.

The pull-out resistance of the solid and model suction anchors was increased with an increase of the anchor diameter for a given depth of embedment. The resistance was increased with an increase of the embedment depth for a given anchor diameter. The ultimate pull-out force was found to be increasing at a slower rate with the increase of the embedment depth for the anchor without suction in comparison with the anchor with suction, for a given anchor diameter. The suction anchors with high suction pressure gave a high ultimate pull-out force. In general, pull-out force increased with increasing burial depth and cavity suction pressure. The pull-out force increased approximately linearly with an increase in the applied suction pressure for a specified embedment depth. The suction time for dewatering from the anchor suction cavity did not affect the pull-out force provided it exceeded two minutes. During the start of the anchor pull-out test, the pressures in the cavity (p_1), below (p_2), above (p_3) and above the anchor top (p_4) increased or decreased by 4.5%, 4.5%, 3.3% and 1.2% respectively. The pressure (p_3) reduced by 61.1% at the ultimate pull-out force.

For model anchors without applied suction pressure in saturated loose sand the factor $\overline{N}_q$ increased up to the values of D/B = 3 and then the values of $\overline{N}_q$ decreased with the increase of D/B values.

The model anchor displacements were up to the values of $d_a/B = 1.87$. The pull-out force increased linearly within the elastic range of the sand. In general, the force rapidly decreased on reaching the peak value as the anchor displacement advanced.

The anchor shaft skin frictional force increased the ultimate pull-out force of the 70, 102, 108 and 145 mm anchors up to 10%, 5.5%, 5% and 3.75% respectively in the loose saturated sand without a suction pressure. The frictional resistance force of the anchor shaft increased the ultimate pull-out force of the 102 mm suction anchor with the cavity suction pressure of 7.5 kN/m^2 by 2.75%.

For one test, the vertical sand movement was 89 mm at the dome apex and its diameter was 275 mm. The shape of the dome was maintained until the applied suction pressure was maintained. The dome collapsed when the suction was put off.

The testing tank appeared to be limited in boundaries for the suction anchors tested.

It was observed during the determination of sand density that the applied suction pressure increased the density to some degree. It was uncertain what density should be taken into account for computing the break-out factors. The submerged density of 9.32 kN/m^3 was used in all calculations.

The effects of the applied suction pressure (p_1) were in descending order, the anchor cavity pressure (p_1), pressure below the anchor (p_2), pressure above the anchor (p_3) and, the cases measured, the pressure above top of the anchor (p_4).

The break-out factors increased with D/B value and with cavity suction pressure for shallow suction anchors. The anchors were buried in the test sand up to a relative depth ratio of 8.5.

A comparison with the results of other investigators shows some degree of agreement because the test results without suction pressure are low in loose sand and with cavity pressure = 2.5 kN/m^2 pass through the curves dense sand to loose sand. The test results with cavity suction pressure above 10 kN/m^2 lie in the range for dense sand.

As far as the author knows there are no theories or experimental data published on embedded suction anchors by any other investigators, excluding Wilson and Sahota, with which comparison could be made.

5.2 SUGGESTIONS FOR FURTHER WORK

The following are the suggestions for the further work to be carried out:-

1. Investigate the effect due to the applied suction pressure in the disturbed soil due to the natural placing of the anchor.

2. Investigate the effect due to the applied suction pressure on the saturated density of the soil.

3. Investigate the effect of soil liquidity due to embedment of the anchor.

4. Investigate the soil consolidation effect due to applied suction pressure and also when the pressure becomes negligible.

5. Develop a general failure equation due to forces and moments.

6. Investigate in detail the pore pressure distribution around the anchor due to the applied suction pressure.

7. Investigate the critical embedment depth for various applied suction pressures.

There are, certainly many other fields of work to be investigated for the embedded-type suction anchors e.g. singly or in groups, vertical or inclined, under static or cyclic loading, pre-stressing the anchor, creep under constant load, stress-strain relationship curve to represent the soil, which have not been mentioned in the study. The further work under the above headings is considered to be essential before a comprehensive understanding of the embedded-type suction anchor behaviour can be fully achieved.

REFERENCES

1. Adams, J. I. and Jaynes, D. C., (1967). "The uplift capacity of shallow foundations". Ontario Hydro Research Qyarterly, Vol. 19, No. 1, pp. 1-13.

2. Adams, J. I. and Klym, T. W., (1972). "A study of anchorages for transmission tower foundations". Canadian Geotechnical Jour., Vol. 9

3. Al-Awadi, M. J., (1971). "Suction Anchors". M.Sc. Thesis, University of Manchester Institute of Science and Technology.

4. Ashbee, R. A., (1969). "A uniaxial analysis for use in uplift foundation calculations". CEGB Central Research Labs., Lab. Note No. RD/L/R1608.

5. Baird, J. A. and Nacci, V. A., (1972). "The shear strength parameters for hydrostatic anchoring". Offshore Tech. Conf. 1972, Paper No. OTC 1534. Vol. 1.

6. Baker, W. H. and Kondner, R. L., (1966). "Pullout load capacity of a circular earth anchor buried in sand". National Academy of Sciences, Highway Research Record 108, pp. 1-10.

7. Balla, A., (1961). "The resistance to breaking out of mushroom foundations for pylons". Proc. of the Fifth International Conf. on Soil Mechanics and Foundation Engineering, Vol. 1, pp. 569-576.

8. Beard, R. M. and Lee, H. J., (1975). "Holding capacity of direct embedment anchors". Proc. Civil Engineering in the Oceans III, ASCE Conf., University of Delaware, Newark, Delaware, June 9-12, 1975. Vol. 1, pp. 470-485, American Society of Civil Engineers.

9. Bemben, S. M. and Kalajian, E. H., (1969). "The vertical holding capacity of marine anchors in sand". Proc. Civil Engineering in the Oceans II, ASCE Conf., Miami Beach, Fl., Dec. 10-12, 1969. New York, American Society of Civil Engineers, 1970, pp. 117-136.

10. Bemben, S. M., Kalajian, E. H. and Kupferman, M., (1973). "The vertical holding capacity of marine anchors in sand and clay subjected to static and cyclic loading". Offshore Tech. Conf., Paper No. OTC 1912, Vol. II

11. Brown, G. A. and Nacci, V. A., (1971). "Performance of hydrostatic anchors in granular soils". Offshore Tech. Conf., Paper No. OTC 1472.

12. Carr, R. W., (1970). "An experimental investigation of plate anchors in sand". Ph.D. Thesis, University of Sheffield.

13. Carr, R. W. and Hanna, T. H., (1971). "Sand movement measurements near anchor plates". Jour. of the Soil Mechanics and Foundations Division, Proc. of the American Society of Civil Engineers, Vol. 97, No. SM5, pp. 833-840.

14. Chmelik, F. B., (1968). "Sediment probes and anchor system for submersible research vehicles". A critical look at Marine Technology, Marine Technology Society, Fourth Annual Conf. and Exh., 8-10 July, Washington D.C.

15. Colp, J. L. and Herbich, J. B., (1975). "Inclined pullout forces for embedded plate anchors". Offshore Tech. Conf., Paper No. OTC 2182.

16. Das, B. M. and Seeley, G. R., (1975). "Pullout resistance of horizontal anchors". Proc. Civil Engineering in

the Oceans/III, Vol L, June 9-12, Speciality Conf. sponsored by American Society of Civil Engineers on Ocean Engineering and Dept. of Civil Engineering, University of Delaware, pp. 435-449.

17. Das, B. M. and Seeley, G. R., (1975). "Breakout resistance of shallow horizontal anchors". Jour. of the Geotechnical Engineering Division, Proc. of the American Society of Civil Engineers, Vol. 101, No. GT9, Sept., pp. 999-1003.

18. Davie, J. R., (1973). "Behaviour of cohesive soils under uplift forces". Ph.D. Thesis, University of Glasgow.

19. Dayal, U., Allen, J. H. and Jones, J. M., (1975). "Use of an impact penetrometer for the evaluation of the in-situ strength of marine sediments". Marine Geotechnology, Vol. 2, Part 1, pp. 73-89.

20. De Beer, E. E., (1970). "Experimental determination of the shape factors and the bearing capacity factors of sand". Geotechnique, Vol. 20, No. 4, pp. 387-411

21. Delflache, A. P.and Bryant, W. R., (1970). "Compressional behaviour of high-void ratio marine sediments". Offshore Tech. Conf. Paper No. OTC 1148.

22. Eggestad, Aa, (1963). "Deformation measurements below a model footing on the surface of dry sand". Proc. of European Conf. on problems of settlement and compressibility of soils. Vol. 1, pp. 233-239.

23. Ehlers, C. J., (1973). "Underreamed footings support offshore platforms in the North Sea". Offshore Tech. Conf., Paper No. OTC 1895.

24. El-Rayes, M. K., (1965). "Behaviour of cohesionless soils under uplift forces". Ph.D. Thesis, University of Glasgow.

25. Esquival-Diaz, R. F. (1967). "Pullout resistance of deeply buried anchor in sand". M.Sc. Thesis, Soil Mechanics Series No. 8, Duke University, Durham, North Carolina.

26. Etter, R. J. and Turpin, F. J. (1967). The feasibility of underwater suction anchors". Underwater Technology Division - Petroleum Division Conf., American Society of Mechanical Engineers, Philadelphia.

27. Finn, W. D., Pickering, D. J. and Bransby, P. L. (1971). "Sand liquefaction in triaxial and simple shear tests". Jour. of the Soil Mechanics and Foundations Division, Proc. of the American Society of Civil Engineers, Vol 97, No. SM4, April, pp. 639-659.

28. Finn, W. D. L. and Byrne, P. M., (1971). "Analysis of ocean bottom sediments". Offshore Tech. Conf., Paper No. OTC 1471.

29. Finn, W. D. L. and Byrne, P. M., (1972). "The evaluation of the breakout force for a submerged ocean platform". Offshore Tech. Conf., Paper No. OTC 1604.

30. Gibson, R. E. and Anderson, W. F., (1961). "In-situ measurement of soil properties with the pressuremeter". Civil Engineering and Public Works Review, Vol. 56, issue 658, pp. 615-618.

31. Goodman, L. J., Lee, C. N. and Walker, F. J., (1961). "The feasibility of vacuum anchorage in soil". Geotechnique, 1, Correspondence, pp. 356-359.

32. Hanna, T. H. and Carr, R. W., (1971) "The loading behaviour of plate anchors in normally and overconsolidated sands". Proc. Fourth Conf. on Soil Mechanics, Budapest, pp. 589-600.

33. Hanna, T. H., Sparks, R. and Yilmaz, M., (1972). "Anchor behaviour in sand". Jour. of the Soil Mechanics and Foundations Division, Proc. of the American Society of Civil Engineers, Vol. 98, Sm11, Nov., pp. 1187-1209.

34. Hanna, T. H. and Sparks, R., (1973). "The behaviour of preloaded anchors in normally consolidated sands". Proc. of the Eighth International Conf. on Soil Mechanics and Foundation Engineering, Part 2, pp. 137-142.

35. Harvey, R. C. and Burley, E., (1973). "Behaviour of shallow inclined anchorages in cohesionless sand". Ground Engineering, Vol. 6, No. 5, Sept., pp. 48-55.

36. Healy, K. A., (1971). "Pullout resistance of anchors buried in sand". Jour. of the Soil Mechanics and Foundations Division, Proc. of the American Society of Civil Engineers, Vol. 97, No. SM11, Nov., pp. 1615-1622.

37. Helfrich, S. C., Brazill, R. L. and Richards, A. F., (1976). "Pullout characteristics of a suction anchor in sand". Offshore Tech. Conf., Paper no. OTC 2469.

38. Howat, M. D., (1969). "The behaviour of earth anchorages in sand". M.Sc. Thesis, University of Bristol.

39. Kalajian, E. H., (1971). "The vertical holding capacity of marine anchors in sand subjected to static and cyclic loading". Ph.D. Thesis, University of Massachusetts, Amherst, M.A.

40. Kolbuszewski, J. J., (1948 a). "An experimental study of the maximum and minimum porosities of sands". 2nd Int. Conf. on Soil Mech. and Found Engg. Rotterdam, Vol. 1, pp. 158-165.

41. Kolbuszewski, J. J., (1948 b). "General investigation of the fundamental factors controlling the loose packing of sands". 2nd. Int. Conf. on Soil Mech. and Found. Engg., Rotterdam, Vol. 7, pp. 47-49.

42. Kolbuszewski, J. J. and Jones, R. H., (1961). "The preparation of sand samples for laboratory testing". Proc. of Midlands Soil Mech. Soc., Vol. 4, pp. 106-123.

43. Lewis, L. F. (1971). "An investigation of deep ocean sediments using the deep ocean sediment probe". Ph.D. Thesis, University of Rhode Island, pp. 237.

44. Littlejohn, G. S., (1976). "Rock anchors". Aberdeen University, Engineering Association, Apr. pp. 3-26.

45. Mackereth, F. J. H., (1958). "A portable core sampler for lake deposits". Limnology and Oceanography, 3, pp. 181-191.

46. Mariupoliskii, L. G., (1965). "The bearing capacity of Anchor foundations". Soil Mechanics and Foundation Engineering, Vol. 3, No. 1, Jan-Feb., pp. 26-32.

47. Matsuo, M., (1967). "Study on the uplift resistance of footing (I)". Soils and Foundations, Japan, Vol. 7, No. 4, Dec., pp. 1-37.

48. Matsuo, M., (1968). "Study on the uplift resistance of footing (II)". Soils and Foundations, Japan, Vol. 8, No. 1, Mar., pp. 18-48.

49. McMullan, D. J., (1974). "The behaviour of inclined ground anchors in sand both singly and in groups". Ph.D. Thesis, University of Bristol.

50. Meyerhof, G. G., (1970). "Safety factors in Soil Mechanics". Canadian Geotechnical Jour. Vol. 7, No. 4, Nov., pp. 349-355.

51. Meyerhof, G. G. and Adams, J. I. (1968). "The ultimate uplift capacity of foundations". Canadian Geotechnical Jour., Vol. 5, No. 4, pp. 225-244.

52. Muga, B. J., (1967). "Bottom Breakout forces". Proc. Civil Engineering in the Oceans, American Society of Civil Engineers, Conf., San Fransisco, CA, Sept. 6-8, pp. 569-600.

53. Nath, B., Harvey, R. C. and Burley, E., (1978). "The development of an embedded anchor to provide multidirectional restraint". Oceanology International, Brighton, March, pp. 97-107.

54. Potyondy, J. G., (1961). "Skin friction between various soils and construction materials". Geotechnique, Vol. 11, Dec., No. 4, pp. 339-353.

55. Rosfelder, A. M., (1966). "Hydrostatic actuation of deep-sea instruments". Jour. of Ocean Tech., Vol 1, No. 1, pp. 53-63.

56. Sahota, B. S., (1978). "Suction anchors". Robert Gordon's Institute of Technology, Aberdeen, March, pp. 1-17.

57. Schofield, A. N., (1974). "Improvements in hydraulic engineering installations". U.K. Patent Specification

1367 881, 25 Sept.

58. Seed, H. B., Martin, P. P. and Lysmer, J., (1976). "Pore-water pressure changes during soil liquefaction". Jour. of the Geotechnical Engineering Division, Proc. of the American Society of Civil Engineers, Vol. 102, No. GT4, pp. 323-346.

59. Smith, R. J. (1962). "Engineering properties of ocean floor soils". Field Testing of Soils, American Society for Testing and Materials, pp. 280-302.

60. "Submersible sounding tool to test North-Sea Floor". Oil and Gas Jour., 70:2, 1972, pp. 74-77.

61. Sutherland, H. B., (1965). "Model studies for shaft raising through cohesionless soils". Proc. of the Sixth International Conf. on Soil Mechanics and Foundation Engineering, Vol. II, pp. 410-413.

62. Taylor, R. J., Jones, D. and Beard, R. M., (1975). "Handbook for uplift-resisting anchors". Deep Ocean Technology, Civil Engineering Laboratory, Naval Construction Battalion Center, Port Hueneme, California 93043, Sept., pp. 1-153.

63. Tudor, W. J., (1967). "Mooring and anchoring of deep ocean platforms". Proc. of the Conf. on Civil Engineering in the Oceans, American Society of Civil Engineers, Conf. San Fransisco, California, Sept. 6-8, pp. 351-390.

64. Turner, E. A., (1962). "Uplift of transmission tower footings". Jour. of the Power Division, Proc. of the American Society of Civil Engineers, Vol. 88, No. PO2, Part 1, pp. 17-33.

65. Valent, R. J., Raecke, D. A. and Hermann, H. G. (1973). "Investigation of the seafloor preconsolidating foundation concept". U.S. Naval Civil Eng. Lab. Tech. Note N-1276, pp. 1-25.

66. Vesic, A. S. and Barksdale, R. D., (1963). "Theoretical studies of cratering mechanisms affecting the stability of cratered slopes. Final report, Project No. A-655, Eng. Expt. Station, Georgia Institute of Technology, Atlanta, Georgia, pp. 103.

67. Vesic, A. S., (1965). "Cratering by explosives as an earth pressure problem". Proc. of the Sixth International Conf. on Soil Mechanics and Foundation Engineering, Vol. II, pp. 427-431.

68. Vesic, A. S., (1971). "The breakout resistance of objects embedded in the ocean bottom". Jour. of the Soil Mechanics and Foundations Division, Proc. of the American Society of Civil Engineers, Vol. 97, No. SM9, pp. 1183-1205.

69. Vesic, A. S., (1972). "Expansion of cavities in infinite soil mass". Jour. of the Soil Mechanics and Foundations Division, Proc. of the American Society of Civil Engineers, Vol. 98, No. SM3, pp. 265-290.

70. Wang, M C., Nacci, V. A. and Demars, K. R. (1975). "Behaviour of underwater suction anchor in soil". Ocean Engineering, Vol. 3, No. 1, Pergamon Press Ltd., London, pp. 47-62.

71. Wang, M. C., Demars, K. R., and Nacci, V. A., (1977). "Breakout capacity of model suction anchors in soil". Canadian Geotechnical Jour., Vol. 14, No. 1, May, pp. 246-257.

72. Wang, M. C., Demars, K. R. and Nacci, V. A., (1978). "Applications of suction anchors in offshore technology". Offshore Tech. Conf., Paper No. OTC 3203.

73. Wilson, Q. and Sahota, B. S., (1977). "Trials with suction anchors". Ocean Industry, Aug., pp. 55-56.

74. Wilson, Q. and Sahota, B. S., (1978). "Suction anchors". European Offshore Petroleum Conf. and Exhibition in London, 24-27 Oct., EUR 16.

75. Yilmaz, M., (1971). "The behaviour of groups of anchors in sand". Ph.D. Thesis, University of Sheffield.

APPENDIX A

PULL-OUT TEST DATA

Page No. A 1 - A 24

Table 1 Pull-out tests for 70 mm suction anchor with a cavity suction pressure = 0.0 KN/m^2. The graph is plotted in Fig. 3.24.

Test No.	Burial depth D (mm)	Pull-out force Qu (N)	Natural consolidation (hrs)	$\frac{Qu}{\gamma' AD}$	$\frac{D}{B}$
1	618	59.5	20.5	2.69	8.83
2	542	56.8	1.0	2.92	7.74
3	493	51.1	1.25	2.89	7.04
4	471	46.4	10.5	2.75	6.73
5	423	44.5	1.0	2.93	6.04
6	382	42.3	1.0	3.08	5.46
7	357	37.9	1.0	2.97	5.10
8	319	36.5	1.0	3.20	4.56
9	317	34.8	49.5	3.06	4.53
10	265	29.5	1.0	3.11	3.79
11	253	30.2	6.5	3.32	3.61
12	235	25.2	1.0	2.99	3.36
13	226	24.1	1.0	2.98	3.29
14	199	21.8	1.0	3.06	2.84
15	158	19.5	1.0	3.44	2.26
16	134	17.4	0.5	3.62	1.91
17	118	15.2	1.0	3.59	1.69
18	101	10.8	1.0	2.98	1.44
19	80	9.1	1.25	3.17	1.14
20	62	8.2	1.0	3.68	0.89
21	42	5.5	1.0	3.65	0.60
22	35	2.4	1.5	1.91	0.50

Table 2 Pull-out tests for 102 mm suction anchor with a cavity suction pressure = 0.0 KN/m^2.

Test No.	Burial depth D (mm)	Pull-out force Qu (N)	Natural consolidation (hrs)	$\frac{Qu}{\gamma' AD}$	$\frac{D}{B}$
1	585	112.6	72.0	2.53	5.74
2	580	107.5	46.5	2.43	5.69
3	564	111.0	29.5	2.59	5.53
4	560	105.5	11.5	2.47	5.49
5	551	107.5	1.0	2.56	5.40
6	537	112.1	1.0	2.74	5.26
7	513	110.1	1.0	2.81	5.03
8	487	106.2	1.0	2.86	4.77
9	453	106.1	1.0	3.08	4.44
10	409	99.5	10.5	3.20	4.01
11	381	101.5	1.0	3.50	3.74
12	358	92.4	1.0	3.39	3.51
13	353	90.5	1.0	3.36	3.46
14	321	80.2	1.0	3.28	3.15
15	316	79.5	13.5	3.30	3.10
16	292	70.5	1.0	3.17	2.86
17	279	65.2	1.0	3.07	2.74
18	255	55.5	72.5	2.85	2.50
19	225	42.5	1.0	2.48	2.21
20	202	40.0	1.0	2.60	1.98
21	203	36.2	1.0	2.34	1.99

Burial depth against pull-out force are plotted in Fig. 3.24 and 3.29. Non-dimensional parameters are plotted in Fig. 4.1, 4.3 and 4.4.

Table 3. Pull-out tests for 108 mm solid anchor. The graph is plotted in Fig. 3.24.

Test No.	Burial depth D (mm)	Pull-out force Qu (N)	Natural consolidation (hrs)	$\frac{Qu}{\gamma' AD}$	$\frac{D}{B}$
1	572	123	21.5	2.52	5.30
2	565	120.5	10.5	2.50	5.23
3	522	113	1.0	2.53	4.83
4	491	115.5	1.0	2.75	4.55
5	446	109.5	1.0	2.88	4.13
6	417	110.0	1.0	3.09	3.86
7	364	99.5	1.0	3.20	3.37
8	332	89.4	1.0	3.16	3.07
9	293	75.3	43.5	3.00	2.71
10	276	69.6	1.0	2.95	2.56
11	269	70.2	1.0	3.06	2.49
12	259	64.5	13.25	2.92	2.40
13	238	56.5	1.0	2.78	2.20
14	218	46.5	1.0	2.50	2.02
15	201	38.1	1.0	2.22	1.86
16	189	32.7	1.0	2.02	1.75

Table 4 Pull-out tests for 145 mm suction anchor with a cavity suction pressure = 0.0 KN/m^2. The graph is plotted in Fig. 3.24.

Test No.	Burial depth D (mm)	Pull-out force Qu(N)	$\frac{Qu}{\gamma' AD}$	$\frac{D}{B}$
1	565	166.5	1.91	3.9
2	562	159.5	1.84	3.88
3	516	162.4	2.05	3.56
4	431	138.8	2.09	2.97
5	380	132.4	2.26	2.62
6	354	115.0	2.11	2.44
7	334	102.2	1.99	2.30
8	305	95.8	2.04	2.10
9	279	88.7	2.07	1.92
10	253	70.8	1.82	1.75
11	246	62.1	1.64	1.70
12	225	53.6	1.55	1.55
13	215	49.5	1.50	1.48
14	197	44.8	1.48	1.36
15	189	40.3	1.39	1.30
16	171	35.5	1.35	1.18
17	173	31.8	1.19	1.19
18	156	31.2	1.30	1.08
19	151	27.0	1.16	1.04
20	134	26.6	1.29	0.92

Table 5 Pull-out tests for 70 mm solid anchor. The graph is plotted in Fig. 3.25.

Test No.	Burial depth D (mm)	Pull-out force Qu (N)	Natural consolidation (hrs)	$\frac{Qu}{\gamma' AD}$	$\frac{D}{B}$
1	542	40.5	72.0	2.08	7.74
2	518	42.8	0.5	2.30	7.4
3	501	42.9	0.5	2.39	7.16
4	465	42.5	66.0	2.55	6.64
5	440	41.0	1.0	2.60	6.29
6	419	40.8	1.0	2.71	5.99
7	407	40.0	1.0	2.74	5.81
8	369	35	1.0	2.64	5.27
9	340	33.8	1.0	2.77	4.86
10	309	33.0	1.0	2.97	4.41
11	280	31.2	1.0	3.11	4.0
12	253	30.8	1.0	3.39	3.61
13	223	26.7	0.5	3.34	3.19
14	196	25.3	0.5	3.60	2.8

Table 6 Pull-out tests for 70 mm suction anchor without pipes. The graph is plotted in Fig. 3.25.

Test No.	Burial depth D (mm)	Pull-out force Qu (N)	Natural consolidation (hrs)	$\frac{Qu}{\gamma' AD}$	$\frac{D}{B}$
1	542	45.8	20.5	2.36	7.74
2	508	43.0	0.5	2.36	7.26
3	470	35.1	0.5	2.09	6.71
4	400	40.0	0.5	2.79	5.71
5	344	39.8	0.5	3.22	4.91
6	281	38.3	0.5	3.79	4.01
7	241	33.1	0.5	3.83	3.44
8	540	42.0	44.5	2.16	7.71
9	502	37.3	0.5	2.08	7.17
10	462	33.1	0.5	2.0	6.60
11	436	34.2	0.5	2.19	6.29
12	383	37.2	0.5	2.71	5.47
13	324	37.2	0.5	3.20	4.63
14	296	37.0	0.5	3.49	4.23
15	262	34.8	0.5	3.71	3.74
16	223	30.0	0.5	3.76	3.19
17	196	24.3	0.5	3.46	2.80
18	185	20.0	0.5	3.02	2.64

Table 7 Pull-out tests for 70 mm suction anchor with pipes. The graph is plotted in Fig. 3.25. Suction pressure $p_i = 0.0$ KN/m^2.

Test No.	Burial depth D (mm)	Pull-out force Qu (N)	Natural consolidation (hrs)	$\frac{Qu}{\gamma' AD}$	$\frac{D}{B}$
1	562	54.2	72.5	2.69	8.03
2	523	46.0	0.5	2.45	7.47
3	511	48.1	0.5	2.62	7.30
4	479	43.3	0.5	2.52	6.84
5	454	42.7	0.5	2.62	6.49
6	370	41.2	1.0	3.10	5.29
7	304	36.2	1.0	3.32	4.34
8	268	35.2	0.5	3.66	3.83
9	235	27.1	0.5	3.22	3.36
10	619	59.8	37.5	2.69	8.84
11	546	55.3	1.0	2.82	7.80
12	514	58.1	1.0	3.15	7.34
13	483	57.2	0.5	3.30	6.90
14	448	56.2	0.5	3.50	6.40
15	417	52.5	0.5	3.51	5.96
16	383	49.0	0.5	3.57	5.47
17	360	47.2	0.5	3.66	5.14
18	338	42.5	0.5	3.51	4.83
19	308	41.0	0.5	3.71	4.40
20	273	40.8	2.5	4.17	3.90
21	256	34.8	0.5	3.79	3.66
22	211	34.8	0.5	4.60	3.01
23	200	34.5	0.5	4.81	2.86
24	181	24.5	17.5	3.77	2.59
25	172	27.3	0.5	4.43	2.46

Table 7 continued.

Test No.	Burial depth D (mm)	Pull-out force Qu (N)	Natural consolidation (hrs)	$\frac{Qu}{\gamma' AD}$	$\frac{D}{B}$
26	159	19.6	0.5	3.44	2.27
27	133	16.5	0.5	3.46	1.90
28	119	14.8	0.5	3.47	1.70
29	99	10.1	0.5	2.84	1.41
30	82	10.0	0.5	3.40	1.17
31	62	8.4	0.5	3.78	0.89
32	45	6.2	0.5	3.84	0.64
33	35	2.5	1.0	1.99	0.50
34	544	57.2	21.75	2.93	7.77
35	498	50	0.5	2.80	7.11
36	473	45.1	0.5	2.66	6.76
37	414	41.8	0.5	2.81	5.91
38	384	41.8	0.5	3.03	5.49
39	354	38.2	0.5	3.01	5.06
40	315	35.6	0.5	3.15	4.50
41	272	30.4	0.5	3.12	3.89
42	211	26.1	0.5	3.45	3.01

Table 8 Pull-out tests for 70 mm suction anchor with a cavity suction pressure = 5.0 KN/m^2 and $P_1/\gamma'B$ = 7.66. The graph is plotted in Fig. 3.28.

Test No.	Burial depth D (mm)	Pull-out force Qu (N)	$\frac{Qu}{\gamma' AD}$	$\frac{P_i}{\gamma' D}$	$\frac{D}{B}$
1	618	216	9.74	0.87	8.83
2	615	207	9.38	0.87	8.79
3	555	201	10.10	0.97	7.93
4	539	189	9.77	0.99	7.70
5	483	197	11.37	1.11	6.90
6	475	185	10.86	1.13	6.79
7	418	165	11.00	1.28	5.97
8	295	134	12.66	1.82	4.21
9	276	106	10.71	1.94	3.94
10	217	103	13.23	2.47	3.10
11	206	93	12.58	2.60	2.94
12	171	79	12.88	3.14	2.44
13	142	51	10.01	3.78	2.03
14	118	37	8.74	4.55	1.69
15	97	28	8.05	5.53	1.39
16	78	27	9.65	6.88	1.11
17	61	23	10.51	8.79	0.87
18	54	19	9.81	9.93	0.77
19	46	17	10.30	11.66	0.66
20	37	12	9.04	14.50	0.53

Table 9 Pull-out tests for 102 mm suction anchor with a cavity suction pressure p_1 = 2.50 KN/m^2 and $P_1/\gamma'B$ = 2.63.

Test No.	Burial depth D (mm)	Pull-out force Qu (N)	Pore pressures (KN/m^2)			$\frac{Qu}{\gamma' AD}$	$\frac{D}{B}$	$\frac{P1}{\gamma' D}$
			below P_2	above P_3	above top P_4			
1	618	391	1.52	1.05	0.86	8.31	6.06	0.43
2	611	361	1.51	1.05	0.85	7.75	5.99	0.44
3	596	349	1.38	1.14	0.89	7.69	5.84	0.45
4	568	340	1.31	1.01	0.78	7.86	5.57	0.47
5	483	245	1.26	0.92	0.81	6.66	4.74	0.56
6	464	206	1.21	0.89	0.80	5.83	4.55	0.58
7	455	242	0.96	0.88	0.62	6.99	4.46	0.59
8	442	237	1.26	0.75	0.69	7.04	4.33	0.61
9	432	222	1.31	1.09	0.73	6.75	4.24	0.62
10	394	218	1.29	0.96	0.64	7.27	3.86	0.68

Table 9 (continued)

Test No.	Burial depth D (mm)	Pull-out force Qu (N)	Pore pressures (KN/m^2)			$\frac{Qu}{\gamma' AD}$	$\frac{D}{B}$	$\frac{P1}{\gamma' D}$
			below P_2	above P_3	above top P_4			
11	393	170	0.64	0.46	0.57	5.68	3.85	0.68
12	366	175	1.08	0.88	0.54	6.28	3.59	0.73
13	335	154	0.63	0.42	0.35	6.04	3.28	0.80
14	309	126	0.61	0.36	0.33	5.36	3.03	0.87
15	291	109	0.51	0.28	0.24	4.91	2.85	0.92
16	251	84	0.50	0.21	0.20	4.39	2.46	1.07
17	238	82	0.50	0.21	0.20	4.52	2.33	1.13
18	187	54	0.41	0.20	0.18	3.79	1.83	1.43
19	148	39	0.38	0.16	0.14	3.46	1.45	1.81
20	117	30	0.36	0.15	0.09	3.36	1.15	2.29

Table 9 (continued)

Test No.	Burial depth D (mm)	Pull-out force Qu (N)	Pore pressures (KN/m^2)			$\frac{Qu}{\gamma' AD}$	$\frac{D}{B}$	$\frac{P1}{\gamma' D}$
			below P_2	above P_3	above top P_4			
21	104	24	0.35	0.11	0.09	3.03	1.02	2.58
22	76	18	0.35	0	0	3.11	0.75	3.53

Burial depth against pull-out force, pore pressures P_2 and P_3 and non-dimensional parameters are plotted in Fig. 3.29, 3.39 and Fig. 4.1 to 4.4 respectively.

Table 10 Pull-out tests for 102 mm suction
$p_1 = 5.0$ KN/m^2 and $p_1/\gamma'B = 5.26$.

Test No.	Burial depth D (mm)	Pull-out force Qu (N)	Pore pressures (kN/m^2)	
			below P_2	above P_3
1	615	553	3.51	2.39
2	595	539	3.49	2.38
3	594	504	3.01	2.22
4	613	482	3.38	2.35
5	571	453	3.02	2.11
6	546	469	3.07	2.41
7	526	456	2.98	2.17
8	488	403	2.65	1.97
9	486	380	2.27	1.84
10	463	345	2.01	1.59

anchor with a cavity pressure

$\frac{Qu}{\gamma' AD}$	$\frac{P1}{\gamma' D}$	$\frac{D}{B}$
11.80	0.87	6.03
11.89	0.90	5.83
11.14	0.90	5.82
10.33	0.88	6.01
10.42	0.94	5.60
11.28	0.98	5.35
11.38	1.02	5.16
10.85	1.10	4.78
10.26	1.10	4.76
9.79	1.16	4.54

Table 10 (continued)

Test No.	Burial depth	Pull-out force	Pore pressures (kN/m^2) below	Pore pressures (kN/m^2) above	$\frac{Qu}{\gamma' AD}$	$\frac{P1}{\gamma' D}$	$\frac{D}{B}$
11	357	250	1.83	1.42	9.19	1.50	3.50
12	336	202	1.71	1.36	7.89	1.60	3.29
13	292	181	1.69	1.34	8.14	1.84	2.86
14	248	122	1.69	1.09	6.45	2.16	2.43
15	208	103	1.49	0.92	6.51	2.58	2.04
16	195	93	1.71	0.96	6.26	2.75	1.91
17	182	81	1.65	0.89	5.84	2.95	1.78
18	151	59	1.55	0.76	5.13	3.55	1.48
19	132	52	1.62	0.61	5.17	4.06	1.29
20	91	40	1.61	0.51	5.76	5.90	0.89

Table 10 (continued)

Test No.	Burial depth D (mm)	Pull-out force Qu (N)	Pore pressures (kN/m^2) below P_2	Pore pressures (kN/m^2) above P_3	$\frac{Qu}{\gamma' AD}$	$\frac{P1}{\gamma' D}$	$\frac{D}{B}$
21	73	31	1.51	0.17	5.77	7.35	0.72
22	51	27	1.51	0.00	6.95	10.52	0.50
23	43	20	1.36	0.00	6.11	12.48	0.42

Burial depth against pull-out force, pore pressures p_2 against p_3 and non-dimensional parameters are plotted in Fig. 3.29, 3.39 and Fig. 4.1 to 4.2 respectively.

Table 11 Pull-out tests for 102 mm suction anchor with a cavity suction pressure p_1 = 6.0 kN/m^2 & $p_1 \gamma' B$ = 6.31

Test No.	Burial depth D (mm)	Pull-out force Qu (N)	$\frac{Qu}{\gamma' AD}$	$\frac{P1}{\gamma' D}$	$\frac{D}{B}$
1	618	656	13.94	1.04	6.06
2	611	656	14.09	1.05	5.99
3	618	628	13.34	1.04	6.06
4	606	596	12.91	1.06	5.94
5	578	541	12.29	1.11	5.67
6	547	544	13.06	1.18	5.36
7	505	452	11.75	1.28	4.95
8	487	478	12.89	1.32	4.77
9	466	450	12.68	1.38	4.57
10	447	413	12.13	1.44	4.38
11	421	394	12.86	1.53	4.13
12	414	339	10.75	1.56	4.06
13	389	312	10.53	1.66	3.81
14	392	303	10.15	1.64	3.84
15	346	266	10.10	1.86	3.39
16	327	225	9.04	1.97	3.21
17	305	213	9.16	2.11	2.99
18	320	197	8.08	2.01	3.14
19	300	191	8.37	2.15	2.94
20	281	191	8.91	2.29	2.75
21	274	188	9.01	2.35	2.69
22	243	155	8.37	2.65	2.38
23	231	129	7.33	2.79	2.26
24	221	127	7.54	2.91	2.17
25	174	99	7.47	3.7	1.71

Table 11 (continued)

Test No.	Burial depth D (mm)	Pull-out force Qu (N)	$\frac{Qu}{\gamma' AD}$	$\frac{P1}{\gamma' D}$	$\frac{D}{B}$
26	165	78	6.21	3.90	1.62
27	153	70	6.01	6.31	1.50
28	144	67	6.11	6.31	1.41
29	126	54	5.63	6.31	1.24
30	112	51	5.98	6.31	1.1

Burial depth against pull-out force and non-dimensional parameters are plotted in Fig. 3.29 and Fig. 4.1 respectively.

Table 12 Pull-out tests for 102 mm suction anchor with a cavity suction pressure $p_1 = 7.50$ KN/m^2 and $p_1/\gamma'B = 7.89$.

Test No.	Burial depth D (mm)	Pull-out force Qu (N)	Pore pressures (KN/m^2) below P_2	Pore pressures (KN/m^2) above P_3	$\frac{Qu}{\gamma' AD}$	$\frac{P1}{\gamma' D}$	$\frac{D}{B}$
1	618	762	3.60	3.10	16.20	1.30	6.06
2	618	743	3.52	3.03	15.76	1.30	6.06
3	609	718	3.48	2.91	15.48	1.32	5.97
4	601	732	3.59	2.71	15.99	1.34	5.89
5	522	601	2.79	2.60	15.11	1.54	5.12
6	504	538	2.72	2.51	14.02	1.60	4.94
7	436	417	2.71	2.33	12.55	1.85	4.27
8	427	423	2.71	2.34	13.01	1.89	4.19
9	409	424	2.37	2.01	13.61	1.97	4.01
10	382	393	2.21	1.89	13.51	2.11	3.75

Table 12 (continued)

Test No.	Burial depth D (mm)	Pull-out force Qu (N)	Pore pressures (KN/m^2) below P_2	above P_3	$\frac{Qu}{\gamma' AD}$	$\frac{P1}{\gamma' D}$	$\frac{D}{B}$
11	339	304	2.03	1.77	11.78	2.37	3.32
12	318	282	1.60	1.44	11.65	2.53	3.12
13	311	253	1.58	1.40	10.68	2.59	3.05
14	296	246	1.56	1.38	10.91	2.72	2.90
15	282	218	1.59	1.31	10.15	2.85	2.77
16	243	166	1.71	1.30	8.98	3.31	2.38
17	199	131	1.56	0.96	8.65	4.04	1.95
18	176	109	1.41	0.93	8.14	4.57	1.73
19	125	68	1.40	0.84	7.14	6.44	1.23

Burial depth against pull-out force and non-dimensional parameters are plotted in Fig. 3.29 and Fig. 4.1 to 4.2 respectively.

Table 13 Pull-out tests for 102 mm suction anchor with a cavity suction pressure $p_1 = 10.0 KN/m^2$ and $p_1/\gamma'B = 10.52$.

Test No.	Burial depth D (mm)	Pull-out force Qu (N)	Pore pressures (KN/m^2) below P_2	Pore pressures (KN/m^2) above P_3	$\frac{Qu}{\gamma'AD}$	$\frac{P1}{\gamma'D}$	$\frac{D}{B}$
1	609	923	7.10	4.91	19.90	1.76	5.97
2	569	862	5.32	4.31	19.89	1.89	5.58
3	556	816	5.19	4.27	19.28	1.93	5.45
4	548	758	5.11	4.21	18.17	1.96	5.37
5	522	742	4.96	4.03	18.67	2.06	5.18
6	501	662	4.89	3.97	17.35	2.14	4.91
7	482	617	4.64	3.89	16.81	2.23	4.73
8	408	502	4.35	3.69	16.16	2.63	4.00
9	384	455	4.24	3.58	15.56	2.79	3.76
10	343	351	3.93	3.14	13.43	3.13	3.36

Table 13 (continued)

Test No.	Burial depth D (mm)	Pull-out force Qu (N)	Pore pressures (KN/m^2) below P_2	above P_3	$\frac{Qu}{\gamma' AD}$	$\frac{P1}{\gamma' D}$	$\frac{D}{B}$
11	327	322	3.58	2.64	12.94	3.28	3.21
12	298	265	3.46	2.51	11.68	3.60	2.92
13	282	241	3.33	2.37	11.22	3.80	2.77
14	246	219	3.29	2.33	11.69	4.36	2.41
15	221	192	3.25	2.25	11.41	4.86	2.17
16	200	161	3.13	2.01	10.57	5.37	1.96
17	181	144	3.09	1.78	10.44	5.93	1.77
18	162	118	3.08	1.81	9.56	6.62	1.59
19	144	111	3.07	1.72	10.12	7.45	1.41
20	128	97	3.07	1.55	9.94	8.38	1.26

Table 13 (continued)

Test No.	Burial depth D (mm)	Pull-out force Qu (N)	Pore pressures (KN/m^2) below P_2	Pore pressures (KN/m^2) above P_3	$\frac{Qu}{\gamma' AD}$	$\frac{P1}{\gamma' D}$	$\frac{D}{B}$
21	102	73	2.67	1.09	9.40	10.52	1.0
22	80	62	2.60	0.54	10.17	13.41	0.78

Burial depth against pull-out force, pore pressures p_2 against p_3 and non-dimensional parameters are plotted in Fig. 3.29, 3.39 and Fig. 4.1 to 4.3 respectively.

Table 14 Pull-out tests for 102 mm suction anchor with a cavity suction pressure p_1 = 12.50 KN/m^2 and $P_1/\gamma' B$ = 13.15.

Test No.	Burial depth D (mm)	Pull-out force Qu (N)	Pore pressures (KN/m^2) below P_2	above P_3	above top P_4	$\frac{Qu}{\gamma' AD}$	$\frac{P1}{\gamma' D}$	$\frac{D}{B}$
1	618	1292	7.11	4.94	4.07	27.45	2.17	6.06
2	585	1113	7.41	5.66	4.92	24.98	2.29	5.74
3	546	965	6.35	4.78	4.30	23.21	2.46	5.35
4	527	842	6.29	4.57	4.21	20.98	2.54	5.17
5	477	761	6.02	4.39	4.01	20.94	2.81	4.68
6	422	560	5.83	4.13	3.72	17.43	3.18	4.18
7	377	489	4.71	3.59	3.17	17.04	3.56	3.70

Burial depth against pull-out force, pore pressures p_2 against p_3 and non-dimensional parameters are plotted in Fig. 3.29, 3.39 and Fig. 4.1 to 4.3 respectively.

APPENDIX B

FLUID PRESSURE DISTRIBUTION IN THE SAND

Page No. B 1 - B 11

Table 1 Pull-out resistance and pressures for 102 mm suction anchor during pull-out. Burial depth D = 614 mm. The graphs are plotted in Fig. 3.31 and 3.42.

Serial No.	Pull-out resistance (N)	Pressures (KN/m^2) cavity P_1	below P_2	above P_3	Anchor displacement mm
1	0.0	5.00	3.39	2.37	10
2	133.4	5.12	3.43	2.35	110
3	269.9	4.99	3.32	2.26	22
4	365.1	4.96	3.02	2.09	34
5	419.1	4.75	2.87	2.01	46
6	450.8	4.65	2.72	1.97	58
7	466.7	4.59	2.60	1.91	70
8	481.1	4.56	2.52	1.89	82
9	485.8	4.50	2.47	1.89	94
10	485.8	4.47	2.39	1.82	106
11	479.4	4.46	2.34	1.76	118
12	473.1	4.43	2.29	1.66	130
13	466.7	4.42	2.22	1.57	142
14	454.0	4.38	2.19	1.50	154

Table 2 Pull-out resistance and pressures for 102 mm suction anchor during pull-out. Burial depth D = 407 mm. The graphs are plotted in Fig. 3.32 and 3.43.

Serial No.	Pull-out resistance (N)	Pressures (KN/m^2)			Anchor displacement (mm)
		cavity P_1	below P_2	above P_3	
1	0	10.00	4.59	3.90	0
2	63.5	10.00	4.59	3.88	2.5
3	285.8	10.16	4.64	3.86	14.5
4	457.2	10.06	4.64	3.77	26.5
5	517.2	9.83	4.56	3.73	38.5
6	533.4	9.64	4.44	3.69	50.5
7	514.3	9.52	4.39	3.60	62.5
8	469.9	9.34	4.23	3.46	74.5
9	428.6	9.17	4.08	3.29	86.5
10	382.3	9.08	3.93	3.14	98.5
11	342.9	8.99	3.78	3.06	110.5
12	304.8	8.92	3.58	2.89	122.5
13	269.9	8.87	3.53	2.81	134.5
14	244.5	8.81	3.43	2.68	146.5
15	222.3	8.79	3.38	2.62	158.5
16	203.2	8.75	3.28	2.47	170.5

Table 3 Pull-out resistance and pressures for 102 mm suction anchor during pull-out. Burial depth D = 381 mm. The graphs are plotted in Fig. 3.33 and 3.43.

Serial No.	Pull-out resistance (N)	Pressures (KN/m^2)			Anchor displacement (mm)
		cavity P_1	below P_2	above P_3	
1	0.0	10.00	4.44	3.69	0
2	95.3	10.09	4.44	3.69	12
3	304.8	10.36	4.39	3.65	24
4	393.7	10.45	4.49	3.77	36
5	469.9	10.00	4.64	3.81	48
6	444.5	9.76	4.59	3.81	60
7	330.2	9.53	4.39	3.65	72
8	304.8	9.24	4.28	3.48	84
9	279.4	9.04	4.11	3.35	96
10	266.7	9.05	3.98	3.23	108
11	250.8	8.95	3.93	3.14	120
12	238.13	8.89	3.83	3.02	132
13	222.3	8.77	3.73	2.93	144
14	206.34	8.72	3.58	2.81	156

Table 4 Pull-out resistance and pressures for 102 mm suction anchor during pull-out. Burial depth D = 609 mm.

Serial No.	Pull-out resistance (N)	Pressures (KN/m^2)			Anchor displacement (mm)
		cavity P_1	below P_2	above P_3	
1	0	10.00	7.06	4.90	0
2	38.1	10.00	7.01	4.86	12
3	190.5	9.85	6.60	4.82	24
4	317.5	9.42	6.50	4.78	36
5	450.9	9.18	6.00	4.57	48
6	584.2	9.0	5.70	4.40	60
7	679.4	8.85	5.39	4.27	72
8	768.4	8.61	5.14	4.15	84
9	831.9	8.50	4.96	4.02	96
10	870.0	8.40	4.81	3.90	108
11	895.5	8.34	4.69	3.90	120
12	908.1	8.28	4.59	3.73	132
13	927.1	8.19	4.49	3.73	144
14	924.0	8.12	4.39	3.69	156
15	908.1	8.04	4.31	3.62	168
16	873.0	8.03	4.23	3.60	180
17	825.5	8.00	4.18	3.52	192
18	787.4	7.96	4.13	3.44	204
19	746.0	7.91	4.03	3.35	216
20	743.0	7.85	3.96	3.29	228
21	615.95	7.80	3.88	3.27	240

Pressures/force, pressures/anchor displacement and pull-out force/anchor displacement are plotted in Fig. 3.34, 3.40 and 3.43 respectively.

Table 5 Pull-out resistance and pressures for 102 mm suction anchor during pull-out. Burial depth D = 614 mm. The graphs are plotted in Fig. 3.35 and 3.42.

Serial No.	Pull-out force (N)	Pressures (KN/m^2) cavity P_1	below P_2	above P_3	Anchor displacement (mm)
1	0.0	15.94	8.67	6.03	0
2	50.8	15.94	9.02	6.03	8
3	330.2	16.01	8.77	6.03	20
4	628.7	15.16	8.27	5.91	32
5	825.5	14.74	7.86	5.82	44
6	952.5	14.29	7.43	5.64	56
7	1028.7	13.86	7.21	5.59	68
8	1069.9	13.60	6.90	5.28	80
9	1073.2	13.26	6.70	5.11	92
10	1073.2	13.21	6.55	4.99	104
11	1054.1	13.11	6.45	4.86	116
12	1025.5	13.05	6.38	4.76	128
13	993.8	12.99	6.28	4.65	140
14	946.2	12.96	6.20	4.53	152
15	901.7	13.01	6.12	4.78	164
16	873.1	12.94	6.10	4.32	176
17	800.1	12.93	6.05	4.23	188
18	752.5	12.97	5.97	4.11	200
19	698.5	12.97	5.85	4.02	212
20	641.4	12.97	5.75	3.93	224
21	565.2	12.99	5.65	3.88	236
22	501.7	13.02	5.52	3.79	248
23	450.9	13.05	5.44	3.71	260
24	412.8	13.04	5.37	3.60	272

Table 6 Pull-out resistance and pressures for 102 mm suction anchor during pull-out. Burial depth D = 614 mm. The graphs are plotted in Fig. 3.36 and 3.42.

Serial No.	Pull-out resistance	Pressures (KN/m^2)			Anchor displacement (mm)
		cavity P_1	below P_2	above P_3	
1	0	16.42	8.97	5.99	0
2	44.5	16.42	9.02	6.03	2
3	222.3	16.68	8.87	5.95	14
4	323.9	16.20	8.42	5.78	26
5	406.4	15.90	7.76	5.55	38
6	482.6	15.71	7.33	5.34	50
7	539.7	15.58	6.96	5.20	62
8	584.2	15.48	6.68	5.03	74
9	615.9	15.43	6.40	4.90	86
10	647.7	15.40	6.15	4.73	98
11	660.4	15.38	6.0	4.50	110
12	679.5	15.34	5.78	4.19	122
13	698.5	15.34	5.59	4.06	134
14	711.2	15.36	5.24	4.06	146
15	717.6	15.36	4.86	3.86	158
16	723.9	15.41	4.71	3.50	170
17	717.6	15.42	4.76	3.35	182

Table 7 Pull-out resistance and pressures for 102 mm suction anchor during pull-out. Burial depth D = 609 mm and cavity suction pressure P_1 = 12.00 KN/m^2. The graph is plotted in Fig. 3.37.

Serial No.	Pull-out resistance (N)	Pressures (KN/m^2) cavity P_1	below P_2	above P_3	above top P_4	Anchor displacement (mm)
1	0.0	12.00	7.06	4.94	4.07	0
2	95.3	12.00	7.06	4.94	4.07	12
3	273.1	11.80	7.16	4.99	4.12	24
4	558.8	11.30	6.65	4.73	4.07	36
5	831.9	11.00	6.20	4.57	3.97	48
6	1016.0	10.6	5.85	4.40	3.88	60
7	1123.9	10.2	5.54	4.27	3.83	72
8	1187.5	10.3	5.34	4.19	3.78	84
9	1230.9	10.1	5.19	4.02	3.67	96
10.	1252.7	10.1	5.04	3.90	3.60	108

Table 7 (continued)

Serial No.	Pull-out resistance (N)	Pressures (KN/m^2) cavity P_1	below P_2	above P_3	above top P_4	Anchor displacement (mm)
11	1252.7	10.1	4.89	3.18	3.45	120
12	1246.6	9.9	4.79	2.60	3.41	132
13	1130.3	9.8	4.69	2.43	3.31	144
14	870.0	9.8	4.39	2.18	3.32	156
15	806.5	9.76	4.38	2.22	3.12	168
16	749.3	9.71	4.28	2.43	3.03	180
17	679.5	9.71	4.18	2.77	2.93	192
18	622.3	9.71	4.13	3.06	2.89	204
19	539.8	9.66	4.08	3.35	2.79	216
20	482.6	9.61	3.98	3.56	2.70	228
21	469.9	9.61	3.88	3.56	2.60	240
22	457.2	9.61	3.88	3.39	2.51	252
23	387.5	9.61	3.68	3.23	2.41	264

Table 8 Pull-out resistance and pressures for 102 mm suction anchor during pull-out. Burial depth D = 589 mm. Pressures against pull-out resistance are plotted in Fig. 3.38.

Serial No.	Pull-out resistance (N)	Pressures (KN/m^2)				Anchor displacement (mm)
		cavity P_1	below P_2	above P_3	above top P_4	
1	0	11.80	7.11	5.70	4.92	0
2	95.3	11.92	7.41	5.74	4.97	3
3	279.4	11.97	7.36	5.66	4.97	15
4	419.1	11.67	7.26	5.53	4.92	27
5	546.1	11.48	6.80	5.36	4.92	39
6	660.4	11.33	6.55	4.75	4.83	51
7	768.4	11.18	6.35	4.19	4.87	63
8	850.9	10.99	6.15	3.77	4.87	75
9	952.5	10.89	5.85	3.78	4.87	87
10	971.6	10.74	5.70	3.23	4.78	99

Table 8 (Continued)

Serial No.	Pull-out resistance (N)	Pressures (KN/m^2)				Anchor displacement (mm)
		cavity P_1	below P_2	above P_3	above top P_4	
11	984.3	10.69	5.54	2.68	4.68	111
12	990.6	10.59	5.39	2.22	4.59	123
13	952.5	10.55	5.29	2.10	4.54	135
14	908.1	10.50	5.19	2.18	4.45	147
15	787.4	10.50	5.14	2.64	4.35	159
16	679.5	10.30	5.14	3.44	4.26	171
17	596.9	10.25	4.99	4.06	4.16	183
18	539.8	10.15	4.89	4.48	4.07	195
19	508.0	10.10	4.84	4.82	3.97	207
20	463.6	10.06	4.74	4.90	3.83	219

APPENDIX C

PORE PRESSURE RÉGIME

Page C 1 to C 7

APPENDIX C

PORE PRESSURE RÉGIME

The 102 mm suction anchor was used for the analysis of the pore water pressure around the anchor. Three different tests were performed.

Test 1: Fig. C.1 shows the plan of the testing tank with the pressure probe and also shows the location of the test anchor. The pressure probe consisted of four small copper tubes. The spacing of the copper tubes was 115 mm centre to centre. Fig. C.2 shows the pore pressure régime of the 102 mm suction anchor on elevation. The anchor was buried at a depth of 204 mm. On achieving the required pressure in the anchor suction cavity the pressure probe was placed at 1. Four pressures were recorded at different depths from position 1 (e.g. 0.13, 0.49, 0.23 and 0.23 kN/m^2). Then, the pressure probe was withdrawn from 1 and placed at 2 and so on for recording the pressures around the anchor. Fig. C.3 shows the pore pressure régime of the 102 mm suction anchor on elevation. The test results appear to be incorrect.

Tests 2 and 3: The tests were performed to study the dissipation of hydrostatic pressure difference in the granular soil as imposed by the suction filter of the anchor. The pressure difference between two equipotential lines represents 5 or 10 percent of the pressure difference between the two potential surfaces. Fig. C.4 shows the pore pressure régime by using an electrolytic tank. Fig. C.5 shows the pore pressure distribution by using an electrical conducting paper.

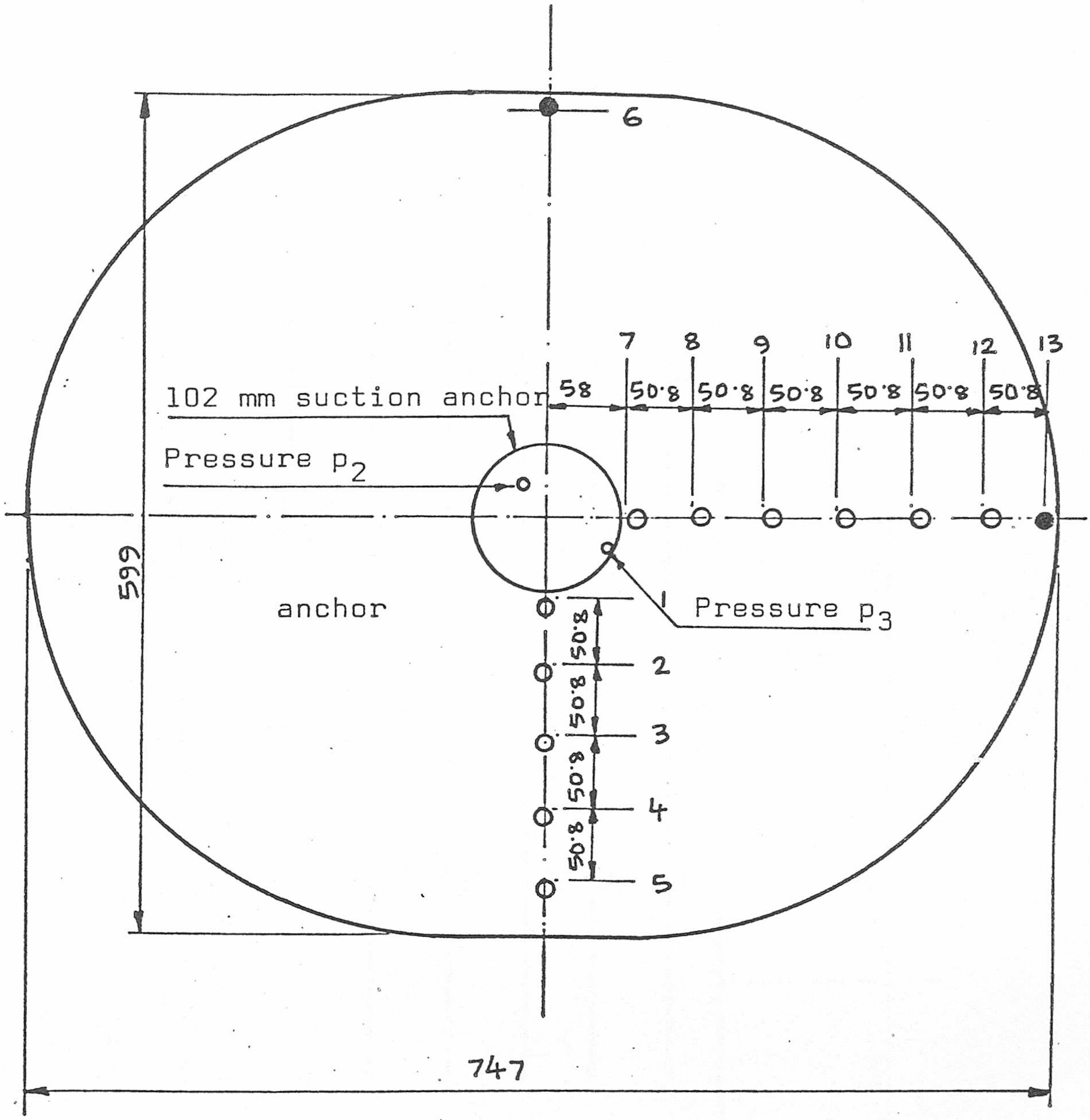

All dimensions are in mm

Fig. C.1 Plan on the testing tank with the pressure probes.

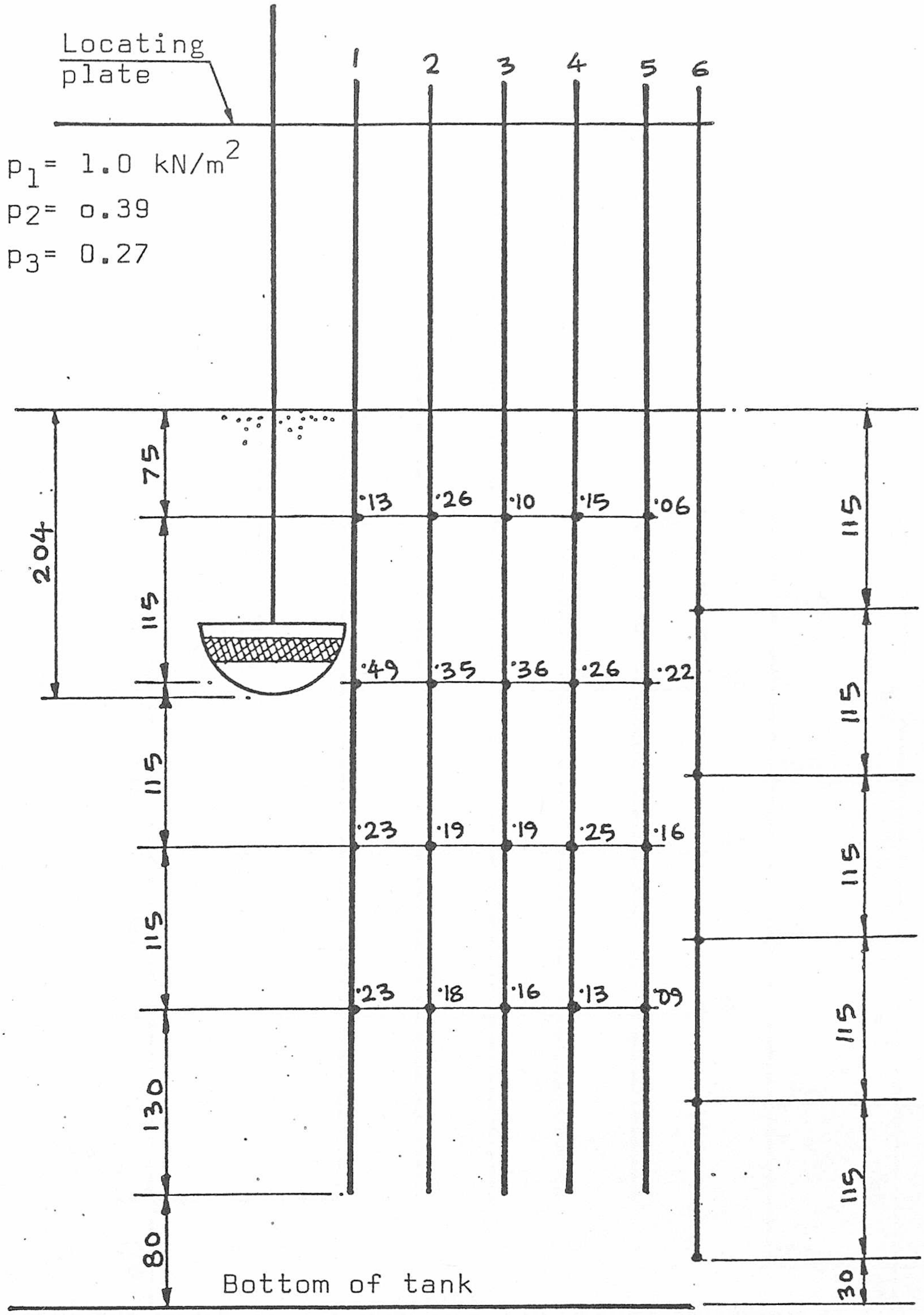

Scale 1:5

Fig. C.2 Pore pressure régime of 102 mm suction anchor on elevation

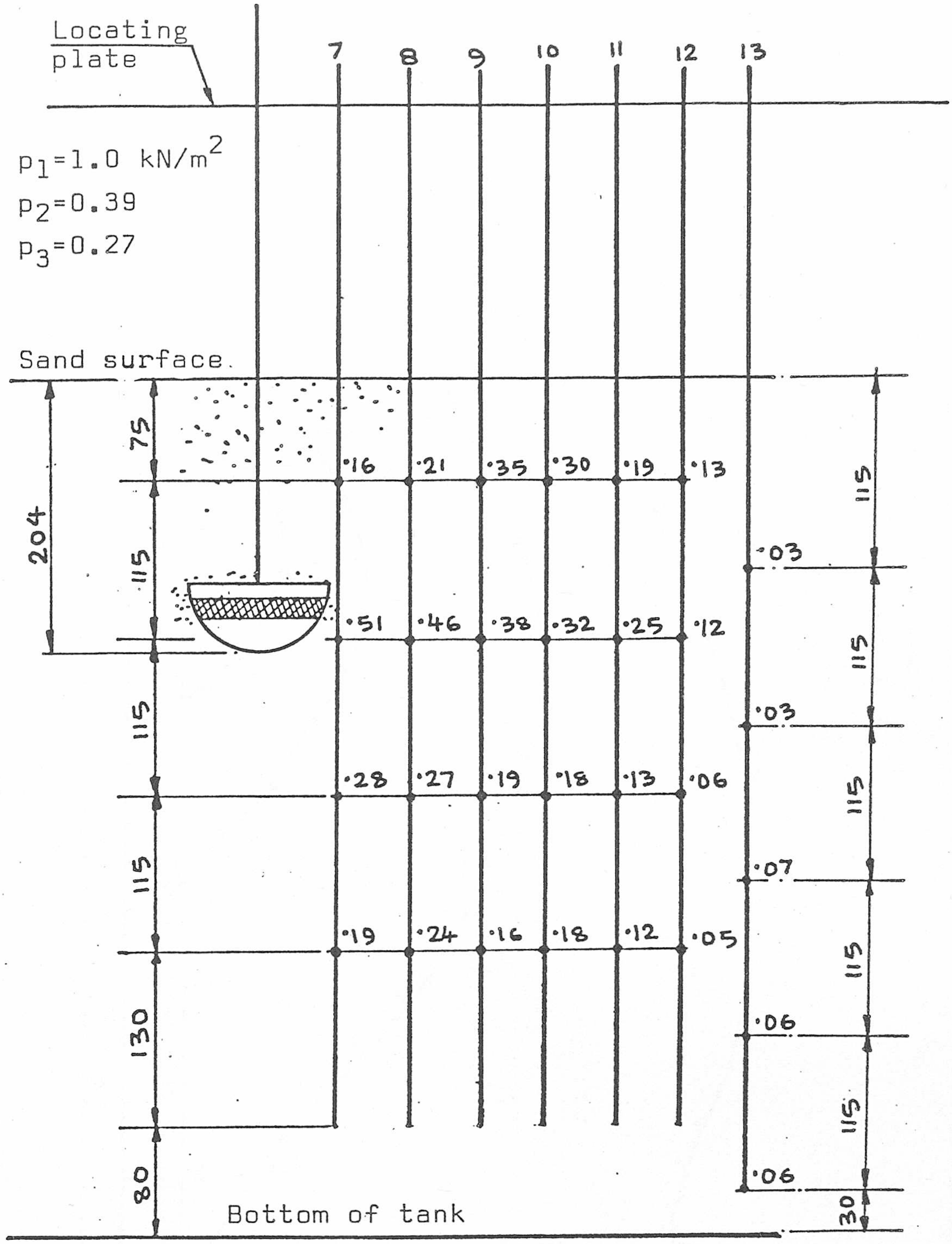

Scale 1:5

Fig. C.3 Pore pressure régime of the 102 mm suction anchor on elevation

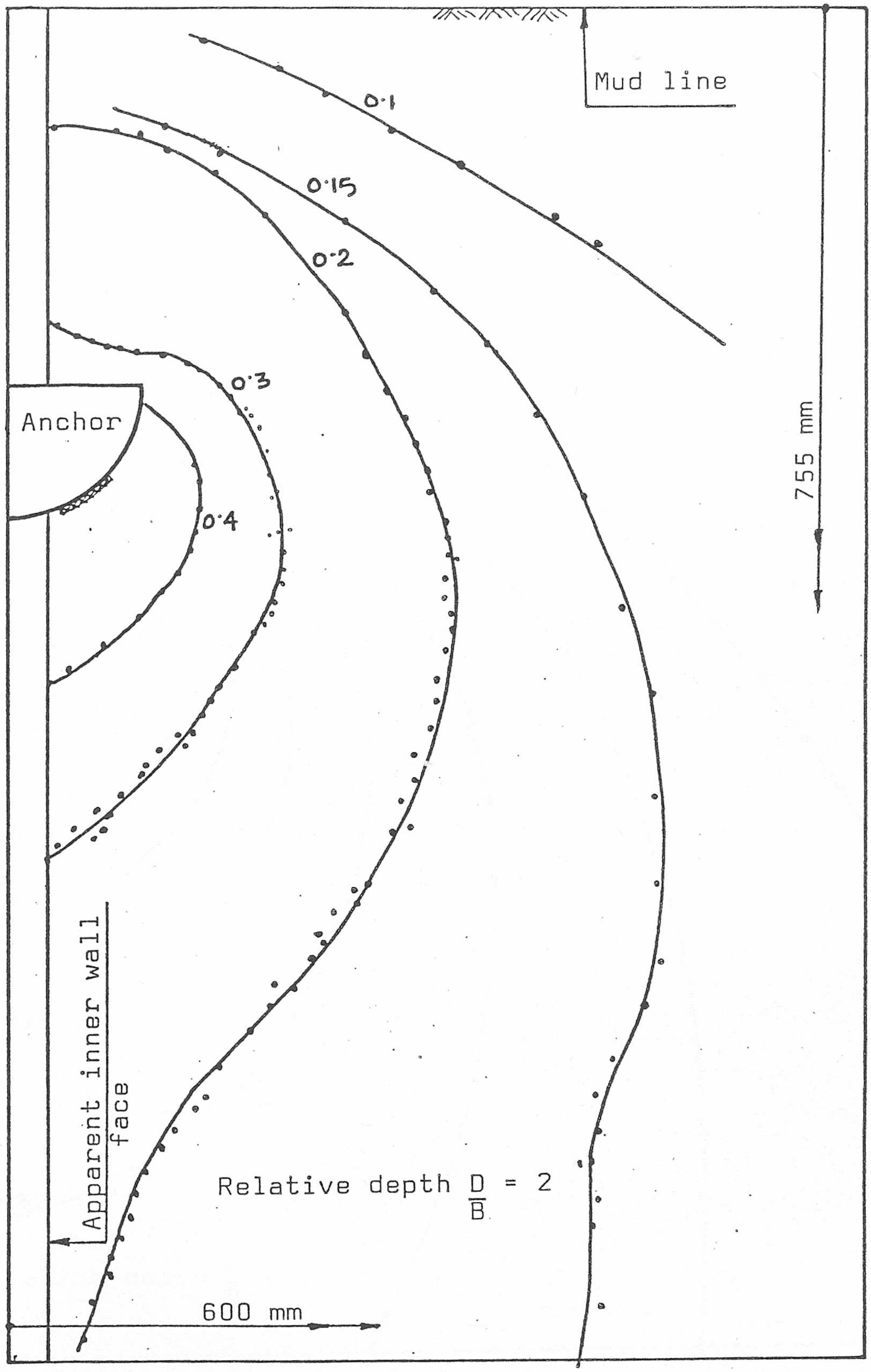

Fig. C.4 Pore pressure régime by using an electrolytic tank.

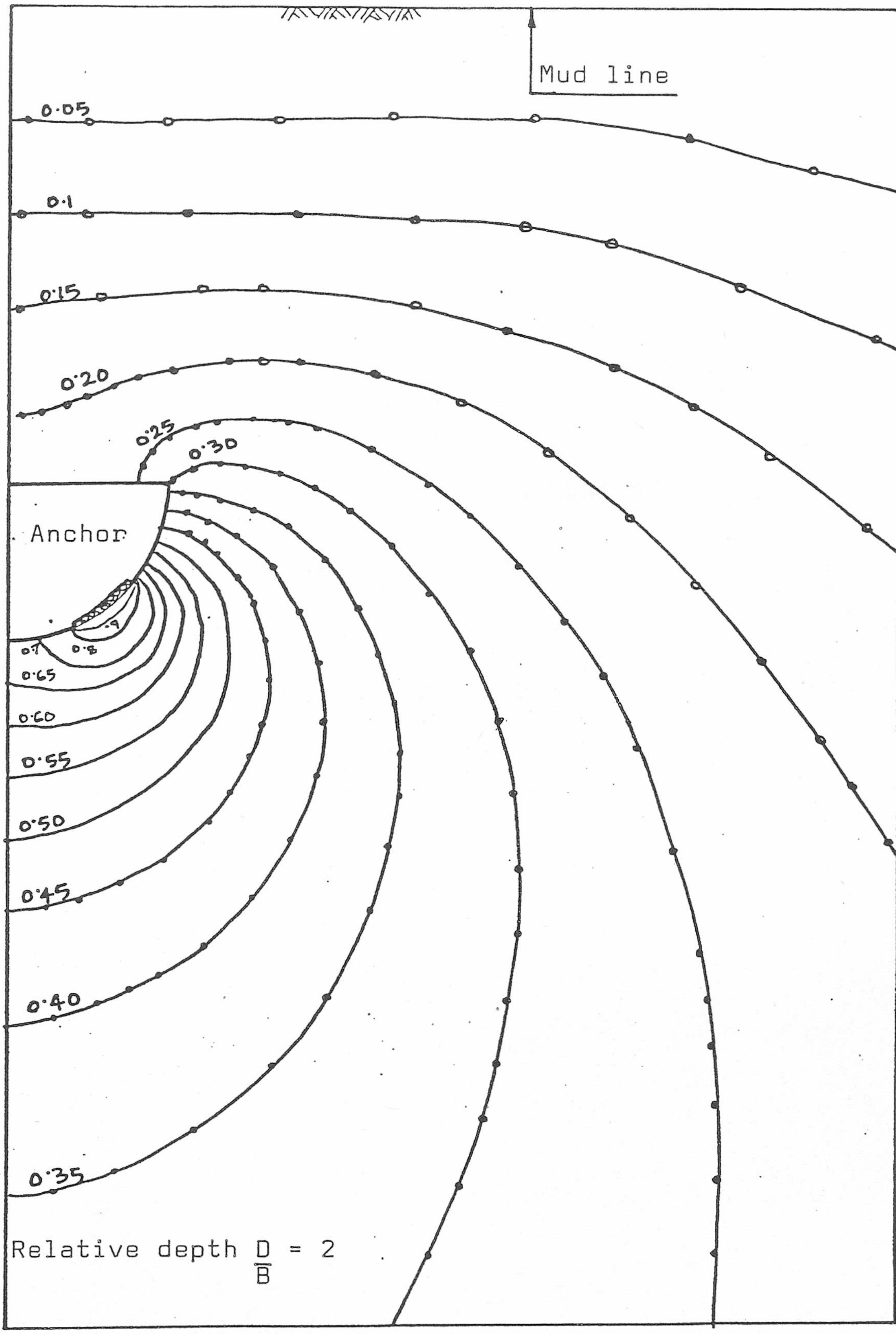

Fig. C.5 Pore pressure distribution by using an electrical conducting paper.

APPENDIX D

SUCTION ANCHOR DISPLACEMENT AT

VARIED SUCTION TIME

Page No. D 1 - D 3

APPENDIX D

SUCTION ANCHOR DISPLACEMENT AT

VARIED SUCTION TIME

The 102 mm suction anchor was used for analysing the anchor displacement at pull-out with varied suction time.

Burial depth D = 619 mm
Cavity suction pressure = 7.50 kN/m^2
Suction time = less than ½ minute to more than 2 minutes
Pull-out speed ≐ 0.60 mm/s

Fig. D.1 shows the relationship between pull-out force and anchor displacement at pullpout for the 102 mm suction anchor.

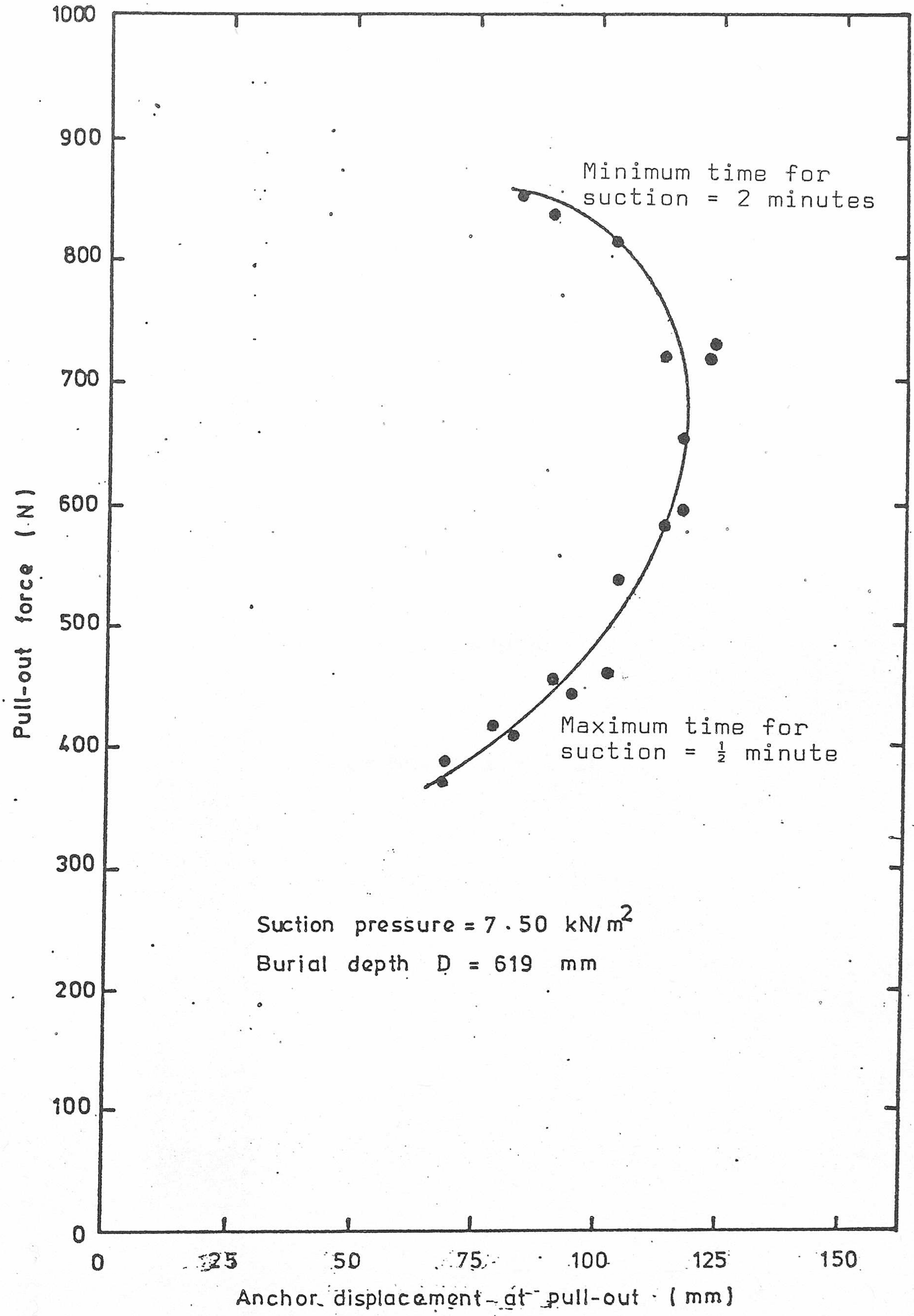

Fig. D.1 Pull-out force / anchor displacement for 102 mm suction anchor.

APPENDIX E

SUCTION ANCHORS

BY

B.S. SAHOTA

Page No. E 1 - E 20

SUCTION ANCHORS

BY

B.S. SAHOTA

RESEARCH STUDENT

This paper was presented on Thursday 25th May 1978 at the Annual General Meeting held at Skean Dhu, Dyce, before the International President, Mr. H. Barton of the Society of Petroleum Engineers and awarded the second prize in the 'Student Paper Competition' which was organised by the Aberdeen branch.

SCHOOL OF MECHANICAL AND OFFSHORE ENGINEERING

ROBERT GORDON'S INSTITUTE OF TECHNOLOGY, ABERDEEN

MARCH, 1978

CONTENTS

SUCTION ANCHORS

B.S. Sahota, SRC Research Student

Robert Gordon's Institute of Technology, Aberdeen

ABSTRACT

Breakout resistance, submerged soil pressure and effective mass of uplift-resisting anchors are considered. To study the feasibility of suction anchors a model 165mm diameter by 100mm deep was tested in submerged fine sand placed in an extented oil drum 850mm deep by 750mm wide. One proto type suction anchor 600mm diameter by 300mm deep was tested in the North Sea off Aberdeen and Stonehaven. Experimental results between the anchors are compared. The study results show that the suction anchors are particularly successful in cohesionless soils.

INTRODUCTION

Ever since man has realized that there was a need for anchors and anchoring facilities in both marine and terrestrial applications, he has been concerned with the development of anchoring devices. Dead weight anchors were introduced because their reaction capabilities could be easily calculated and these anchors are still in use.

On land, earth anchors are being used increasingly in place of large deadweight foundations. Most of the holding power is achieved by the mass and strength of the soil above the anchor.

Several types of anchor are available and are in use in the ocean environment. The growth of the ocean operations and construction over the last decade has resulted in increased application of floating equipment anchored in shallow or deep water; a substantial mooring is often required in deep water far from land and this puts into question the economics of transporting heavy masses of concrete, steel, etc. to act/

act as anchors for such systems. The need is for anchors which can resist uplift and are highly efficient, reliable, light weight, occupying a small surface area and are simple to handle. Embedded seabed anchors are capable of providing a higher pullout/weight ratio in comparison with a conventional anchor and are capable of providing short-term and long-term upward resistance to breakout for precisely positioned submersibles and bottom resting equipment.

RECENT RESEARCH AND DEVELOPMENT

Investigators have learned of the need for uplift-resisting anchors and have introduced other types (5) such as propellant-actuated, vibrated, screw-in, implosive, pulse-jet, jetted, padlock, hydrostatic and vacuum anchors. A few of these anchors advanced to development stage, others still require further attention for development and some of these are abandoned due to encountered problems. Still some hidden difficulties remain unsolved and much has to be learned about the security of holding capacity of anchors in shallow and deep waters.

The scope of this paper is limited to suction anchors. Initial research on model suction anchors took place in the United States of America on the development of a short-term high-efficiency anchor which utilized vacuum to develop its capacity. Further research commenced (3, 4, 6) at Robert Gordon's Institute of Technology (RGIT) Aberdeen, United Kingdom for the investigation and development of suction anchors.

Suction anchors are capable of providing large upward forces in comparison to their own weight,. Suction anchors may be designed as a surface attachment anchor, embedded anchor or platform-type anchor.

BREAKOUT RESISTANCE

To determine the breakout resistance (7) of anchors designed to resist upward forces involves considerations and techniques which are not required for conventional anchors. Conventional anchors are designed to/

to embed as they are dragged and generally maintain their approximate design holding capacity. Uplift-resisting anchors should be embedded in the ocean bottom by means of applied forces except the service loading.

SUBMERGED SOIL PRESSURE

Fig. 1 shows that the suction anchor is buried in the seabed at a depth z and the height of water above the seabed level is z_1. Total pressure at AA is given by,

$$\sigma_{A-A} = g\gamma_{sat} z + g\gamma_w z_1 \quad \text{.......................(1)}$$

$$\text{Pore pressure } u = g\gamma_w z + g\gamma_w z_1 \quad \text{...............(2)}$$

$$\begin{aligned} \text{Effective pressure } \sigma' &= \sigma_{A-A} - u \\ &= g\gamma_{sat} z + g\gamma_w z_1 - g\gamma_w z - g\gamma_w z_1 \\ &= g\gamma_{sat} z - g\gamma_w z \\ &= g(\gamma_{sat} - \gamma_w) z \\ &= g\gamma' z \quad \text{..................(3)} \end{aligned}$$

Hence the effective pressure is equal to the thickness of the soil multiplied by the submerged density of soil. It does not depend upon the height z_1 of the water column. Even if z_1 reduces to zero, σ' will remain equal to $g\gamma' z$ so long as the soil mass above AA remains fully saturated. At BB, the total pressure is equal to the water pressure $g\gamma_w z_1$ and hence the effective pressure is zero. Thus the effective pressure varies linearly as shown in Fig. 1.

EFFECTIVE WEIGHT OF ANCHOR AND SOIL MASS

Effective weight of anchor = Anchor's total weight in air - buoyancy in water

$$W' = W - U \quad \text{.......................(4)}$$

The submerged unit mass γ' is given by,

$$\gamma' = \frac{(G_s - 1)\gamma_w}{1 + e} \quad \text{....................(5)}$$

where/

where, G_s = the specific gravity of solids

γ_w = unit mass of water

e = void ratio of the soil

For saturated soil,

$$e = mG_s$$

in which m = water content of the soil.

If there is a steady vertical seepage of gradient i in the soil mass under investigation the apparent soil mass will be changed to

$$\gamma'' = \gamma' \pm \gamma_w i \qquad (6)$$

in which the plus sign applies to downward and the minus sign to upward flow of water.

PRINCIPLE OF THE RGIT SUCTION ANCHORS

Suction type anchors may be of any shaped object, a can, a box, a cone, a hemisphere, a legged platform, etc., with an open, close or suitable end at the bottom. Water under pressure is supplied to a system of water jets. The burying of this anchor can be achieved by the water supply through the peripheral and, or middle jets which fluidize the seabed sediments underneath and within the skirt of the anchor because the jets produce a region of high turbulence which excavates the surrounding solids. To bury the anchor to a certain depth in the seafloor, underlying solid particles need to be removed and forced to move upwards or discharged in the sea water above it. Fig. 2 shows the burying and pulling action of a can anchor. The main force is provided by the collapse of the overlying material above the anchor. Once the anchor is buried by a few diameters, its own weight contributes little to the burying action. The anchor has a self levelling action. This is due to a cross-flow from the water jets which develops from a sloping seabed and increases the scouring rate on the high side of the anchor. Once the required burial depth is achieved the water supply to the jets is/

is cut-off and suction is applied. Water is extracted from the anchor cavity, which reduces the pressure in the anchor cavity, then the porewater pressure in the surrounding soil, and the continuation of dewatering reduces the volume of water present in the fluidized soil Dewatering consolidates the disturbed soil and provides an extra breakout resistance or an equivalent height of soil due to the applied suction pressure in addition to the overlying deposits. By dewatering, the cohesionless soil strength can be restored within a short time, allowing the anchor to be brought into almost immediate use. A large reduction in pullout can be achieved by use of the water jets if it is desired to retrieve the anchor.

TYPICAL TEST PROCEDURE FOR MODEL SUCTION ANCHOR

The apparatus was set up as shown in Fig. 3. The test model suction anchor was 165mm diameter by 100mm deep and shown in Fig. 4. The weight of the anchor in air and water was noted. A soil datum was marked and the anchor was lowered on to this datum. Water under pressure was supplied to the anchor through a 6mm bore plastic tubing from the mains. The chain was lowered gradually at a set speed, using the hounsfield tensometer motor. The anchor embedded itself in the soil and so that the top was just visible. It then began to oscillate and did not embed itself any further. The anchor was then gently pushed into the soil by hand, whereupon it began to bury itself further. Alternatively, suction was applied when the water supply was turned off for a few minutes and then the jet supply was turned on; if it did not embed itself further then it was gently pushed into the soil by hand so that it started to embed itself again. Jet and cavity heads were recorded and the water supply discontinued. Suction was then applied to the anchor by the pump for some minutes and it consolidated the soil while extracting water through the suction cavity. The anchor was then brought to the surface under suction by the hounsfield tensometer motor. A steady pull of 130mm/minute was maintained by the hounsfield tensometer. On completion of the breakout test, the anchor was brought above the water/

water surface and washed until the attached soil was removed. After each test, the soil in the tank was resurfaced and prepared for additional testing. The anchor was tested under several depths but the testing location was approximately the same.

The test soil was fine sand, with a specific gravity of 2.67.

TYPICAL TEST PROCEDURE FOR PROTO TYPE SUCTION ANCHOR

The apparatus was set up as shown in Fig. 5 and Fig. 6 shows the prototype suction anchor. The weight of the anchor was noted in air and in water. The anchor was lowered to the seabed. Water supply under pressure was delivered to the anchor by a centrifugal pump (Godwin DPC3). The jet supply was continued until the anchor stopped to bury further. If it was found that no further burial was achieved, the pump was switched off and the hoses were exchanged as shown in Fig. 5. The pump was switched on and dewatering was continued to consolidate the soil. The anchor was pulled out either by the help of tides or the manually operated winch of the Robert Gordon while the dewatering was in operation. Pressures were noted from the gauges before exchanging the hoses for suction and also when suction was applied. Once the pressure difference was built up the breakout test was applied. The breakout force was recorded on a chart recorder. The anchor was tested in several different locations but the sea water depth was limited due to the availability of the hoses.

The tests were carried out at Aberdeen beach and Stonehaven Harbour, North Sea.

COMPARISON BETWEEN THE ANCHORS

The comparison between the model suction anchor and prototype suction anchor is tabulated in Table 1.

CONCLUSIONS/

CONCLUSIONS

1. The breakout resistance of the suction anchors was a function of the pressure difference. The greater pullout force was achieved when the greater pressure difference was achieved.

2. An excessive dewatering time before the test and the variation in water depth did not have any effect on the breakout resistance of the model anchor. By dewatering, the soil strength was restored within a short time, allowing the anchor to be brought into almost immediate use for the test.

3. The central jet-ahead nozzle excavated the soil below the anchor level and made a difference in the burying motion of the anchor.

4. By applying jets the model anchor buried in sand up to its own depth. Further burial was not achieved and this was due to the built up upward pressure within the anchor which made it buoyant in the fluidized sand. Provision has been made on the prototype suction anchor for control of buoyancy but this has not been done so far.

5. By applying jets and suction in sequence to bury the model anchor in the sand, a deeper penetration could be achieved but the embedment depth was not consistent.

6. Manual power for winding the winch was very restricted and excessive loads were caused by the movement of the vessel due to the waves or swell. One field test had to be abandoned after nine minutes for the safety of the crew and the vessel when a succession of pulsating forces caused by the movement of the vessel reached a maximum force of 67.5 kN without causing breakout and on several occasions the pulsating forces reached well over 50 kN. On one breakout test a large plug of soil was brought above the sea water level from the seabed. It was held by the anchor as long as suction was maintained and the weight of this soil was 1.25 kN. It seems that the prototype suction anchor can be/

be successful in the fine grained sediments of the ocean bottom. Further, the breakout resistance depends upon anchor weight and geometry, soil strength parameters, soil permeability and pump capacity. Results of the study indicated that underwater suction anchoring in soil is feasible and that among the important anchor components a filter is necessary for preventing the soil underneath the anchor to fluidize. For a shallow burial depth, continual pumping is required for dewatering but continual pumping may not be necessary for deeper embedment.

APPLICATIONS OF SUCTION ANCHORS

Suction anchors may be used as surface attachment anchors, embedded anchors and platform-type anchors depending on the service required from the anchor and, or the ocean bed sediments. The application of these anchors are briefly described below:-

1. Surface attachment anchor

   If the anchor is buried to its own depth or a shallow burial is achieved, the achievement of burial depth being governed by the ocean bed sediments and the pump used, continual dewatering is necessary when the anchor is in use to maintain a working (breakout) force so that the vessel is kept precisely on the required position. A low pump power is required in cohesive soil due to low degree of seepage through this type of soil and a higher pump power is required for cohesionless soil because of the higher degree of permeability. This type of anchor can be used for driving piles, positioning and as a guide for embedded anchors, and is also capable of providing a short-term anchored position for semi-submersible objects.

2. Embedded anchor

   This/

This type of suction anchor is capable of embedding into the ocean bed, depending on the pump capacity and the ocean bed sediments. Dewatering is only used to consolidate the surrounding disturbed soil which was fluidized by the jetting action of the anchor. This type of anchor may be used for short or long term operation.

3. Platform-type anchor

A large embedded suction anchor may be capable of providing large upward forces provided the anchor is designed and built to resist such forces. This type of anchor may be very useful in deep water because of its uplift-resisting capacity.

ACKNOWLEDGEMENTS

The research described herein was carried out in the School of Mechanical and Offshore Engineering, RGIT, Aberdeen.

The author is deeply indebted to his Director of Studies, Mr. Q. Wilson for his general guidance and thanks are also due to Mr. M.D. Lowndes for his helpful suggestions.

Thanks are also due to the workshop staff for their help but particularly to Mr. A. Whyte who took keen interest in making the prototype suction anchor and helped during the field tests.

REFERENCES

1. Brown, G.A., and Nacci, V.A., "Performance of hydrostatic anchors in granular soils". Third Annual Offshore Technology Conference, Houston, TX, Apr 19-21, 1971. Dallas, TX, Offshore Technology Conference, vol 2, 1971, pp 533-542.

2. Kerr, N., "A Self-Burying Anchor of Considerable Holding Power". Offshore Technology Conference, 6200 North Central Expressway, Dallas, TX 75206, 1976.

3. Røsbak, T., "An investigation into the Feasibility of Suction Anchors". Diploma in Offshore Engineering Thesis, R.G.I.T., Aberdeen, 1975.

4. Sahota, B.S., "Suction Anchor". Diploma in Offshore Engineering Thesis, R.G.I.T., Aberdeen, 1977.

5. Taylor, R.J., Jones, D., and Beard, R.M., "Handbook for Uplift - Resisting Anchors". Civil Engineering Laboratory, Naval Construction Battalion Centre, Port Hueneme, California 93043, September, 1975.

6. Torbjørnsen, E., "Further Development of Suction Anchors". Diploma in Offshore Engineering Thesis, R.G.I.T., Aberdeen, 1976.

7. Vesic, A.S., "Breakout Resistance of Objects Embedded in Ocean Bottom". Journal of the Soil Mechanics and Foundations Division, Proceedings of the American Society of Civil Engineers. Vol. 97, No. SM9, Sep., 1971, pp 1183 - 1205.

8. Wang, M.C., Demars K.R., and Nacci, V.A., "Breakout capacity of model suction anchors in soil". Can. Geotech. I, Vol. 14, 1977.

9. Wilson, Q , and Sahota, B.S., "Trials with suction anchors". Ocean Industry, August, 1977, pp 55-56.

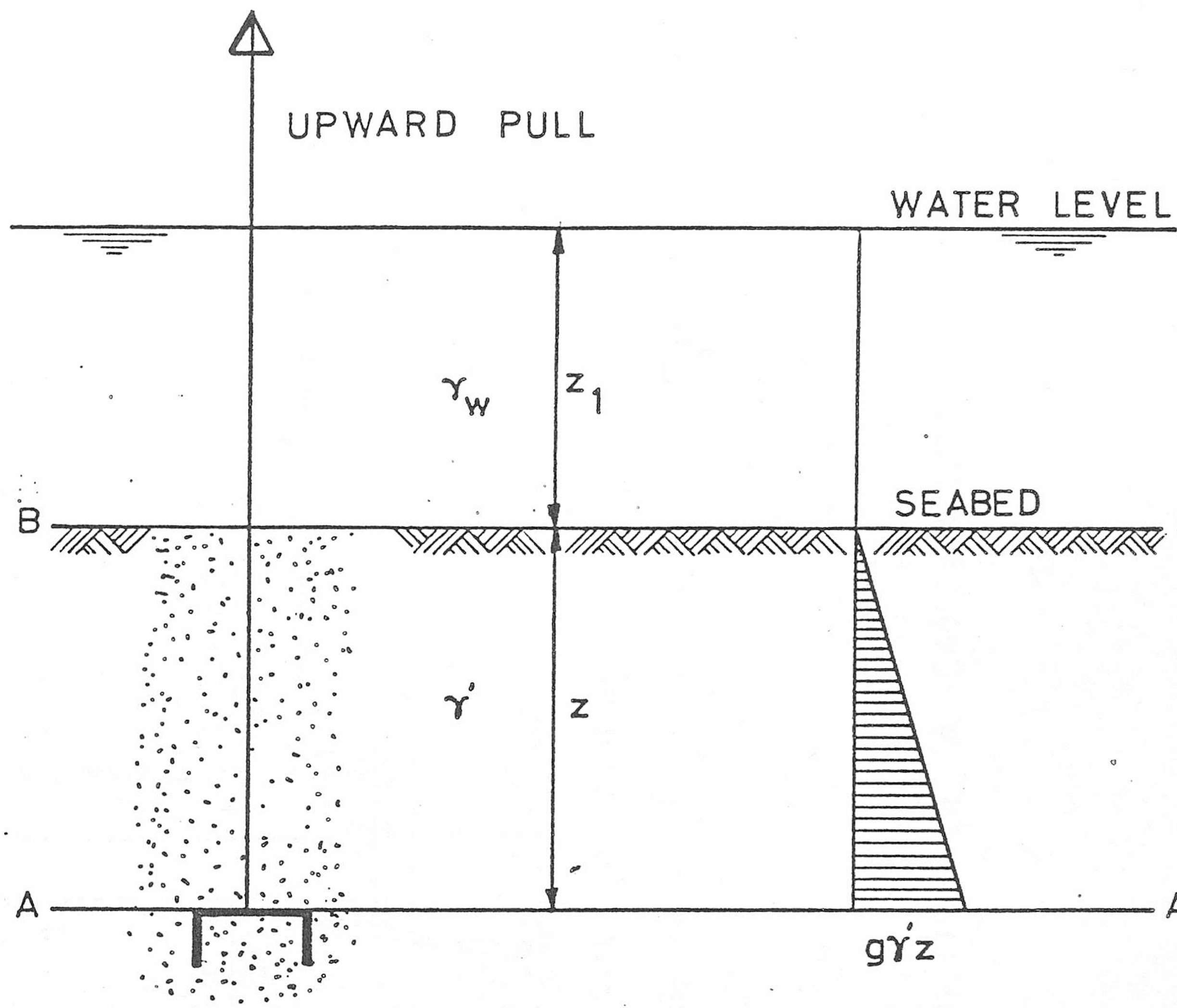

γ_w = UNIT MASS OF WATER

γ' = SUBMERGED UNIT MASS OF SOIL

$$\gamma' = \frac{(G_s - 1)\gamma_w}{1 + e}$$

FIG. 1 EMBEDDED ANCHOR BURIED IN THE OCEAN BOTTOM.

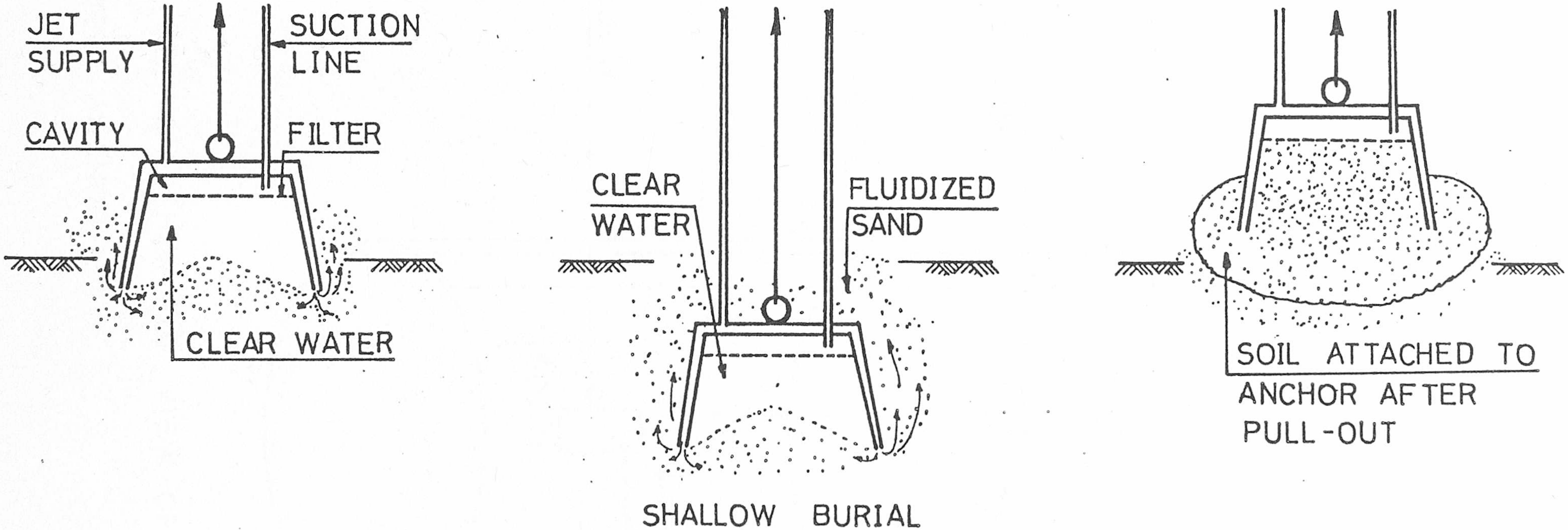

FIG. 2a JETS ONLY

FIG. 2b JETS ONLY

FIG. 2c SUCTION ONLY

FIG. 2 BURYING AND PULLING OUT ACTION OF A CAN ANCHOR.

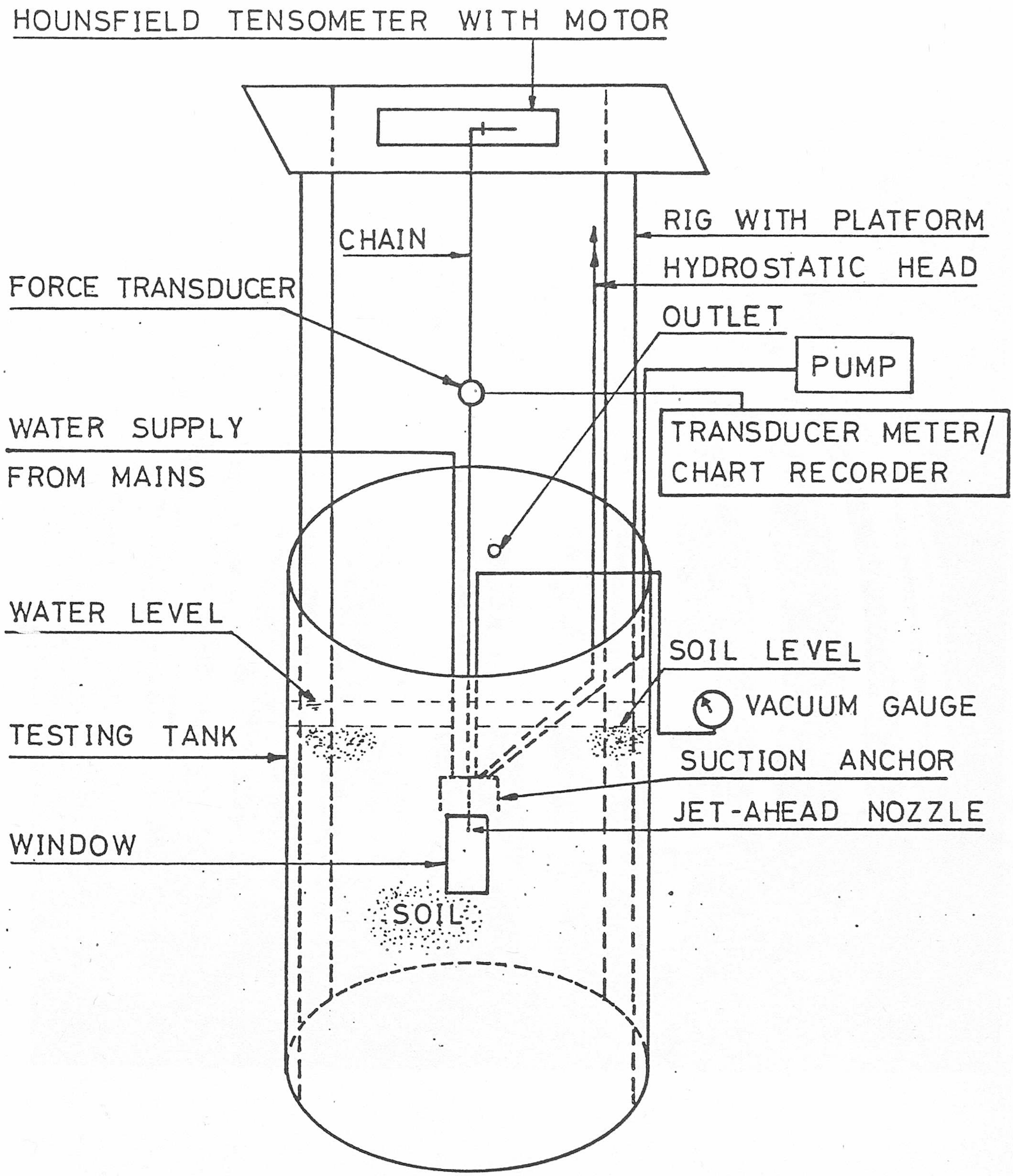

FIG. 3 SCHEMATIC VIEW OF TEST SETUP FOR THE MODEL ANCHOR.

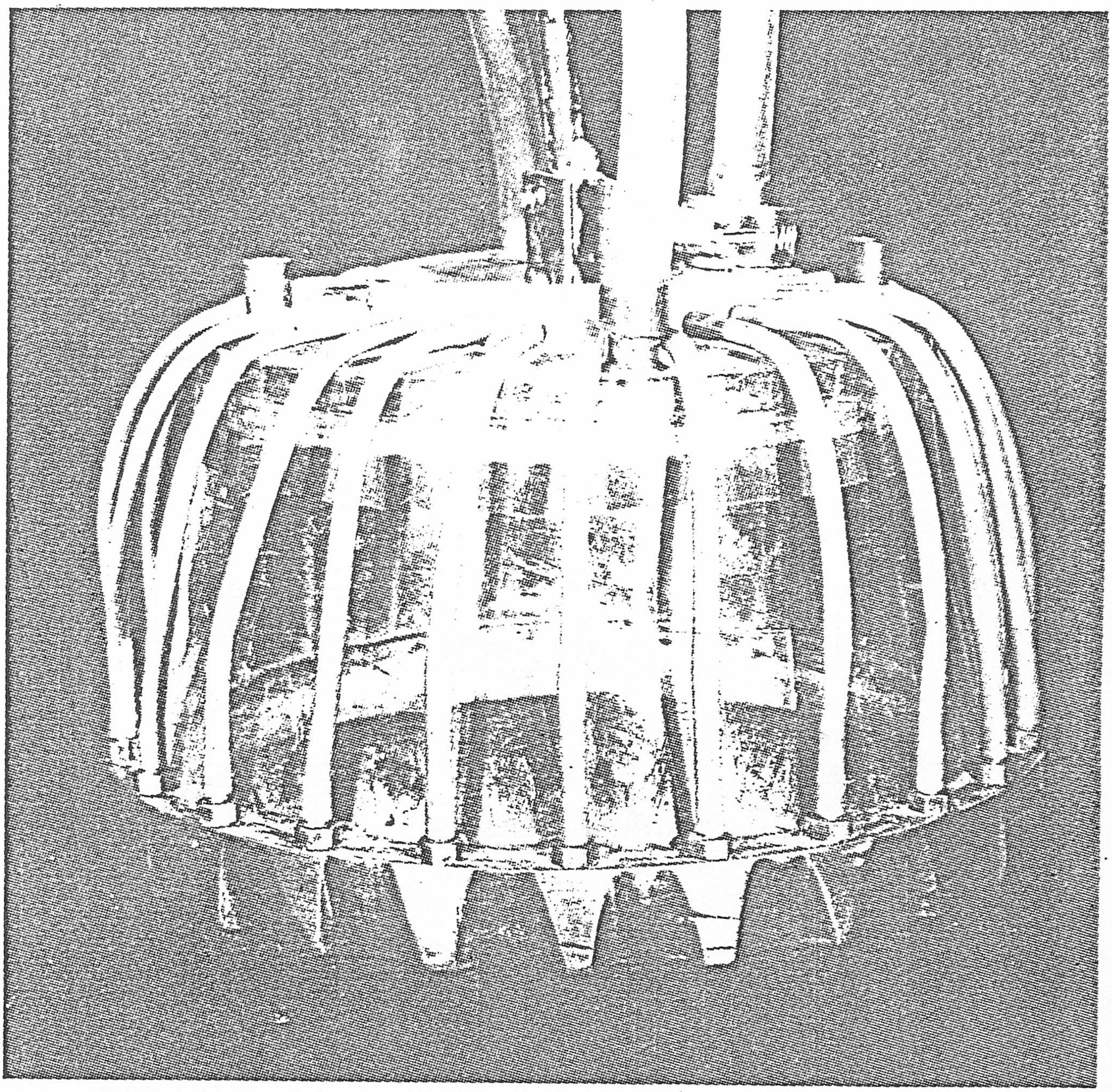

Fig. 4 Photograph of the model suction anchor

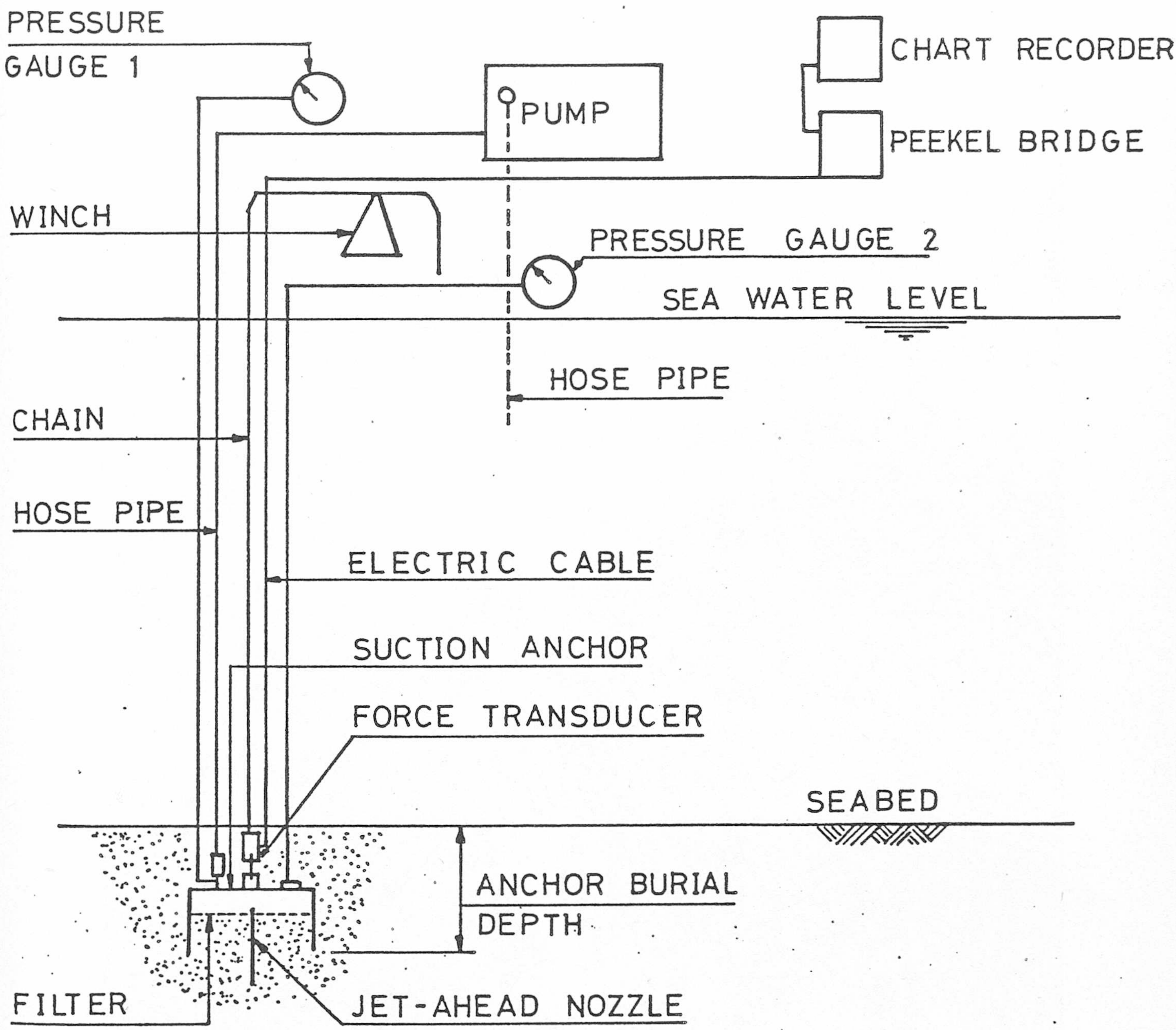

FIG. 5 SCHEMATIC VIEW OF TEST SETUP FOR THE PROTOTYPE SUCTION ANCHOR. ROBERT GORDON (BOAT) IS NOT SHOWN.

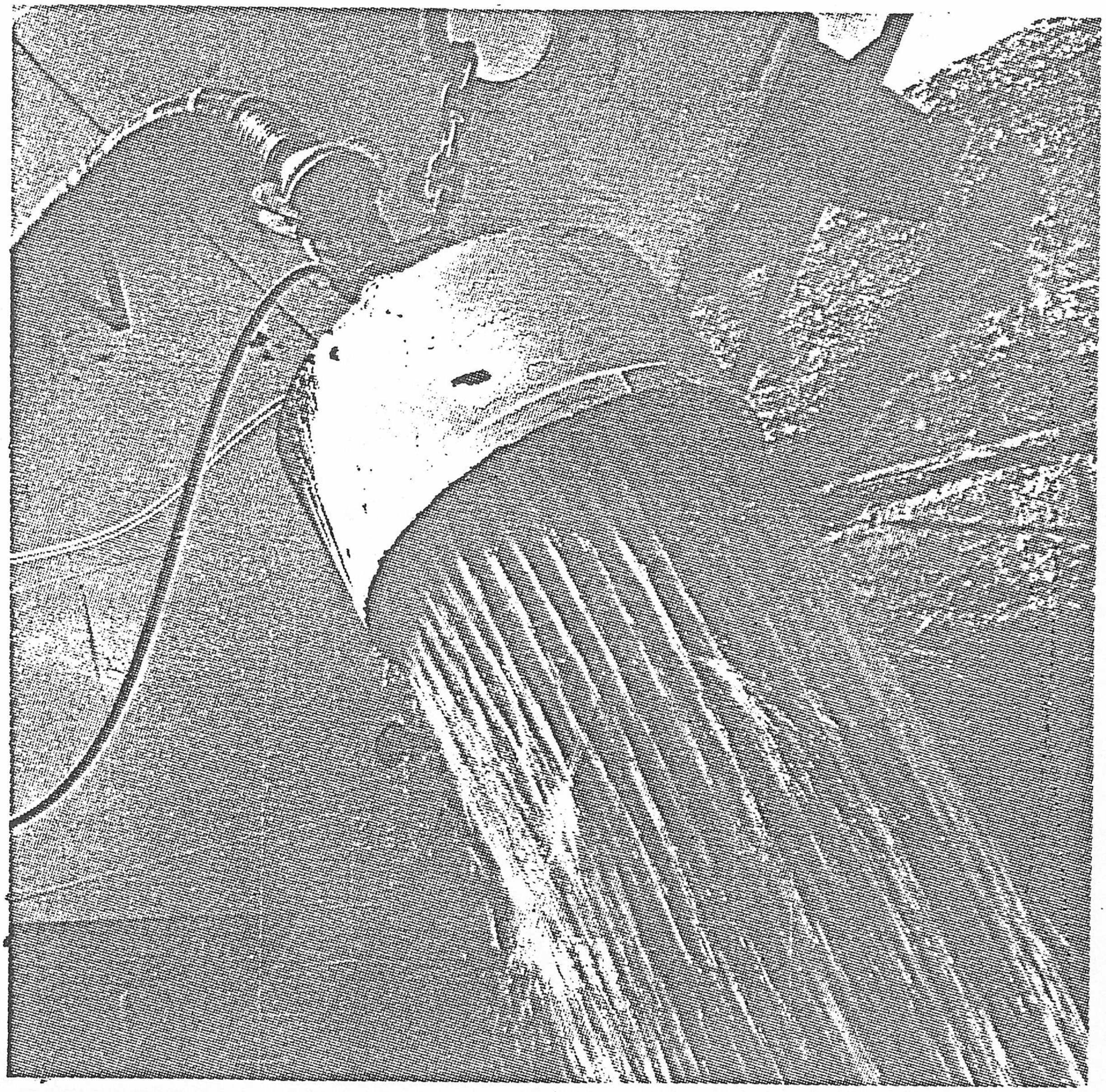

Fig. 6 Photograph of the prototype suction anchor - water jets

Table 1 Comparison between the suction anchors

Details	Model Anchor	Prototype Anchor
Diameter	165 mm	600 mm
Depth	100 mm	300 mm
Weight of anchor	8 N	750 N
Material used for fabrication	Perspex - brass	Mild steel
Area ratio	1	14
Length/Diameter ratio	0.5	0.32
Weight of soil attached	15 N	1250 N
Weight ratio	1	94
Weight of soil attached ratio	1	83
Jet flow	0.014 m^3/min.	0.9 m^3/min. (Designed)
No. of peripherial jets	24	48
Jet static pressure	34.5 kN/m^2	200 kN/m^2
Power	7.4 W	3 kW assessed
Suction flow	80×10^{-6} m^3/s	--
Uplift force	10N	555 N
Maximum pulsating force	--	67.5 kN
No. of buoyancy control	None	2
Size of filter	100 μm	100 μm
Designed for breakout force	600 N	0.1×10^6 N

APPENDIX F

SUCTION ANCHORS

BY

Q. WILSON & B.S. SAHOTA

Page No. F 1 - F 7

EUR 16

SUCTION ANCHORS

by Quentin Wilson and Baldev S. Sahota,
Robert Gordon's Institute of Technology

ABSTRACT

The development of self-burying suction anchors is described and data on pull-out forces presented for both inverted-cup and solid hemispherical types embedded in fine sand at depths up to three times anchor diameter. Observations made during sea trials of both anchor types are discussed. It is shown that the application of anchor suction increases the force necessary for pull-out of deeply embedded anchors and that suction anchors can have a low power requirement.

INTRODUCTION

Marine ground-anchors may be classified according to their capacity for withstanding uplift force and horizontal drag force. In recent years, many forms of uplift-resisting anchors have been proposed [4,5,9], each anchor type having its own characteristics and range of applications. One type, the suction anchor, has been investigated at a number of centres [1,2,3,10,11,12]. Most of these studies were based on anchors in the shape of an inverted cup (Fig. 1), with a skirt and internal filter or porous stone between the soil and an internal cavity from which water is drawn by means of a suction line connected to a pump. The reduction of pressure within the anchor and the adjacent soil produces a downward-acting force which presses the anchor onto the soil bed and creates compressive increments in the effective stresses in the soil below the anchor.

A vertical force is required to lift an anchor hanging freely in water. The extra force F required for pull-out of an embedded cup anchor comprises the resultant of the normal and shear stresses applied to the outer surfaces of the anchor by the soil and a force to cause failure of the soil below the anchor by further modification of the effective stresses.

Schofield [7,8] proposed an alternative to the cup anchor in the form of an anchor plate or an arrangement of interconnecting beams lying on the sea bottom and covered by an impermeable sheet. By creating a difference in hydrostatic pressure between the upper and lower sides of the sheet the anchor assembly was pressed onto the soil, thereby making the anchor capable of resisting uplift forces.

All of these anchors are surface attaching devices with little or no overburden to contribute to the pull-out force. Also, the cup anchors have a very limited capacity for self burial, usually requiring a downward push into the soil.

References and illustrations at end of paper.

DEVELOPMENT OF SELF-BURYING ANCHORS

At R.G.I.T., work on suction anchors was carried out by students Røsbak and Torbjørnsen. By the end of 1974 Røsbak had tested a cup-type model (Fig.1) in a submerged bed of fine sand and obtained results similar to Wang et al[10]. In general, this model would not embed itself by suction alone. Sea trials with a simple anchor made from a small oil drum were encouraging though they confirmed the belief that suction alone would not give consistant embedment of a free anchor. If the anchor was part of a sea-bed structure[11] then the weight of that structure might be sufficient to push the anchor into the soil. The weight of the anchor was unlikely to give sufficient initial penetration for suction to develop to complete the embedment.

In order to give the anchor a self-burying action various arrangements of water jets were fitted to the original model. Effective sand fluidization was produced by a ring of downward-acting jets around the edge of the anchor skirt. A new model in acrylic with a brass jet ring was designed by Torbjørnsen (Fig.2). A secondary function of this ring was to give the model a low centre of mass and stability during burial. In the fine sand in the test tank the new model buried rapidly to filter level.

Up to this time the suction anchor had been regarded as a surface attachment device, and it was a somewhat surprised Torbjørnsen who on one occasion watched the model bury to filter level in the normal way and then disappear downwards into the sand bed. The forces required for pull-out increased significantly with burial depth.

THE SELF-BURYING ACTION OF CUP ANCHORS

A curious feature of the deep-burial action of the acrylic and brass model was its inconsistency. Sometimes the model anchor would give the impression of floating in the fluidized sand. At other times it would disappear downwards with little hesitation.

Two experiments were set up to investigate the burial action. In the first, a half-model of the acrylic and brass anchor was constructed and held against the glass wall of a tank so that the behaviour of the sand around the model could be observed. The experiment showed that the skirt jets excavated a trench (Fig.2) and that the sand within the model, because of its free running nature, fell into the turbulent region created by the jets and was then carried by the flow of water up the outside of the anchor. The water within the model remained clear since there was insufficient vertical flow to maintain the sand particles in suspension.

A clear plastic tube connected to the anchor cavity acted as a manometer and indicated pressure increases within the model during jetting (Fig.3). It was observed that the jets increased the hydrostatic pressure within the model and that the manometer rise Z_m was independent of the jet supply pressure and flow, provided that the water supply was sufficient to maintain the soil in a fluid state. The jet-induced pressure rise increased linearly with burial depth Z. This pressure rise was attributed to the difference in density between the column of clear water inside the anchor and the column of fluidized sand outside the anchor (Fig.3).

Similar results were obtained with other models jetted into the same sand (Fig.5). If the pressure rise is considered on a purely hydrostatic basis, the assumption of equal pressure at a level common to both the internal and external fluid columns gives

$$\gamma_w(Z_m + Z_1 + Z) = \gamma_w Z_1 + \gamma_f Z \quad \ldots\ldots\ldots(1)$$

Hence, the unit weight of the fluidized soil may be derived from Fig.5 using the relationship that

$$\gamma_f = \gamma_w \left(\frac{Z_m}{Z} + 1\right) \quad \ldots\ldots\ldots(2)$$

For the soil in the test tank $\gamma_f \simeq 16$ kN/m^3 (102 lbf/ft^3)

Most of the tests on complete models were conducted with the anchor attached to the loading apparatus by a chain, so that the anchor could bury in a natural manner. By replacing the chain by a steel rod the anchor model was constrained and any change in vertical force measured by means of a load cell and chart recorder. This procedure showed that, as the model anchor buried, the "weight" of the anchor measured by the load cell reduced until the top of the model was level with the top of the sand bed. As burial continued below this level a small increase in "weight" occurred, then the vertical force measured by the load cell became constant, except for unsteady surging effects in the fluidized sand.

It was now apparent that the burial action was being affected by buoyancy forces as the anchor and any clear water enclosed within its profile displaced a corresponding volume of fluidized sand. The buoyancy force F_b is given by

$$F_b = (\gamma_f - \gamma_w)(\text{volume of fluidized soil displaced}) \quad \ldots\ldots\ldots\ldots(3)$$

When the top of the anchor passed below sand level, particles collected until a cone of sand covered the anchor top, offsetting the buoyancy given by (3).

The acrylic and brass model and entrapped water had a volume of 1.43×10^{-3}m^3 (87.3 in^3). Thus the maximum buoyancy force from (3) is

$$(16.0 - 9.81) \times 1.43 \times 10^{-3}\ \text{kN} = 8.9\text{N (2 lbf)}$$

The buoyant weight of the sand cone that collected on top of the anchor was estimated to be about 2N (0.5 lbf). These values agreed closely with the changes in vertical force measured during burial. The inconsistent burial action of the brass and acrylic model was due to the near balance of the weight and buoyancy forces.

When the same ideas were applied to a 600 mm diameter by 300 mm deep anchor of sheet steel it was found that the 750 N (170 lbf) weight in air reduced to 650 N (145 lbf) in salt water and 150 N (34 lbf) in fluidized sand of similar type to that in the test tank. Thus the buoyancy effect may be significant on large scale anchors employing water jets for burial.

PULL-OUT TESTS WITH SELF-BURYING CUP ANCHORS IN SAND

Once the required burial depth had been achieved, the water supply to the jets was cut off and suction applied. The sand surrounding the anchor was drawn towards the filter, filling the anchor cup and causing a general sinkage as dewatering reduced the proportion of water present in the fluidized soil.

When the model anchors were pulled-out from the sand bed they retained a sand plug of the form shown in Fig. 4. A similar plug was observed during sea trials with a 600 mm diameter steel prototype anchor.

The maximum vertical force F during pull-out of the model anchor (D = 165 mm) divided by the anchor plan area A is plotted against burial depth ratio d_e/D on Fig. 6 for cavity suction pressures Δp of 5 kN/m^2 and 10 kN/m^2 (0.7 psi and 1.5 psi). As a rule-of-thumb for surface-attaching cup anchors in sand, the pull-out pressure $F/A \simeq 0.5\ \Delta p$. The test results show that values considerably in excess of this are attainable by buried anchors.

The water flow through the model varied from 95×10^{-6} m^3/s (3.4×10^{-3} ft^3/s) with the anchor hanging freely in the water ($\Delta p = 0$) to 77×10^{-6}m^3/s (2.7×10^{-3} ft^3/s) for the embedded condition. The product of cavity suction pressure and water flow gives the anchor power requirement. For the model anchors this was of the order of 1 W (0.0013 hp). This very low power demand may be satisfied most efficiently by intermittant pumping and use of a reservoir system as proposed by Schofield[8].

All sea trials were conducted from the Institute schooner "Robert Gordon" using the vessel's anchor chain and windlass. Since the tension that could be applied by the windlass was too low for break-out of the 600 mm anchor the procedure adopted was to lock the windlass and allow the rise in tide to create the necessary force. A typical section of test record (Fig.7) obtained during calm conditions off Aberdeen shows the frequent load peaks that occurred when applying a vertical load through a taut mooring that had little flexibility. During this test the burial depth did not exceed 300 mm (1 ft.). An earlier trial conducted in a more active sea-state gave a succession of load peaks that reached 67.5 kN (15000 lbf) before the test was abandoned for safety reasons. This load was greatly in excess of the maximum static load that the anchor might have been expected to hold with $\Delta p \simeq 30$ kN/m^2 (4.4 psi). The result may have been exceptional but it does suggest that suction anchors have a good capacity for holding dynamic loads.

When the pull-out force is applied by a surface vessel, the anchor, soil, mooring cable and vessel become one dynamic system with sea-state excitation.

The 600 mm anchor used for the sea trials had internal non-return valves and a single 75 mm (3 inch) internal-diameter armoured hose. By reversing the hose connection at the pump the valves directed the water supply to the jets or the suction flow from the cavity to the pump as required.

DEVELOPMENT OF OTHER ANCHOR TYPES

The penetration of an anchor into the sea bed depends on the balance of the vertical forces that come into action. Buoyancy effects alone may be sufficient to reduce the downward force on a cup-type suction anchor to a value inadequate for burial, even in an easily fluidized sand, unless the anchor is pushed downwards. More generally, any form of anchor that depends on jetting and forces of the order of anchor weight may not bury if hard strata or large stones are encountered. Never-the-less, an improvement in performance can be obtained by reducing the enclosed volumes full of clear water and by making the anchor heavier. Increase in weight may be a retrograde step if taken to the point of causing handling difficulties and increased costs. (An alternative is the use of an air-lift pump, as in the National Engineering Laboratory "Hydropin" [4], to carry the fluidized soil up the inside of the anchor.)

Experimental investigation of the pore pressure changes due to anchor suction showed that for a cup anchor with a deep skirt a large proportion of the cavity suction pressure Δp is dissipated in the soil contained within the skirt region. This led to speculation that the position and size of the anchor filter should be such that the most favourable effective stresses are produced by extending the low pressure region as far into the soil mass as possible.

The concept of an anchor cast in concrete, solid except for the minimum of internal ducting and with the filter on the outer surface, was first realized in the form of a 145 mm (5.7 in) diameter hemispherical model. Soil fluidization was produced by a single nozzle unit containing a number of jets that directed water outwards from the bottom of the hemisphere (Fig.8). In the test tank, this model buried quickly and consistently. A 600 mm (2 ft) diameter anchor of similar form buried to a depth of 5 metres (16 ft) in 10 minutes in sand off Ardersier in the Moray Firth, when supplied with water at 70 m^3/h (2470 ft^3/h) flow rate and 350 kN/m^2 (50 p.s.i.) pressure. This anchor had provision for a secondary jet ring (Fig.8) which could be used to supply additional energy to the flow around the anchor.

The 600 mm anchor weighed 1510 N (340 lbf) in air and 1170 N (260 lbf) in salt water. In fluidized sand its weight was estimated to be 835 N (190 lbf).

A combination of the cup and "solid" anchor types is suggested in Fig. 9, in which the "solid" anchors are used as footings on columns which extend downwards from a skirted platform. Resistance to vertical forces is due to anchor weight, overburden and reduction in pore pressure by dewatering. The platform skirts, columns and footings give resistance to horizontal loads and over-turning moments. During embedment the platform's buoyant weight in water is available to push the footings into the soil until the skirts begin to penetrate. Thereafter, the platform limits the embedment so that the mooring attachment remains above soil level. Many variations on these basic ideas are possible. A few have been given initial feasibility trials at model scale.

PULL-OUT TESTS WITH HEMISPHERICAL ANCHORS

Pull-out tests under vertical loading were performed with the 145 mm diameter model (Fig.8) at displacement rates of 2 mm/s (4.7 in/min) and 0.08 mm/s (0.18 in/min) with a cavity suction pressure Δp equal to 5 kN/m^2 (0.7 p.s.i). Similar forces were recorded in both test series (Fig.10). Due to pump flow limitations Δp = 10 kN/m^2 could not be attained.

In a third test series, the jets were used to fluidize the sand in the tank and then turned off. After the pore pressure changes around the anchor had returned to zero, 5 kN/m^2 suction was applied for one minute. Once the pore pressure changes had again returned to zero the model was pulled out at 0.08 mm/s. Pore pressure changes during pull-out were less than 4 mm water gauge (0.006 p.s.i.).

Comparison of the results for Δp = 0 and Δp = 5 kN/m^2 (Fig.10) shows that applied suction causes a significant increase in pull-out pressure F/A. The data for Δp = 5 kN/m^2 are similar to the results given by the cup model (Fig.6) at the same cavity pressure, but the comparison may be misleading since investigation of the pore pressure distribution created by an anchor of hemispherical form has shown that the pore pressure changes in the surrounding sand increase with increasing filter area. Though cavity suction Δp is an important variable, there is insufficient information available at present to confirm the validity of comparing the pull-out behaviour of different anchor types on the basis of Δp without reference to the filter arrangement and anchor geometry. Helfrich et al [3] directed attention towards suction flow rate as a parameter to which pull-out force in a specified sand can be related. A combination of pressure and flow rate data may provide a basis for comparison of anchor performance.

During one trial with the 600 mm diameter concrete anchor, when it buried to the 2.1 metre (6.8 ft) test depth in 2.7 minutes, the suction flow rate reduced from 0.81 m^3/hr (29 ft^3/hr) shortly after initiation of suction to 0.22 m^3/hr (7.8 ft^3/hr) one hour later. The maximum cavity suction during this period was 52 kN/m^2 (7.5 p.s.i.). The greatest anchor power corresponding to these figures is 12 W (0.016 hp). The pump installed on the "Robert Gordon" for the most recent tests is driven by a 22 kW (30 hp) diesel engine. This power is required during jetting but the use of such a pump is a grossly inefficient method of maintaining suction at low flow rates.

Pull-out data are not yet available for the 600 mm diameter concrete anchor due to damage to the load-cell cable during trials. When buried to 5 metres (16 ft) in sand the anchor could not be broken-out by the "Robert Gordon", though it was easily retrieved by using the jets to fluidize the sand.

CONCLUDING REMARKS

Deeply-embedded suction anchors have certain features in common with buried plate anchors. Considered in this context, the new parameter introduced is the reduction in pore pressure in the surrounding soil and the influence of this pressure change on the forces required for pull-out. All pull-out tests, in the laboratory and at sea, were carried out after anchor embedment had created a pit of disturbed soil within a region of naturally consolidated material. The data presented show that the application of anchor suction can have a significant effect on the forces required for pull-out. The extent of this effect and the relative contributions made by applied suction and overburden require further exploration by extension of the range of suction pressures and burial depths.

An undesirably feature of suction anchors is the need for continuous pumping. The results presented show that, even in sand, the power requirement is low and that only intermittent pumping may be necessary. Many different anchor arrangements are possible and the power requirement may be reduced further by means of impermeable plates, platforms, sheets or clay beds on the sea bottom.

The results obtained so far give encouragement that suction anchors will become useful in the field of Ocean Technology, but it is apparent that much more development and basic research remain to be done.

NOMENCLATURE

A = anchor plan area $(= \frac{\pi}{4} D^2)$
D = anchor external diameter
d_e = burial depth (See Fig.6 and Fig.10)
F = total vertical pull-out force less anchor weight in water
F_b = buoyancy force
Z = distance from sand level to bottom of internal water column
Z_m = cavity manometer rise during jetting
Z_1 = water depth
γ_w = unit weight of water
γ_f = unit weight of fluidized soil
Δp = cavity suction pressure
v = pull-out speed

ACKNOWLEDGEMENTS

The authors are grateful to Robert Gordon's Institute of Technology and to the Science Research Council for their support of this work.

Acknowledgement is also due to Mr. A. Whyte, project technician, whose enthusiasm made the experimental work possible.

REFERENCES

1. Al-Awadi, M.J.: "Suction Anchors", M.Sc. Thesis, University of Manchester Inst. Sci. and Tech., 1971.
2. Brown, G.A. and Nacci, V.A.: "Performance of Hydrostatic Anchors in Granular Soils", Offshore Tech. Conf., OTC 1472, 1971.
3. Helfrich, S.C., Brazill, R.L. and Richards, A.F.: "Pullout Characteristics of a Suction Anchor in Sand", Offshore Tech. Conf., OTC 2469, 1976.
4. Kerr, N.: "A Self-Burying Anchor of Considerable Holding Power", Offshore Tech. Conf., OTC 2466, 1976.
5. Nath, B., Harvey, R.C. and Burley, E.: "The Development of an Embedded Anchor to provide Multi-Directional Restraints", Oceanology International Conf., Brighton, 1978, 97 - 107.
6. Sahota, B.S.: "Suction Anchors", Robert Gordon's Inst. of Tech., Aberdeen, 1978, 17 pages.
7. Schofield, A.N.: "Suction Anchors Could Eliminate Pile Driving", *Offshore Services*, 7:3, 1974, 37-39.
8. Schofield A.N.: "Improvements in Hydraulic Engineering Installations", U.K. Patent Specification 1367 881, 25 Sept. 1974.
9. Taylor, R.J., Jones, D. and Beard, R.M.: *Handbook for Uplift-Resisting Anchors*, Naval Civil Eng. Lab., Port Hueneme, Calif., 1975, 153 pages.
10. Wang, M.C., Nacci, V.A. and Demars, K.R.: "Vertical Breakout Behaviour of the Hydrostatic Anchor", Naval Civil Eng. Lab., Port Hueneme, Calif., Report CR 74.005, 1974, 39 pages.
11. Wang, M.C., Demars, K.R. and Nacci, V.A.: "Applications of Suction Anchors in Offshore Technology", Offshore Tech. Conf., OTC 3203, 1978.
12. Wilson, Q. and Sahota, B.S.: "Trials with Suction Anchors", *Ocean Industry*, Aug. 1977, 55-56.

APPENDIX - DATA FOR SAND IN TEST TANK

Soil type	Fine sand
Specific gravity G_s of sand particles	2.67
Unit weight γ (sand + water)	18.9 kN/m^3 (120 lbf/ft^3)
Buoyant unit weight γ' in fresh water	9.1 kN/m^3 (58 lbf/ft^3)
Internal angle of friction ϕ (loose state)	29°
Internal angle of friction ϕ (dense state)	37°
Depth of sand bed	580 mm (23 in)

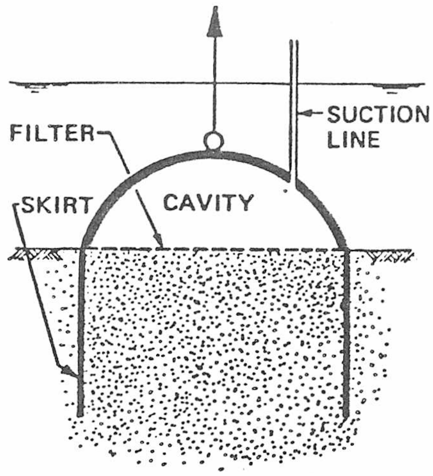

Fig. 1 - Basic cup-type suction anchor.

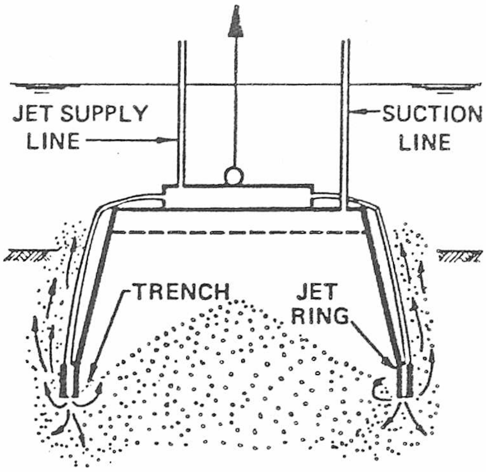

Fig. 2 - Cup-type suction anchor with jet ring.

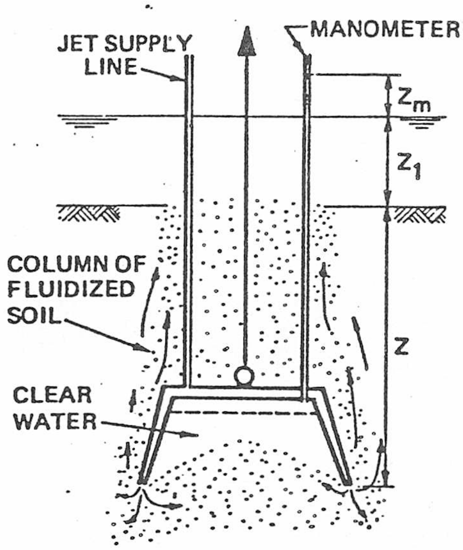

Fig. 3 - Fluid columns during jetting.

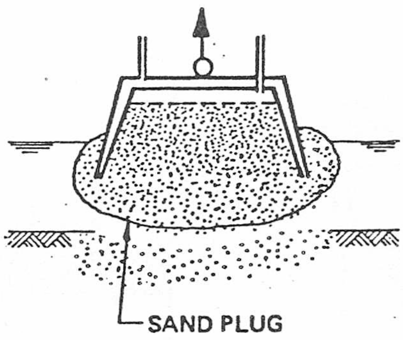

Fig. 4 - Sand plug retained after break-out.

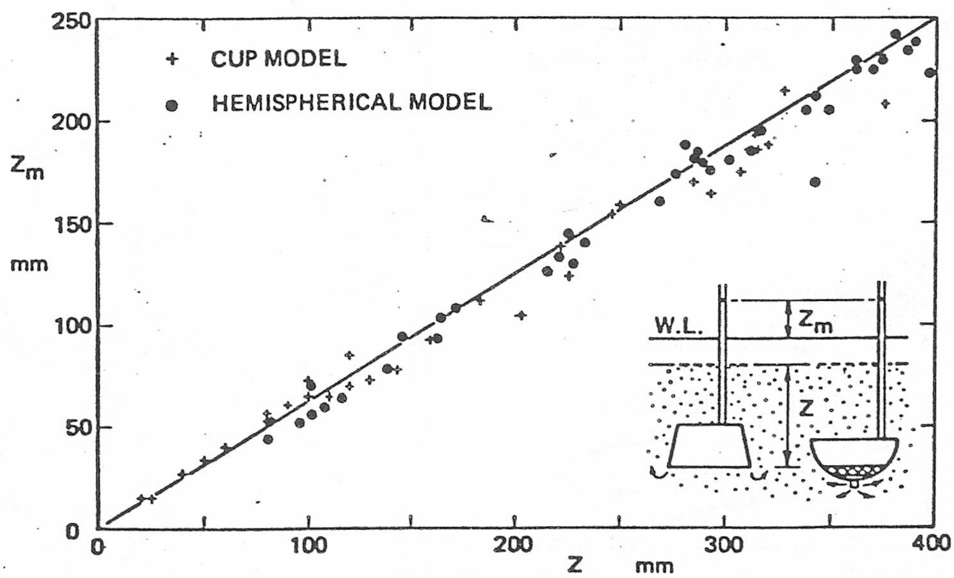

Fig. 5 - Cavity head rise Z_m during jetting.

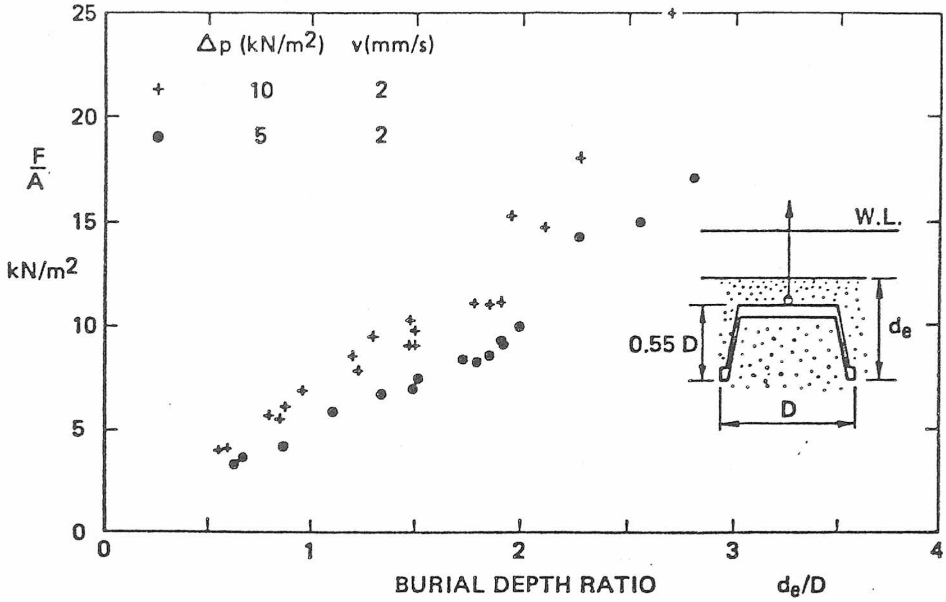

Fig. 6 - Pull-out test data for acrylic and brass model (D = 165 mm).

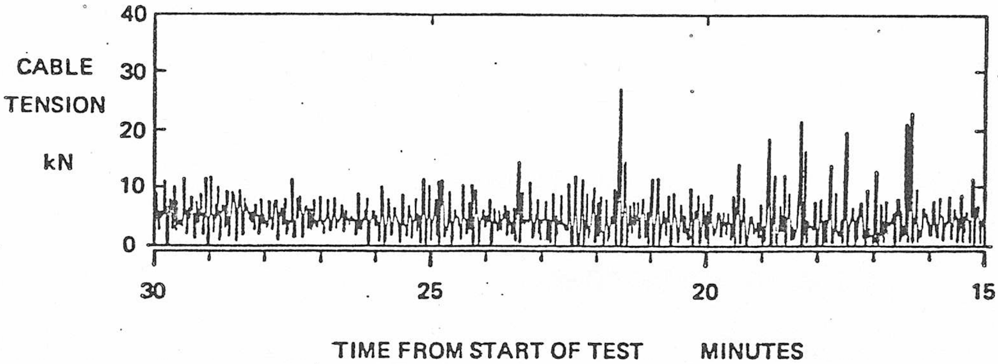

Fig. 7 - Typical force variation in anchor cable during sea trials.

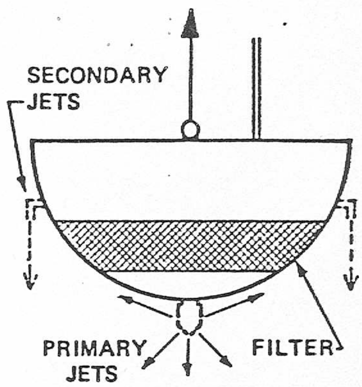

Fig. 8 - Hemispherical suction anchor.

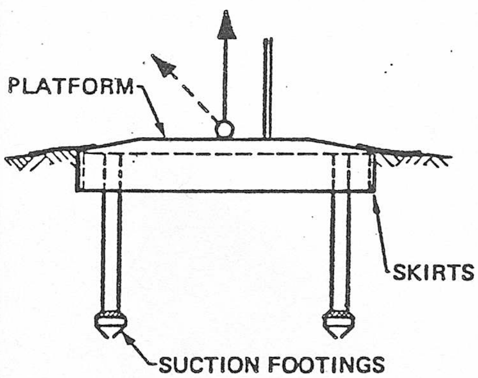

Fig. 9 - Platform-type suction anchor.

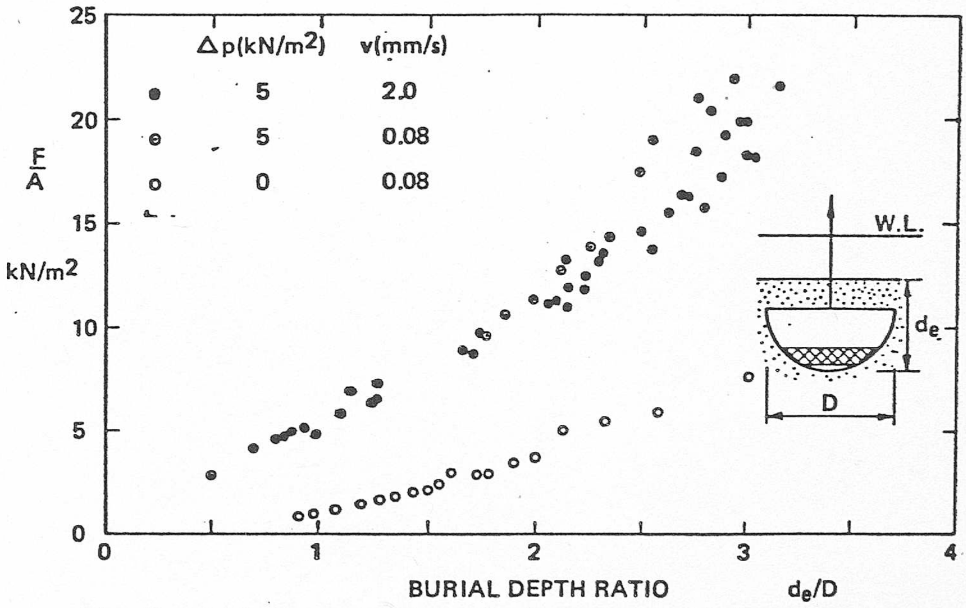

Fig. 10 - Pull-out test data for hemispherical model (D = 145 mm).

APPENDIX G

STATEMENT OF THE ADVANCED STUDIES
UNDERTAKEN IN CONNECTION WITH THE
PROGRAMME OF WORK

Page No. G1 - G2

APPENDIX G

STATEMENT OF THE ADVANCED STUDIES UNDERTAKEN IN CONNECTION WITH THE PROGRAMME OF WORK

During the period of the research programme the writer attended the von Karman Institute for Fluid Dynamics, Belgium for a four week training in research methods.

The Shell laboratory at Rijswyk, Holland, was visited and suction anchors were discussed with Shell research personnel. Visits were made to the National Engineering Laboratory, U.K. and to the Civil Engineering Laboratories of the University of Glasgow to discuss the uplift-resisting-anchor problem with other workers in this field. In the company of Mr. Quentin Wilson, a day was spent with Professor Schofield in the Civil Engineering Laboratories including the Centrifuge facility of the University of Cambridge.

Research seminars were regularly attended and papers were presented in Aberdeen and before an invited audience at the von Karman Institute. The writer attended the EUROPEC conference in London and contributed to the paper on Suction Anchors (Appendix F).